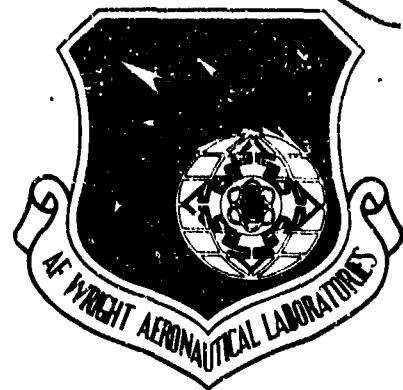(2)

# AD-A207 215

AFWAL-TR-86-3017
VOLUME II

ADVANCED DURABILITY ANALYSIS
VOLUME II - ANALYTICAL PREDICTIONS, TEST RESULTS
        AND ANALYTICAL CORRELATIONS

S. D. Manning

General Dynamics Corporation
Fort Worth Division
P.O. Box 748
Fort Worth, Texas  76101

J. N. Yang

United Analysis Incorporated
2100 Robin Way Court
Vienna, Virginia  22180

February 27, 1989

DTIC
S ELECTE
APR 2 5 1989
D

FINAL REPORT OCTOBER 1984 - FEBRUARY 1989

Approved for public release; distribution unlimited

FLIGHT DYNAMICS LABORATORY
AIR FORCE WRIGHT AERONAUTICAL LABORATORIES
AIR FORCE SYSTEMS COMMAND
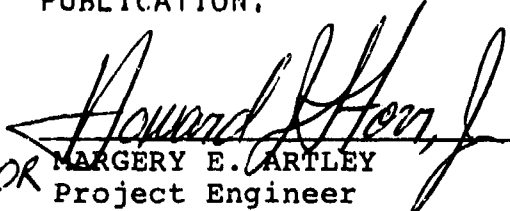WRIGHT-PATTERSON AIR FORCE BASE, OH  45433-6553
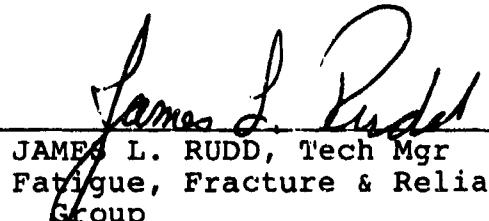
089  4  24  093

# NOTICE

WHEN GOVERNMENT DRAWINGS, SPECIFICATIONS, OR OTHER DATA ARE USED FOR ANY PURPOSE OTHER THAN IN CONNECTION WITH A DEFINITELY GOVERNMENT-RELATED PROCUREMENT, THE UNITED STATES GOVERNMENT INCURS NO RESPONSIBILITY OR ANY OBLIGATION WHATSOEVER. THE FACT THAT THE GOVERNMENT MAY HAVE FORMULATED OR IN ANY WAY SUPPLIED THE SAID DRAWINGS, SPECIFICATIONS, OR OTHER DATA, IS NOT TO BE REGARDED BY IMPLICATION, OR OTHERWISE IN ANY MANNER CONSTRUED, AS LICENSING THE HOLDER, OR ANY OTHER PERSON OR CORPORATION; OR AS CONVEYING ANY RIGHTS OR PERMISSION TO MANUFACTURE, USE, OR SELL ANY PATENTED INVENTION THAT MAY IN ANY WAY BE RELATED THERETO.
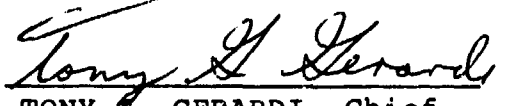
THIS REPORT HAS BEEN REVIEWED BY THE OFFICE OF PUBLIC AFFAIRS (ASD/CPA) AND IS RELEASABLE TO THE NATIONAL TECHNICAL INFORMATION SERVICE (NTIS). AT NTIS, IT WILL BE AVAILABLE TO THE GENERAL PUBLIC, INCLUDING FOREIGN NATIONS.

THIS TECHNICAL REPORT HAS BEEN REVIEWED AND IS APPROVED FOR PUBLICATION.

FOR MARGERY E. ARTLEY
Project Engineer

JAMES L. RUDD, Tech Mgr
Fatigue, Fracture & Reliability Group
Structural Integrity Branch

FOR THE COMMANDER

TONY G. GERARDI, Chief
Structural Integrity Branch
Structures Division

IF YOUR ADDRESS HAS CHANGED, IF YOU WISH TO BE REMOVED FROM OUR MAILING LIST, OR IF THE ADDRESSEE IS NO LONGER EMPLOYED BY YOUR ORGANIZATION PLEASE NOTIFY AFWAL/FIBEC , WRIGHT-PATTERSON AFB, OH 45433-6553 TO HELP US MAINTAIN A CURRENT MAILING LIST.

COPIES OF THIS REPORT SHOULD NOT BE RETURNED UNLESS RETURN IS REQUIRED BY SECURITY CONSIDERATIONS, CONTRACTUAL OBLIGATIONS, OR NOTICE ON A SPECIFIC DOCUMENT.

# REPORT DOCUMENTATION PAGE

| 1a. REPORT SECURITY CLASSIFICATION Unclassified | | 1b. RESTRICTIVE MARKINGS | | | |
|---|---|---|---|---|---|
| 3a. SECURITY CLASSIFICATION AUTHORITY | | 3. DISTRIBUTION/AVAILABILITY OF REPORT Approved for public release; distribution unlimited | | | |
| 3b. DECLASSIFICATION/DOWNGRADING SCHEDULE | | | | | |
| 4. PERFORMING ORGANIZATION REPORT NUMBER(S) | | 5. MONITORING ORGANIZATION REPORT NUMBER(S) AFWAL-TR-86-3017, Volume II | | | |
| 6a. NAME OF PERFORMING ORGANIZATION General Dynamics - FWD | 6b. OFFICE SYMBOL (If applicable) | 7a. NAME OF MONITORING ORGANIZATION Flight Dynamics Lab. (AFWAL/FIBEC) Air Force Wright Aeronautical Laboratories | | | |
| 6c. ADDRESS (City, State and ZIP Code) P.O. Box 748 Fort Worth, Texas 76101 | | 7b. ADDRESS (City, State and ZIP Code) Wright-Patterson AFB OH 45433-6553 | | | |
| 8a. NAME OF FUNDING/SPONSORING ORGANIZATION Wright Aeronautical Laboratories | 8b. OFFICE SYMBOL (If applicable) FIBEC | 9. PROCUREMENT INSTRUMENT IDENTIFICATION NUMBER F33615-84-C-3208 | | | |

| 8c. ADDRESS (City, State and ZIP Code) | 10. SOURCE OF FUNDING NOS. | | | |
|---|---|---|---|---|
| | PROGRAM ELEMENT NO. | PROJECT NO. | TASK NO. | WORK UNIT NO. |
| 11. TITLE (Include Security Classification) Advanced Durability Analysis - Vol. II - Analytical Predictions, Test Results & Analytical Correlations | 62201F | 2401 | 01 | 89 |

**12. PERSONAL AUTHOR(S)**
S. D. Manning and J. N. Yang

| 13a. TYPE OF REPORT Final | 13b. TIME COVERED FROM Oct 84 TO Feb 89 | 14. DATE OF REPORT (Yr., Mo., Day) 89 02 27 | 15. PAGE COUNT 287 |
|---|---|---|---|

**16. SUPPLEMENTARY NOTATION**
The associate investigator for this report was Dr. J. N. Yang of United Analysis, Inc.

| 17. COSATI CODES | | | 18. SUBJECT TERMS (Continue on reverse if necessary and identify by block number) |
|---|---|---|---|
| FIELD | GROUP | SUB. GR. | Durability, fatigue, equivalent initial flaw size (EIFS), |
| 0103 | 1404 | 1305 | initial fatigue quality (IFQ), crack initiation (TTCI), deterministic and stochastic crack growth. |

**19. ABSTRACT (Continue on reverse if necessary and identify by block number)**
Advanced durability analysis "design tools" have been developed for metallic aircraft structures. These tools can be used to evaluate durability design requirements for functional impairments due to (1) excessive cracking and (2) fuel leakage/ligament breakage. The methodology accounts for the initial fatigue quality variation of structural details, the crack growth accumulation for a population of structural details under specified design conditions and structural properties. Step-by-step procedures are provided. This volume is limited to the analytical methods, technical aspects, concepts and philosophy for the durability analysis of metallic aircraft structures.

The methodology reflects a probabilistic approach, a fracture mechanics philosophy and both deterministic and stochastic crack growth methods. It can be used to predict the probability of crack exceedance at any service time and/or the cumulative distribution of the time

| 20. DISTRIBUTION/AVAILABILITY OF ABSTRACT UNCLASSIFIED/UNLIMITED ☒ SAME AS RPT. ☐ DTIC USERS ☐ | 21. ABSTRACT SECURITY CLASSIFICATION Unclassified | |
|---|---|---|
| 22a. NAME OF RESPONSIBLE INDIVIDUAL Margery E. Artley | 22b. TELEPHONE NUMBER (Include Area Code) (513) 255-6104 | 22c. OFFICE SYMBOL AFWAL/FIBEC |

**DD FORM 1473, 83 APR**    EDITION OF 1 JAN 73 IS OBSOLETE.

18. (continued) probability of crack exceedance, cumulative distribution of TTCI.

19. (continued) to reach any crack size. The methodology applies to the small crack size range associated with excessive cracking (e.g., <0.05") and to large through-the-thickness cracks (e.g., 0.5" - 0.75") associated with fuel leakage/ligament breakage.

No matter what form, location or combination the as-manufactured flaws may have in fastener holes (e.g., scratches, burrs, microscopic imperfections, etc.) or whatever the source of fatigue cracking may be, a practical method of representing the reality of the as-manufactured condition is needed for durability analysis. This is taken care of by the equivalent initial flaw concept.

Initial fatigue quality of a structural detail (e.g., fastener holes, cut-outs, fillets, lugs, etc.) is represented by an equivalent initial flaw size distribution. An equivalent initial flaw (EIFS) is an artificial crack size which results in an actual crack size at an actual point in time when the initial flaw is grown forward. It is determined by back-extrapolating fractographic results. It has the following characteristics: (1) an EIFS is an artificial crack assumed to represent the initial fatigue quality of a structural detail in the as-manufactured condition whatever the source of fatigue cracking may be, (2) it has no direct relationship to actual initial flaws in fastener holes such as scratches, burrs, microdefects, etc., and it cannot be verified by NDI, (3) it has a universal crack shape in which the crack size is measured in the direction of crack propagation, (4) EIFSs are in a fracture mechanics format but they are not subject to such laws and limitations as the "short crack effect," (5) it depends on the fractographic data used, the fractographic crack size range used for the back-extrapolation and the crack growth rate model used, (6) it must be grown forward in a manner consistent with the basis for the EIFS, and (7) EIFSs are not unique - a different set is obtained for each crack growth law used for the back-extrapolation.

Recommendations for durability analysis are as follows: (1) define the equivalent initial flaw size distribution (EIFSD) using fractographic data in the small crack size region (e.g., 0.01"-0.05"), (2) use fractographic data pooling procedure and statistical scaling technique to estimate the EIFSD parameters in a "global sense" for a "single hole population" basis (3) use the deterministic crack growth approach (DCGA) in the small crack size region and (4) use the two-segment deterministic-stochastic crack growth approach (DCGA-SCGA) for applications in the large crack size region (e.g., 0.50"-0.75"); the two-segment deterministic crack growth approach (DCGA-DCGA) is also reasonable but it is slightly less conservative than the DCGA-SCGA.

Procedures have been developed for defining initial fatigue quality. These procedures could be used to standardize the way initial flaw sizes are determined from fractographic data. A better understanding of initial flaw sizes (i.e., what they are and limitations) has been developed. For consistent durability analysis predictions, equivalent initial flaws must be used in the same context for which they were defined. This means that equivalent initial flaws must be grown forward in the same manner the EIFSs were established by back-extrapolating fractographic results.

## FOREWORD

This report was prepared by General Dynamics, Fort Worth Division, under the "Advanced Durability Analysis" program (Air Force Contract F33615-84-C-3208) for the Air Force Wright Aeronautical Laboratories (AFWAL/FIBEC). Margery E. Artley was the Air Force Project Engineer; Dr. John W. Lincoln of ASD/ENFS and James L. Rudd of AFWAL/FIBEC were technical advisors. Dr. S. D. Manning of the General Dynamics' Structures Technology Staff was the program manager and co-principal investigator along with Dr. J. N. Yang of United Analysis Incorporated (Vienna, VA).

The advanced durability analysis methodology developed under this program is evaluated in this report (Vol. II). Analytical predictions, test results and analytical correlations are considered. Other volumes for this program are as follows:

- o     Volume I     -   Analytical Methods

- o     Volume III   -   Fractographic Test Data

- o     Volume IV    -   Executive Summary

- o     Volume V     -   Durability Analysis Software User's Guide

| Accesion For | | |
|---|---|---|
| NTIS    CRA&I | | ☑ |
| DTIC    TAB | | ☐ |
| Unannounced | | ☐ |
| Justification | | |
| By | | |
| Distribution / | | |
| Availability Codes | | |
| Dist | Avail and / or Special | |
| A-1 | | |

DTIC COPY INSPECTED 4

## Table of Contents

Table of Contents (Continued)

# Table of Contents (Continued)

Table of Contents (Concluded)

# LIST OF FIGURES

List of Figures (Continued)

List of Figures (Continued)

List of Figures (Continued)

List of Figures (Continued)

List of Figures (Continued)

List of Figures (Concluded)

# LIST OF TABLES

List of Tables (Continued)

List of Tables (Concluded)

# SECTION I
## INTRODUCTION

The purpose of this Volume is to evaluate the advanced durability analysis methodology documented in Volume I [1] and the test/fractographic results documented in Volume III [2].

# SECTION II

## EVALUATION OF DURABILITY TEST/FRACTOGRAPHIC RESULTS

### 2.1  INTRODUCTION

Test and fractographic results acquired under this program (Volume III) [2] are reviewed, evaluated and compared in this section with results from two previous test programs [3, 4]. The overall test program and results are described. Test and fractographic results are evaluated; conclusions and recommendations are presented.

### 2.2  TEST PROGRAM

A two-phase test program was conducted. Dog-bone specimens were fatigue tested to failure under spectrum loading. Fractographic and strain survey results were acquired. Details of the test program, test and fractographic results are given in Volume III [2].

The Phase I test matrix is described in Table 1 and specimen details are shown in Fig. 1. Data acquired under Phase I was used to (1) evaluate/verify statistical scaling method for multi-hole dog-bone specimens and (2) investigate the initial fatigue quality and crack growth behavior of countersunk fastener holes.

The Phase 2 test matrix is described in Table 2. Specimen details are shown in Figs. 2 and 3. The purpose of these tests was to (1) acquire data for verifying the durability analysis extension for large through-the-thickness cracks associated with fuel leaks and ligament breakage, and (2) conduct a strain survey to verify the present bolt load transfer for a double-reversed dog-bone type specimen.

Table 1. Phase 1 Test Matrix.

| SPECIMEN | MATERIAL | TEST SERIES | NO. HOLES PER SPECIMEN | % LOAD TRANSFER | LOAD SPECTRA | MAX. STRESS LEVEL (KSI) | FASTENER I.D. | NO. SPECIMEN |
|---|---|---|---|---|---|---|---|---|
| | 7475-T7351 | I(a) | 3 | 0 | F-16 400HR | 34 | MS90353-08(1/4) | 15 |
| | | I(b) | | | B-1 BOMBER | 36 | | 16 |

Note: All tests performed at room temperature in lab air
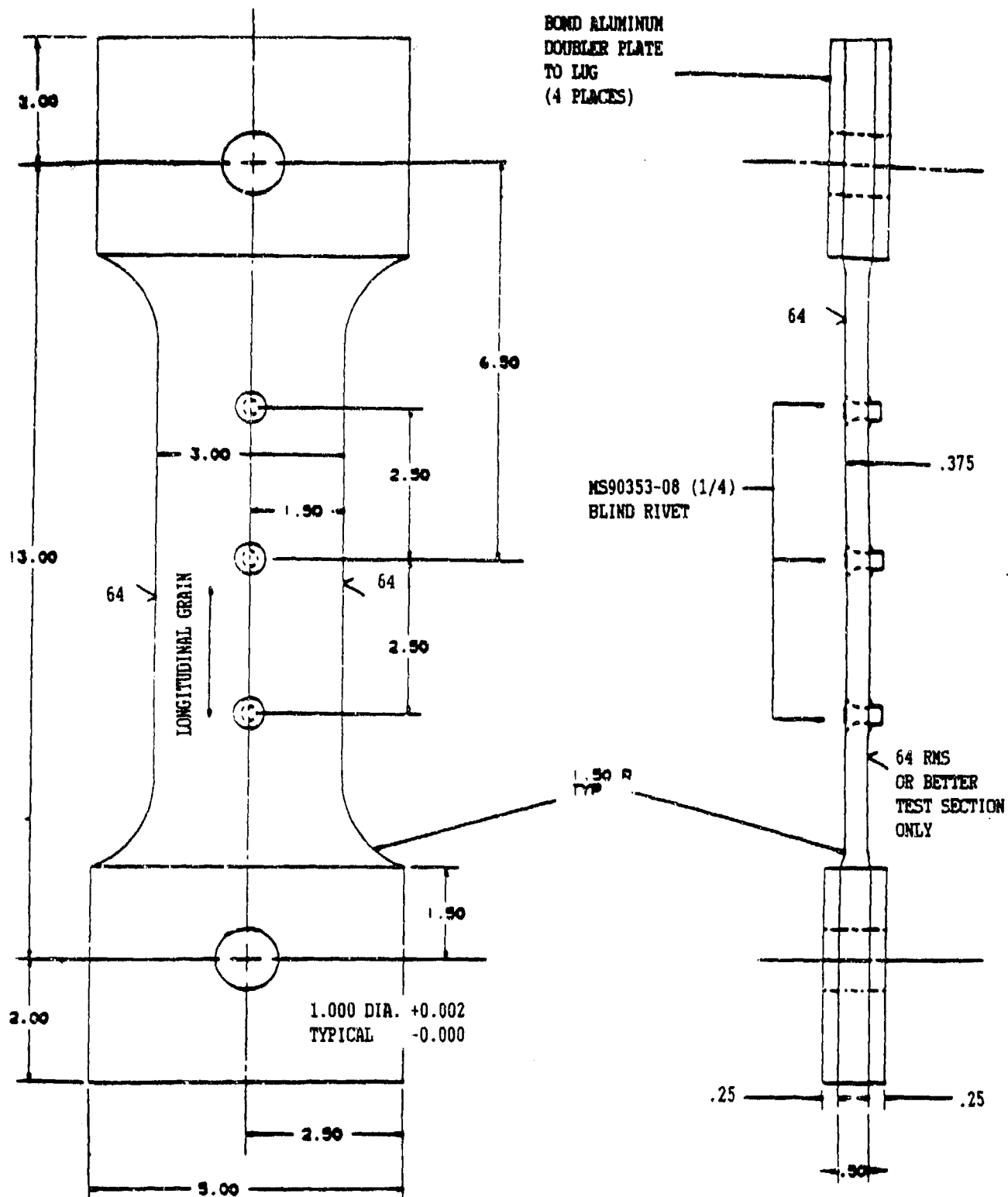
3

NOTES: 1. MATERIAL: 7475-T7351 Aluminum Plate (1/2" stock)
2. Match drill holes using Modified Winslow Spacematic (no deburring)
3. Drill and install MS90353-08 Rivets per M198
4. All dimensions in inches

**Figure 1.** <u>Design Details for WFI Data Set Specimens.</u>

Table 2. Phase 2 Test Matrix.

| Specimen | Material | Test Series | No. Holes per Specimen | Load Transfer | Load Spectra | Max Stress Level (ksi) | Fastener Type | Dia (in) | ID | No. Specimens Tested |
|---|---|---|---|---|---|---|---|---|---|---|
| (Fig 2) | 7475-T7351 Al | IV(a) | 1 | 0 | F-16 400-Hr | 34 | PH | 1/4 | NAS6204 | 9 |
|  |  | IV(b) |  |  | B-1 Bomber | 34 |  |  |  | 8 |
|  |  | IV(c) |  |  | F-16 C/D | 34 |  |  |  | 5 |
|  |  |  |  |  |  | 40.8 |  |  |  | 8 |
|  |  | IV(h) |  |  | F-16 400-Hr | 34 | Open Hole (1/4" Dia.) |  |  | 15 |
| (Fig 3) |  | IV(d) | 4 | 15% | F-16 400-Hr | 34 | CSK | 1/4 | MS90353-08 | 15 |
|  |  | IV(e) |  |  | F-16 400-Hr | 40.8 |  |  |  |  |
|  |  | IV(f) |  |  | B-1 Bomber | 34 |  |  |  |  |
|  |  | IV(g) |  |  | B-1 Bomber | 40.8 |  |  |  |  |
|  |  | IV(i) |  |  | Strain Survey | — |  |  |  | 1 |

Note: All tests performed at room temperature in lab air
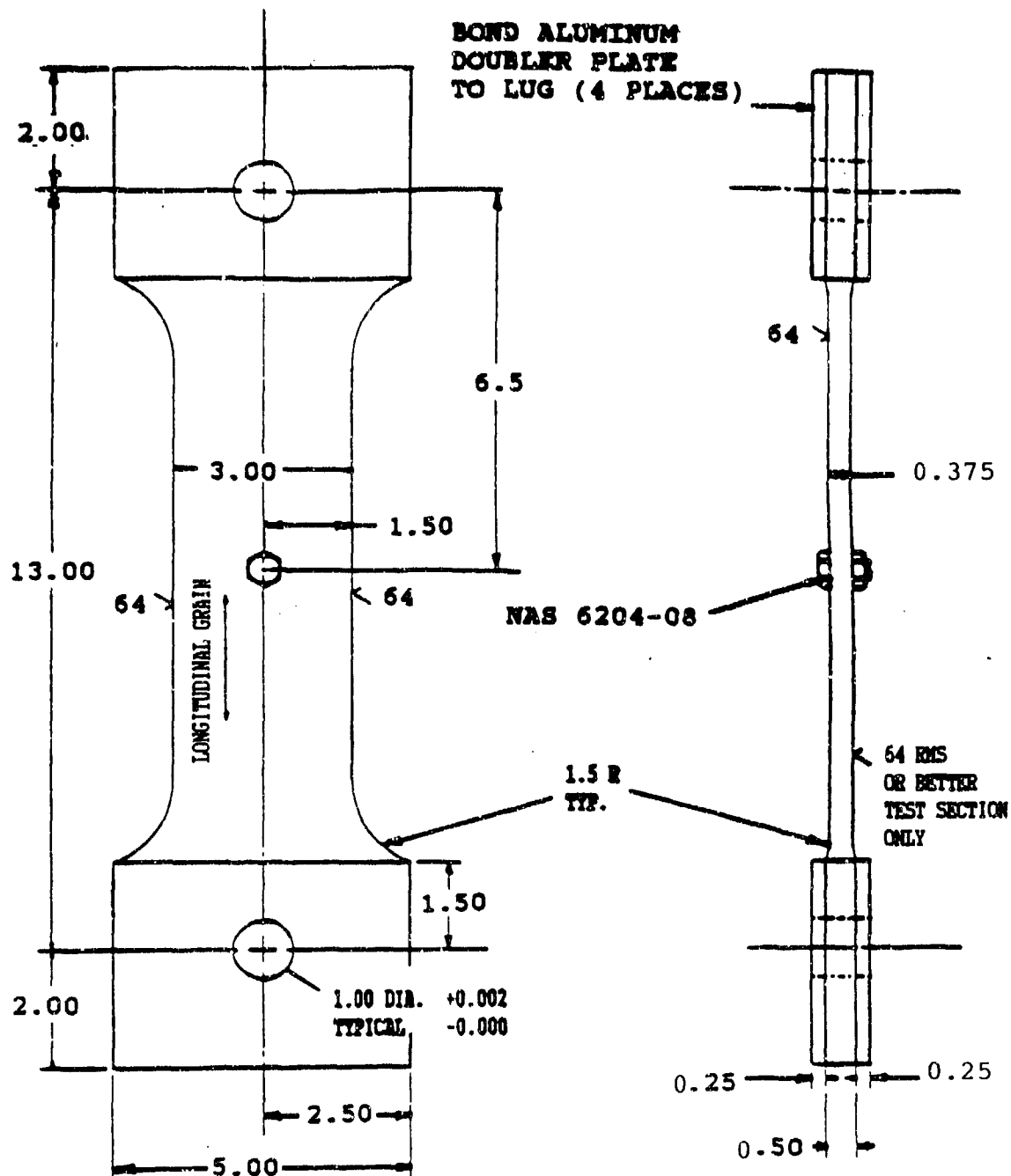
5

NOTES: 1. MATERIAL: 7475-T7351 Aluminum Plate (1/2" stock)
2. Match drill holes using Modified Winslow Spacematic (no deburring)
3. Drill and install NAS 6204-08 Bolt per M198
4. All dimensions in inches

Figure 2. **Dog-Bone Specimen with Single Hole.**
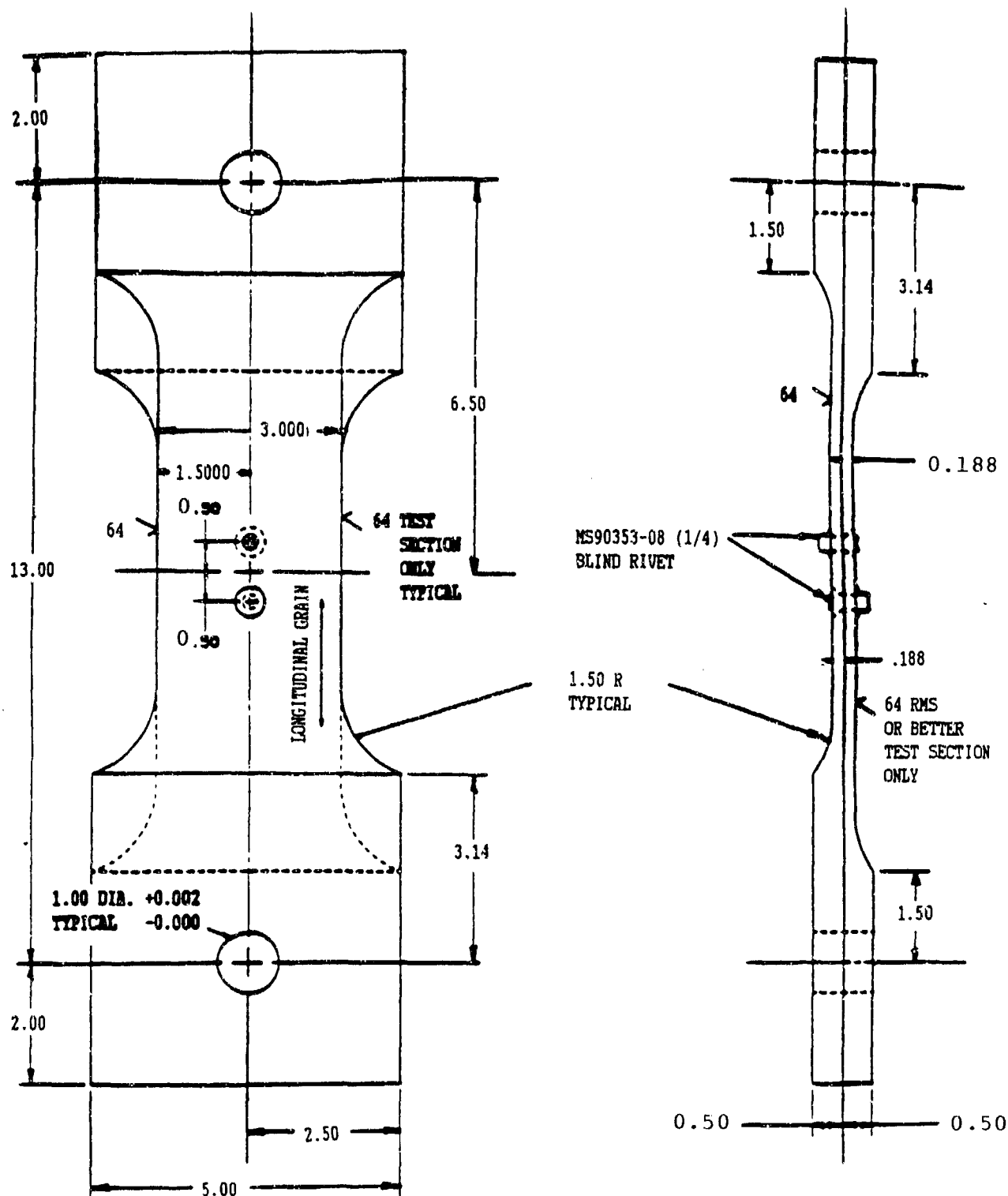
NOTES: 1. MATERIAL: 7475-T7351 Aluminum Plate (1/2" stock)
2. Match drill holes using Modified Winslow Spacematic (no deburring)
3. Drill and install MS90353-08 Rivets per M198
4. All dimensions in inches

Figure 3. **Double-Reversed Dog-Bone Specimen (15% Load Transfer).**

7

Specimen details are shown in Figs. 4 through 6 for those specimens used in the "Fastener Hole Quality" [2] and "Durability Methods Development" [4] programs. Applicable fractographic results for these specimens are referred to in this Volume (II).

## 2.3 FRACTOGRAPHIC DATA SCREENING

Fractographic data should be screened before using the data for any durability analysis purpose. Screening is essential to determine the uniformity, quality and behavior of the fractographic data. Software has been developed for surveying and plotting the fractographic data for a given data set. The software is briefly described in Appendix A and details are given in Volume V [5].

A comprehensive fractographic data screening investigation is documented in Appendix B. Each data set from this program was surveyed and the fractographic data (i.e., a(t) versus t) was plotted. Refer to Appendix B for details.

## 2.4 CRACK INITIATION ORIGINS AND TRENDS

Crack initiation origins and trends were investigated for both straight-bore and countersunk fastener holes. Results from this program were also compared with those from two other programs [3,4].

The following crack initiation origins were observed.

1. Some fatigue cracks originated in the bore of the fastener hole for straight-bore holes. Multiple origins and crack branching in the bore of the hole were observed for both fighter and bomber load spectra and for specimens with or without a fastener in the hole. For example, specimen for

Figure 4. No-Load Transfer Specimen Geometry.

9
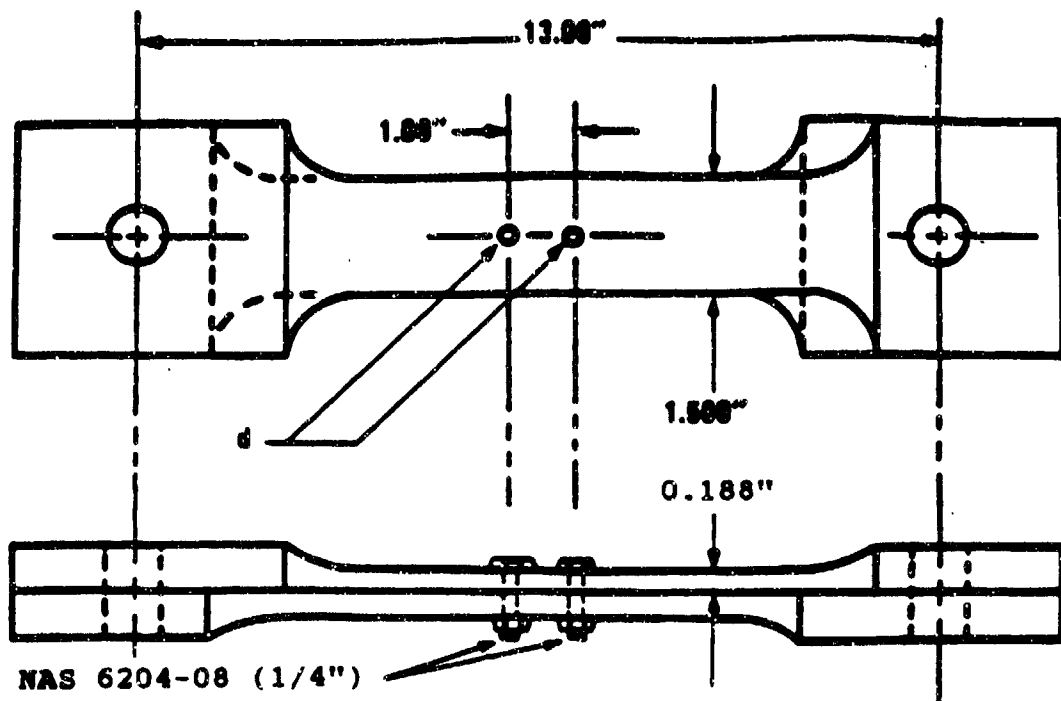
**Figure 5.** <u>Double-Reversed Dog-Bone Specimen Design with Straight Shank Bolts.</u>
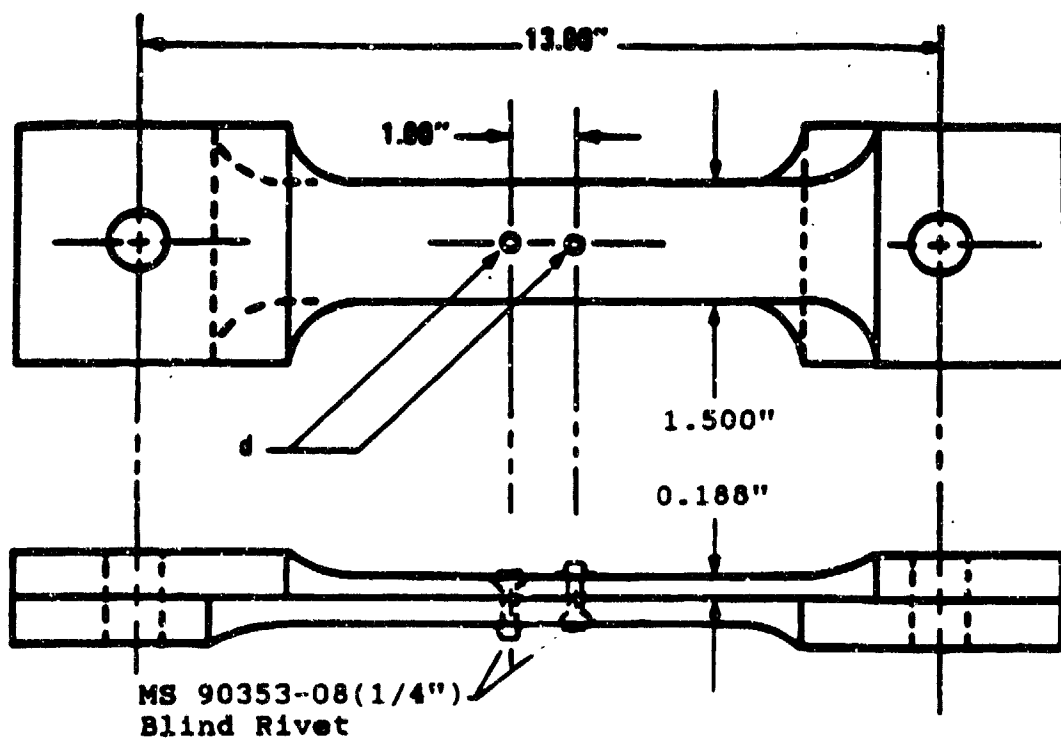


**Figure 6.** <u>Double-Reversed Dog-Bone Specimen Design with Blind Countersunk Rivets.</u>

10

the WWPFO data sets contained a single straight-bore hole without a fastener installed. All data sets with a straight-bore fastener hole were a "no load transfer" type (i.e., bolt passive).

2.   Most fatigue cracks originated in the bore of the countersunk fastener holes for the WFI and WBI data sets (both "no load transfer" type specimen). A few fatigue cracks also originated on the surface of the countersink.

3.   For data sets with countersunk fastener holes with bolt load transfer, most fatigue cracks originated at the corner of the fastener hole at the interface. Some cracks originated on the surface of the countersink. Also, in one or two cases fatigue cracks originated on the faying surface instead of the fastener hole.

The fatigue crack initiation origins and trends observed for this program for both straight bore and countersunk fastener holes are very comparable with those for the "Fastener Hole Quality" program [3] and the prototype "Durability Methods Development" program [4].

## 2.5   STRAIN SURVEY

A strain survey was performed in Phase 2 on a double reversed dog-bone specimen like the one shown in Fig. 3. The purpose of the strain survey was to estimate the actual amount of bolt load transfer, as a function of the applied load level, for this type of specimen. Details of the strain survey are given in Appendix G.

The double-reversed dog bone specimen shown in Fig. 3 is a "15% bolt load transfer design." If the fasteners perfectly fit the holes, the specimen will theoretically transfer 15% of the applied load to specimen through the bolts. The

11

actual amount of bolt load transfer for this type specimen varies depending on the fastener type and fit.

The percent bolt load transfer is an important consideration for durability analysis for (1) tuning or curve fitting the analytical crack growth program [e.g., 1] to the fractographic data base that is used to define IFQ or the EIFSD parameters and (2) determining the service crack growth master curve (SCGMC) for desired durability analysis conditions.

## 2.6 FRACTOGRAPHIC DATA APPLICATIONS

The fractographic data acquired under this program are used extensively in this Volume (II) to (1) conduct initial fatigue quality studies for fastener holes, (2) evaluate/verify the statistical scaling method developed in Volume I [1], (3) evaluate the sensitivity of crack growth rate parameters $Q$ and $\sigma_Z$ with respect to the fractographic crack size range used, (4) study mean EIFSs for different data sets, (5) investigate the initial flaw size for different EIFSD functions and crack exceedance probabilities and (6) evaluate/compare time-to-crack initiation (TTCI) and time-to-failure (TTF) statistics and trends for narrow (W = 1.5") and wide (W = 3.0") specimen data sets.

Most of the investigation mentioned above are documented in other sections of this Volume (II), such as Sections III and IV and Appendices B, C and E-J.

TTCIs (mean, high and low extremes) for $a_0$ = .05" are compared in Tables 3-5 for various data sets. The mean TTCI is denoted by an open or solid circle and the extremes by tic marks. An open circle is used to denote data sets from either the "Fastener Hole Quality" program [3] or the "Durability Methods Development" program [4].

12

**Table 3.** Comparison of TTCIs ($a_0 = 0.05''$) for Narrow and Wide Specimen Data Sets (Straight Bore Holes with NAS 6204-08 Bolt).



| DATA SET | $\sigma$ (ksi) | WIDTH (in.) | z LT | TTCI ($a_0 = 0.05''$) |
|---|---|---|---|---|
| WPF (N=33) | 34 | 1.5 | 0 | |
| WWPF (N=13) | 34 | 3.0 | 0 | |
| WWPFO (N=14) | 34 | 3.0 | 0 | (open hole w/o bolt) |
| WPB (N=32) | 34 | 1.5 | 0 | |
| WWPB (N=12) | 34 | 3.0 | 0 | |
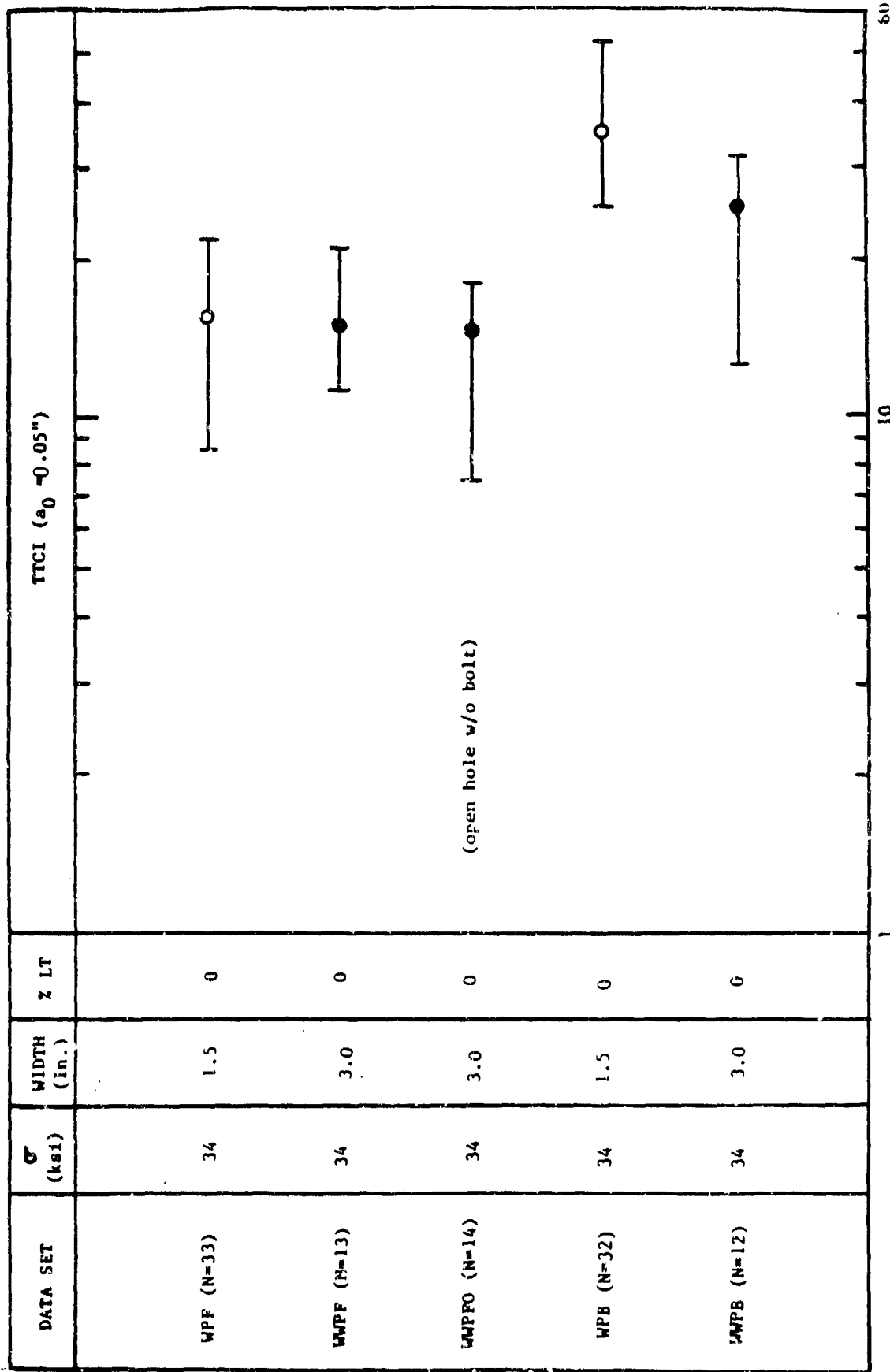
Table 4. Comparison of TTCIs ($a_0 = 0.05''$) for Narrow and Wide Specimen Data Sets (Countersunk Holes with MS 90353-08 Rivets).



| DATA SET | $\sigma$ (ksi) | WIDTH (in.) | % LT |
|---|---|---|---|
| AFXLR4 (N=10) | 32 | 1.5 | 15 |
| AFXMR4 (N=9) | 34 | 1.5 | 15 |
| AFXHR4 (N=10) | 38 | 1.5 | 15 |
| WAFXMR4 (N=14) | 34 | 3.0 | 15 |
| WAFXHR4 (N=13) | 40.8 | 3.0 | 15 |

TTCI ($a_0 = 0.05''$)

14
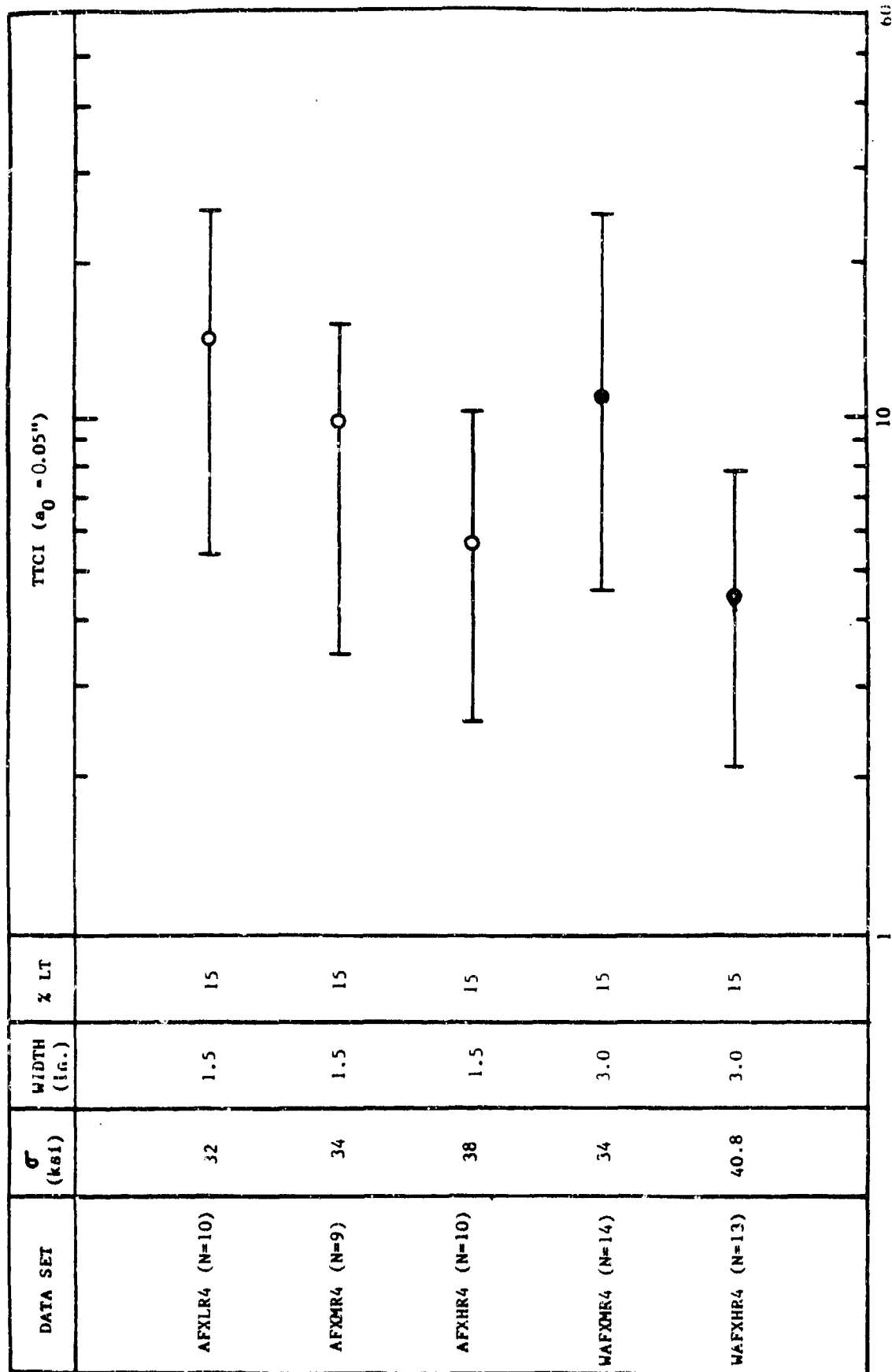
# Table 5. Comparison of TTCIs ($a_0 = 0.05''$) for Wide Specimen Data Sets.



TTCI ($a_0 = 0.05''$)

| DATA SET | $\sigma$ (ksi) | WIDTH (In.) | % LT |
|---|---|---|---|
| WWPCL (N=4) | 34 | 3.0 | 0 |
| WWPCH (N=6) | 40.8 | 3.0 | 0 |
| WFI (N=14) | 34 | 3.0 | 0 |
| WBI (N=12) | 36 | 3.0 | 0 |
| WXWTB (N=15) | 34 | 3.0 | 15 |
| WABXHR4 (N=15) | 40.8 | 3.0 | 15 |

15
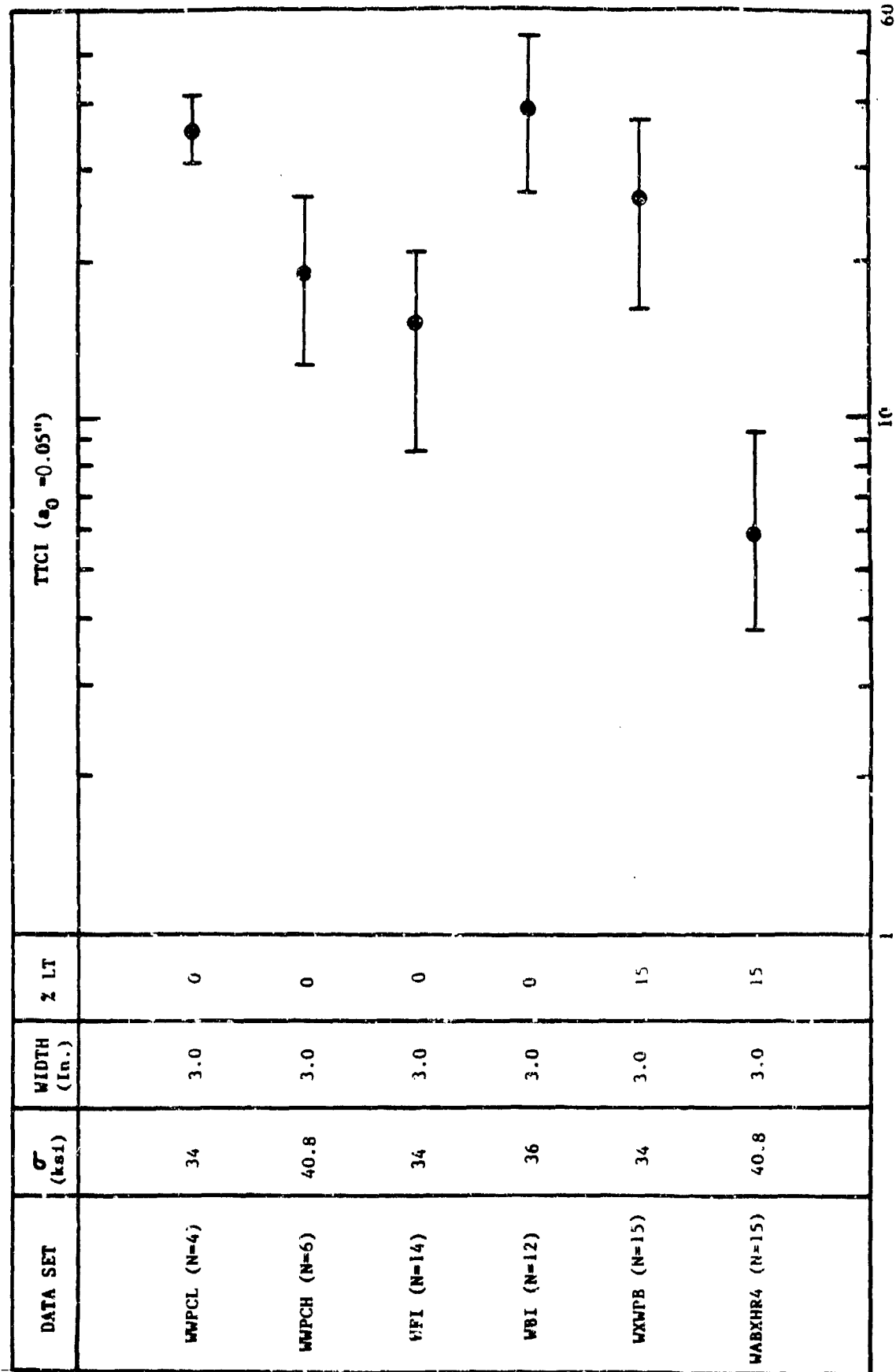
In Table 3, the mean and extreme TTCI values for narrow and wide specimen data sets are compared for the fighter and bomber load spectra. For example, the results for the narrow specimen data set WPF are compared with the wide specimen data sets WWPF and WWPFO. The specimen details for data sets WWPF and WWPFO are identical except no bolt is installed in the fastener hole for the WWPFO data set. In this case the mean and extreme TTCIs for the narrow and wide specimen data sets are the same order of magnitude.

TTCIs for the WPB data set (bomber load spectrum) are compared with those for the WWPB data in Table 3. In this case, the mean and extreme TTCIs, for some reason, do not have the same degree of agreement as those for the fighter data set.

TTCI results for selected countersunk data sets are shown in Table 4. The specimens and test conditions for data sets AFXMR4 and WAFXMR4 are identical except the latter is 3.0" wide and the former is 1.5" wide. In this case, the mean TTCIs and extremes compare reasonably well. This suggests that specimen width doesn't have a significant affect on the TTCIs for a relatively small referenced crack size (i.e., $a_0 = 0.05$"). Since other data sets do not have comparable stress levels, the results cannot be compared directly.

The TTCI mean and extreme values are shown in Table 5 for six other fractographic data sets acquired under this program. Data sets WWPCL and WWPCH reflect straight-bore fastener holes and the other data sets reflect countersunk fastener holes.

## 2.7 CONCLUSIONS, RECOMMENDATIONS AND GUIDELINES

The following observations, conclusions and recommendations are based on the extensive evaluations and experience with the test and fractographic results of this program and two other programs [3,4].

1. Test specimens for acquiring IFQ data should be fatigue tested to failure. "Mixing and Matching" fractographic results for both failures and runouts (or survivors) may lead to one of the following potential problems. The fractographic data (i.e., a(t) versus t) for each test specimen may not cover the desired AL-AU crack size range. Hence, fractographic results may have to be "extrapolated" to a given crack size and/or service time.

2. Fractographic data should be surveyed and censored before using the data for any durability analysis purpose. Data screening is needed to determine the quality and character of the data and to reject suspicious data. Questionable fractographic data should be censored from the data set.

3. Software is available for an IBM or IBM-compatible PC for plotting fractographic results for any data set [5]. This software is useful for studying the behavior of fractographic data for a selected AL-AU range and for identifying fatigue cracks with abnormal behavior.

4. The fractographic data sparsity problem needs to be investigated further. For example, fractographic data may not be available, for one reason or another, in the desired AL-AU crack size range. There are three possibilities regarding the fractographic data: (1) it covers the selected AL-AU range completely (i.e., $a(t) \leq AL$ and $a(t) > AU$), (2) it has some data in the AL-AU range, and (3) it has no data in the

AL-AU range. If the (a(t), t) fractographic data does not cover the AL-AU range, then data may have to be extrapolated for the durability analysis.

5. When fractographic data is extrapolated, don't extrapolate too far beyond the limits of the actual data. Two problems with extrapolations are (1) extrapolated values may be meaningless if they are far removed from the limits of the actual size, and (2) there's no way to separate the effects of fractographic data extrapolations and interpolations on the overall variability.

6. Considerable scatter was observed for some of the fractographic data sets. The following factors probably contributed to the scatter: (1) inherent variability of material properties, (2) specimen manufacturing variability, (3) testing procedures/environment, and (4) fractographic readers and readings.

7. Considerable care should be used to prepare the test specimens for fractographic evaluation because fracture surfaces can be easily damaged by saw marks when cracks are broken open.

8. The TTCI mean and extremes for the WPF (W = 1.5"), the WWPF (W = 3.0") and the WWPFO (W = 3.0") straight-bore data sets ($a_0$ = 0.05") were comparable. This was expected for relatively small fatigue cracks in fastener holes.

9. The fractographic data acquired under this program was very useful for evaluating/refining the durability analysis methods described in Volume I [1]. The data was particularly useful for (1) investigating/evaluating the IFQ of fastener holes, (2) evaluating/justifying the statistical scaling method developed, (3) estimating the % bolt load transfer for double-reversed dog-bone specimens, and (4) conducting numer-

ous durability related studies.

10.    Only straight shank and countersunk clearance fit fasteners in 7475-T7351 aluminum were investigated under this program.  The effect of interference fit fasteners and cold working on the IFQ of fastener holes needs to be investigated.  Whatever type fastener is used, however, the same general guidelines presented herein apply.

11.    The double-reversed dog-bone type specimens used in this program were "designed" for 15% bolt load transfer.  The actual amount of bolt load transfer varied depending upon the fastener type and fit.  From the strain survey we determined that the actual amount of % bolt load transfer was approximately 7% for the specimen used at 100% specimen load.  Only one reversed dog-bone specimen was used in the strain survey.  We would expect the actual amount of the % bolt load transfer to vary for each specimen - depending on the particular fastener type and fit for each specimen.  The % bolt load transfer for a given fractographic data set can be estimated in one of the following two ways:  (1) strain survey or (2) by tuning or curve fitting the analytical crack growth program to the EIFS master curve.

12.    In a few cases fatigue cracks originated on the faying surface instead of the bore of the hole.  Two possible reasons for this behavior are  (1) surface finish too rough, and (2) mating surface rubbing together at the faying surface.

# SECTION III

## DEMONSTRATION/EVALUATION OF INITIAL FATIGUE QUALITY

### 3.1  INTRODUCTION

The purpose of this section is to demonstrate and evaluate the refined methods, described in Volume I [1], for determining the initial fatigue quality of countersunk and straight-bore fastener holes. Initial fatigue quality (IFQ) characterizes the initially manufactured state of a structural detail or details (e.g., fastener holes, lugs, cutouts, fillets, etc.) with respect to initial flaws in a part, component, or airframe prior to service. Actual initial flaws in a fastener hole are typically random scratches, burrs, microscopic imperfections, etc. Initial flaws are represented by the equivalent initial flaw size (EIFS) in this program. An EIFS is an artificial crack size which results in an actual crack size at an actual point in time when the EIFS is grown forward. It is determined by back-extrapolating fractographic results using a suitable empirical crack growth rate model. The IFQ, represented by an equivalent initial flaw size distribution (EIFSD), is the "cornerstone" of the durability analysis method. Once the IFQ has been determined and justified for durability analysis, it can be used to make predictions for the probability of crack exceedance at any service time, $\tau$ , and the cumulative distribution of service time to reach any crack size, $x_1$.

In this section, we will determine the EIFSD parameters for the Weibull compatible distribution for countersunk and straight bore fastener holes (with clearance fit and no cold working) and then justify the resulting EIFSD for durability analysis. For this purpose, we will use available fractographic results for 7475-T7351 aluminum [2-4] and available durability software [5]. This section concerns IFQ and fatigue

cracking in the small crack size region (e.g., AL - AU = 0.01"
- 0.05"). However, the IFQ results of this section will be
used later in Section III to demonstrate and evaluate the dur-
ability analysis extension for the large crack size region
(e.g., AL - AU = 0.05" - 1").

The general procedure for estimating the EIFSD parameters
for the Weibull compatible distribution using fractographic re-
sults is presented in Volume I [1]. The procedure, essential
equations, and details are summarized in this section. The
same approach for determining IFQ applies to both countersunk
and straight-bore fastener holes.

### 3.2 METHOD FOR DETERMINING INITIAL FATIGUE QUALITY

The general procedure for defining IFQ is summarized below
and key elements are described in Figs. 7-9.

1. Select a suitable EIFSD function for representing the
initial fatigue quality (e.g., Weibull compatible or Lognormal,
or lognormal/compatible). The Weibull compatible distribution
function proposed by Yang and Manning [6,7] has been found to
be reasonable for representing the EIFS cumulative distribution
[6-16].

$$F_{a(0)}(x) = \exp\left\{-\left[\frac{\ln(x_u/x)}{\phi}\right]^\alpha\right\} ; \quad 0 \le x \le x_u$$
$$= 1.0 \qquad\qquad\qquad ; \quad x > x_u \qquad (1)$$

in which $F_{a(0)}(x) = P[a(0) \le x]$, $a(0)$ = EIFS = crack size at time
$t = 0$, $x_u$ = EIFS upper bound limit, and $\alpha$ and $\phi$ are empirical
parameters.

2. Select fractographic data set(s) to be used to de-
termine the EIFSD. The data sets should be for the same mate-
rial, same type load spectrum (e.g., fighter, bomber, or trans-
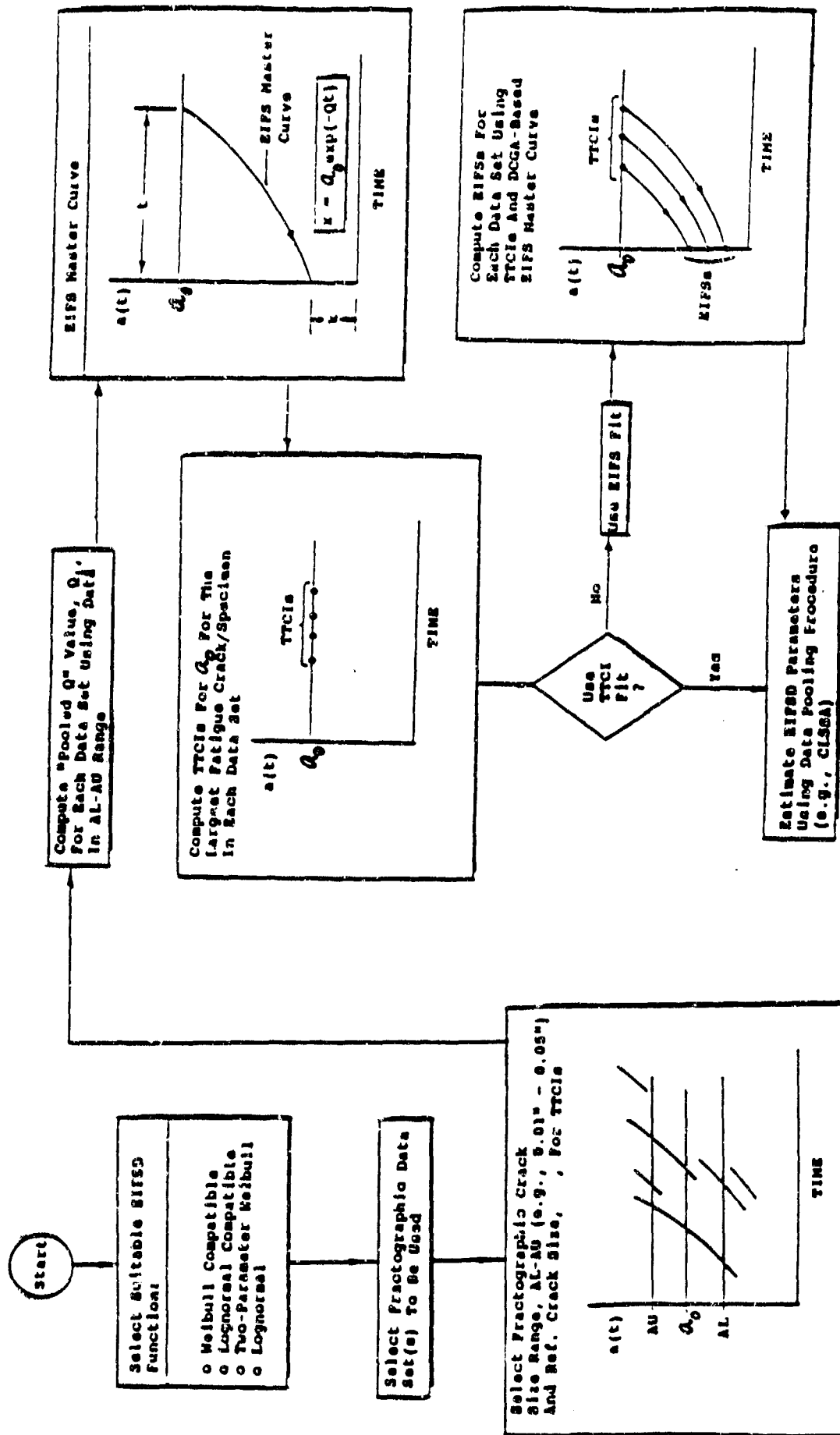
Figure 7. Initial Steps in Procedure Leading to Estimation of EIFSD Parameters.
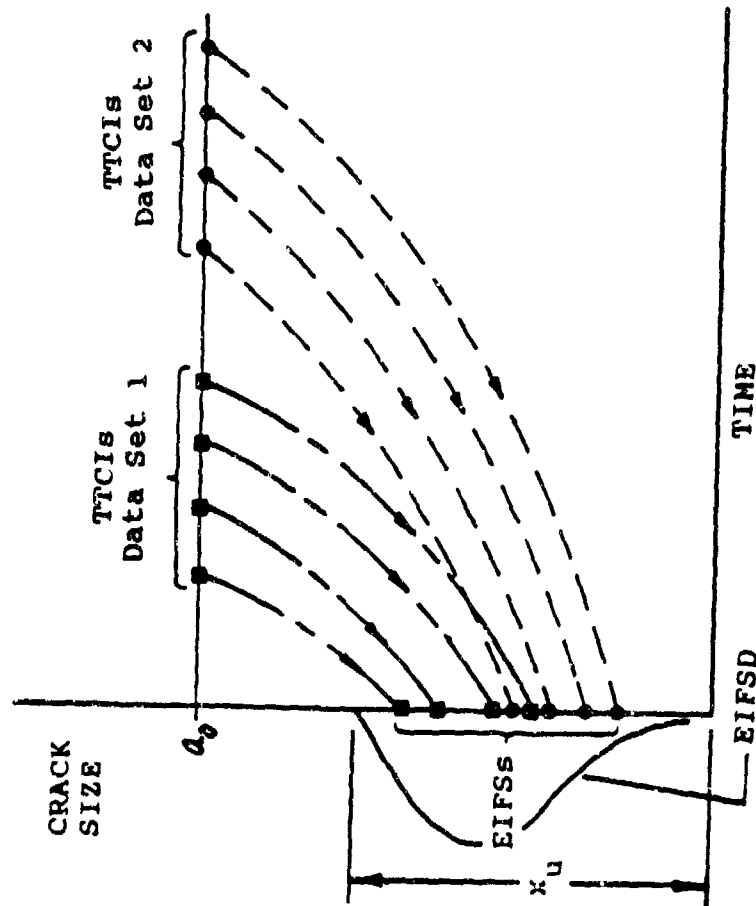
(a) Estimate EIFSD Parameters
Using EIFSs
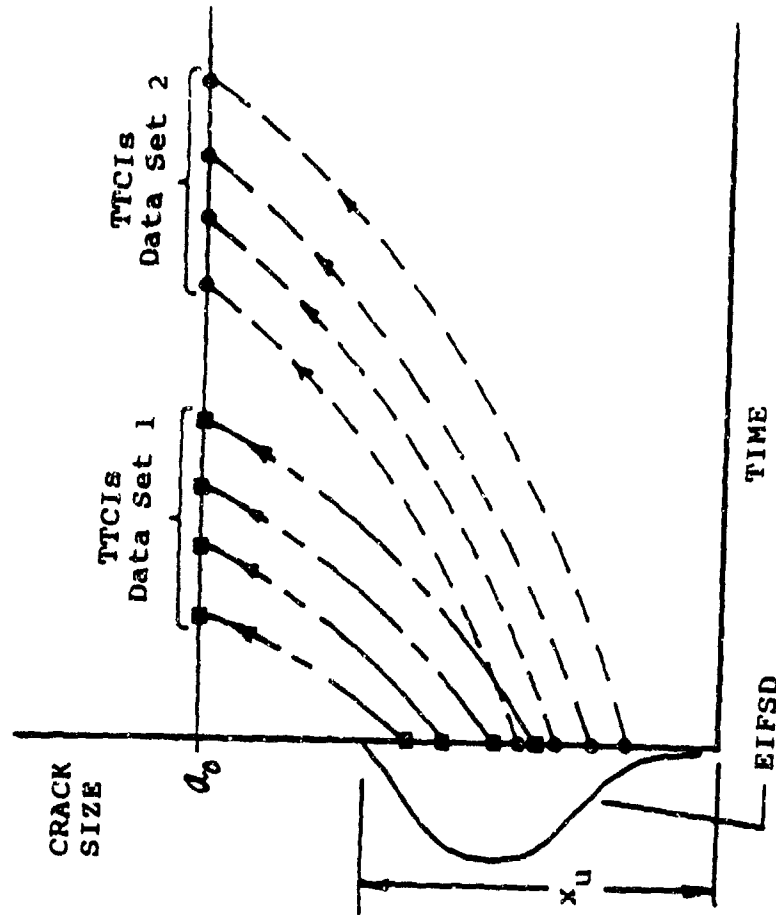
(b) Estimate EIFSD Parameters
Using TTCIs

Figure 8. Two Different Philosophies for Estimating EIFSD Parameters
Using Fractographic Data Pooling Procedures and DCGA.

23
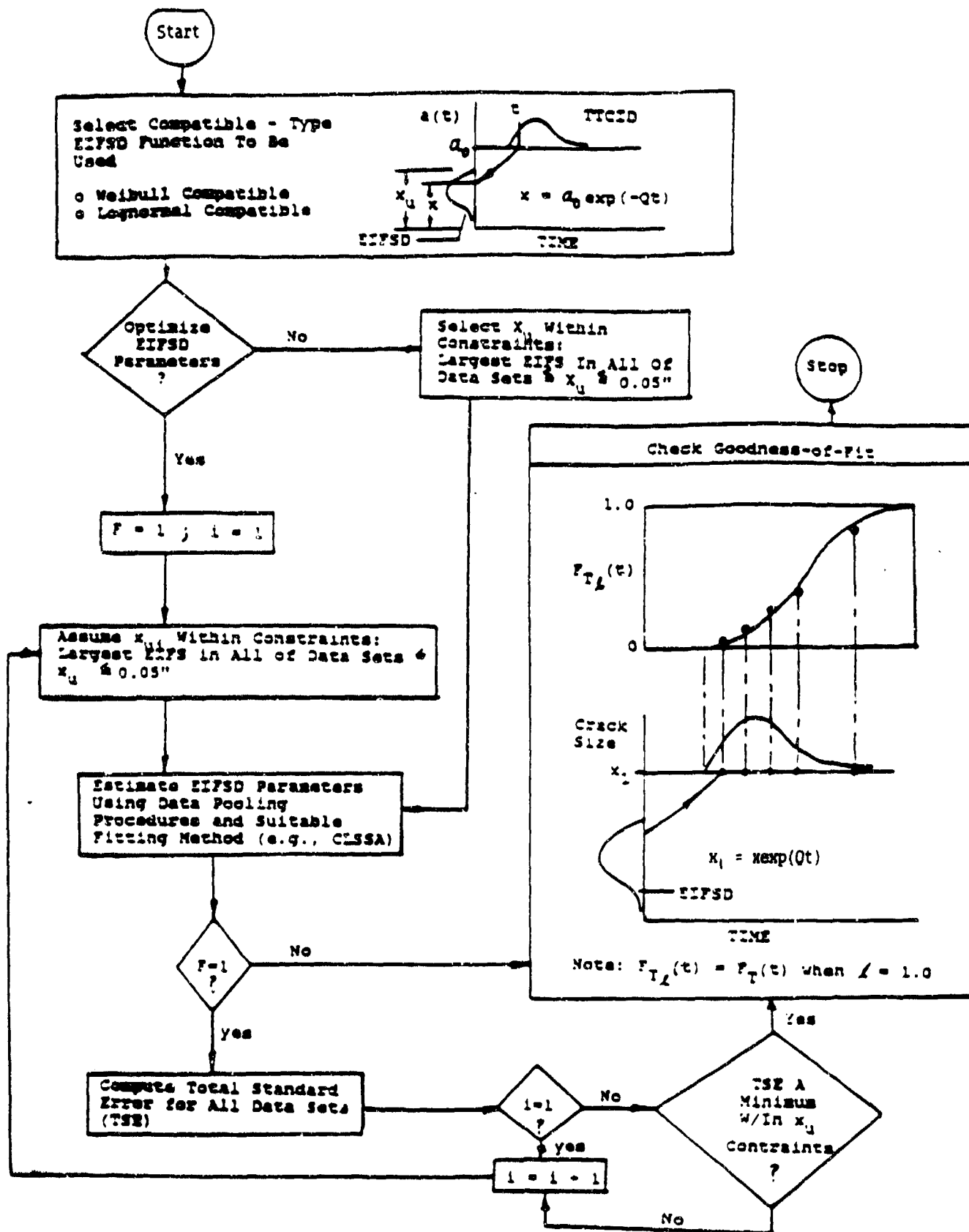
**Fi Figure 9.** General Procedure for Optimizing EIFSD Parameters and Checking Goodness-of-Fit for Compatible Type EIFSD Function.

24

port) and type fastener/hole/fit (e.g., straight-bore or coun-
tersunk). Screen and censor the data for any unusual abnormal-
ities.

3. Select fractographic crack size range, AL-AU. Frac-
tographic data in this range will be used to determine the
crack size-time relationship and deterministic crack growth
rate parameters. Also select a reference crack size, $a_0$, for
the TTCIs for each fractographic data set, see Fig. 7. Use the
largest fatigue crack per speciman in each data set.

4. Estimate the crack growth rate parameters Q in the
model suggested by Yang and Manning for the small crack size
region [6,7]

$$da(t)/dt = Qa(t) \tag{2}$$

in which $da(t)/dt$ = crack growth rate, $a(t)$ = crack size at
time, t, and Q is an empirical crack growth rate parameter.

This model, Eq. 2, has been found to be very reasonable
for durability analysis [8-11,14,16]. Integration of Eq. 2
leads to a relation between $a(0)$ or EIFS and the crack size
$a(t)$ at any service time t, i.e.,

$$EIFS = a(0) = a(t)\exp(-Qt) \tag{3}$$

If $a_0$ is the reference crack size, say 0.03", and T is the time
to initiate the crack size $a_0$, i.e., $a(T) = a_0$, then the
deterministic relation between EIFS = $a(0)$ and TTCI = T, is
referred to as the "EIFS master curve." Such an EIFS master
curve is obtained from Eq. 3 by setting t = T and $a(T) = a_0$, as
follows

$$EIFS = a_0\exp(-QT) \tag{4}$$

Hence, for every TTCI = T in a given fractographic data set, there is a corresponding EIFS value and vice versa as shown in Eq. 4 (also, see Volume I [1]).

Q in Eqs. 2-3 is an empirical crack growth rate parameter, which can be used from a particular fractographic data set. This parameter is used to define EIFSs for a given fractographic data set using Eq. 4.

Suppose the ith fractographic data set contains a total of m fatigue cracks, where each fatigue crack is denoted by $j = 1$, 2, ..., m. The jth fatigue crack has a total number of N pairs of fractographic data in the AL-AU range, denoted by $[a_j(t_k)$, $t_k]$, i.e., $a_j(t_k)$ = kth crack size for the jth fatigue crack at service time $t_k$ in the AL-AU range, where $k = 1, 2, \ldots, N$.

The crack growth rate parameter for a single fatigue crack, say the jth fatigue crack, denoted by $Q_j$, is estimated from fractographic data of the jth fatigue crack in the AL-AU range using Eq. 3 and the least squares fit procedure as follows

$$Q_j = \frac{N \sum_{k=1}^{N} X_k Y_k - \sum_{k=1}^{N} X_k \sum_{k=1}^{N} Y_k}{N \sum_{k=1}^{N} X_k^2 - \left(\sum_{k=1}^{N} X_k\right)^2} \tag{5}$$

in which $X_k = t_k$ and $Y_k = \ln a_j(t_k)$.

$Q_j$ given in Eqs. 3-5 is the crack growth rate parameter for the jth crack and it is obtained using the fractographic data of the jth crack. Let $Q_i$ be the crack growth rate parameter for the ith data set consisting of m cracks. Then, $Q_i$ is referred to as the "pooled Q" value for the ith data set. It is ob-

26

tained using all the fractographic data in the ith data set, i.e., all fractographic data for m cracks in the AL-AU range, and the least squares fit procedure. $Q_i$ or the "pooled Q" value for the ith data set can be obtained as follows

$$Q_i = exp\left[\frac{1}{m} \sum_{j=1}^{m} \ln Q_j\right] \qquad (6)$$

where, $Q_j$ = crack growth rate parameter Q for the jth fatigue crack and m = total number of fatigue cracks in the ith data set (i.e., j = 1, 2, ..., m).

5.     Determine TTCI values for each data set(s) for the chosen reference crack size, $a_0$, by either interpolation or extrapolation of fractographic results. Refer to Fig. 7.

6.     Use (i) the data pooling procedure described in Volume I [1], (ii) TTCI results from Step 5, and (iii) the combined least square sums approach (CLSSA), to estimate and optimize the Weibull compatible EIFSD parameters (i.e., $\alpha$ and $\phi$ for a  given $x_u$) given in Eq. 1. Other EIFSD functions could also be used if appropriate (e.g., lognormal compatible, lognormal, two-parameter Weibull, etc.). The general procedure for optimizing the EIFSD parameters is described in Fig. 9 and Volume I [1].

NOTE:  The EIFSD parameters can  be  estimated  using either  a "TTCI fit" or a "EIFS fit." Either fitting method will yield the same  EIFSD  parameter  values. The formulation for the "EIFS fit" is given elsewhere [1,21].   In  the durability analysis design handbook [21] the "EIFS fit" is recommended because  the  EIFS statistics (mean  and  standard deviation) provide a basis for comparing and  cataloging  initial  fatigue quality  results  from various sources; whereas, TTCI statistics (mean  and  standard  deviation)  do  not

27

provide such a basis. The "TTCI fit" formulation, reflected in the following, is considered herein as a part of the overall evaluation of methods for estimating EIFSD parameter values.

The Weibull compatible EIFSD parameters $\alpha$ and $\phi$ in Eq. 1 can be determined for a given $x_u$ as follows. Let M = total number of fractographic data sets to be used for estimating the EIFSD parameters. For each fractographic data set there is a corresponding "TTCI" or "EIFS" data set. Therefore, M also applies to either TTCI or EIFS data sets. The ith TTCI data set (i.e., i = 1, 2, ..., M) contains a number of $N_i$ TTCIs based on the largest fatigue crack per specimen, where each TTCI is denoted by j = 1, 2, ..., $N_i$. Further, let $Q_i$ = pooled crack growth rate parameter for the ith fractographic data set based on Eq. 6 and $\ell_i$ = scaling factor for the ith fractographic data set.

Then, $\alpha$ and $\phi$ for a given $x_u$ can be determined as follows:

$$\alpha = \frac{n \Sigma XY - (\Sigma X)(\Sigma Y)}{n \Sigma X^2 - (\Sigma X)^2} \tag{7}$$

$$\phi = exp\left\{\frac{\alpha n \Sigma X - \Sigma Y}{\alpha n}\right\} \tag{8}$$

The terms in Eqs. 7 and 8 are defined as follows:

$$X_{ij} = \ell n \left[\ell n (x_u/a_0) + Q_i t_{ij}\right] \tag{9}$$

$$Y_{ij} = \ell n \left\{-(1/\ell_i)\ell n \left[1 - \frac{j}{(N_i+1)}\right]\right\} \tag{10}$$

28

$$\Sigma X = \sum_{i=1}^{M} \sum_{j=1}^{N_i} X_{ij}$$

$$\Sigma X^2 = \sum_{i=1}^{M} \sum_{j=1}^{N_i} X_{ij}$$

$$\Sigma Y = \sum_{i=1}^{M} \sum_{j=1}^{N_i} Y_{ij}$$

$$\Sigma XY = \sum_{i=1}^{M} \sum_{j=1}^{N_i} X_{ij} Y_{ij}$$

$$n = \sum_{i=1}^{M} N_i$$

(11)

All notations in Eqs. 9 - 11 have been previously defined except the following. In Eq. 9, $t_{ij}$ = jth TTCI value for the ith TTCI data set (i.e., j = 1, 2, ..., $N_i$). In Eq. 10, the TTCIs for the ith data set are ranked in ascending order, i.e., j = 1, 2, ..., $N_i$. Similar expressions to those in Eqs. 9 and 10 have been developed for an "EIFS fit" [1, 21].

The expression for the total standard error is given in Eq. 12 [1],

$$TSE = \sqrt{ \frac{ \sum_{i=1}^{M} \sum_{j=1}^{N_i} \left\{ \left[ \frac{j}{(N_i + 1)} - 1 + exp\left( -l_i \left[ \frac{ln(z_u/A_u) + Q_i l_i}{\phi} \right]^{\alpha} \right) \right] \right\}^2 }{ \sum_{i=1}^{M} N_i } } \quad (12)$$

where all terms have been previously defined in Eqs. 6-11. Equation 12 is used in the optimization of EIFSD parameters.

For a given $x_u$ there is a corresponding $\alpha$, $\phi$ and TSE. Within the user's selected limits for minimum and maximum $x_u$ values, the TSE can be minimized with respect to $x_u$ using a trial and error procedure.

7.   Verify the goodness-of-fit of the resulting EIFSD us-

ing the fractographic data sets that have been used to estimate
the EIFSD parameters. For example, correlate theoretical pre-
dictions for (i) the probability of crack exceedance, $p(i, \mathcal{T})$,
at a given service time, $\mathcal{T}$, and (ii) the cumulative distribu-
tion of service time to reach any crack size $x_1$, $F_{T(x_i)}^{(\mathcal{T})}$ with
actual fractographic results for those data sets that have been
used to define the IFQ, see Fig. 10. Other fractographic data
sets (e.g., for different stress levels, load spectra, % load
bolt load transfer, etc.) that have not been used to estimate
the EIFSD parameters can also be used to justify the candidate
EIFSD for durability analysis.

Software is available for an IBM or IBM-compatible PC for
implementing the procedures described above, including a good-
ness-of-fit plotting capability. The software user's guide is
given in Volume V [5].

### 3.3 DEMONSTRATION FOR DOG-BONE SPECIMENS

The general procedure described in Section 3.2 is used to
demonstrate and evaluate the IFQ methods for countersunk and
straightbore fastener holes in 7475-T7351 aluminum (clearance-
fit fasteners without cold working) in the following.

### 3.3.1 Countersunk Fastener Hole Specimens

Three fractographic data sets from the "Durability Method
Development" program [4] will be used to determine the IFQ of
countersunk fastener holes. The three data sets, referred to
as "AFXLR4", "AFXMR4", and "AFXHR4", are described in Table 6.
Specimen geometry and design details for these data sets are
shown in Fig 6. The fractographic results, i.e., a(t) versus t
data, for each fatigue crack in each data set were screened for
abnormal behavior (see Figs. B.23-B.28). Only one fatigue
crack, i.e. crack number 8, was deleted from the AFXLR4 data
set, see Fig. 11. Fractographic data screening is an important

30
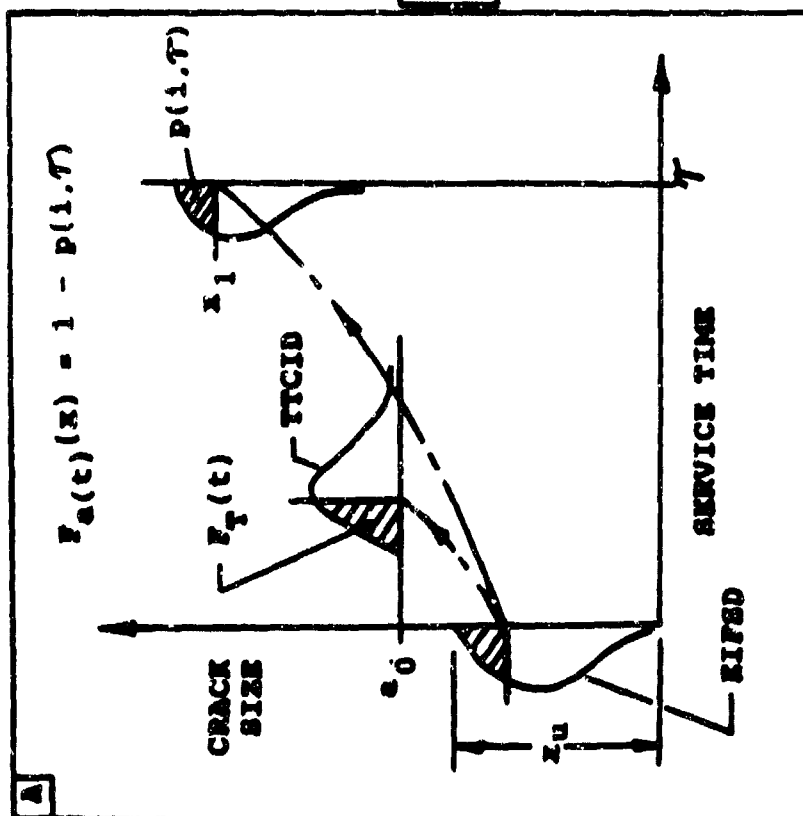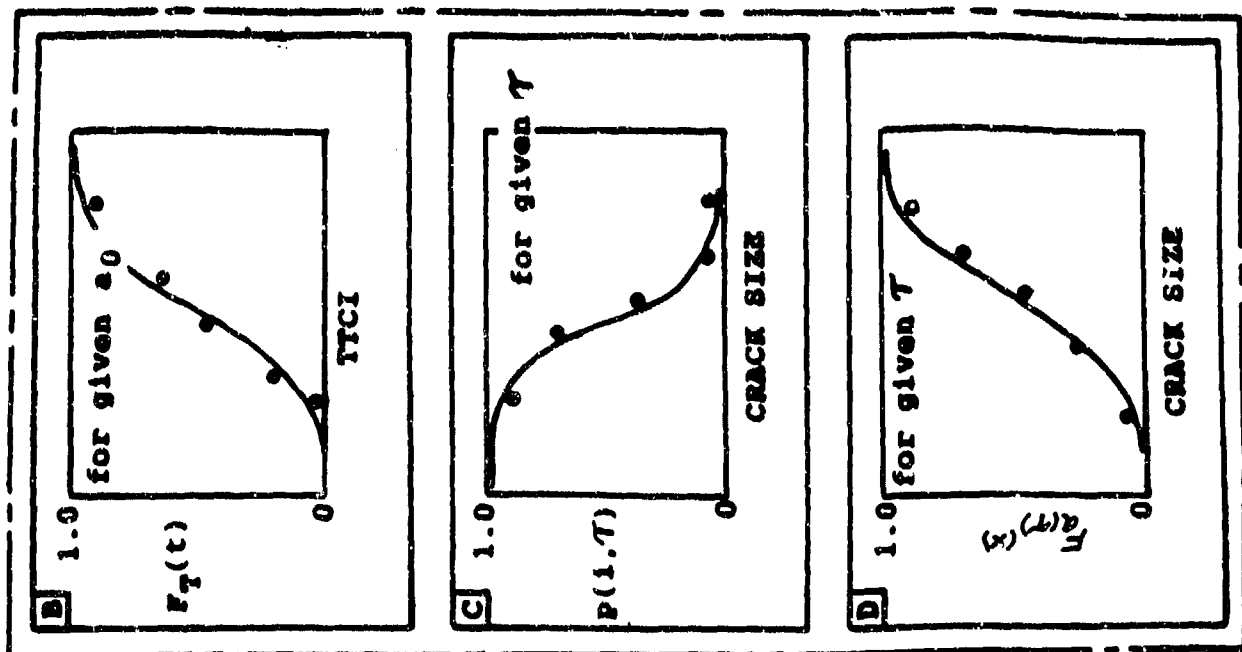
Figure 10. Elements for Justifying EIFSD and Goodness-of-fit Plots.

Table 6.    Description of Fractographic Data Sets Used to Determine
            the IFQ for Countersunk Fastener Holes

| Data Set | No. of Specimens Used (4) | (3) KSI | LT % | W (In) | t (In) | Fastener (2) | Load Spectrum | Ref. |
|---|---|---|---|---|---|---|---|---|
| AFXLR4 | 10/11 (5) | 32 | 15 | 1.5 | .1875 | MS 90353-08 (1/4D) | F-16 400 Hr | 4 |
| AFXHR4 | 9/9 | 34 | ↓ | ↓ | ↓ | ↓ | ↓ | |
| AFXHR4 | 10/10 | 38 | | | | | | |

NOTES:
(1)  Material:  7475-T7351 Aluminum
(2)  Blind pull-through rivet (countersunk head)
(3)  Gross section stress
(4)  XX/YY = No. of specimens used/total no. of specimen in data set
(5)  Deleted crack No. 8 from data set (ref. Fig. 11)
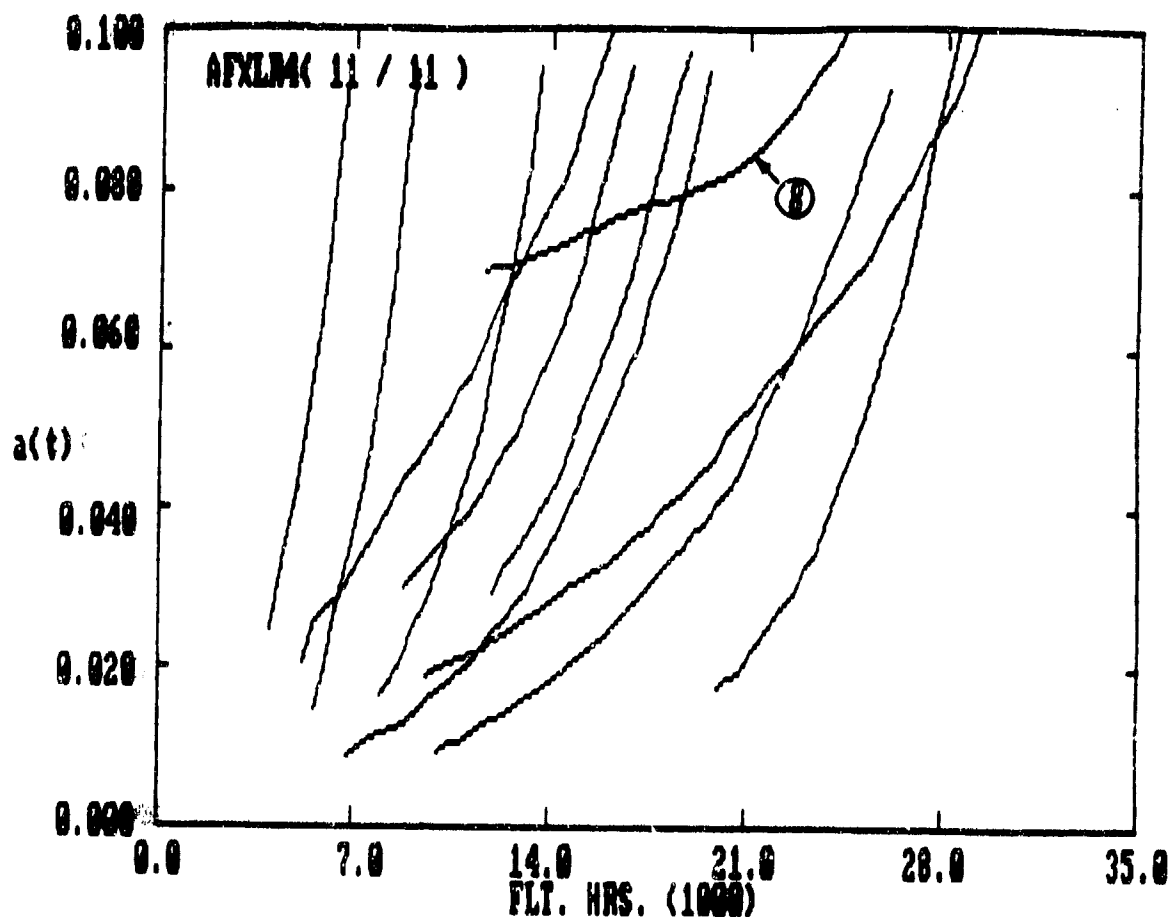


Figure 11.    Fractographic Data Survey for AFXLR4
              Data Set in the AL-AU = 0-.1" Crack
              Size Range.

consideration in determining IFQ.

The IFQ or EIFSD will be determined for each of the three data sets shown in Table 6 separately. Then, these three data sets will be pooled together as a "pooled data set" to increase the sample size. The IFQ will be determined for the pooled data set using the data pooling procedures described in Volume I [1]. Elements of this procedure for determining an EIFSD for the pooled data set are conceptually described in Fig. 12. Once the EIFSD has been determined, the candidate EIFSD must be justified for desired durability analysis applications. An EIFSD, based on one or more fractographic data sets, should be justified by showing that the given EIFSD can be grown forward to make reasonable predictions for one or more of the following: (1) cumulative distribution of TTCI, $F_T(t)$, at a given reference crack size $x_1$, (2) probability of crack exceedance, $p(i, \mathcal{T})$, at any given service time, $\mathcal{T}$, and (3) cumulative distribution of crack size, $F_{a(t)}(x)$, at a given service time, t. Elements for justifying an EIFSD for durability analysis are described in Fig. 10.

The IFQ analysis that follows is divided into three parts: (1) estimate the deterministic crack growth rate parameter, pooled Q (2) estimate the EIFSD parameters (i.e., $\alpha$ and $\phi$ for given $x_u$) for the Weibull compatible distribution function, and (3) justify the EIFSD for desired durability analyses. Details are provided in the following subsections.

3.3.1.1 <u>Estimation of Crack Growth Rate Parameters.</u> Pooled Q values for AFXLR4, AFXMR4, and AFXHR4 data sets obtained using Eq. 6, are summarized in Table 7. Q values were determined using the software documented in Volume V [5]. Example problems and computer output for Q are given in Volume V. The Q values shown in Table 7 will be used to estimate the EIFSD parameters.
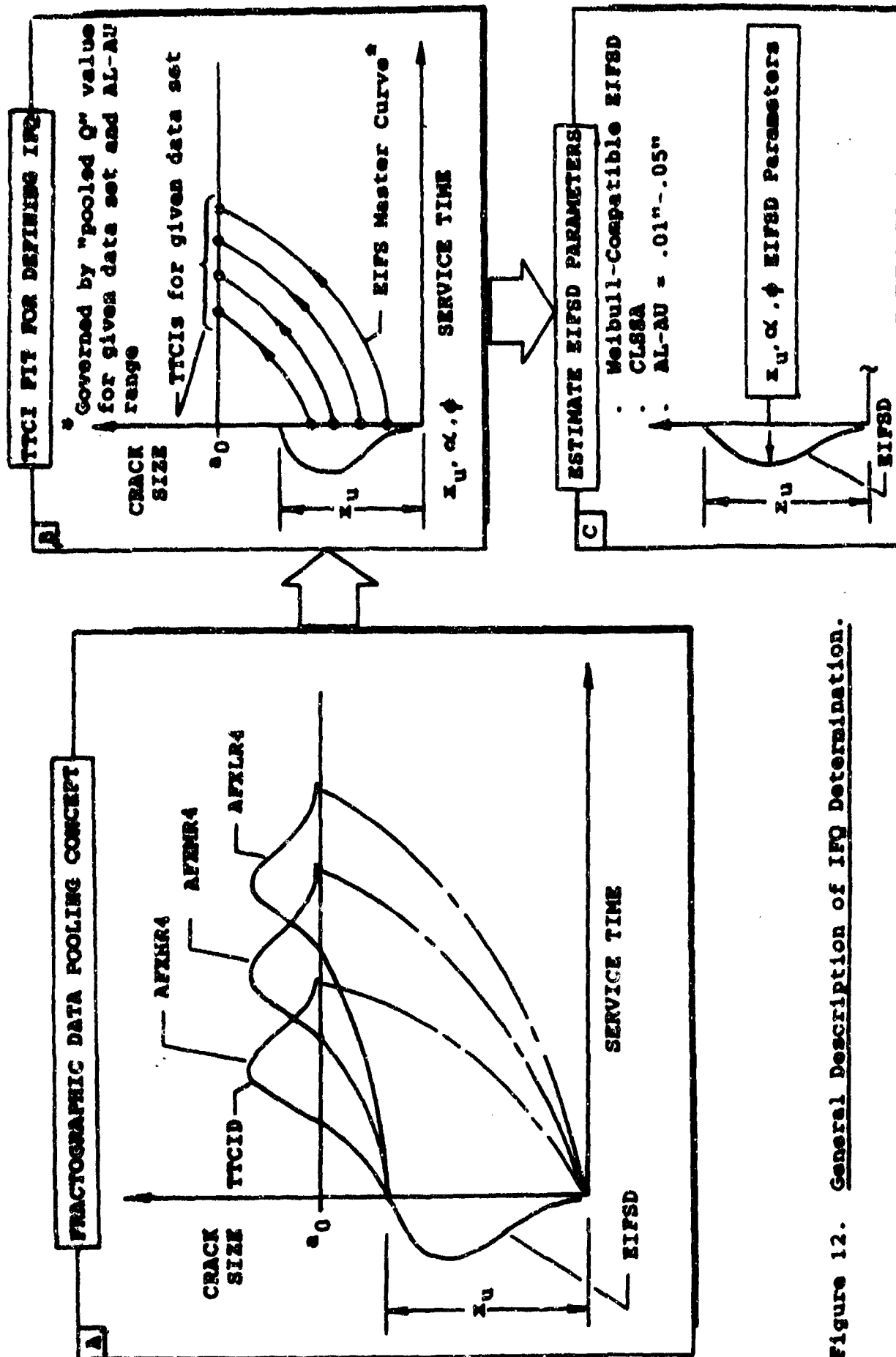
Figure 12. General Description of IFQ Determination.

**Table 7.** Summary of Pooled Q Values for Double-Reversed Dog-Bone Specimens (15% LT) with Countersunk Fastener Holes.

| Data Set | % LT | No. Cracks | (KSI) | W (IN.) | t (IN.) | AL-AU | Qx10⁴ (1/HR) | Load Spectrum |
|----------|------|------------|-------|---------|---------|-------|-------------|---------------|
| AFXLR4 | 15 | 10 | 32 | 1.5 | .1875 | .01"-.05" | 2.101 | F-16 400 HR |
| AFXMR4 | ↓ | 9 | 34 | ↓ | ↓ | ↓ | 2.514 | ↓ |
| AFXHR4 | ↓ | 10 | 38 | | | | 6.062 | |

3.3.1.2 <u>Estimation of EIFSD Parameters</u>. The EIFSD parameters (i.e., $\alpha$ and $\phi$) for the Weibull compatible distribution, Eq. 1, for a given $x_u$ will be estimated for individual fractographic data sets and for the pooled data sets. Essential features, conceptually described in Fig. 12, will be briefly discussed.

The cumulative distribution of TTCI, $F_T(T)$, can be obtained using the distribution of EIFS given by Eq. 1 and the EIFS master curve relationship given in Eq. 12. The resulting expression, given in Eq. 13, is derived in Volume I [1].

$$F_T(T) = 1 - exp\left\{-\left[\frac{Y(T)}{\phi}\right]^{\alpha}\right\} ; \quad Y(T) \geq 0 \tag{13}$$

where

$$Y(T) = \ell_n(x_u/x_1) + QT ; \quad T \geq 0 \tag{14}$$

In Eq. 13, $x_u$ = EIFS upper bound limit, $x_1$ = $a_0$ = reference crack size for TTCIs, and $T$ = TTCIs for given $x_1$.

It can easily be shown that Eqs. 13 and 14 are simply the three-parameter Weibull distribution as follows:

$$F_T(T) = 1 - exp\left\{-\left[\frac{T-\epsilon}{\phi/Q}\right]^{\alpha}\right\} ; \quad T \geq \epsilon \tag{15}$$
$$= 0 \qquad\qquad\qquad ; \quad T < \epsilon$$

where

$$x_u = x_1 \, exp(-QT) \tag{16}$$

Recall that the Weibull compatible EIFS distribution given by Eq. 1 was derived from Eqs. 15 and 16, where $\phi = Q\beta$ with $\beta$ being the scale parameter of TTCI.

The EIFSD parameters        in Eq. 13 can be estimated
for a given $x_u$ value using either the combined least square
sums approach (CLSSA), Eqs. 7-11, the method of moments (MM),
or the homogeneous EIFS (HEIFS) approach [1]. Detailed proce-
dures and equations are given in Volume I [1], and software for
determining $\alpha$ and $\phi$ is documented in Volume V [5].

A statistical scaling factor $\ell$ which accounts for the
number of fastener holes per specimen, is used to determine
the EIFSD parameters. The scaling concept is developed and
discussed in Volume I. For example, each specimen in the
AFXLR4, AFXMR4, and AFXHR4 data sets contains 4 fastener holes
per specimen (i.e., two holes per dog bone and there are two
dog bones per specimen). However, fractographic data were
acquired for only the largest fatigue crack in any one of 4
holes per specimen. Hence, $\ell = 4$ should be used.

EIFSD parameters for individual data sets and for pooled
data sets, based on the CLSSA, are summarized in Table 8 for
selected $x_u$ values (i.e., .02", .03" and .05"). These results
are based on $\ell = 4$. Similar EIFSD parameter values have been
obtained using the method of moments [42]. Mean EIFS values
for each of the three data sets are also shown for comparison.
The mean EIFS values or each data set should first be compared
before all data sets are pooled together to determine the EIFSD
parameters for the pooled data sets. Ideally, the mean EIFS
values or each data set used in the data pooling procedure
should be of he same order of magnitude. Data sets with large
differences in mean EIFS values should be carefully scrutinized
before such data sets are used to estimate the EIFSD paramet-
ers.

3.3.1.3 <u>Goodness-of-Fit Plots</u>. A given EIFSD should be
justified by showing that reasonable predictions for $F_T(t)$,
$p(i, \mathcal{T})$, or $F_{a(t)}(x)$ can be made for (1) those data sets that
were used to define the IFQ and/or (2) data sets that were not
considered in the EIFSD determination. Basic concepts of such

Table 8. Summary of IFQ Model Parameters for Countersunk Data Sets.

| DATA SET | $\sigma$ (ksi) | NO. OF CRACKS USED | AL - AU | POOLED Q x$10^4$ (1/Hr.) | $x_u$ (In.) | $\alpha$ | $\phi$ | $\ell$ | MEAN EIFS (In.) | METHOD (5) |
|---|---|---|---|---|---|---|---|---|---|---|
| AFKLR4 (1) | 32 | 10/11 | .01"-.05" | 2.101 | 0.03 | 1.960 | 5.708 | 4 | .0042 | CLSSA |
| | | | | | 0.03 | 2.309 | 5.020 | | | MM |
| | | | | | 0.05 | 2.450 | 5.918 | | | CLSSA |
| AFXMR4 (1) | 34 | 9/9 | .01"-.05" | 2.514 | 0.03 | 1.960 | 4.355 | 4 | .0062 | CLSSA |
| | | | | | 0.05 | 2.545 | 4.646 | | | CLSSA |
| AFXHR4 (1) | 38 | 10/10 | .01"-.05" | 6.062 | 0.03 | 1.870 | 6.857 | 4 | .0034 | CLSSA |
| | | | | | 0.05 | 2.240 | 7.108 | | | CLSSA |
| | | | | | 0.05 | 2.607 | 6.386 | | | MM |
| AFKLR4 AFXMR4 (2) AFXHR4 | 32 34 38 | 10/11 9/9 10/10 | .01"-.05" | 2.101 2.514 6.062 | 0.02 0.03 0.05 | 1.330 1.716 2.132 | 6.794 6.308 6.453 | 4 4 4 | .0042 .0062 .0034 | CLSSA |

Notes: (1) Individual fractographic data set

(2) Pooled fractographic data sets

(3) Scaling factor used to define IFQ

(4) Weibull compatible EIFSD function used

(5) CLSSA = Combined Least Square Sums Approach; MM = Method of Moments; $a_{0} = 0.05"$ (ref. crack size for TTCIs)

38

justification procedures are shown in Figs. 13 and 14.

Expressions for $p(i, \mathcal{T})$ and $F_{a(t)}(x)$ developed in Volume I
[1], are given in Eqs. 17 and 18, respectively. The expression
for $Y(\mathcal{T})$ in Eq. 17 is given in Eq. 14.

$$p(i, \mathcal{T}) = 1 - exp\left\{-\left[\frac{Y(\mathcal{T})}{\phi}\right]^{\alpha}\right\}; \ Y(\mathcal{T}) \geq 0 \qquad (17)$$
$$= 0 \qquad\qquad ; \ Y(\mathcal{T}) \leq 0$$

$$F_{a(t)}(x) = 1 - p(i, \mathcal{T}) \qquad (18)$$

Let $T(x_1)$ be the time to reach any specific crack size $x_1$
and $F_{T(x_1)}(\mathcal{T})$ be the corresponding cumulative distribution,
i.e., $F_{T(x_1)}(\mathcal{T}) = P[T(x_1) \leq \mathcal{T}]$. The distribution function of
$T(x_1)$ is the probability that the crack will reach a crack size
$x_1$ before the service time $\mathcal{T}$. Such a probability is equal to
the probability that the crack size $a(\mathcal{T})$ at service time $\mathcal{T}$
will exceed $x_1$, which is simply the probability of crack ex-
ceedance. Hence,

$$F_{T(x_1)}(\mathcal{T}) = P[T(x_1) \leq \mathcal{T}] = P[a(\mathcal{T}) \geq x_1] = p(i, \mathcal{T}) \qquad (19)$$

Therefore, the cumulative distribution of service time to reach
any crack size $x_1$ is obtained by computing the crack exceedance
probability, $p(i, \mathcal{T})$, at different values of $\mathcal{T}$.

Various goodness-of-fit plots for $F_{T(x_i)}(t)$ and $p(i, \mathcal{T})$ are
shown in Figs. 15-30 for testing different EIFSDs for the AFXLR4,
AFXMR4, and AFXHR4 data sets. Plots are presented for each of
the three data sets using the EIFSD for a single data set and
for pooled data sets. Different goodness-of-fit plots are pre-
sented so that comparisons can be made for different sets of
EIFSD parameters.

39
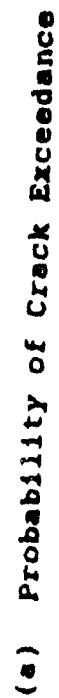
Figure 13. Probability of Crack Exceedance and Goodness-of-Fit for Small Crack Size Range.

(a) Probability of Crack Exceedance

(b) P(1,T) Goodness-of-Fit

40

(b)  $F_T(t)$ Goodness-of-Fit

(a)  Cumulative Distribution of TTCI
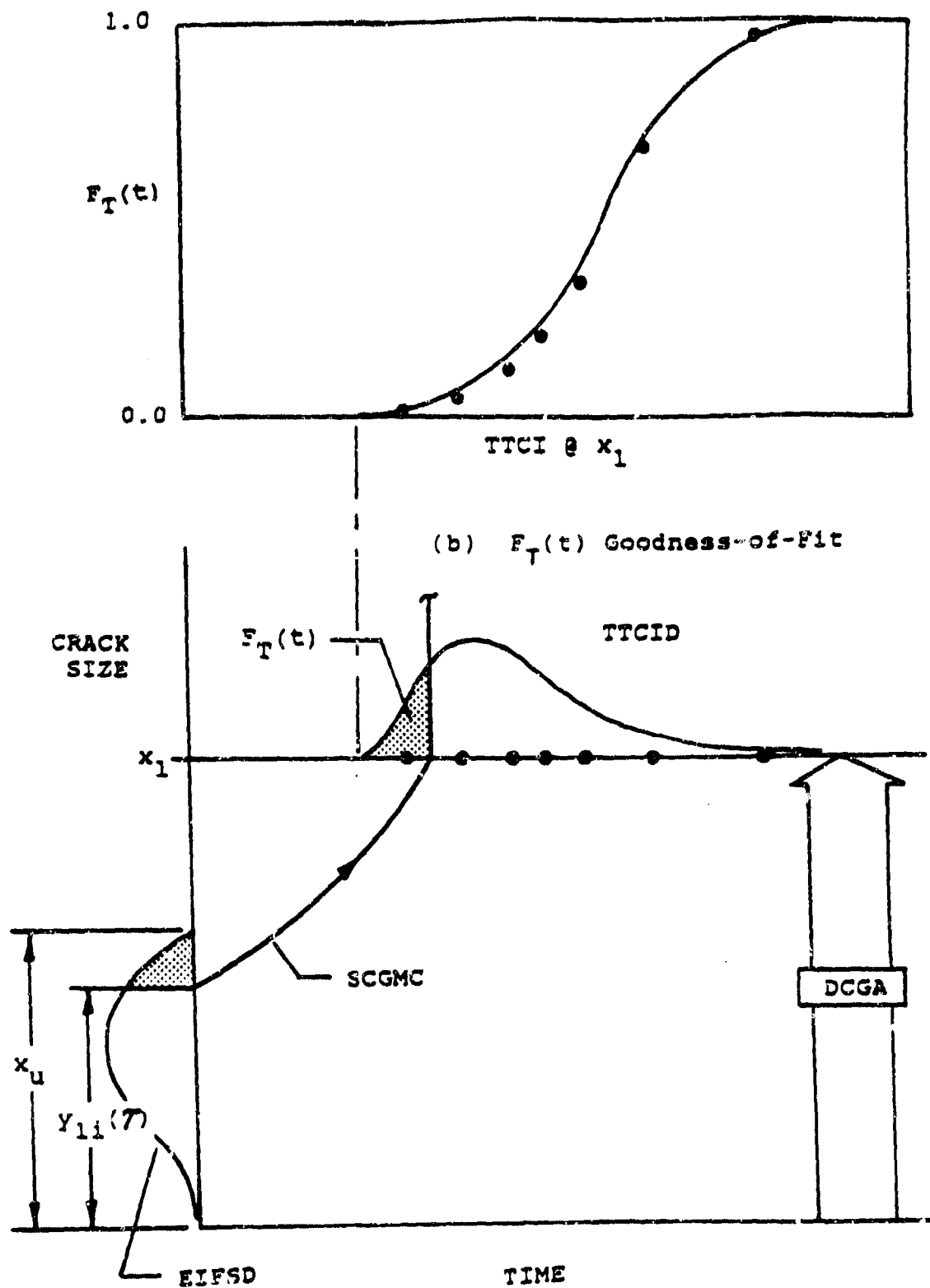
Figure 14.  Cumulative Distribution of TTCI and Goodness-of-Fit for Small Crack Size Range.

41
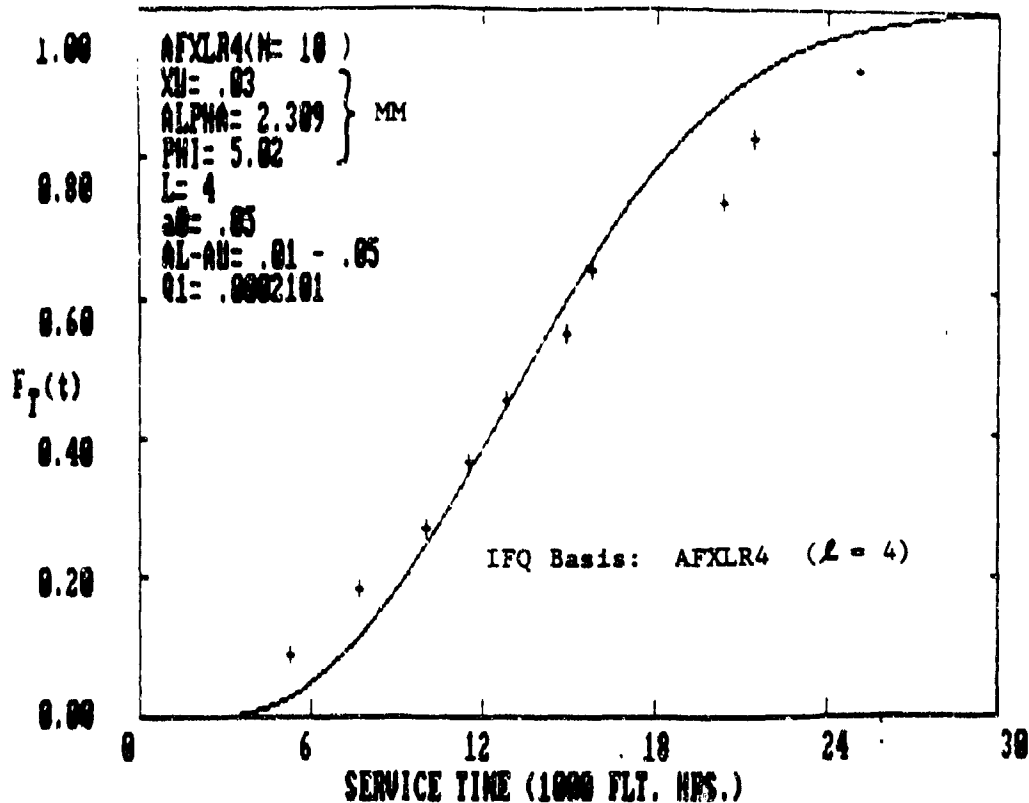
Figure 15. $F_T(t)$ Versus TTCI Plot for AFXLR4 (IFQ Basis: AFXLR4: $x_u = .03''$, $\alpha = 2.309$, $\phi = 5.02$, $\ell = 4$, Method of Moments)
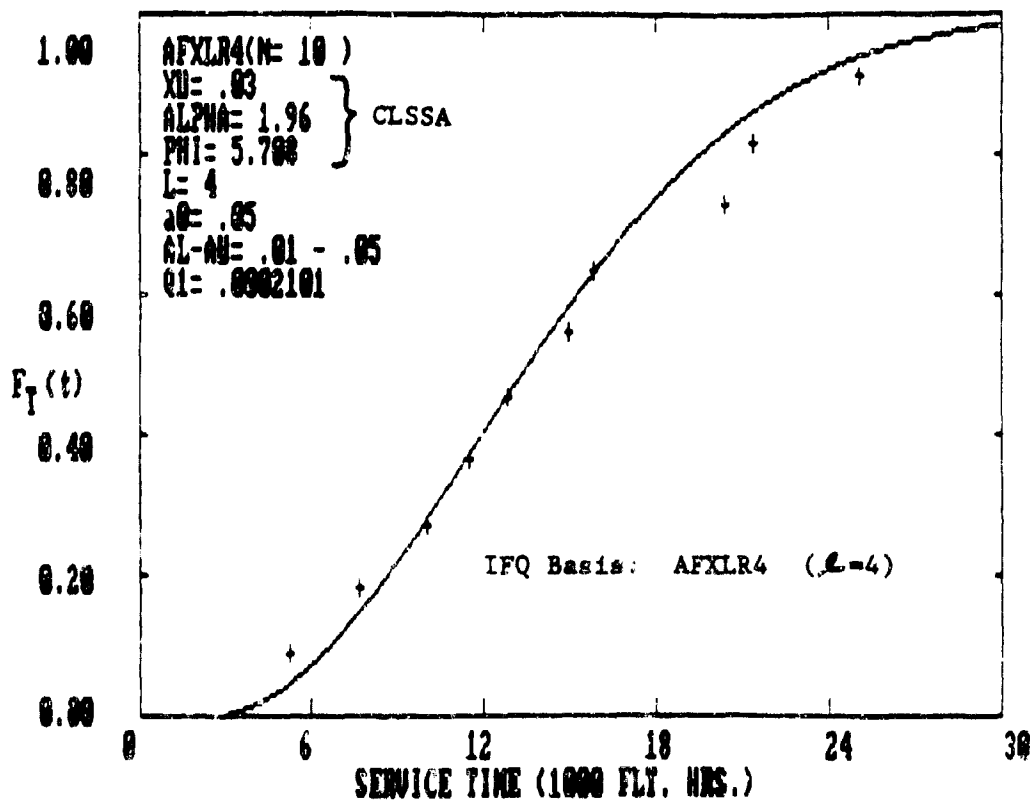


Figure 16. $F_T(t)$ Versus TTCI Plot for AFXLR4 (IFQ Basis: AFXLR4; $x_u = .03''$, $\alpha = 1.96$, $\phi = 5.708$, $\ell = 4$; CLSSA)
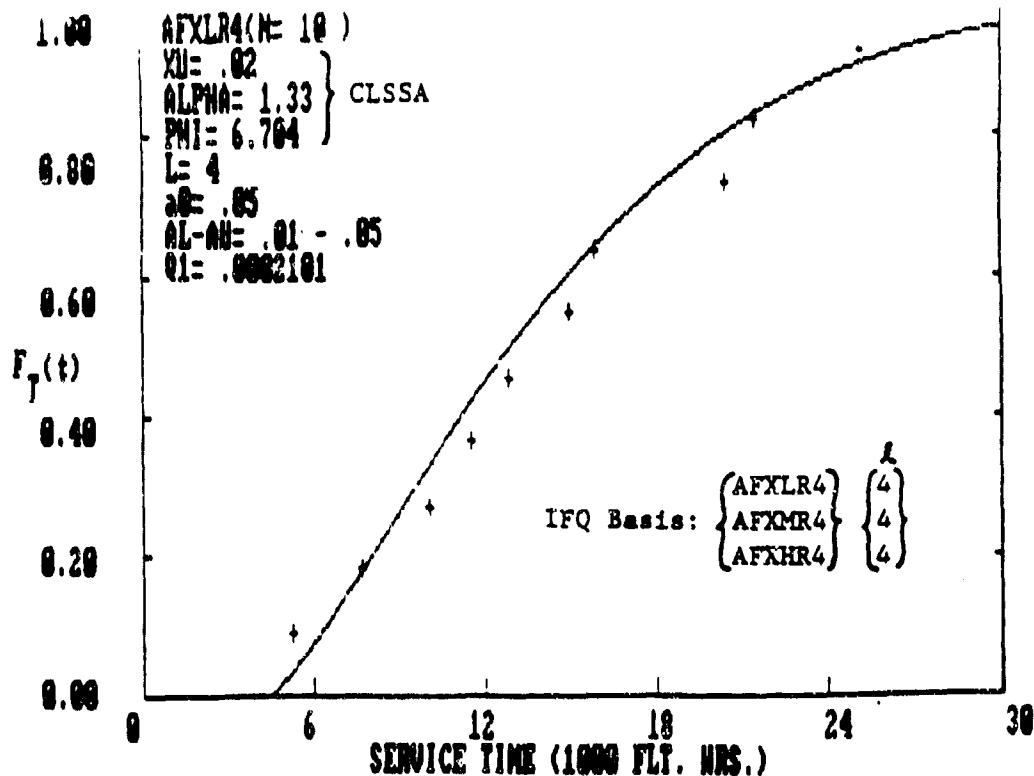
Figure 17.    $F_T(t)$ Versus TTCI Plot for AFXLR4
(IFQ Basis:   AFXLR4 + AFXMR4 + AFXHR4; $x_u$ = 0.02",
$\alpha$ = 1.33, $\phi$ = 6.704, $\ell$ =4, CLSSA)
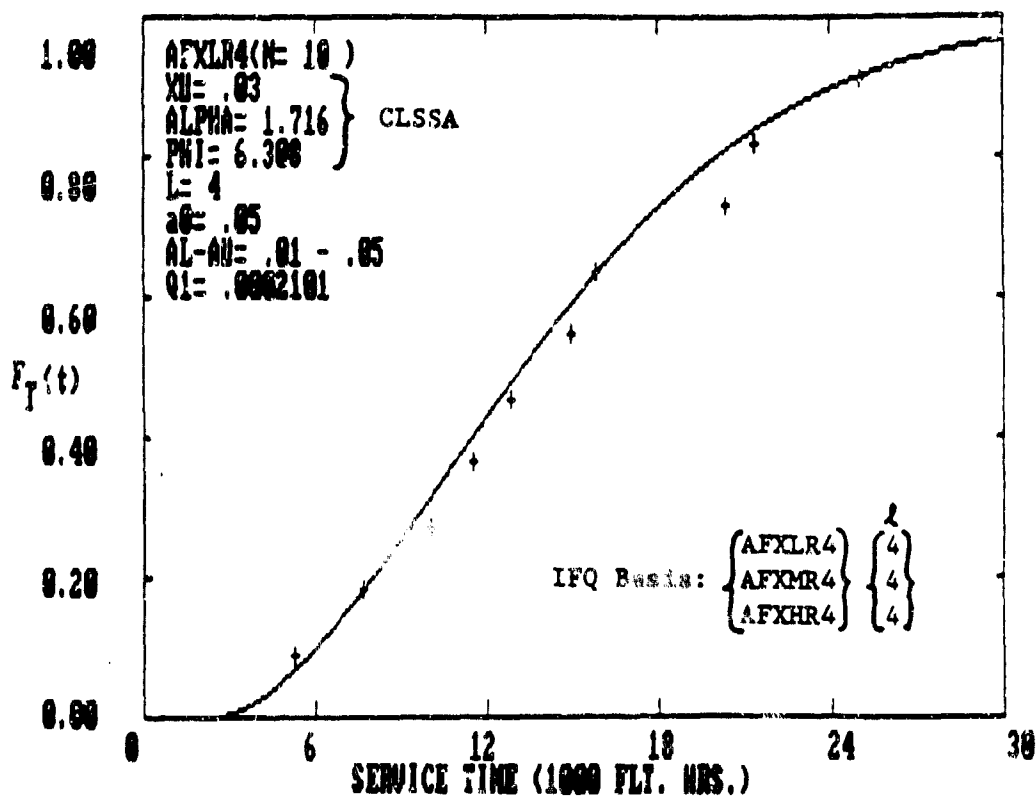


Figure 18.    $F_T(t)$ Versus TTCI Plot for AFXLR4
(IFQ Basis:   AFXLR4 + AFXMR4 + AFXHR4; $x_u$ = 0.03",
$\alpha$ = 1.716, $\phi$ = 6.309, $\ell$ =4; CLSSA)

43
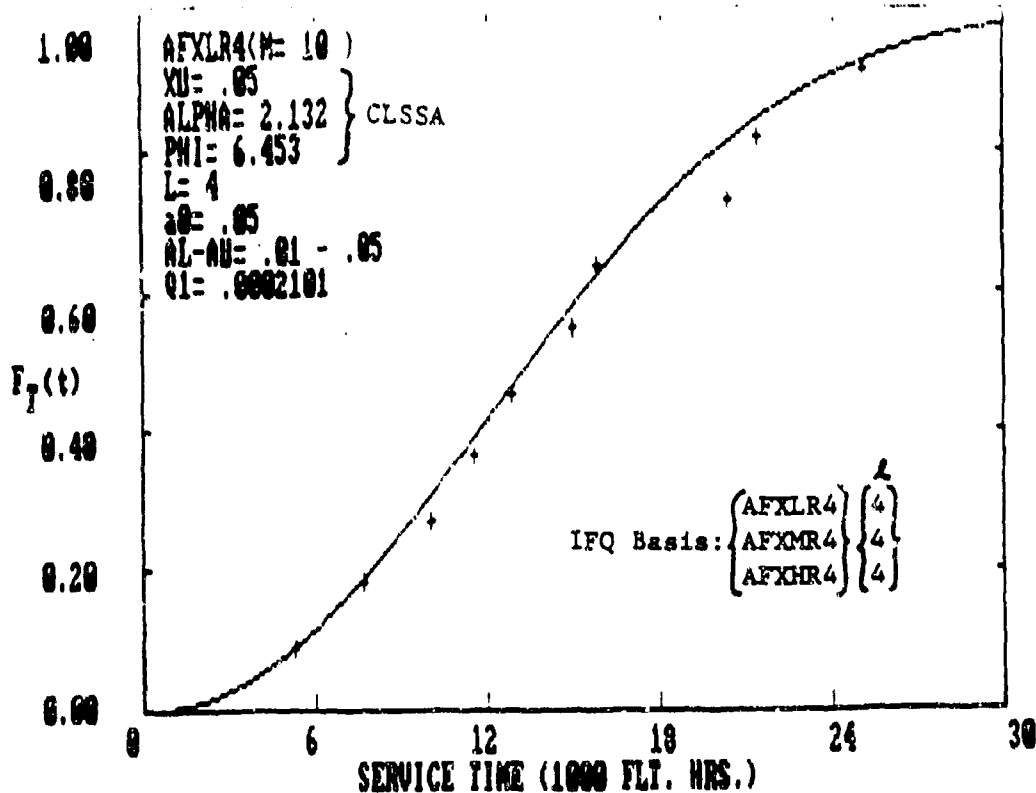
Figure 19.   $F_T(t)$ Versus TTCI Plot for AFXLR4
(IFQ Basis:   AFXLR4 + AFXMR4 + AFXHR4;
$x_u = 0.05''$, $\alpha = 2.132$, $\phi = 6.453$, $\mathcal{L} = 4$; CLSSA)
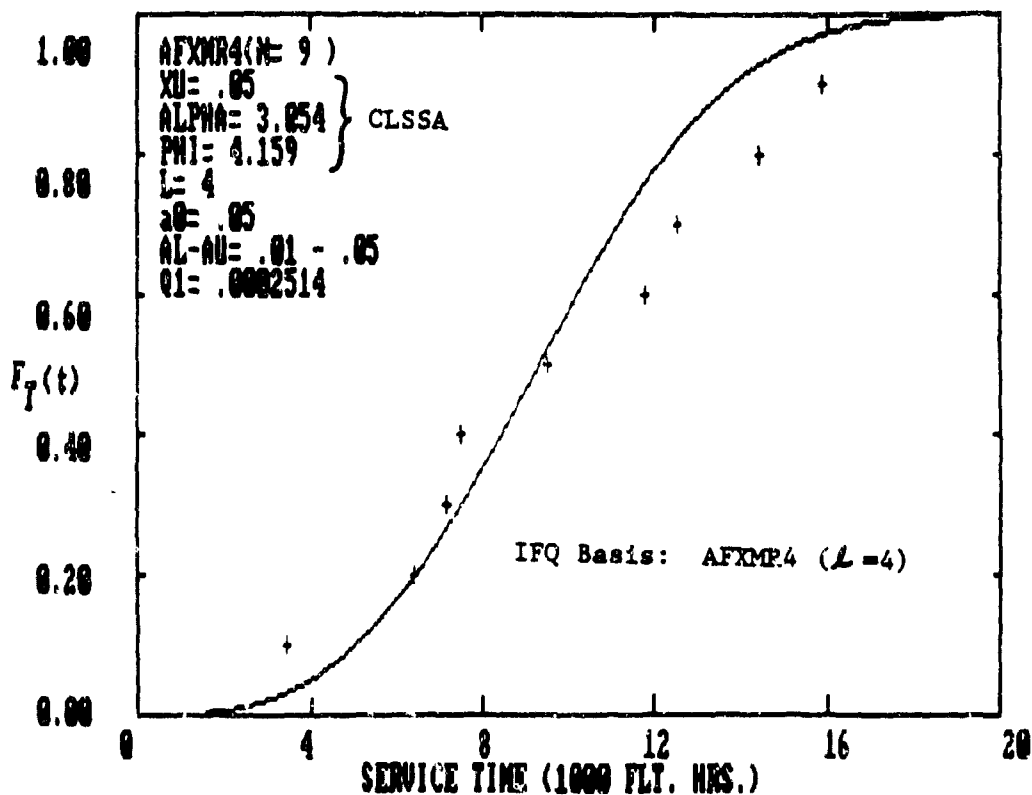


Figure 20.   $F_T(t)$ Versus TTCI Plot for AFXMR4
(IFQ Basis:   AFXMR4; $x_u = 0.05''$, $\alpha = 3.054$,
$\phi = 4.159$, $\mathcal{L} = 4$; CLSSA)

44
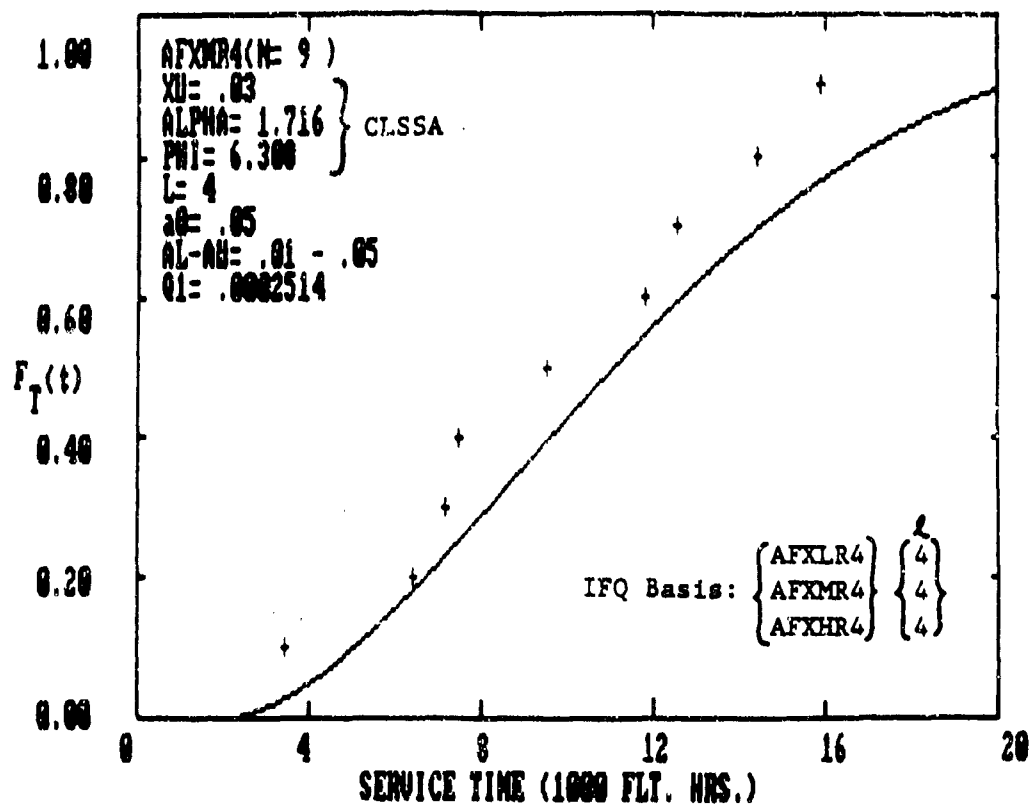
Figure 21. $F_T(t)$ Versus TTCI Plot for AFXMR4
(IFQ Basis: AFXLR4 + AFXMR4 + AFXHR4; $x_u = 0.03$"
$\alpha = 1.716, \phi = 6.308, \mathcal{L} = 4$; CLSSA)
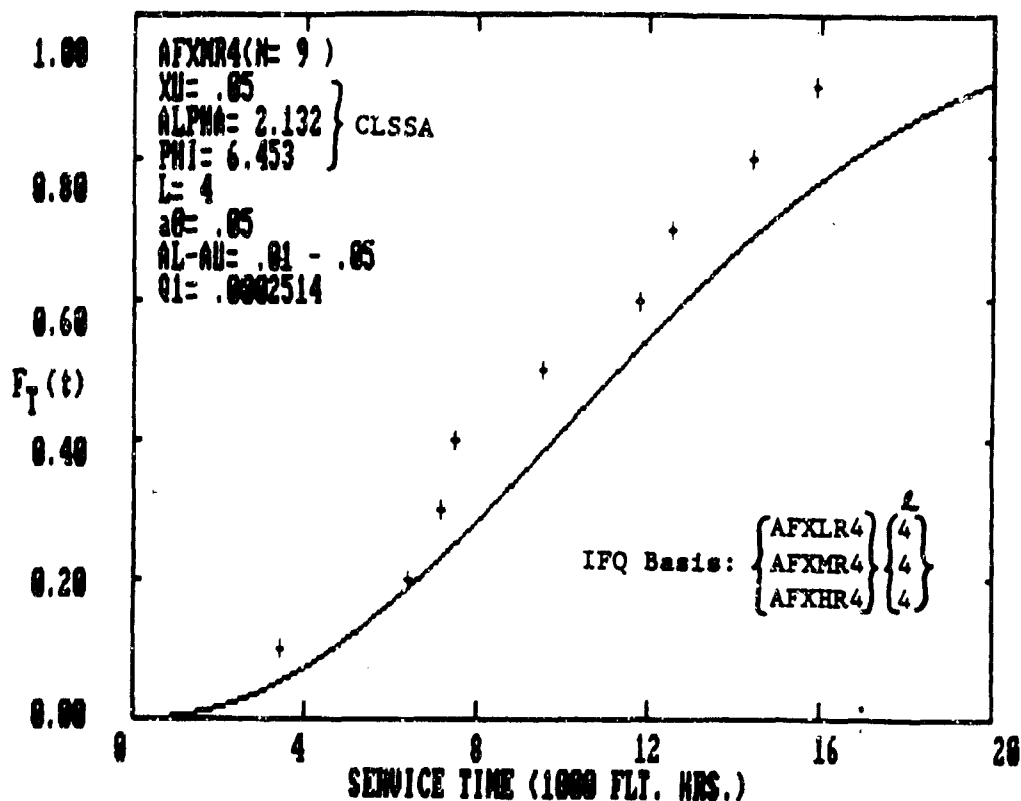


Figure 22. $F_T(t)$ Versus TTCI Plot for AFXMR4
(IFQ Basis: AFXLR4 + AFXMR4 + AFXHR4; $x_u = 0.05$"
$\alpha = 2.132, \phi = 6.453, \mathcal{L} = 4$; CLSSA)

45
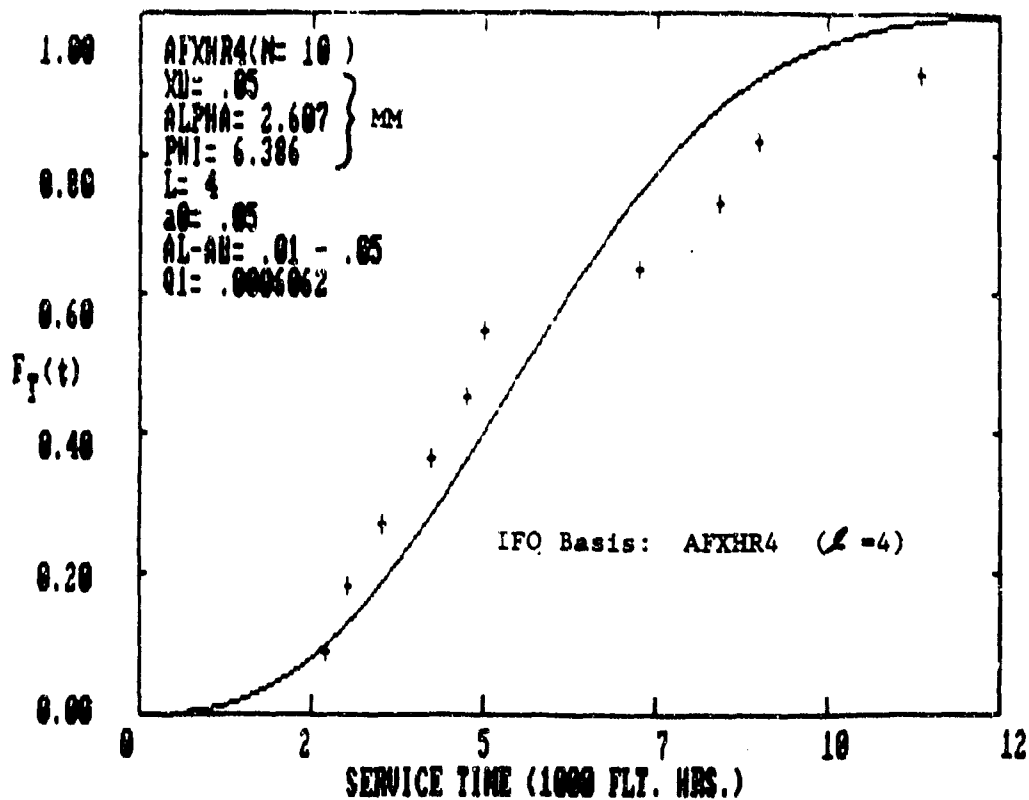
Figure 23. $F_T(t)$ Versus TTCI Plot for AFXHR4
(IFQ Basis: AFXHR4; $x_u = 0.05"$, $\alpha = 2.607$, $\phi = 6.386$,
$\ell = 4$; Method of Moments)
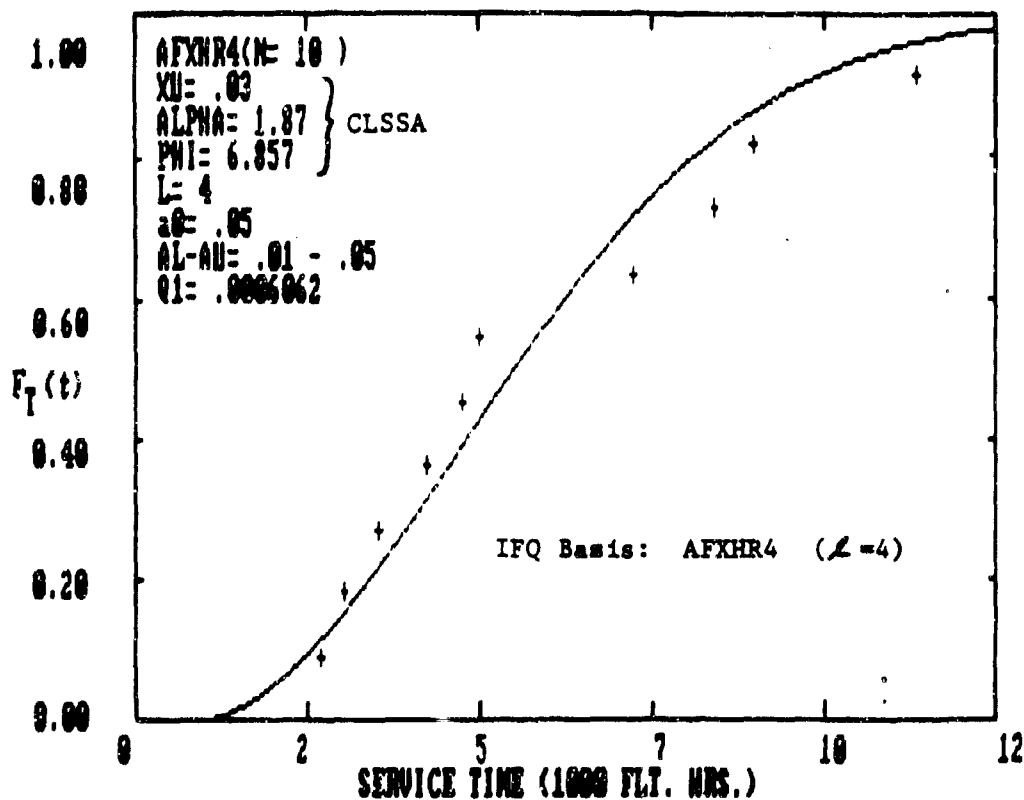


Figure 24. $F_T(t)$ Versus TTCI Plot for AFXHR4
(IFQ Basis: AFXHR4; $x_u = 0.03"$, $\alpha = 1.87$,
$\phi = 6.857$, $\ell = 4$; CLSSA)

46
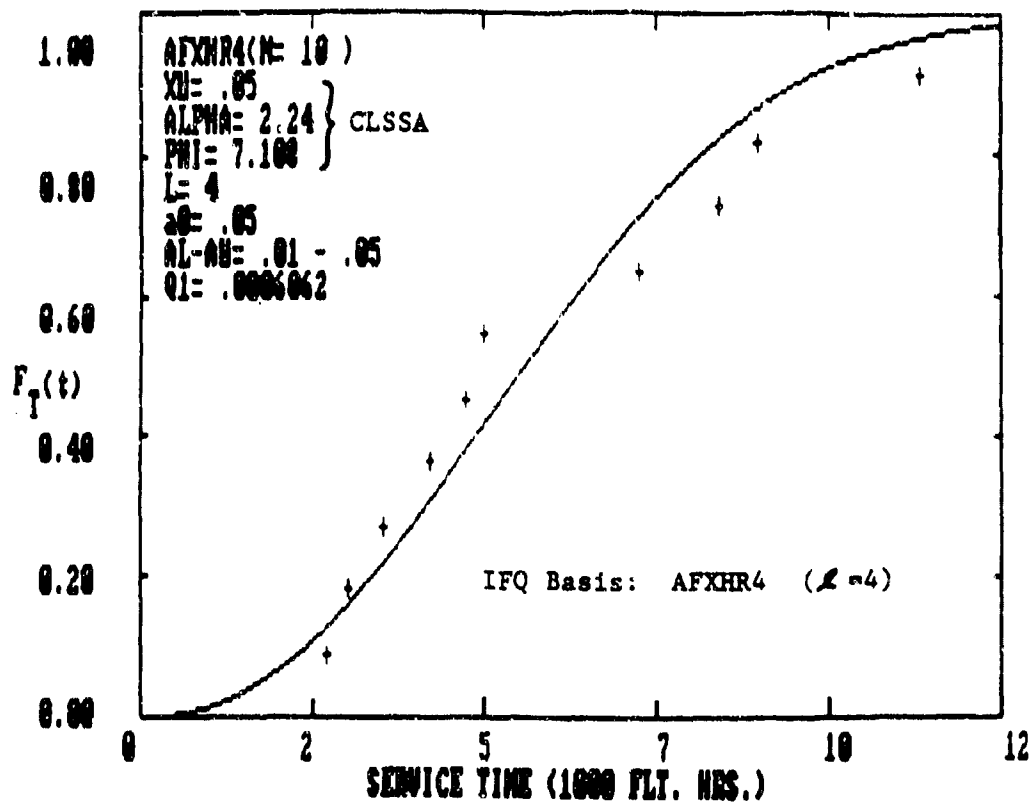
Figure 25.  $F_T(t)$ Versus TTCI for AFXHR4
(IFQ Basis:  AFXHR4; $x_u = 0.05$", $\alpha = 2.24$, $\phi = 7.108$,
$\mathcal{L} = 4$; CLSSA)
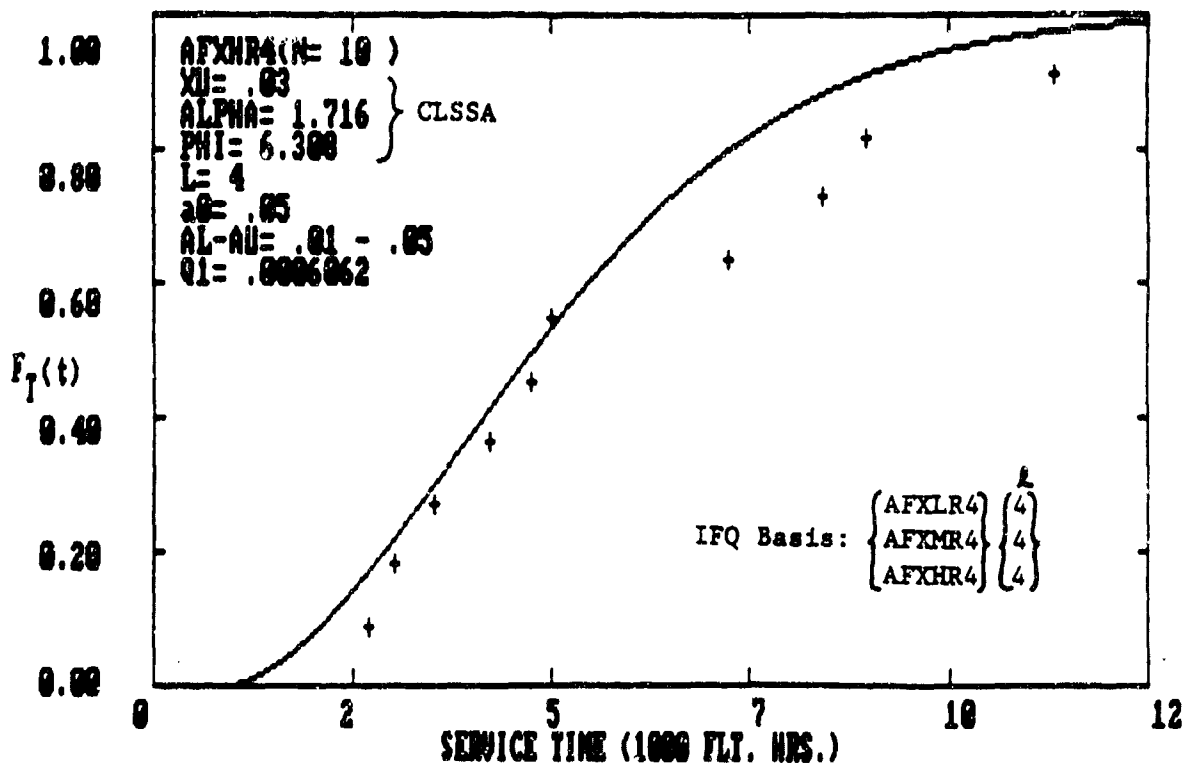


Figure 26.  $F_T(t)$ Versus TTCI for AFXHR4
(IFQ Basis:  AFXLR4 + AFXMR4 + AFXHR4; $x_u = 0.03$"
$\alpha = 1.716$. $\phi = 6.308$, $\mathcal{L} = 4$; CLSSA)
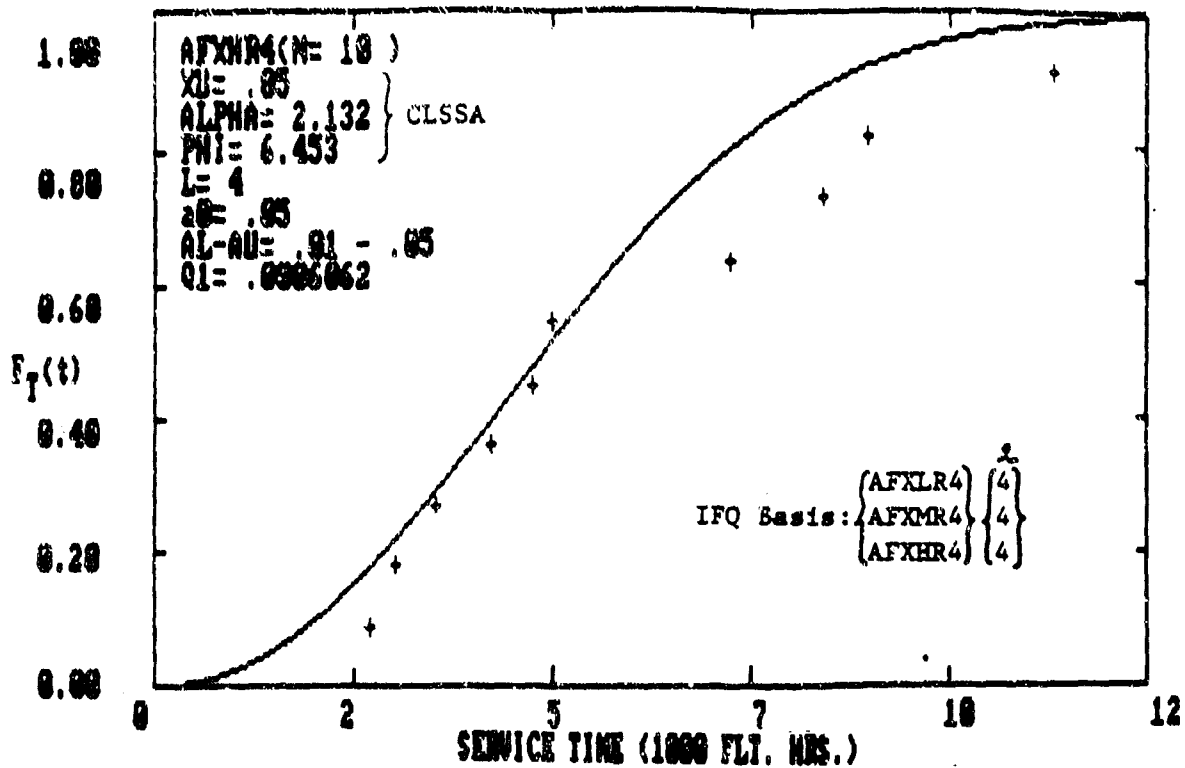
Figure 27. $F_T(t)$ Versus TTCI for AFXHR4
(IFQ Basis: AFXLR4 + AFXMR4 + AFXHR4; $x_u = 0.05''$,
$\alpha = 2.132$, $\phi = 6.453$, $\ell = 4$; CLSSA)
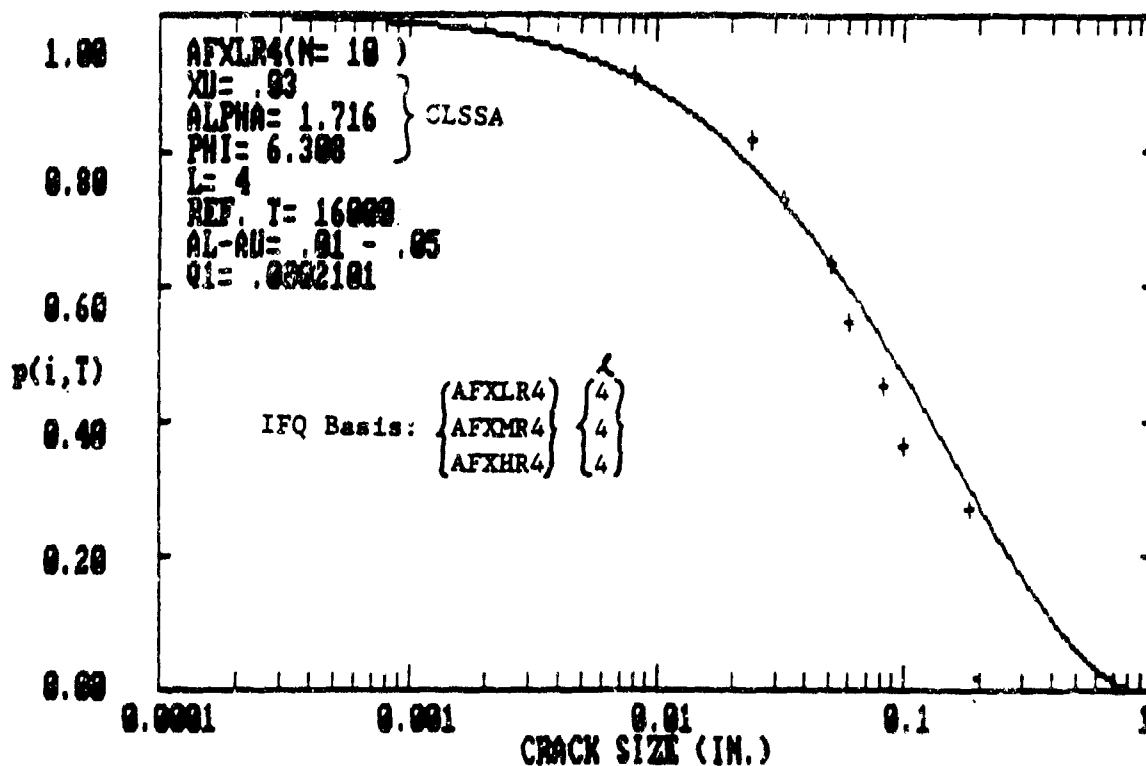


Figure 28. $p(i, \mathcal{T})$ Versus Crack Size for AFXLR4
(IFQ Basis: AFXLR4 + AFXMR4 + AFXHR4; $x_u = 0.03''$,
$\alpha = 1.716$, $\phi = 6.308$, $\ell = 4$; CLSSA)
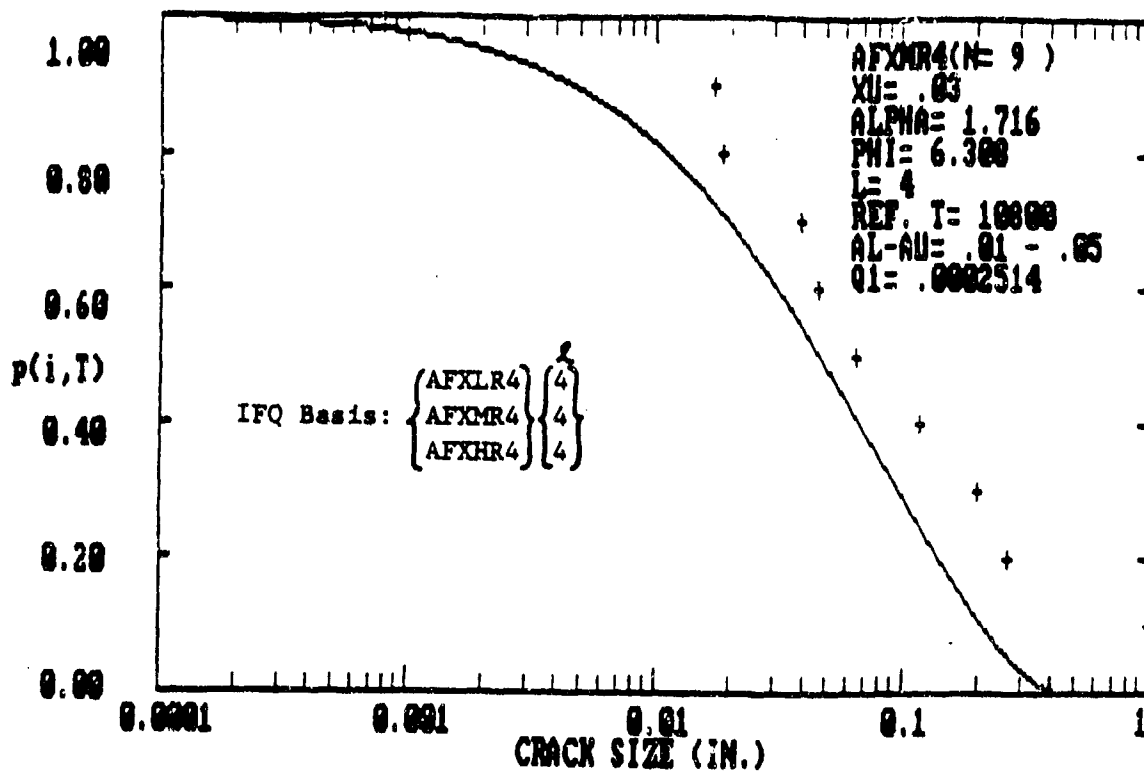
Figure 29.  p(i, $\mathcal{T}$) Versus Crack Size for AFXMR4
(IFQ Basis:  AFXLR4 + AFXMR4 + AFXHR4; $x_u$ = 0.03",
$\alpha$ = 1.716, $\phi$ = 6.308, $\mathcal{L}$ =4; CLSSA)
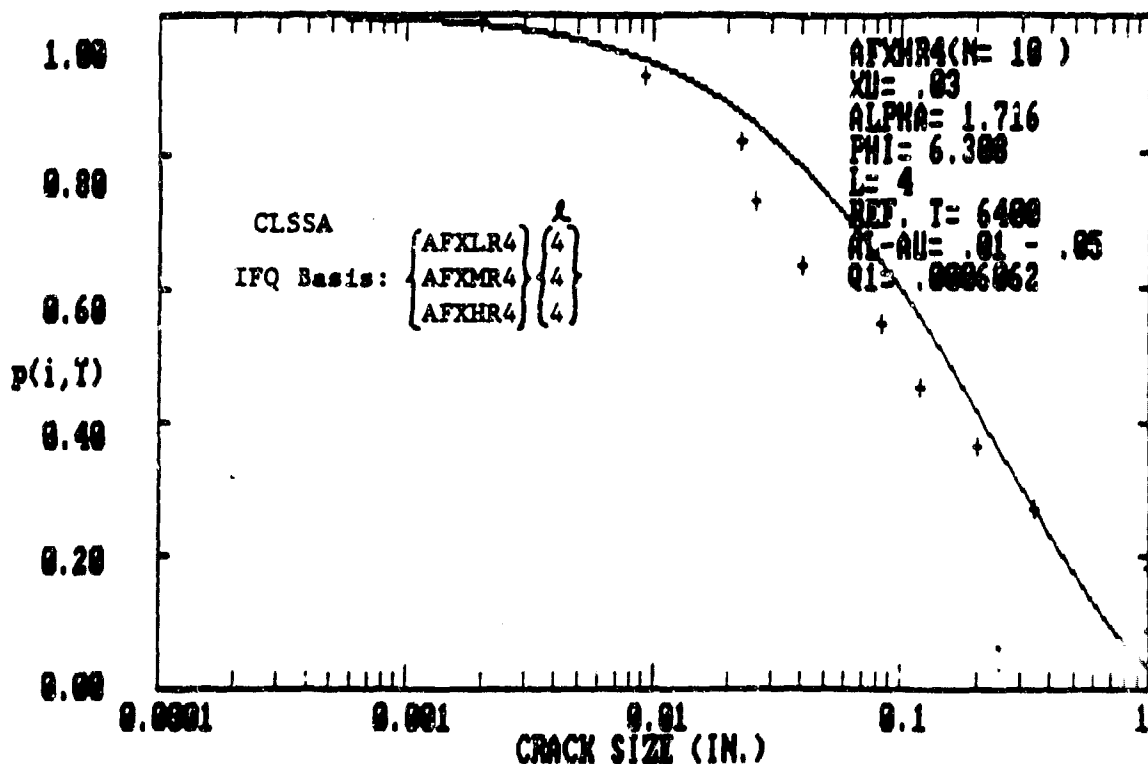


Figure 30.  p(i, $\mathcal{T}$) Versus Crack Size for AFXHR4
(IFQ Basis:  AFXLR4 + AFXMR4 + AFXHR4; $x_u$ =0.03",
$\alpha$ = 1.716, $\phi$ = 6.308, $\mathcal{L}$ =4; CLSSA)

3.3.1.4    Discussion of Results.  The following observa-
tions, comments, and conclusions are based on Figs. 15-30.


1.   The EIFSD parameters for the Weibull compatible distri-
bution depend on the chosen fractographic crack size range, AL-
AU.  A fractographic crack size range of AL-AU = 0.01" - 0.05"
was used in the demonstration.


2.     The EIFS parameters have been estimated  using  the
CLSSA  and  the method of moments (MM) [1,42].  Goodness-of-fit
plots for $F_T(t)$ versus TTCI using the  MM  and  the  CLSSA  are
shown  in  Figs. 15 and 16, respectively.  In general, however,
the CLSSA seems to give a better overall fit than the MM.  This
has been expected because $\alpha$ and $\phi$ are determined by  minimizing
the total sum squared error.


3.   With the IFQ that is determined from pooled data sets
(i.e.,  AFXLR4  +  AFXMR4  +  AFXHR4) goodness-of-fit plots for
$F_T(t)$ are shown in Figs. 17-19 for the AFXLR4 data set  and  in
Figs.  26  and 27 for the AFXHR4 data set.  These plots reflect
different $x_u$ values.  For all three data sets $x_u = 0.03"$ appears
to give the best fit in the lower tail.  Plots for  $x_u$ = 0.05"
also give reasonable fits for the three data sets   The theore-
tical  predictions  based on $x_u$ = 0.02" do not correlate as well
with actual test results as either $x_u$ = 0.03" or 0.05".


4.   The crack exceedance probability plots, $p(i, \mathcal{T})$,  in
Figs.  28 - 30 are shown for crack sizes up to 1.0".  Theoreti-
cal predictions are based  on  the  corresponding  EIFS  master
curve.   The   crack  size range of most interest for justifying
the EIFSD is for AL-AU = 0.01" - 0.05".


5.   The theoretical predictions for  $F_T(t)$  and  $p(i, \mathcal{T})$
based  on the IFQ that is determined from the pooled data sets,

50

correlate reasonably well with the actual test results for each of the three countersunk fastener hole data sets, separately. We then conclude that the EIFSD parameters $x_u$ = .03", $\alpha$ = 1.716, and $\phi$ = 6.308 (for the pooled data sets) are reasonable for the durability analysis of countersunk fastener holes in 7475-T7351 aluminum for the situation considered. The EIFSD parameters $x_u$ = .05", $\alpha$ = 2.132, and $\phi$ = 6.453 are also considered reasonable for durability analysis. A slightly more conservative durability analysis prediction for $x_u$ = 0.05" than for $x_u$ = 0.03" would be expected. The EIFSD parameters $x_u$ = 0.02", $\alpha$ = 1.33, and $\phi$ = 6.704 are a poor third choice for representing the IFQ.

### 3.3.2 Straight-Bore Fastener Hole Specimens

Two fractographic data sets from the "Fastener Hole Quality" (FHQ) program [3] will be used to determine the initial fatigue quality (IFQ) of stright-bore fastener holes in 7475-T7351 aluminum. The two data sets, referred to as "WPF" and "XWPF" are described in Table 9. Specimen geometry and design details for WPF and XWPF data sets are shown in Figs. 4 and 5, respectively. The specimens for both data sets have NAS 6204 (1/4" dia) protruding head bolts installed with a clearance fit. No special life enhancement hole processing, such as cold working and interference fit bushings, were reflected in any of the test specimens considered.

The fractographic results (i.e., a(t) versus t data) for the largest fatigue crack per specimen in the bore of the hole of each specimen in each data set were screened for extreme behavior. Screening was conducted using the computer software in Volume V [5]. Fractographic results in AL-AU = 0-.05" are shown in Figs. 31 and 32 for the WPF and XWPF data sets, respectively. Two fatigue cracks were deleted from each of the two data sets as indicated in Figs. 31 and 32.

**Table 9.** Description of Fractographic Data Sets Used to Determine the IFQ for Straight-Bore Fastener Holes

| Data Set (1) | No. of Specimens Used | (4) σ (KSI) | % KT | W (In.) | Fastener | Load Spectrum | Ref. Fig. |
|---|---|---|---|---|---|---|---|
| WPF (5) | 31/33 (2) | 34 | 0 | 1.5 | NAS6204-8 | F-16 400 HR | 4 |
| XWPF | 31/33 (3) | 34 | 15 | 1.5 | | | 5 |

Notes:
(1) 7475-T7351 Aluminum
(2) Deleted fatigue cracks #2 and 6
(3) Deleted fatigue cracks #11 and 16
(4) Gross section stress for peak spectrum load
(5) Ref. FHQ program [3]
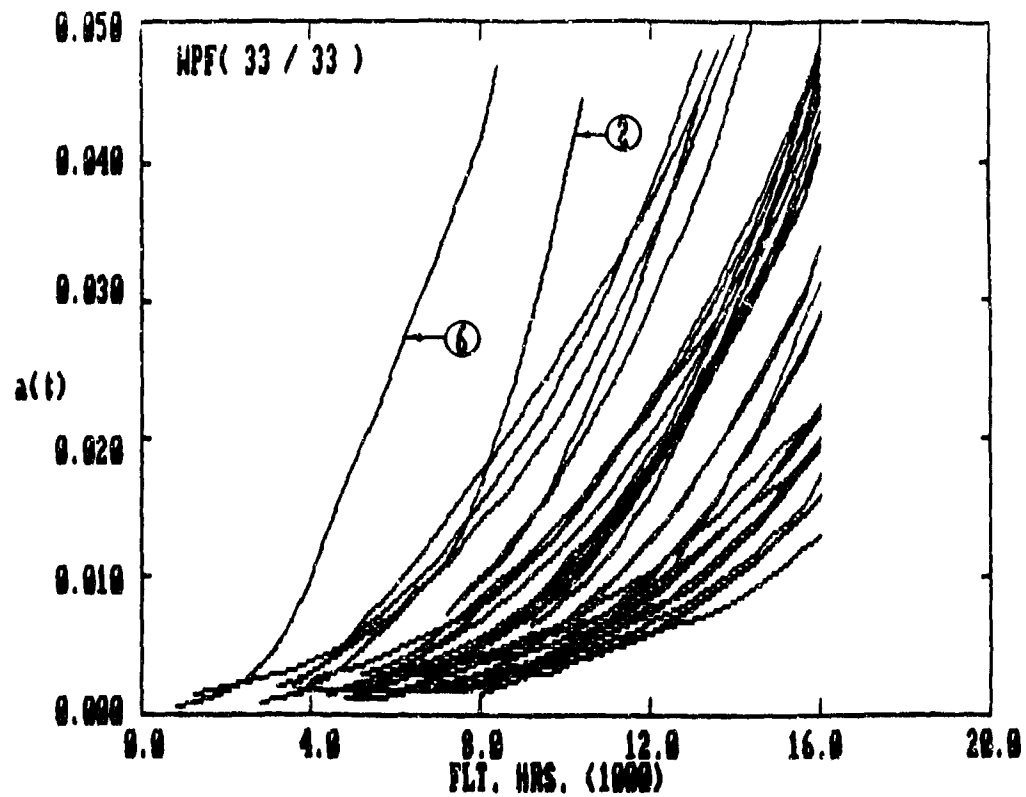
Figure 31.   Fractographic Data Survey for WPF Data
             Set in the AL-AU = 0-.05" Crack Size Range.
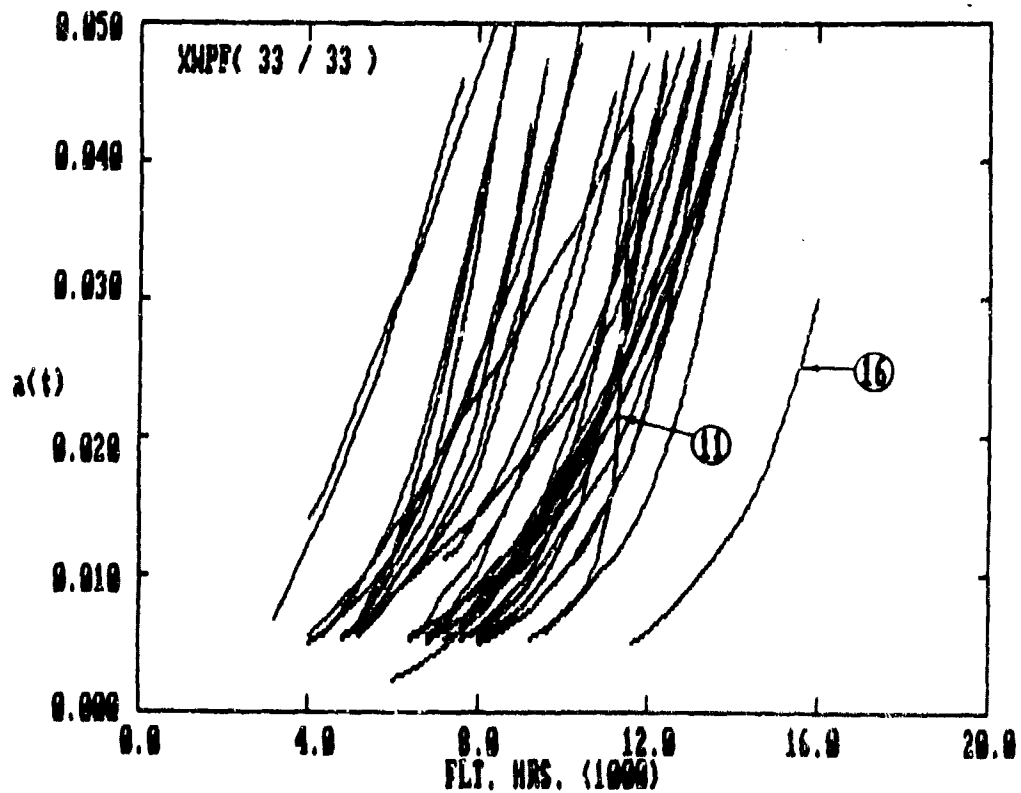


Figure 32.   Fractographic Data Survey for XWPF Data
             Set in the AL-AU = 0-.05" Crack Size Range.

Two criteria were used to censor the fractographic data:
(1) eliminate fatigue cracks with abnormally fast crack
growth rates (e.g., cracks no. 2 and 6 for the WPF and crack
no. 11 for the XWPF data set), and (2) delete cracks with
little useful data in the desired AL-AU range, e.g., the
crack data is sparse for fatigue crack no. 16 of the XWPF
data set and would require extrapolation to $a_0 = 0.05"$.
There are no hard and fast rules for fractographic data cen-
soring. However, fractographic data screening is essential
when defining the IFQ to assure data consistency and compat-
ibility.

The IFQ analysis procedures described previously for
countersunk fastener holes will be repeated herein for
straight-bore hole specimens in the following.

3.3.2.1 <u>Estimation of Crack Growth Rate Parameters.</u>
The crack growth parameter Q in Eqs. 10 - 12 is determined
for the WPF and XWPF data sets using the same procedure des-
cribed in Section 3.3.1.1 for countersunk fastener holes.
Pooled Q values were determined using the applicable fracto-
graphic data in the AL-AU range = 0.01"-0.05". Pooled Q val-
ues for the WPF and XWPF data sets are shown in Table 10.
Similar Q values are also shown in Table 10 for the WWPF,
LYWPF and HYWPF data sets. Experimental results for these
three data sets will be used later to correlate with theore-
tical predictions for $p(i, \mathcal{T})$ or $F_{T(x_i)}(\mathcal{T})$. In this case
predictions will be based on an EIFSD determined using two
data sets (i.e., WPF and XWPF) and the data pooling procedure
described in Volume I [1]. Specimen geometries for the WWPF,
LYWPF and HYWPF data sets are also shown in Table 10. Speci-
men geometries for the WWPF data set are shown in Fig. 2.
Except for specimen width, the specimen for the WWPF data set
is identical to that for the WPF data set in the test sec-
tion. The width of the WPF and WWPF specimens is 1.5" and
3.0", respectively.

Table 10. Summary of Pooled Q Values for Data Sets Used
for Straight-Bore Fastener Hole Demonstration

| (1) Data Set | Number of Specimens Used | (4) (KSI) | W (In.) | % LT | (5) AL-AU | (6) Qx10$^4$ (1/HR.) | Load Spectrum | Ref. Fig. |
|---|---|---|---|---|---|---|---|---|
| YPF | 32/33 (2) | 34 | 1.5 | 0 | .01"-.05" | 2.329 | F-16 400 HR. | 4 |
| XWPF | 31/33 (3) | 34 | 1.5 | 15 | | 3.671 | | 5 |
| WWPF | 13/13 | 34 | 3.0 | 0 | | 2.742 | | 2 |
| LYWPF | 5/6 | 30.6 | 1.5 | 15 | | 2.140 | | 5 |
| HYWPF | 8/8 | 40.6 | 1.5 | 15 | | 9.969 | | 5 |

Notes:

(1) Ref. FHQ program [3]
(2) Deleted fatigue crack #2 and 6
(3) Deleted fatigue crack #11 and 16
(4) Gross section stress for peak spectrum load
(5) Fractographic crack size range used to compute Q
(6) Based on Eq. 3

55

3.3.2.2 Estimation of EIFSD Parameters. EIFSD parameters are estimated using fractographic results for individual data sets and for pooled data sets. Three different initial fatigue quality (IFQ) cases are considered as shown in Table 11. The IFQ for cases 1 and 2 is based on the fractographic data for individual data sets (i.e., WPF and XWPF). Statistical scaling factors of $l = 1$ and 4 were used for the WPF and XWPF data sets, respectively for IFQ case 3. The statistical scaling procedure used is described in Volume I [1].

Specimens for the WPF data set have a single fastener hole (Fig. 4), whereas each specimen for the XWPF data set (Fig. 5) contains two common fastener holes in two dog-bones or a total of four holes per specimen. Fractographic results are available for the largest fatigue crack in each specimen for both data sets.

The EIFSD parameters for the Weibull-compatible distribution function (i.e., $\alpha$ and $\phi$), Eq. 1, will be estimated for $x_u = 0.03"$ using the WPF and XWPF data sets described in Table 9. The same procedures, equations, and details used in Section 3.3.1.2 for countersunk fastener holes will be used for the straight-bore fastener hole demonstration.

EIFSD parameters $\alpha$ and $\phi$ can be estimated for a given $x_u$ using either an "EIFS fit" or a "TTCI fit" and the combined least square sums approach (CLSSA). Details of the estimation procedure are given in Volume I [1]. In this section $\alpha$ and $\phi$ were estimated for each IFQ case using $x_u = 0.03"$, an "EIFS fit," and the CLSSA. Software for an IBM or IBM-compatible PC, documented in Volume V [5], was used to determine the EIFSD parameters. Results for the three IFQ cases are summarized in Table 11.

56

Table 11. Summary of EIFSD Parameters for Straight-Bore Fastener Holes Based on Weibull-Compatible Distribution Function

| IFQ Basis | No. Spec. | AL-AU (In.) | $Qx10^4$ (1/HR) | $\ell$ | $x_u$ (In.) | $\alpha$ | $\phi$ | IFQ Case |
|---|---|---|---|---|---|---|---|---|
| WPF | 31 | .01-.05 | 2.329 | 1 | .03 | 6.920 | 3.808 | 1 (1) |
| XWPF | 31 | | 3.671 | 4 | | 5.136 | 5.440 | 2 (1) |
| $\begin{bmatrix} WPF \\ XWPF \end{bmatrix}$ | $\begin{bmatrix} 31 \\ 31 \end{bmatrix}$ | | $\begin{bmatrix} 2.329 \\ 3.671 \end{bmatrix}$ | $\begin{bmatrix} 1.0 \\ 4.0 \end{bmatrix}$ | | 4.782 | 4.658 | 3 (2) |

NOTES: (1) Based on individual fractographic data set
(2) Based on pooled fractographic data sets

57

3.3.2.3 **Goodness-of-Fit Plots.** A candidate EIFSD can be tested as follows. The EIFSD is grown forward to predict the probability of crack exceedance, $p(i, \mathcal{T})$, at any service time and/or the cumulative distribution of service time, $F_T(t)$, at any given crack size. Then, analytical predictions can be plotted and correlated with available fractographic results to determine if reasonable predictions can be obtained with the candidate EIFSD. Such plots are referred to as "goodness-of-fit plots." The three IFQ cases shown in Table 11 are evaluated in the following.

$p(i, \mathcal{T})$ predictions, based on IFQ cases 1 and 2 (individual data sets), are correlated with fractographic results as shown in Figs. 33 and 34 for the WPF and XWPF data sets, respectively. Similar plots for $F_T(t)$ are shown in Figs. 35 and 36 for the same data sets.

$p(i, \mathcal{T})$ predictions based on IFQ case 3 for pooled data sets (i.e., WPF and XWPF), are correlated with fractographic results in Figs. 37 and 38 for the WPF and XWPF data sets, respectively. Similar plots for $F_T(t)$ are shown in Figs. 39 and 40.

Predictions for $p(i, \mathcal{T})$ and/or $F_T(t)$ were also made and correlated with fractographic results for three data sets (i.e., WWPF, LYWPF and HYWPF) not used to estimate the IFQ. Theoretical predictions were based on IFQ case 3. Results for the WWPF data set are shown in Figs. 41 and 42 for $p(i, \mathcal{T})$ and $F_T(t)$, respectively. Specimen details for the WWPF data set are shown in Fig. 2. Crack growth parameters for determining $p(i, \mathcal{T})$ and $F_T(t)$ and other details are shown in Table 10.

$F_T(t)$ predictions for the LYWPF and HYWPF data sets were also made using IFQ case 3 (Table 11). Specimen details are shown in Fig. 5 and other particulars are shown in Table
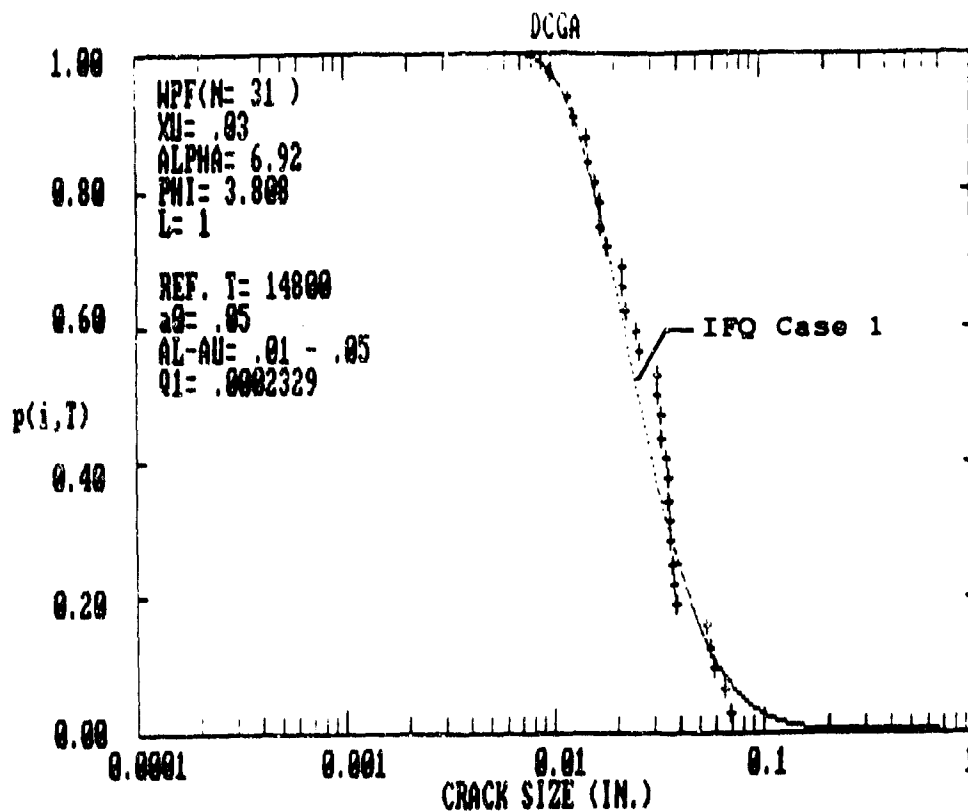
Figure 33. p(i,$\mathcal{T}$) Versus Crack Size Goodness-of-Fit Plot for WPF Data Set (IFQ Basis: Case 1) at $\mathcal{T}$ = 14800 Flight Hours.
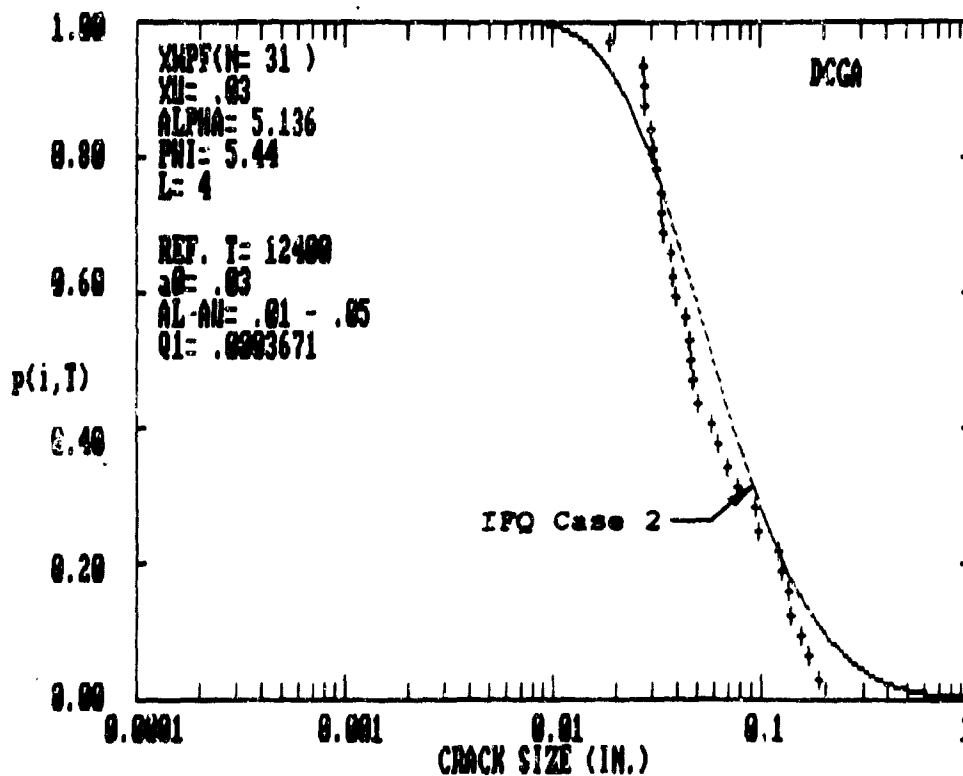


Figure 34. p(i,$\mathcal{T}$) Versus Crack Size Goodness-of-Fit Plot for XWPF Data Set (IFQ Basis: Case 2) at $\mathcal{T}$ = 12400 Flight Hours.
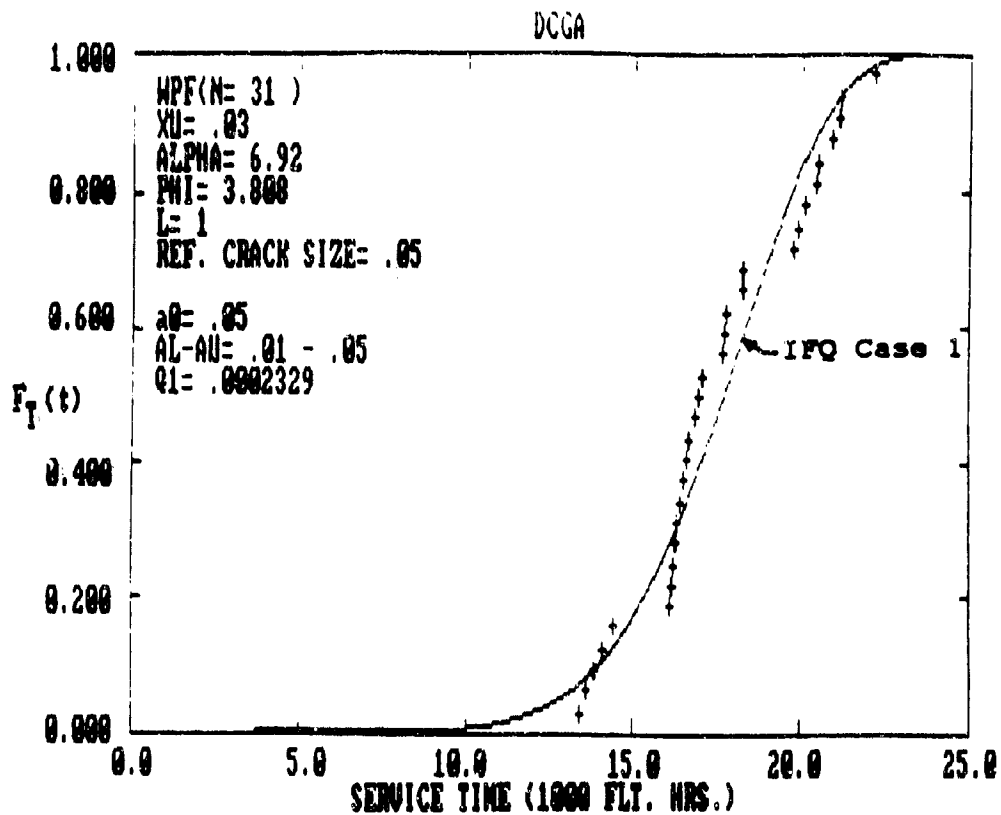
**Figure 35.** $F_T(t)$ Versus TTCI Goodness-of-Fit Plot for WPF Data Set (IFQ Basis: Case 1) at $a_o$ = .05".
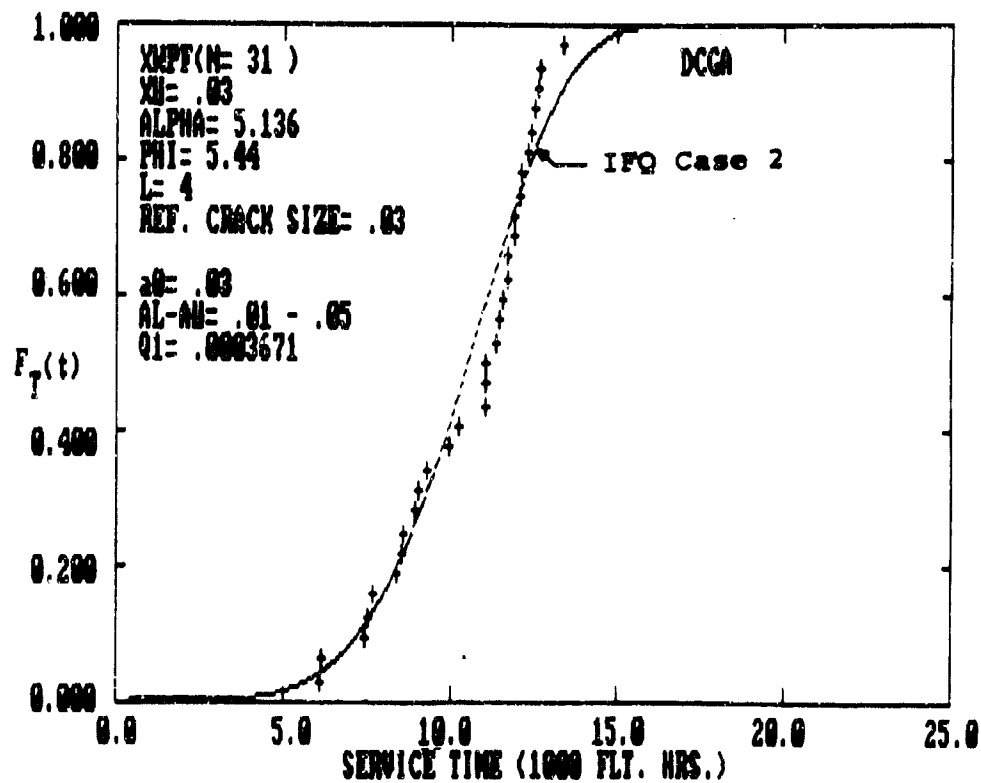


**Figure 36.** $F_T(t)$ Versus TTCI Goodness-of-Fit Plot for XWPF Data Set (IFQ Basis: Case 2) at $a_o$ = .05".
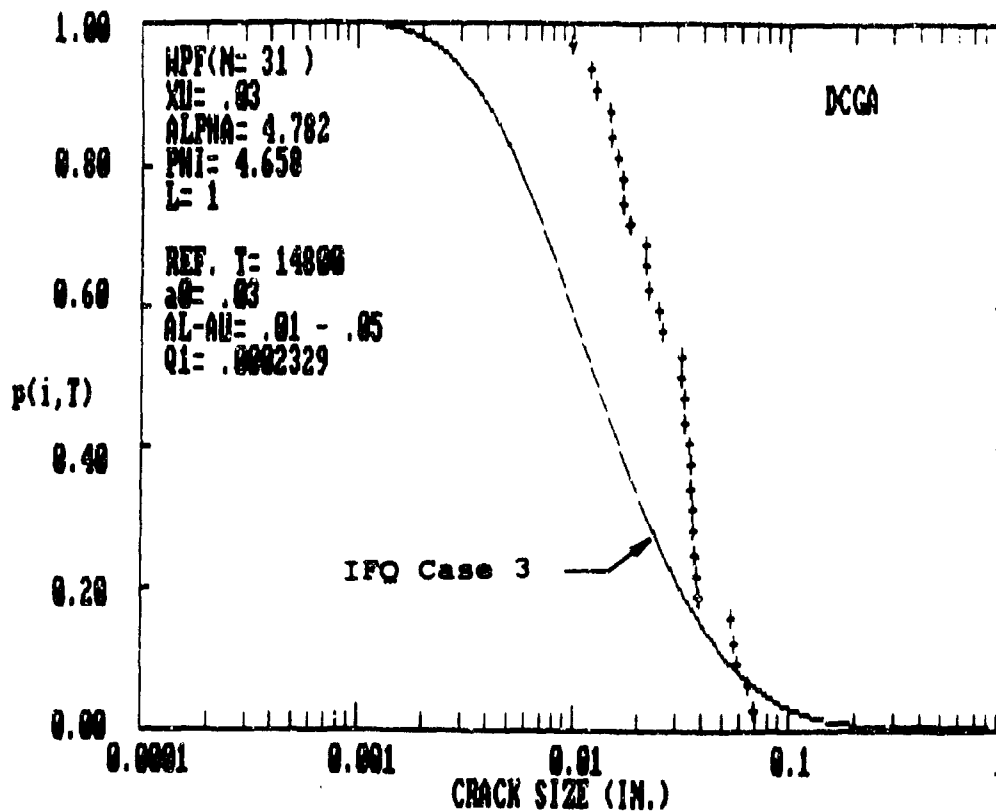
**Figure 37.** p(i,T) Versus Crack Size Goodness-of-Fit Plot for WPF Data Set (IFQ Basis = WPF+XWPF) at T = 14800 Flight Hours.
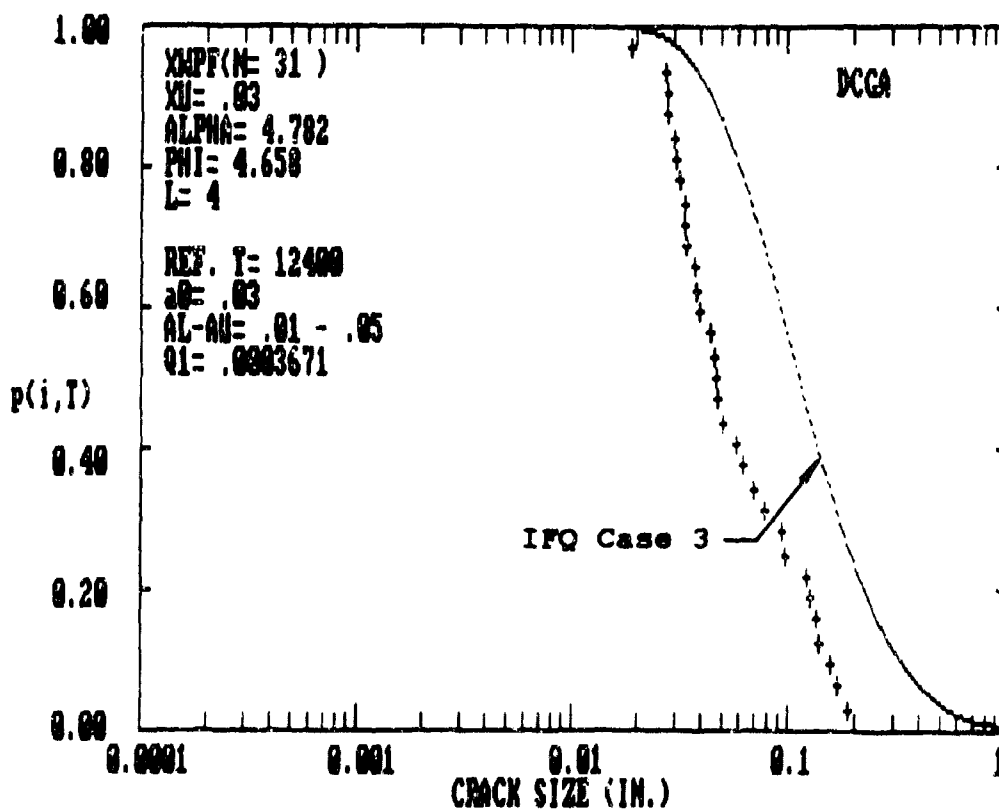


**Figure 38.** p(i,T) Versus Crack Size Goodness-of-Fit Plot for XWPF Data Set (IFQ Basis = WPF+XWPF) at T = 12400 Flight Hours.
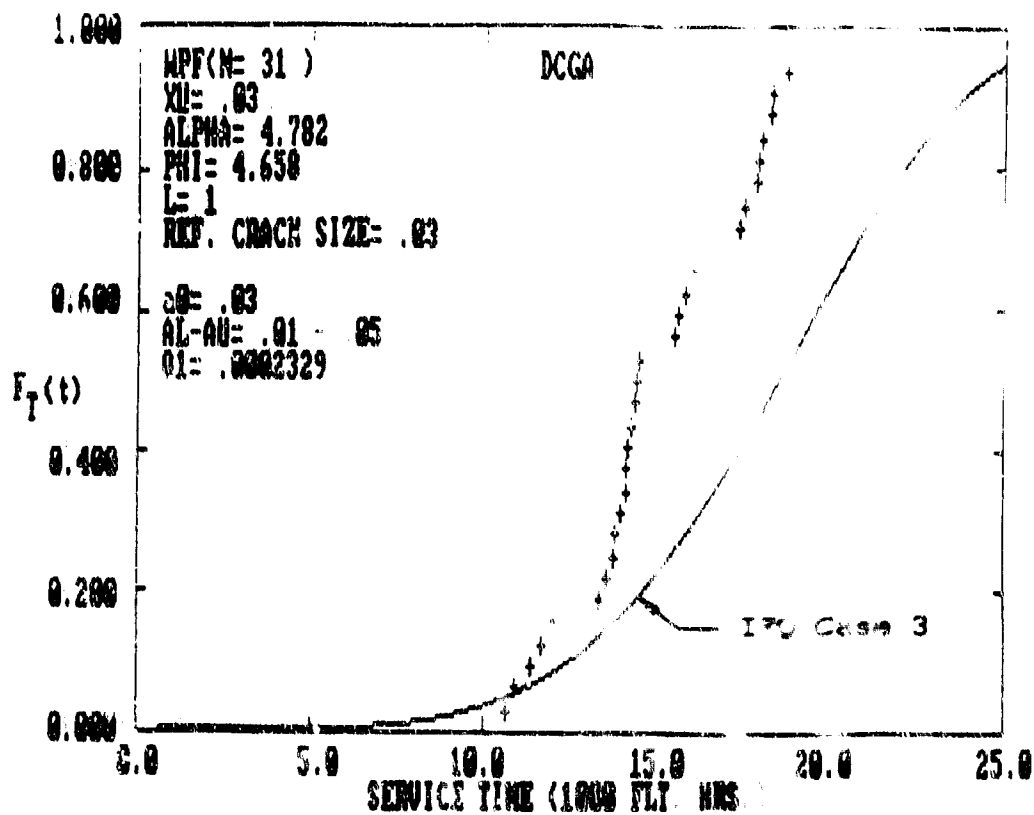
Figure 39.  $F_T(t)$ Versus TTCI Goodness-of-Fit Plot for
WPF Data Set (IFQ Basis = WPF+XWPF) for
$a_0 = 0.03''$.
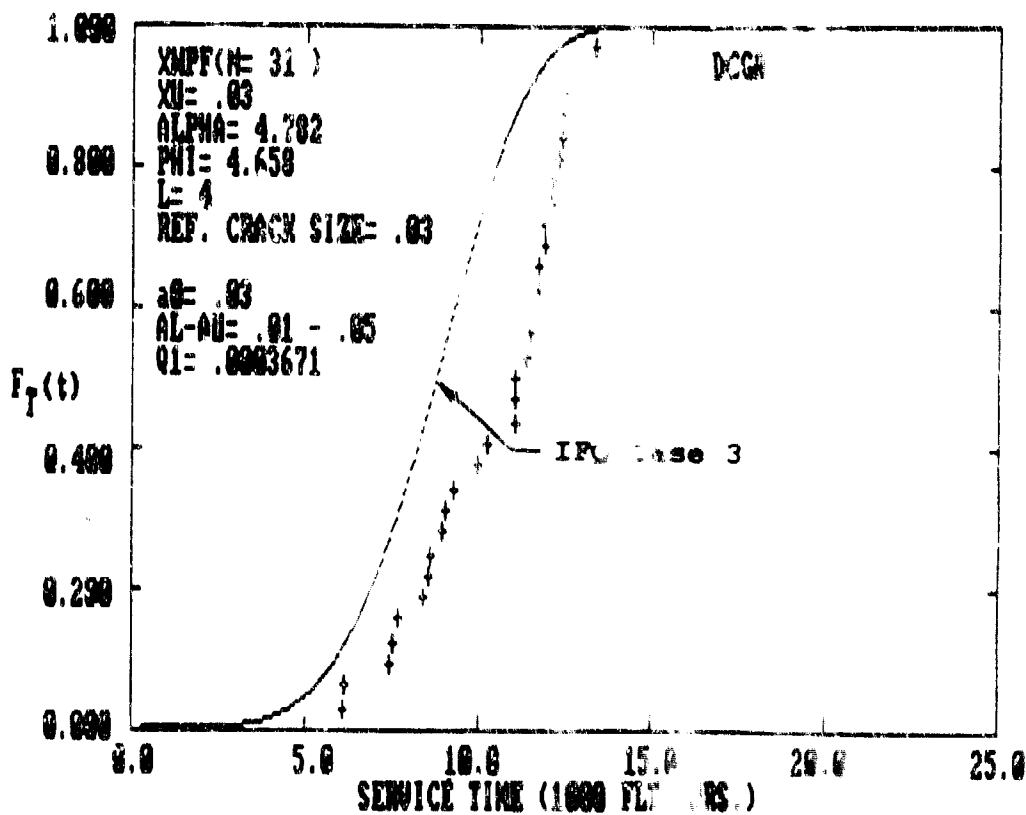


Figure 40.  $F_T(t)$ Versus TTCI Goodness-of-Fit Plot for
XWPF Data Set (IFQ Basis = WPF+XWPF) for
$a_0 = 0.03''$.

62
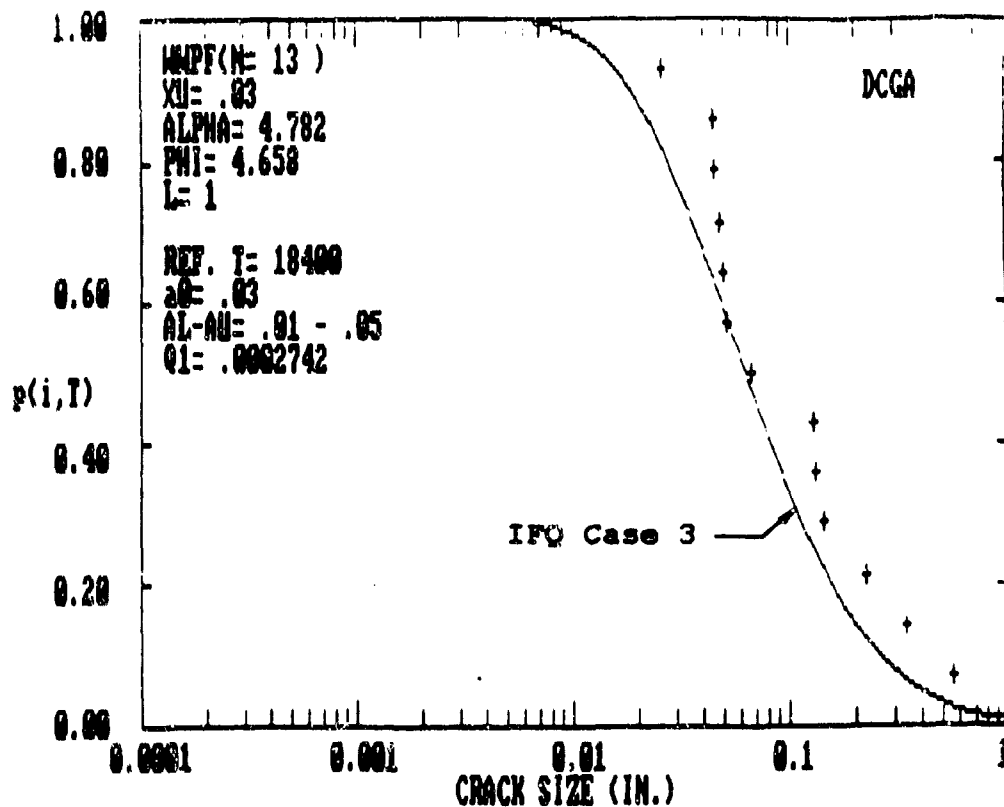
**Figure 41.** p(i,$\mathcal{T}$) Versus Crack Size Goodness-of-Fit Plot for WWPF Data Set (IFQ Basis = WPF+XWPF) at $\mathcal{T}$ = 18400 Flight Hours.
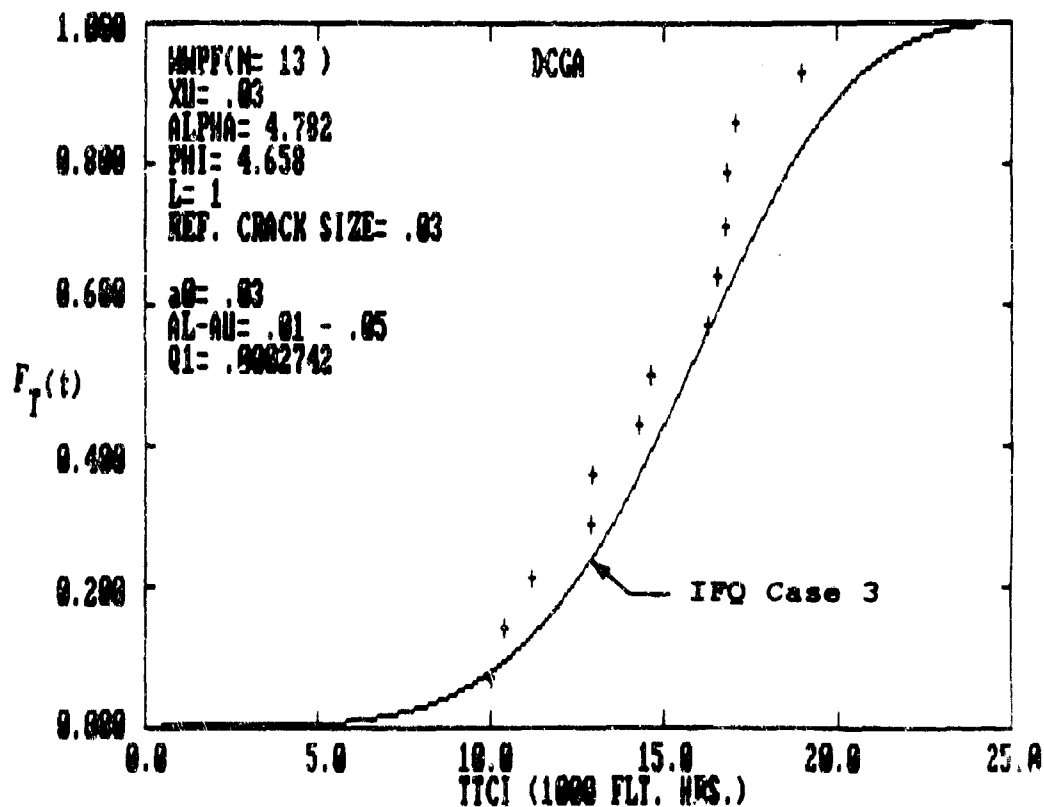


**Figure 42.** $F_T$(t) Versus TTCI Goodness-of-Fit Plot for WWPF Data Set (IFQ Basis = WPF+XWPF) for $a_0$ = 0.03".

10.    $F_T(t)$   predictions  are  correlated with actual fracto-
graphic results for the LYWPF and HYWPF data sets in Figs. 43
and 44, respectively. Experimental results for all plots
shown in Figs. 33-44 are based on the largest fatigue crack
per specimen -- irrespective of the number of fastener holes
per specimen.

3.3.2.4    Discussion of Results.   The following observa-
tions, comments and conclusions are based on  the  demonstra-
tion presented herein.

1.    $p(i, \mathcal{T})$  and  $F_T(t)$ predictions for an individual
fractographic data set (i.e., WPF and XWPF)  correlated  very
well with fractographic results when the IFQ was based on the
fractographic results of that given data set.   For example,
see Figs. 33-36.

2.    Theoretical predictions for $p(i, \mathcal{T})$  and  $F_T(t)$  for
the  WPF  and  XWPF data sets, based on IFQ case 3 (see Table
11), did not correlate as well with experimental  results  as
those  based  on IFQ cases 1 and 2.   For example, compare re-
sults shown in Figs. 33-40.

3.  The WWPF, LYWPF and HYWPF  fractographic  data  sets
were  not  used  to  define  the IFQ for any of the three IFQ
cases shown in Table 11.   Theoretical predictions for $p(i, \mathcal{T})$
and $F_T(t)$, based on the DCGA, correlated reasonably well with
experimental results for the WWPF data set (see Figs. 41  and
42).    Poorer  correlations  were  obtained for the LYWPF and
HYWPF data sets as shown in Figs. 43  and  44,  respectively.
Better correlations were obtained for the HYWPF data set than
for  the  LYWPF data set.  Theoretical predictions for $F_T(t)$
were more conservative (i.e., shorter service times to  reach
a  specified  crack  size)  than the experimental results for
both the LYWPF and HYWPF data sets.   It should be noted  that
the LYWPF and HYWPF data sets had a limited number of useable
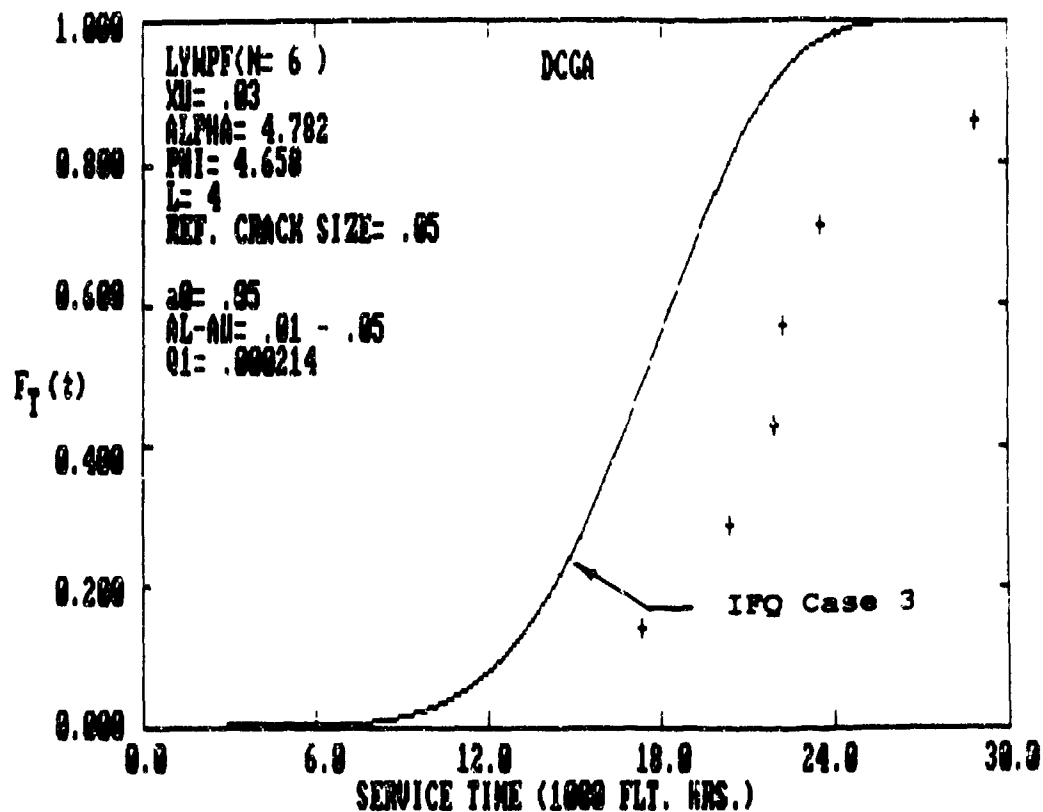
**Figure 43.** $F_T(t)$ Analytical and Experimental Correlations for LYWPF Data Set.
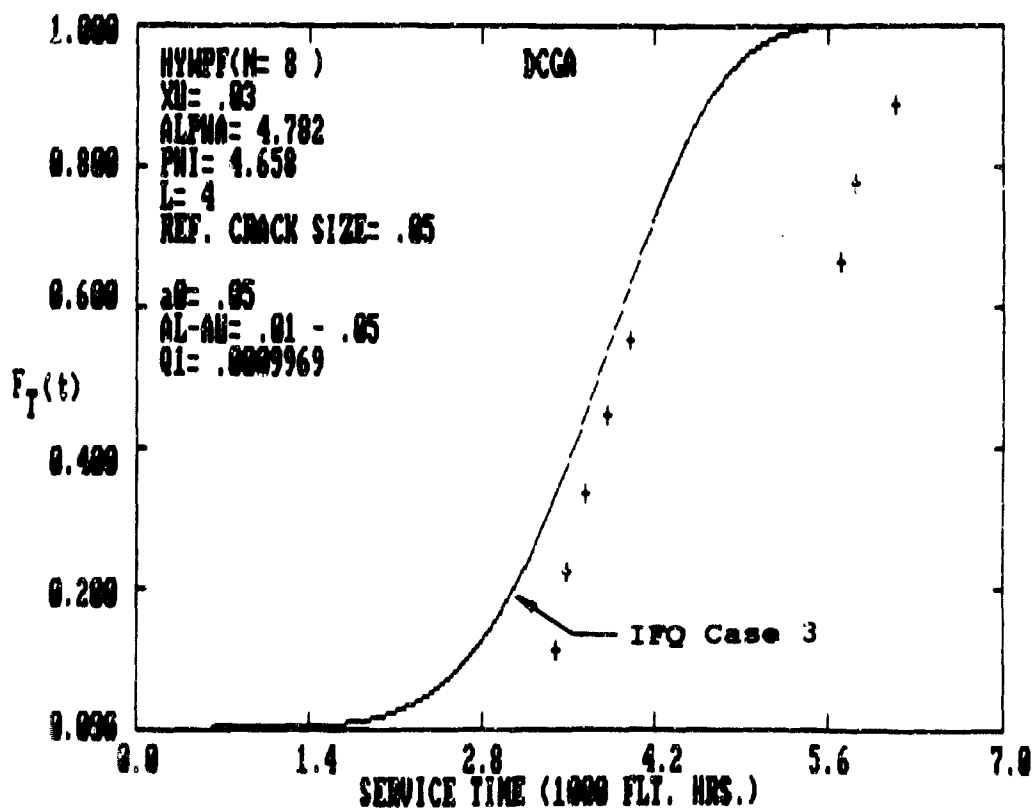


**Figure 44.** $F_T(t)$ Analytical and Experimental Correlations for HYWPF Data Set

65

fatigue cracks per data set (e.g., N = 6 for LYWPF and N = 8 for HYWPF).

4. Goodness-of-fit plots for $p(i, \mathcal{T})$ and/or $F_T(t)$ are essential to justify an EIFSD and statistical scaling for durability analysis.

5. The following aspects of statistical scaling need to be investigated further: (1) statistical independence of dominant fatigue cracks in fastener holes, (2) effect of variable stress level on scaling, (3) effect of bolt load transfer and variance on scaling, and (4) how to deal with fractographic data sets with significantly different mean EIFS values when estimating the EIFSD parameters using the data pooling procedure.

# SECTION IV
# DEMONSTRATION/EVALUATION OF DURABILITY ANALYSIS EXTENSION

## 4.1 INTRODUCTION

The purpose of this section is to demonstrate and evaluate the durability analysis extension for predicting the probability of crack exceedance in the large crack size range that may result in functional impairment such as fuel leaks and ligament breakage. Various theoretical approaches have been proposed for the durability analysis extension in Vol. I[1]. In this section, only the two-segment deterministic-deterministic (DCGA-DCGA) and deterministic-stochastic (DCGA-SCGA) crack growth analysis methodologies will be demonstrated, because these two approaches are the most promising. Other durability extension methodologies will be presented in the Appendix.

The demonstration/evaluation is performed at two levels: (1) coupon specimens, and (2) full-scale aircraft structure. Fractographic results for 1.5" wide double-reversed dog-bone type specimens [4] and the Weibull-compatible EIFSD function, given in Eq.1, are used to define the initial fatigue quality (IFQ) of straight-bore holes and countersunk fastener holes.

Durability analysis predictions will be made for 3" wide double-reversed dog-bone type specimens and for the F-16 lower wing skins. Analytical predictions will be correlated with actual test results for 3" wide test specimens [2] and for the F-16 durability test article [4]. Specifically, straight-bore holes and countersunk fastener holes in 7475-T7351 aluminum will be considered. The durability analysis extension will cover the large crack size regions, involving functional impairment, such as fuel leakage and ligament breakage.

The advanced durability analysis methodology is documented in Volume I [1]. Volume I should be referred to for further details about equations, concepts and methods. Key equations from Volume I, which will be used in the durability analysis, will be presented in the following.

This section includes the demonstration/evaluation of the following three parts: (1) countersunk fastener holes in dog-bone specimen (2) straight bore holes in dog-bone specimen, and (3) F-16 lower wing skins. Details of the investigation are given in the following sections. Results of this investigation are discussed, and observations/conclusions and recommendations are presented.

### 4.2 EQUATIONS FOR DURABILITY ANALYSIS EXTENSION

Two-segment crack growth approaches for the durability analysis extension are described in Fig. 45. Key equations for the durability analysis extension, derived in Volume I [1], for the two-segment DCGA-DCGA and DCGA/SCGA are presented in the following.

### 4.2.1 Deterministic-Deterministic Crack Growth Approach (DCGA-DCGA)

In the crack size region smaller than a reference crack size $a_0$, referred to as the first region, the service crack growth rate model is given by

$$da(t)/dt = Q_1[a(t)]^{b_1} \; ; \; a(t) \leq a_0 \tag{20}$$

The service crack growth rate model in the crack size region larger than $a_c$, referred to as the second region, is

68
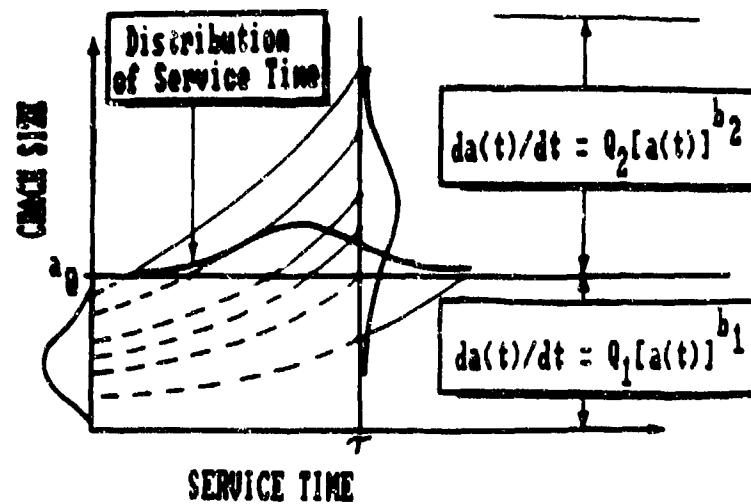
(a) Two-Segment Deterministic Crack
    Growth Approach (DCGA-DCGA)
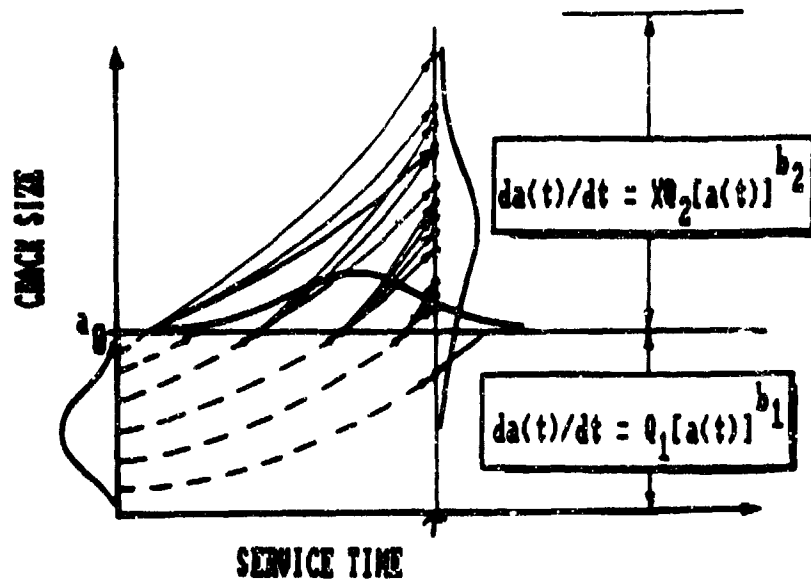
(b) Two-Segment Deterministic-Stochastic
    Crack Growth Approach (DCGA-SCGA)

Figure 45. Two-Segment Crack Growth Approaches
for Durability Analysis Extension.

69

$$da(t)/dt = Q_2 [a(t)]^{b_2}; \quad a(t) \geq a_0 \tag{21}$$

With the EIFSD given in Eq. 1 and the service crack growth rate models given in Eqs. 20 and 21 for $b_1 = b_2 = 1$, the distribution function, $F_{a(T)}(x_1) = P[a(T) \leq x_1]$, of the crack size, $a(T)$, at any service time $T$ can be derived as

$$F_{a(T)}(x_1) = F_{a(0)}[y(x_1; T)] \tag{22}$$

in which

$$y(x_1; T) = x_1 \exp(-qT); \quad x_1 \leq a_0 \tag{23}$$

and

$$y(x_1; T) = \left\{(x_1)^{Q_1/Q_2}\right\} \exp(\Lambda - q_1 T); \quad x_1 > q_0 \tag{24}$$

where

$$\Lambda = [1 - (Q_1/Q_2)] \ln a_0 \tag{25}$$

The probability of crack exceedance, $p(i, T)$, and the distribution of service time to reach a given crack size $x_1$, $F_{T(x_1)}(T)$, are derived as follows

$$p(i, T) = 1 - F_{a(T)}(x_1) = F_{T(x_1)}(T) \tag{26}$$

70

in which $F_{a(\mathcal{T})}(x_1)$ is given by Eqs. 22 - 25.

In using Eq. 26 for computing either the probability of crack exceedance $p(i,\mathcal{T})$ or the distribution of service time to reach any crack size $x_1$, $F_{T(x_1)}(\mathcal{T})$, the following distinction should be made: (1) for the crack exceedance probability $p(i,\mathcal{T})$ prediction, $\mathcal{T}$ is a selected fixed service time and $x_1$ is a variable crack size for crack exceedance, and (2) for $F_{T(x_1)}(\mathcal{T})$ prediction, $x_1$ is a selected fixed crack size and $t$ is a service time variable.

When the predictions are made for the largest crack in specimens with $l$ holes, i.e., the scaling factor is $l$, the solutions for $p(i,\mathcal{T})$ and $F_{T(x_1)}(\mathcal{T})$ are given in the following.

$$p(i,\mathcal{T}) = F_{T(x_1)}(\mathcal{T}) = 1 - \left\{ F_{a(0)}[y(x_1;\mathcal{T})] \right\}^{l} \tag{27}$$

### 4.2.2 Equations for the Two-Segment DCGA-SCGA

The service crack growth rate model in the first region is given in Eq. 20 whereas a stochastic crack growth rate model is used in the second region

$$da(t)/dt = X Q_2 [a(t)]^{b_2} ; \; a(t) \geq a_0 \tag{28}$$

in which X is a lognormal random variable with a unit median value. Thus, the statistical variability of the crack growth rate in the large crack size region is taken into account by the lognormal random variable X. Equation 28 is referred to as the lognormal random variable model [12-17, 39-40].

The probability density function of the lognormal random variable X with a median 1.0 is given by

$$f_X(u) = \frac{\log e}{\sqrt{2\pi}\, u\, \sigma_z}\, \exp\left\{-\frac{1}{2}\left[\frac{\log u}{\sigma_z}\right]^2\right\} \; ; \; u \geq 0 \qquad (29)$$
$$= 0 \qquad\qquad\qquad ; \; u < 0$$

in which $\sigma_z$ is the standard deviation of the normal random variable $Z = \log X$. Equation 29 is used when $\sigma_z$ is estimated using the log to base 10 form. If $\sigma_z$ is based on the natural log form, $f_X(u)$ given in Eq. 30 should be used.

$$f_X(u) = \frac{1}{\sqrt{2\pi}\, u\, \sigma_z}\, \exp\left\{-\frac{1}{2}\left[\frac{\ln u}{\sigma_z}\right]^2\right\} \; ; \; u \geq 0 \qquad (30)$$
$$= 0 \qquad\qquad\qquad ; \; u < 0$$

Two different expressions for $\sigma_z$, derived in Appendix C of Volume I [1], are given in Eqs. 31 and 32 for the natural log basis.

$$\sigma_z = \sqrt{\frac{1}{N}\sum_{j=1}^{m}\sum_{k=1}^{N_j}\left[\ln\left(da(t)/dt\right)_{jk} - \ln Q - \ln a_j(t_k)\right]^2} \qquad (31)$$

$$\sigma_z = \sqrt{\frac{1}{m}\sum_{j=1}^{m}\left[\ln\left(Q_j/Q\right)\right]^2} \qquad (32)$$

In Eqs. 31 and 32, m = the total number of fatigue cracks in the fractographic data set, $N_j$ = number of da(t)/dts for a(t)s in the second region for the jth fatigue crack, $N = \sum_{j=1}^{m} N_j$ = total number of [da(t)/dt, a(t)] pairs in the second region (da(t)/dt)$_{jk}$ = the kth crack growth rate value for the jth fatigue crack , $a_j(t_k)$ = crack size for the jth fatigue crack , $a_j(t_k)$ = crack size for the jth fatigue crack at the kth service time $t_k$ (i.e., k = 1, 2, ..., $N_j$), $Q_j$ = crack growth rate parameter for the jth fatigue crack defined by Eq. 5 and Q = "pooled Q" value for the fractographic data set defined by Eq. 6 in which $Q = Q_i$.

The distribution function, $F_{a(\mathcal{T})}(x_1) = P[a(\mathcal{T}) \leq x_1]$, of the crack size, $a(\mathcal{T})$, at any service time $\mathcal{T}$ can be derived from the distribution functions of $a(0)$ and $X$ given by Eqs. 1 and 29, respectively, through the transformation of Eqs. 20 and 28. The result for $b_1 = b_2 = 1$ is given as follows

(i) for $x_1 \leq a_0$

$$F_{a(\mathcal{T})}(x_1) = F_{a(0)}[y(x_1;\mathcal{T})] \tag{33}$$

in which $F_{a(0)}(y)$ is given by Eq. 1 and

$$y(x_1;\mathcal{T}) = x_1 \exp(-Q_1\mathcal{T}) \tag{34}$$

(ii) for $x_1 > a_0$

$$F_{a(\mathcal{T})}(x_1) = \int_0^\infty F_{a(0)}[G(x_1;\mathcal{T}\,|\,X = u)]\,f_X(u)\,du \tag{35}$$

in which $f_X(u)$ is given in Eq. 30 or 31 and

$$G(x_1;\mathcal{T}\,|\,X = u) = a_0 \exp(-Q_1\mathcal{T})(x_1/a_0)^{\gamma/u} \tag{36}$$

$$\gamma = Q_1/Q_2 \tag{37}$$

The probability of crack exceedence at a particular service time, $p(i,\mathcal{T})$, and the distribution function of service time to reach a given crack size $x_1$, $F_{T(x_1)}(\mathcal{T})$, are obtained from the distribution of $a(\mathcal{T})$ derived above

73

$$p(i, T) = F_{T(x_1)}(T) = 1 - F_{2(T)}(x_i) \tag{38}$$

For the prediction of largest cracks in specimens with a scaling factor of $\ell$, Eq. 27 should be used.

### 4.2.3 Extent of Damage Statistics

The extent of damage in an aircraft structure can be quantitatively defined in terms of the number of structural details expected to exceed any given crack size $x_1$ at a given service time $T$. The mean and upper/lower bound limits for the "extent of damage" can be estimated using the Binomial distribution [1,9-11,21,23,41]. From a functional impairment standpoint, the extent of damage can be interpreted as the average number of locations where the accumulated crack size exceeds limiting crack sizes for functional impairment. For example, a through-the-thickness crack in a fuel tank may cause fuel leakage and the dimension between adjacent structural details may be considered as a crack size limit for ligament breakage.

The number of details in the ith stress region with a crack size greater than $x_1$ at the service time $T$, is a statistical variable, the mean value $N(i, T)$, and the standard deviation, $\sigma_N(i, T)$, are determined using the Binomial distribution:

$$\bar{N}(i, T) = N_i \, p(i, T) \tag{39}$$

$$\sigma_N(i, T) = \left\{ N_i \, p(i, T)[1 - p(i, T)] \right\}^{1/2} \tag{40}$$

in which $N_i$ denotes the total number of details in the ith stress region. The average number of details with a crack size exceeding $x_1$ at the service time $T$ for m stress regions, $L(T)$, and the standard deviation, $\sigma_L(T)$, can be computed using Eqs. 41 and 42, respectively.

$$\bar{L}(T) = \sum_{\lambda=1}^{m} \bar{N}(\lambda, T) \qquad (41)$$

$$\sigma_{\bar{L}}(T) = \left[ \sum_{\lambda=1}^{m} \sigma_{N}^{2}(\lambda, T) \right]^{1/2} \qquad (42)$$

Equations 41 and 42 can be used to quantify the extent of damage for a single detail, a group of details, a part, a component, or an airframe. $\bar{L}(T)$ approximately corresponds to a 50% probability. Upper and lower bound limits for the "extent of damage" can be estimated using the Binomial distribution, e.g., $\bar{L}(T) \pm z\sigma_{\bar{L}}(T)$, with $z$ being the number of standard deviations, from the mean, $\bar{L}(T)$. Equations 39 - 42 are valid when the crack growth accumulation for each detail is statistically independent [6,9,23].

## 4.3 DEMONSTRATION FOR DOUBLE REVERSED DOG-BONE SPECIMENS

### 4.3.1 Countersunk Fastener Hole Specimens

The initial fatigue quality of countersunk fastener holes will be determined using the narrow specimen (Fig. 6) test results, i.e., AFXLR4, AFXMR4 and AFXHR4 data sets. Then, the durability analysis prediction will be made for the test results of wide specimen (Fig. 3), i.e., WAFXMR4 and WAFXHR4 data sets where large fatigue cracks exist. Correlations between the theoretical predictions and test results will be made to demonstrate the validity of the durability analysis methodology. The procedures are given as follows:

The WAFXMR4 and WAFXHR4 data sets are described in Table 12. Specimen design details are shown in Fig. 3. Specimen design details for the WAFXMR4 and WAFXHR4 data sets are the same as those for the AFXLR4, AFXMR4 and AFXHR4 data sets except the specimen width. For the latter three data sets the specimen width is 1.5" and for the former two data sets it is 3.00".

75

Table 12    Summary of Q   and   $\sigma_z$ for WAFXMR4 and WAFXHR4 Data Sets

| DATA SET [1] | % LT | NO. CRACKS | MAX. STRESS (ksi) | WIDTH (In.) | CRACK SIZE RANGE $a_o - AU'$ | Q x10⁴ (1/Hr.) | $\sigma_z$ [2] |
|---|---|---|---|---|---|---|---|
| WAFXMR4 | 15 | 14 | 34 | 3.00 | .05″-.5″ | 2.906 | .449 |
| WAFXHR4 | 15 | 13 | 40.8 | 3.00 | .05″-.5″ | 3.854 | .322 |

Notes:    (1)  Ref. Fig. 3 for specimen design details (7475-T7351 aluminum)
          (2)  Ref. Eq. 32 (Natural log basis)

1. Use the EIFSD parameters obtained from the pooled data set (i.e., AFXLR4, AFXMR4 and AFXHR4) in Section 3.3.1 to define the IFQ of countersunk fastener holes in 7475-T7351 aluminum for $x_u$ = 0.03". These parameter values are $x_u$ = 0.03", $\alpha$ = 1.716 and $\phi$ = 6.308 (see Table 13).

2. Determine the crack growth rate parameter $Q_1$ for WAFXMR4 and WAFXHR4 data sets in the small crack size region, (i.e., AL-AU = 0.01" - 0.05"), using the pooled Q values from AFXMR4 and AFXHR4 data sets, respectively. Determine the crack growth rate parameter $Q_2$ and the corresponding variability $\sigma_z$ for WAFXMR4 and WAFXHR4 data sets in the large crack size region (i.e., $a_0$ - AU' = 0.05"-.5") using the fractographic results for WAFXMR4 and WAFXHR4 data sets, respectively.

3. Predict the crack exceedance probability $p(i, \mathcal{T})$ in the large crack size region and the distribution of service time $F_{T(x_i)}(\mathcal{T})$ to reach any specified large crack size $x_1$. The two-segment DCGA-DCGA and DCGA-SCGA approaches will be used.

4. Correlate analytical predictions with the actual test results for two wide specimen data sets; i.e., WAFXMR4 and WAFXHR4. The investigation plan is described in Fig. 46.

WAFXMR4 and WAFXHR4 data sets were tested using the F-16 400 hour spectrum with a maximum peak gross stress of 34 ksi and 40.8 ksi, respectively. Theoretically, there is no significant difference in the peak stress at the edge of the fastener hole for narrow (W = 1.5") or wide (W = 3.0") specimen subjected to the same gross section stress. The narrow specimen has a slightly larger net section stress than the wide specimen. However, the narrow specimen has a smaller stress concentration factor than the wide specimen. These compensating factors are the reason the maximum peak stress

Table 13. Summary of IPQ Parameters for Pooled Countersunk Data Sets.

| DATA SET | NO. CRACKS | MAX. STRESS (ksi) | $\ell$ | AL-AU | $Qx10^4$ (1/HR.) | x (IN.) | $\alpha$ | $\phi$ | MEAN EIFS $x10^4$ |
|---|---|---|---|---|---|---|---|---|---|
| AFXLR4 | 10 | 32 | 4 | .01"-.05" | 2.101 | .02 | 1.330 | 6.704 | 42.40" |
| AFXMR4 | 9 | 34 | 4 | | 2.514 | .03 | 1.716 | 6.308 | 62.43" |
| AFXHR4 | 10 | 38 | 4 | | 6.062 | .05 | 2.132 | 6.453 | 34.29" |

Notes:  1.  CLSSA used
2.  Used data pooling procedure

78
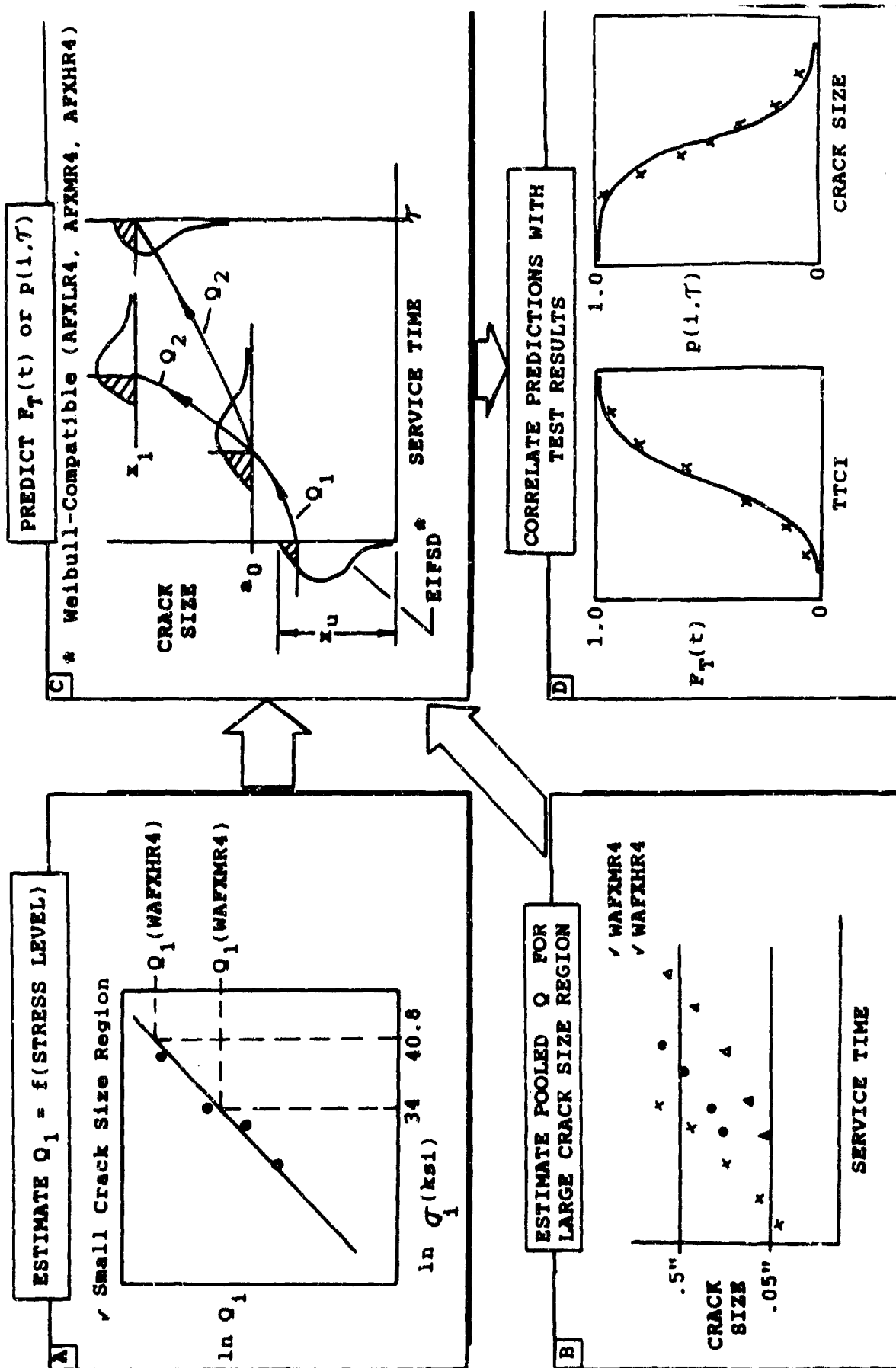
Figure 46. General Approach Used to Demonstrate the Two-Segment DCGA for WAFXMR4 and WAFXHR4 Data Sets.

79

at the edge of the fastener hole is virtually the same for both narrow and wide specimens subjected to the same gross section stress.

4.3.1.1 Estimation of Service Crack Growth Parameters. The crack growth behavior in the small and large crack size region must be characterized to implement the two-segment DCGA-DCGA and DCGA-SCGA. In the following demonstrations, AL-AU = 0.01" - 0.05" is chosen for the small crack size region whereas $a_0$-AU' = 0.05" - 0.5" is chosen for the large crack size region.

In reality, however, crack growth rate data are usually not available for service conditions in which the crack exceedance probability should be predicted. For instance, crack growth rate data in various stress regions of the F-16 lower wing skins are not available. Hence, crack growth parameters $Q_1$ and $Q_2$ should be estimated using either an analytical crack growth program [e.g., 18,19] or suitable fractographic results [e.g., 2-4] if available. In any case, $Q_1$ should be compatible with the basis in which the EIFS master curve(s) is established for defining the EIFSD parameters. This aspect is discussed in Volume I [1].

EIFSD parameters for countersunk fastener holes were defined in Section 4.2.3 using three narrow width (w = 1.5") specimen data sets (i.e., AFXLR4, AFXMR4, AFXHR4). Pooled Q values for these three data sets are shown in Table 13.

The crack growth rate parameters $Q_1$ and $Q_2$ vary with respect to service loading conditions. However, when all service loading conditions are identical, such as loading spectra, percentage of load transfer, type of fastener holes, etc., except the maximum gross section stress level $\sigma$, a very reasonable model relating the crack growth rate parameter Q and the maximum gross section stress has been proposed by

Yang and Manning as follows [6,8,20].

$$Q = C\sigma^V \tag{43}$$

in which C and V are empirical parameters.

Thus, if fractographic data sets are available under several different gross stress levels, $\sigma$, the empirical parameters C and V can be determined from Eq. 43 using the least square fit procedure. Then, an alternate approach to determine the crack growth rate parameters $Q_1$ and $Q_2$ is to use Eq. 43. For demonstrative purpose, since applicable fractographic results in the small crack size region are available for AFXLR4, AFXMR4 and AFXHR4 narrow specimen data sets, Eq. 43 will be used to determine the crack growth rate parameters $Q_1$ for WAFXMR4 and WAFXHR4 data sets as well as various stress regions in the lower wing skin of F-16 aircraft.

In the small crack size region of AL-AU = 0.01" - 0.05", Q values versus gross stresses for the AFXLR4, AFXMR4 and AFXHR4 data sets shown in Table 13 are plotted in Fig. 47 as solid circles. Using the model of Eq. 43 and a least-squares-fit procedure, a straight line is obtained in Fig. 47; with C = $4.829 \times 10^{-4}$ and V = 6.38. With the values of C and V given above as well as the gross stresses for WAFXMR4 and WAFXHR4 data set, $Q_1$ values for these two data sets are computed from Eq. 43 as $2.851 \times 10^{-4}$ per hour and $9.126 \times 10^{-4}$ per hour, respectively.

Fractographic results available in the large crack size range, i.e., $a_0$ - AU' = 0.05" - 0.5", for AFXLR4, AFXMR4 and AFXHR4 data sets are not sufficient to determine the respective pooled $Q_2$ values, because the specimens for these data sets are only 1.5" wide. As a result, the crack growth rate parameters $Q_2$ and the corresponding variabilities $\sigma_2$ in segment 2, i.e., $a_0$ - AU' = 0.05" - 0.5", for WAFXMR4 and WAFXHR4

GROSS STRESS, MPa

CRACK GROWTH RATE PARAMETER: $Q_1 \times 10^4$

AL-AU = .01"-.05"

Segment 1

AFXHR4

AFXMR4

AFXLR4

$Q_1 = 4.829 \times 10^{-14} \sigma^{6.380}$

$\sigma$ Basis (ksi)
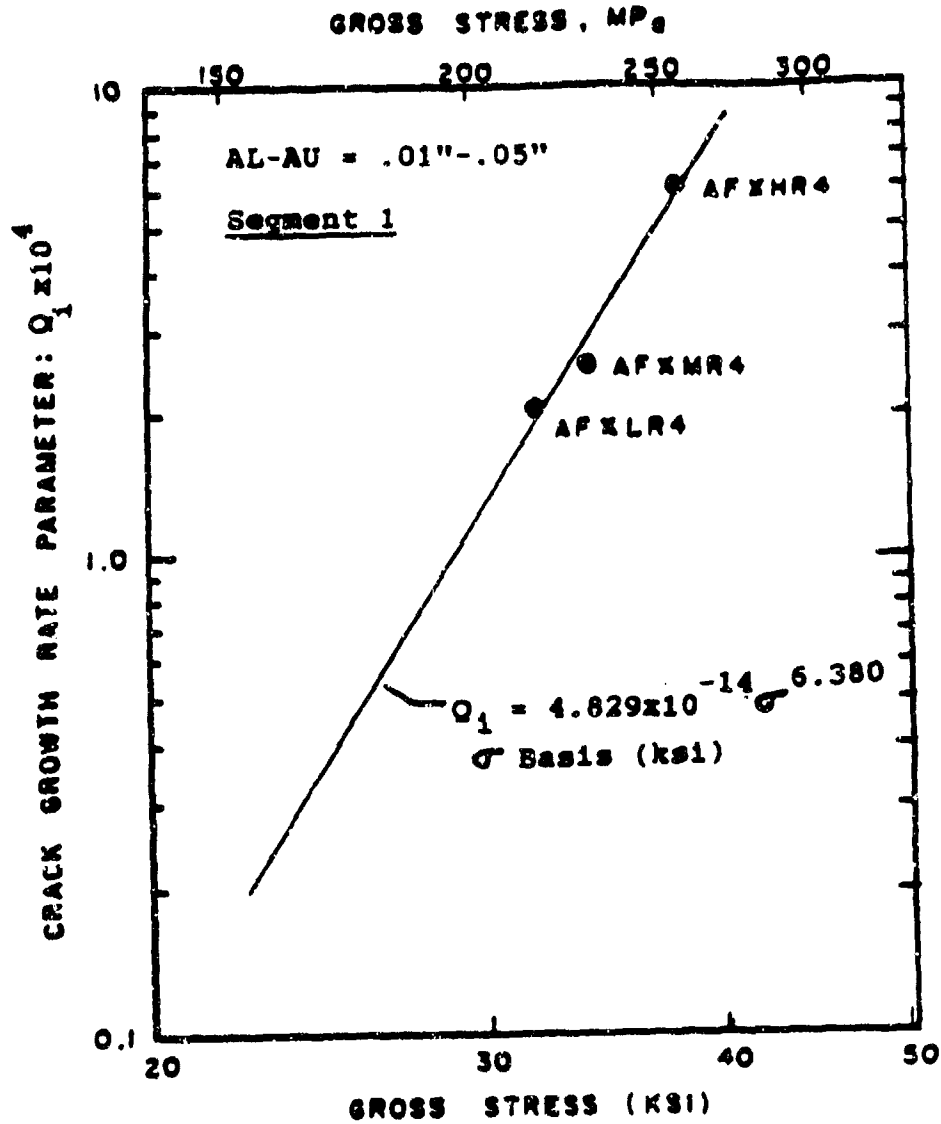
GROSS STRESS (KSI)

Figure 47. Crack Growth Parameter Q Versus Gross Stress for Narrow Specimen Data Sets (AFXLR4, AFXMR4, AFXHR4).

82

were determined using the fractographic results of these two data sets. $Q_2$ and $\sigma_Z$ values for WAFXMR4 and WAFXHR4 are summarized in Table 12 in which the value of $Q_2$ is denoted as $Q$.

4.3.1.2 Theoretical/Experimental Correlations. Theoretical predictions for the probability of crack exceedance $p(i,T)$, and the cumulative distribution of service time to reach any crack size $x_1$, $F_{T(x_i)}(t)$, for the WAFXMR4 and WAFXHR4 data sets have been computed using the DCGA-DCGA and the DCGA-SCGA. All results are based on the following EIFSD parameters for the Weibull compatible distribution function: $x_u = 0.03"$, $\alpha = 1.716$, $\phi = 6.308$ (see Table 13).

The following results are presented for the DCGA-DCGA: (1) Probability of crack exceedance plots at $T = 11608$ and 7000 flight hours are shown in Figs. 48 and 49, respectively for the WAFXMR4 and WAFXHR4 data sets. (2) The cumulative distributions of service time to reach a crack size $x_1 = 0.73"$ and $0.59"$ are shown in Figs. 50 and 51, respectively for WAFXMR4 and WAFXHR4. In these figures, the theoretical predictions are shown by the solid curves; whereas, experimental results are displayed by solid circles.

Using the DCGA-SCGA, theoretical/experimental correlation plots corresponding to Figs. 48-51 are presented in Figs. 52 - 55.

4.3.1.3 Discussion of Results. The following observations are made based on the results presented in Figs. 48-55:

1. The DCGA-DCGA predictions correlated reasonably well with the experimental results for the WAFXMR4 and the WAFXHR4 data sets in the central portion of the population. However, the correlation was poor at the tail portion of the distribution (see Figs. 48 - 51).
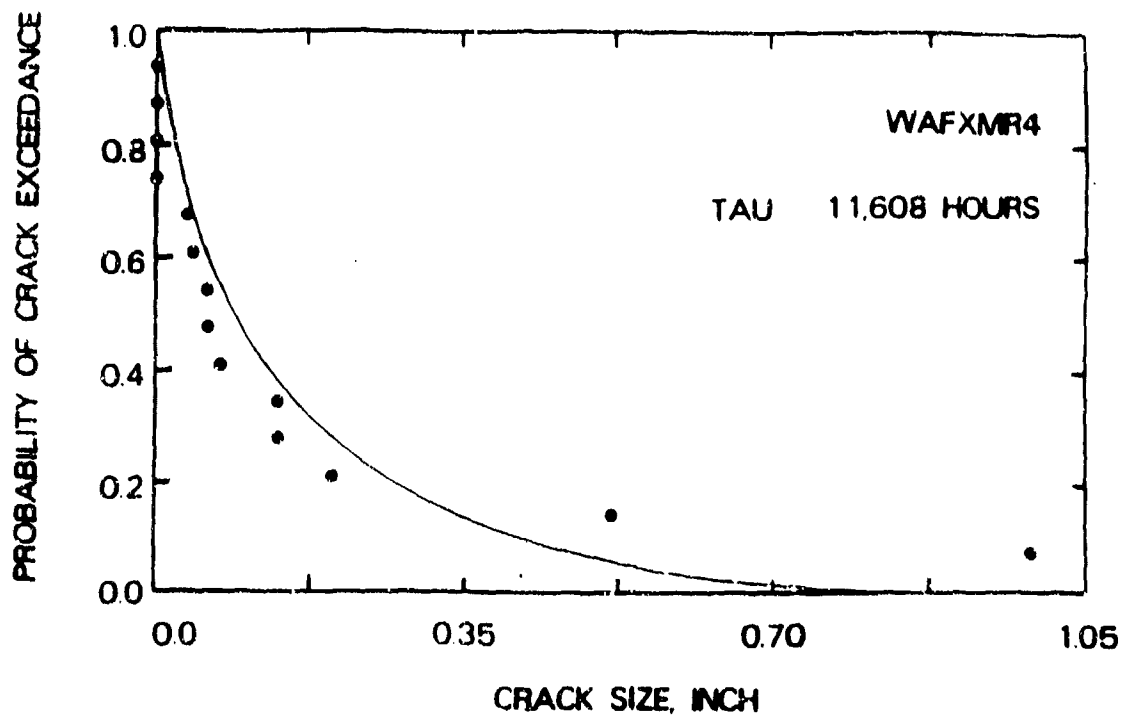
Figure 48.　Correlations Between Theoretical Predictions and Experimental Results (WAFXMR4 Data Set) for Crack Exceedance Probability p(i, $\mathcal{T}$) at $\mathcal{T}$ = 11608 Flight Hours Based on DCGA-DCGA.
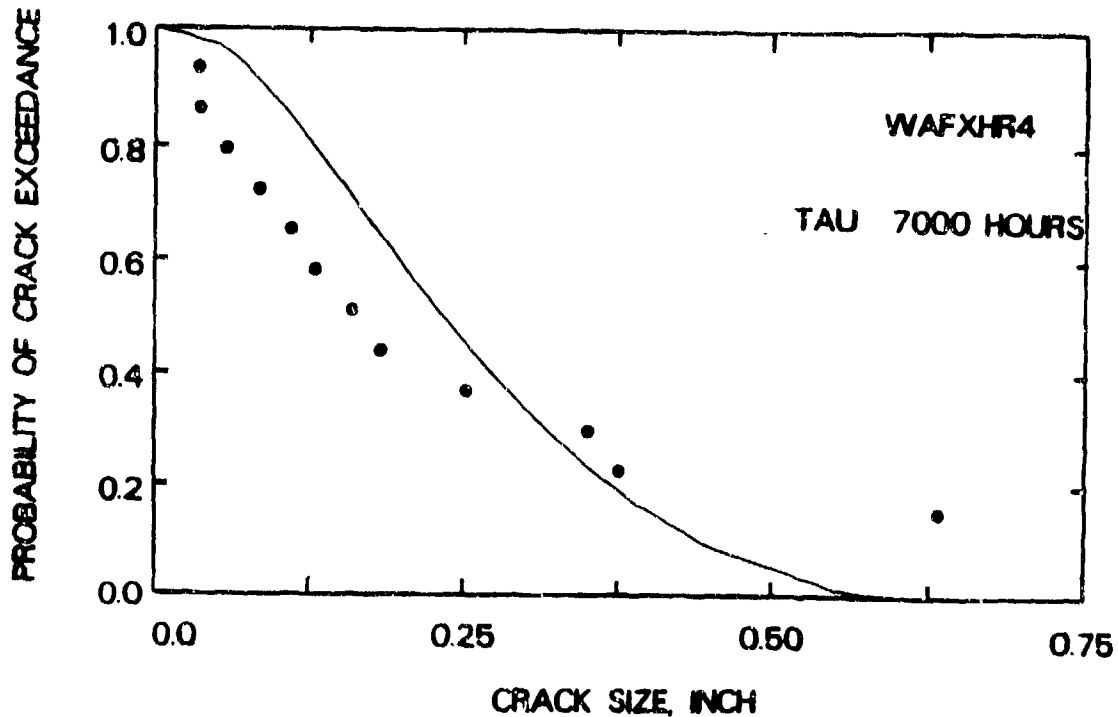


Figure 49.　Correlations Between Theoretical Predictions and Experimental Results (WAFXHR4 Data Set) for Crack Exceedance Probability p(i, $\mathcal{T}$) at $\mathcal{T}$ = 7000 Flight Hours Based on DCGA-DCGA.

84
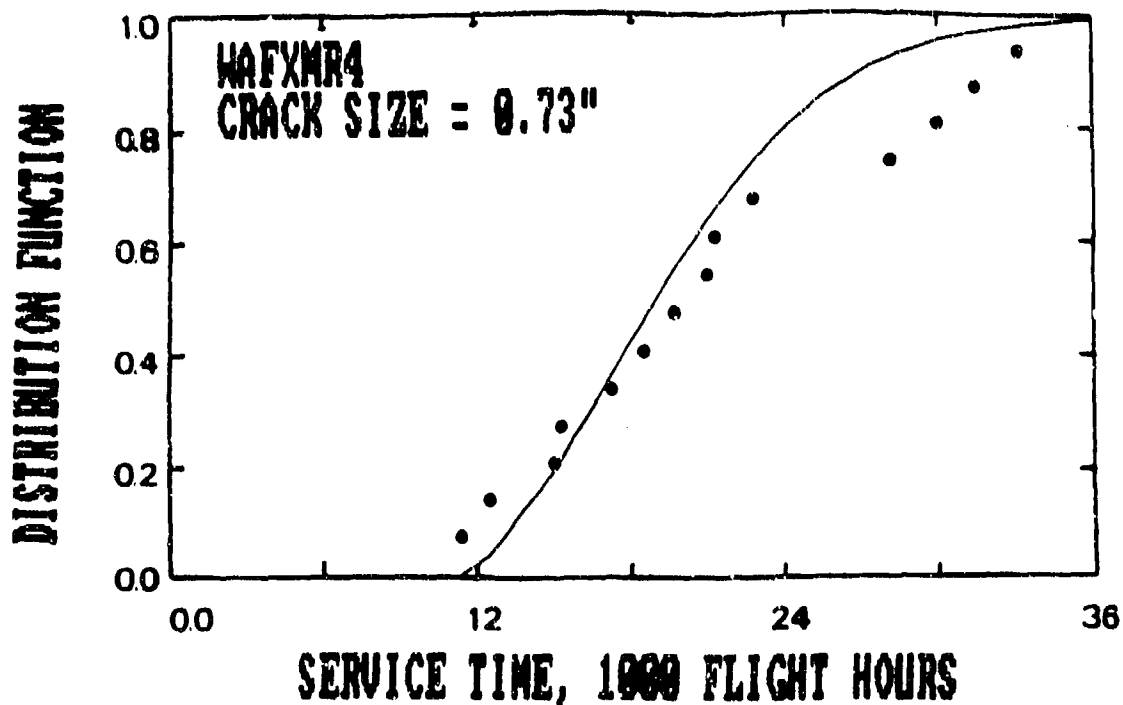
Figure 50.    Correlations Between Theoretical Predictions and
              Experimental Results (WAFXMR4 Data Set) for Cumulative
              Distribution of Service Time to Reach Crack Size $x_1$ =
              .73" Based on DCGA-DCGA.
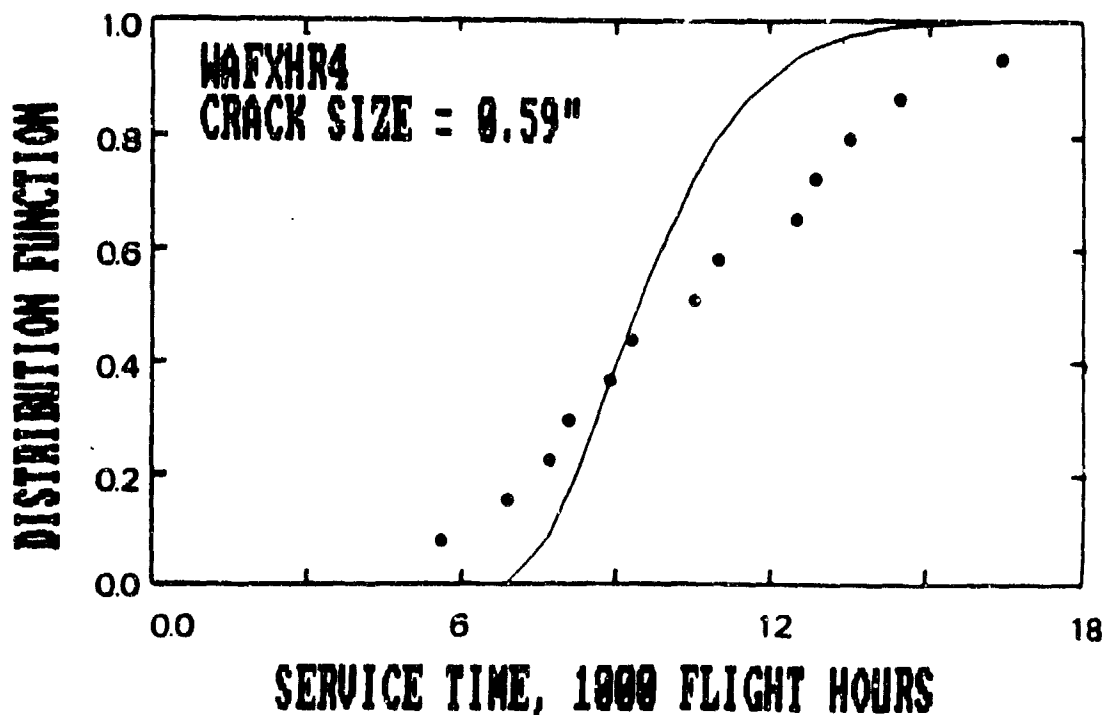


Figure 51.    Correlations Between Theoretical Predictions and
              Experimental Results (WAFXHR4 Data Set) for Cumulative
              Distribution of Service Time to Reach Crack Size $x_1$ =
              .59" Based on DCGA-DCGA.

WEIBULL COMPATIBLE
TAU    11,608 HOURS          WAFXMR4
ALPHA 1.716,PHAI 6.308,XU 0.03
STD. 0.449,Q .0002851,Q1 0.0002906
2-SEGMENT DCGA-SCGA APPROACH
SCALING FACTOR 4, POOLED DATA
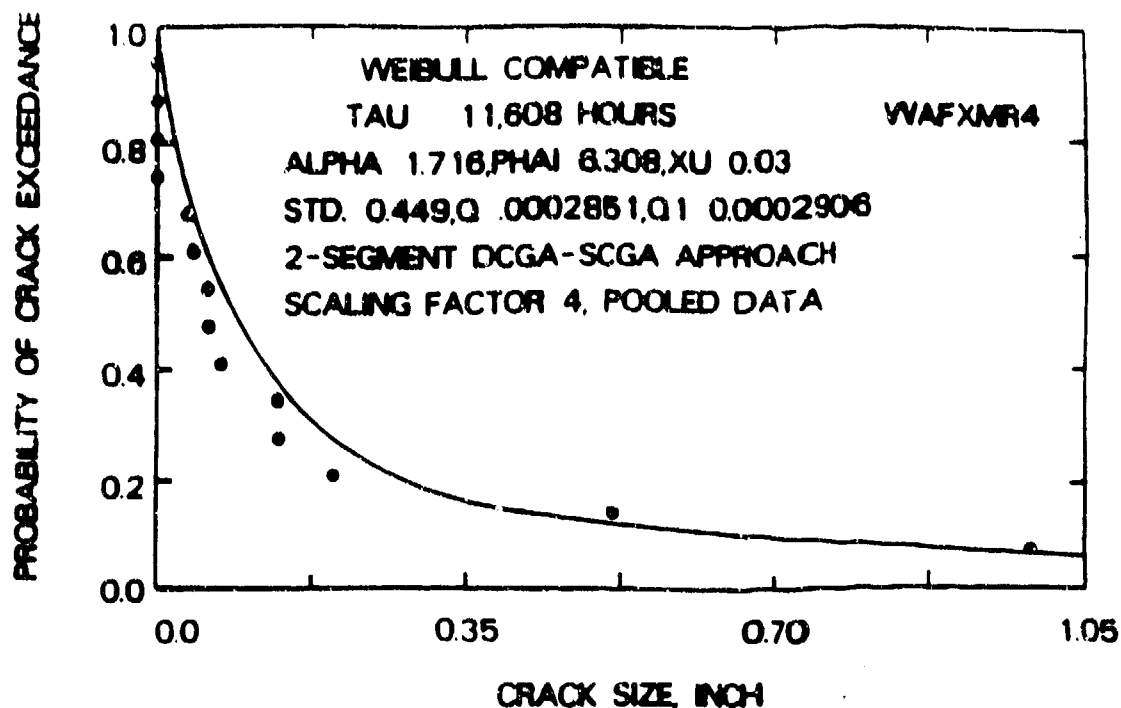
Figure 52.   Correlations Between Theoretical Predictions and Experimental Results (WAFXMR4 Data Set) for Crack Exceedance Probability $p(i, \mathcal{T})$ at $\mathcal{T}$ = 11608 Flight Hours Based on DCGA-SCGA.



WAFXHR4
WEIBULL COMPATIBLE
TAU    7000 HOURS
ALPHA 1.716,PHAI 6.308,XU 0.03
STD. 0.322,Q .0009126,Q1 0.0003854
2-SEGMENT DCGA-SCGA APPROACH
SCALING FACTOR 4, POOLED DATA
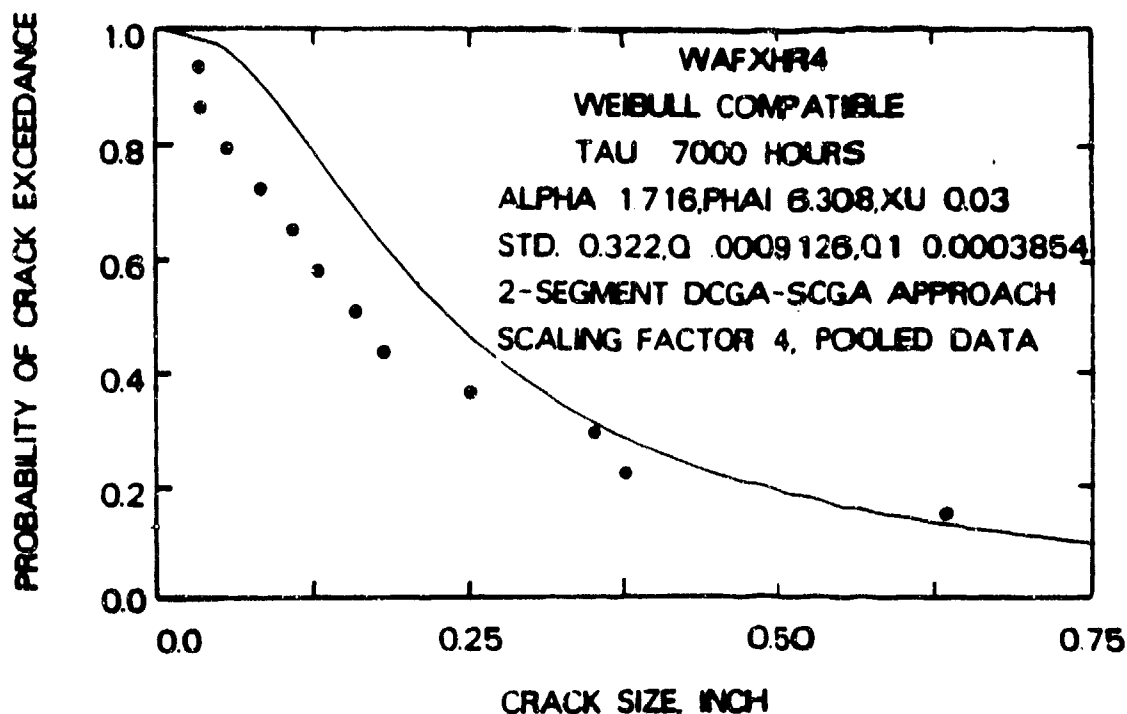
Figure 53.   Correlations Between Theoretical Predictions and Experimental Results (WAFXHR4 Data Set) for Crack Exceedance Probability $p(i, \mathcal{T})$ at $\mathcal{T}$ = 7000 Flight Hours Based on DCGA-SCGA.

86

CRACK SIZE 0.73 IN
ALPHA 1.7 ι6,PHAI 6.308,XU 0.03
STD. 0.449,Q .0002851,Q1 0.0002906
2-SEGMENT DCGA-SCGA APPROACH
SCALING FACTOR 4, POOLED DATA
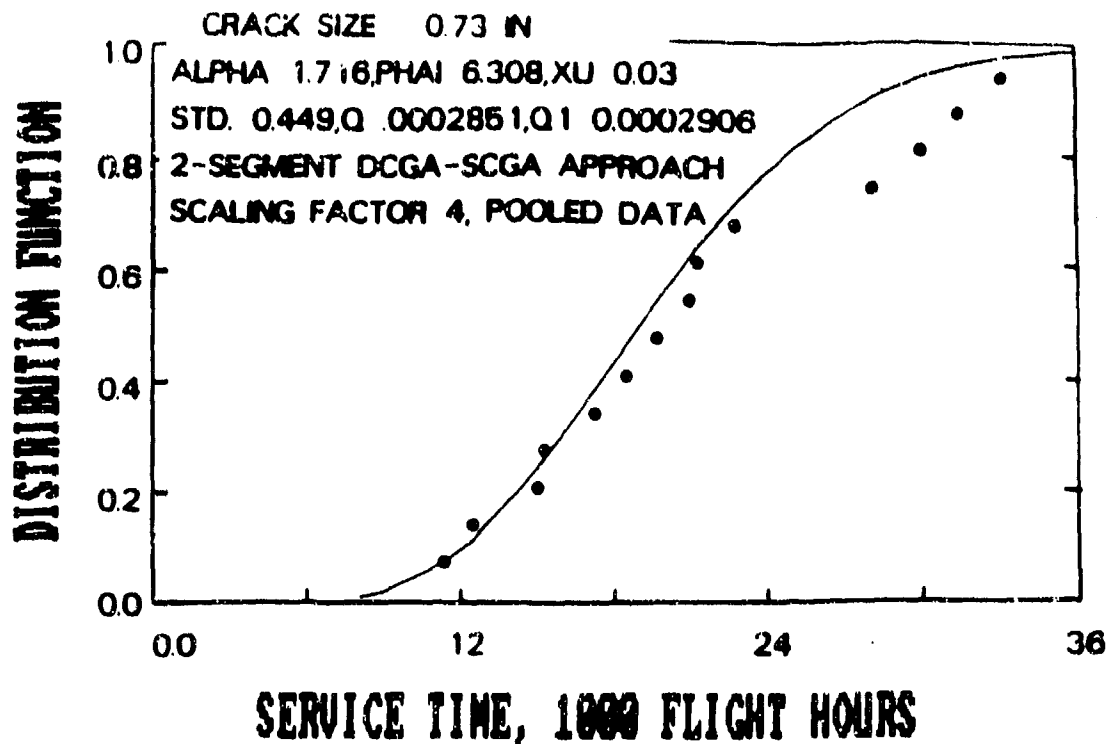
Figure 54. Correlations Between Theoretical Predictions and Experimental Results (WAFXMR4 Data Set) for Cumulative Distribution of Service Time to Reach Crack Size $x_1$ = .73" Based on DCGA-DCGA.



CRACK SIZE 0.59 IN
ALPHA 1.716,PHAI 6.308,XU 0.03
STD. 0.322,Q .0009126,Q1 0.0003854
2-SEGMENT DCGA-SCGA APPROACH
SCALING FACTOR 4, POOLED DATA
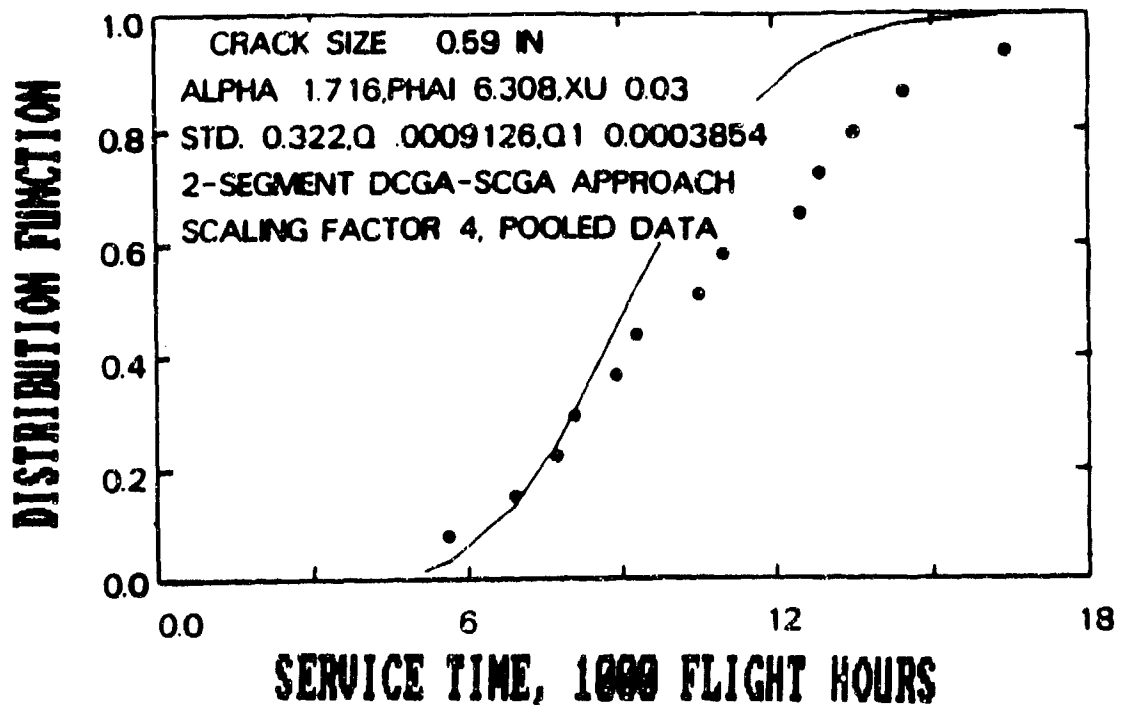
Figure 55. Correlations Between Theoretical Predictions and Experimental Results (WAFXHR4 Data Set) for Cumulative Distribution of Service Time to Reach Crack Size $x_1$ = .59" Based on DCGA-SCGA.

87

2. Excellent correlations were obtained for the WAFXMR4 and WAFXHR4 data sets for the DCGA-SCGA. In this case, better overall correlations were obtained using the DCGA-SCGA than the DCGA-DCGA.

3. The correlations for the WAFXMR4 data sets were slightly better than those for the WAFXHR4 data set for both the DCGA-DCGA and the DCGA-SCGA.

4.3.2 Straight-Bore Fastener Hole Specimens

The durability analysis extension for the DCGA-DCGA and the DCGA-SCGA are demonstrated for straight-bore clearance-fit fastener holes in 7475-T7357 aluminum herein. Procedures for the demonstration are given as follows.

1. The IFQ for straight-bore clearance-fit fastener holes is based on the Weibull-compatible EIFSD. Two narrow width (W = 1.5") specimen data sets (WPF and XWPF; see Figs. 4 and 5, respectively) and a data pooling procedure [1] were used to estimate the EIFSD parameters with the results: $x_u$ =0.03", $\alpha$ = 4.782 and $\phi$ = 4.658. These parameters are given in Table 11 under IFQ case 3 and they will be used for demonstration purposes herein. Details for estimating these parameters are given in Section 3.3.2.2.

2. The crack growth rate model of Eqs. 20 and 28 (with $b_1 = b_2 = 1$) and fractographic data for the WWPF data set are used to estimate the crack growth parameter $Q_1$ and $Q_2$ respectively, in the small and large crack size regions. In the present demonstrations, AL-AU = 0.01" - 0.05" is used for the small crack size region (i.e., "segment 1") and $a_0$ - AU' = 0.05" - 1" is used for the large crack size region (i.e., "segment 2"). Results for $Q_1$, $Q_2$ and $\sigma_z$ for the WWPF data set are summarized in Table 14.

Table 14. Summary of Pooled Q and $\sigma_z$ Values for WWPF Data Set.

| DATA SET (1) | NO. SPECIMENS | SEGMENT 1 (3) Q x10$^4$ (1/HR.) | SEGMENT 2 (4) Q x10$^4$ (1/HR.) | $\sigma_z$ |
|---|---|---|---|---|
| WWPF (2) | 13 | 2.742 | 3.124 | 0.177 |

Notes: (1) Material: 7475-T7351 aluminum; straight-bore fastener holes with clearance-fit fasteners (NAS 6204-08)
(2) Ref. Fig. 2
(3) $AL - AU = 0.01" - 0.05"$
(4) $a_0 - AU = 0.05" - 1"$
(5) Ref. Eq. 32 (natural log basis)

3. Theoretical predictions for the probability of crack exceedance, $p(i,T)$, at service time $T = 18,400$ flight hours, are shown in Figs. 56 and 57 for the DCGA-DCGA and the DCGA-SCGA, respectively. In both figures experimental results for the WWPF data set are plotted as plus signs (+) for comparison.

4. Theoretical predictions for the cumulative distribution of service time to reach a crack size $x_1 = 0.5"$ are shown in Figs. 58 and 59 for the DCGA-DCGA and the DCGA-SCGA, respectively. Experimental results for the WWPF data set are plotted as plus signs (+) for comparison.

The following observations are based on the plots shown in Figs. 56 - 59 for the WWPF data set and the lessons learned under this program.

1. Excellent correlations were obtained between predictions for $p(i,T)$ and $F_{T(x_1)}(T)$ and experimental results for the WWPF data set for both the DCGA-DCGA and DCGA-SCGA (see Figs. 56 - 59).

2. A statistical scaling procedure was developed in Vol. 1 [1] so that fractographic results for specimens with a different number of holes per specimen could be used to estimate the EIFSD parameters in a global sense. IFQ case 3 (see Table 11) was used for the demonstration herein. The statistical scaling technique reflected in IFQ case 3 is recommended for durability analysis predictions. However, scaling the fractographic results for specimens with a different number of fastener holes involves complex issues, e.g., fatigue cracking interactions in fastener holes, bolt load transfer, assumption of independent cracking, etc. Further research on statistical scaling is needed to better understand the ef-
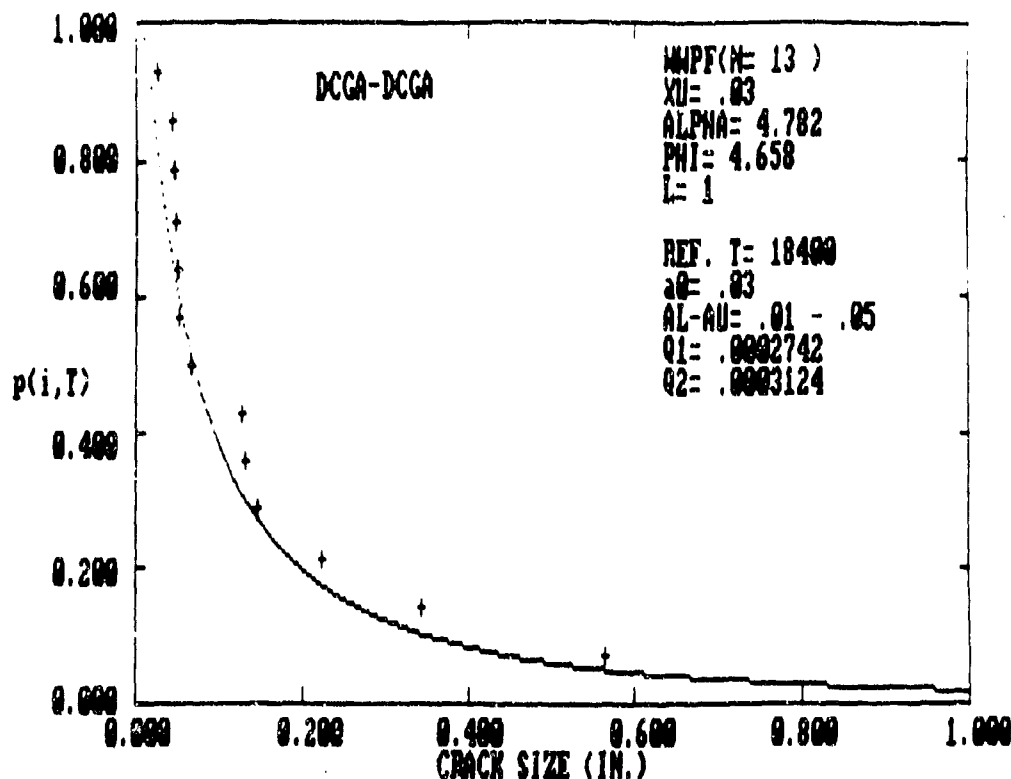
Figure 56. Correlations Between Theoretical Predictions and Experimental Results (WWPF Data Set) for Crack Exceedance Probability p(i,$\mathcal{T}$) at $\mathcal{T}$ = 18400 Flight Hours Based on DCGA-DCGA.
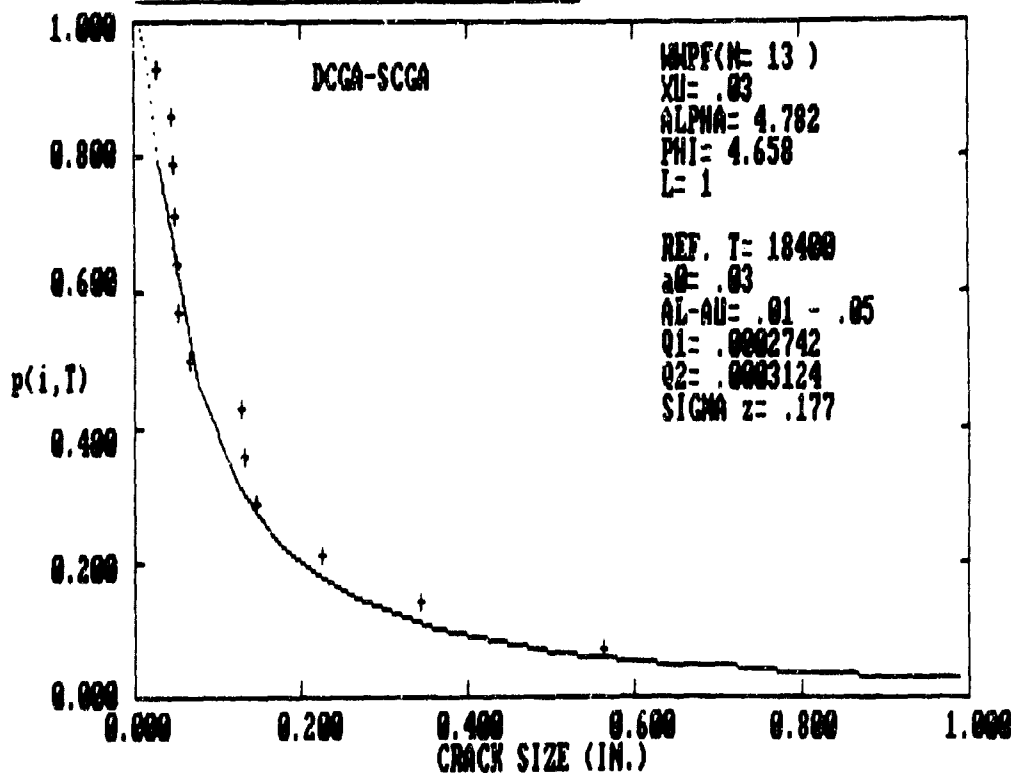


Figure 57. Correlations between Theoretical Predictions and Experimental Results (WWPF Data Set) for Crack Exceedance Probability p(i,$\mathcal{T}$) at $\mathcal{T}$ = 18400 Flight Hours Based on DCGA-SCGA.

91
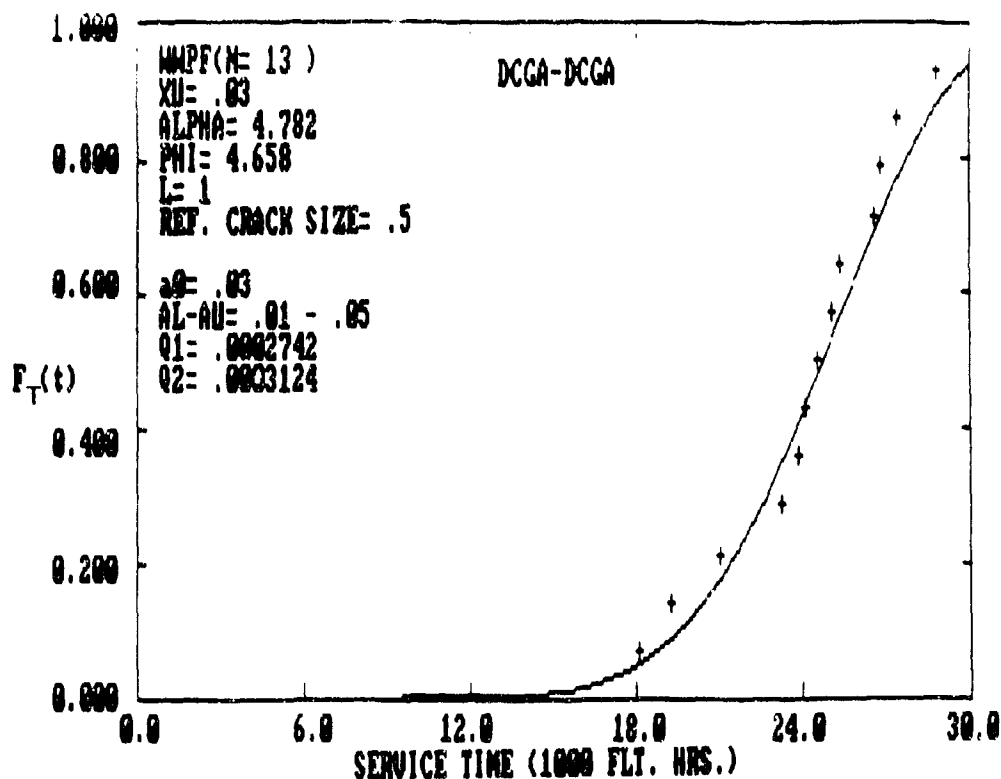
**Figure 58.** Correlations Between Theoretical Predictions and Experimental Results (WWPF Data Set) for Cumulative Distribution of Service Time to Reach Crack Size $x_1$ = 0.5" Based on DCGA-DCGA.
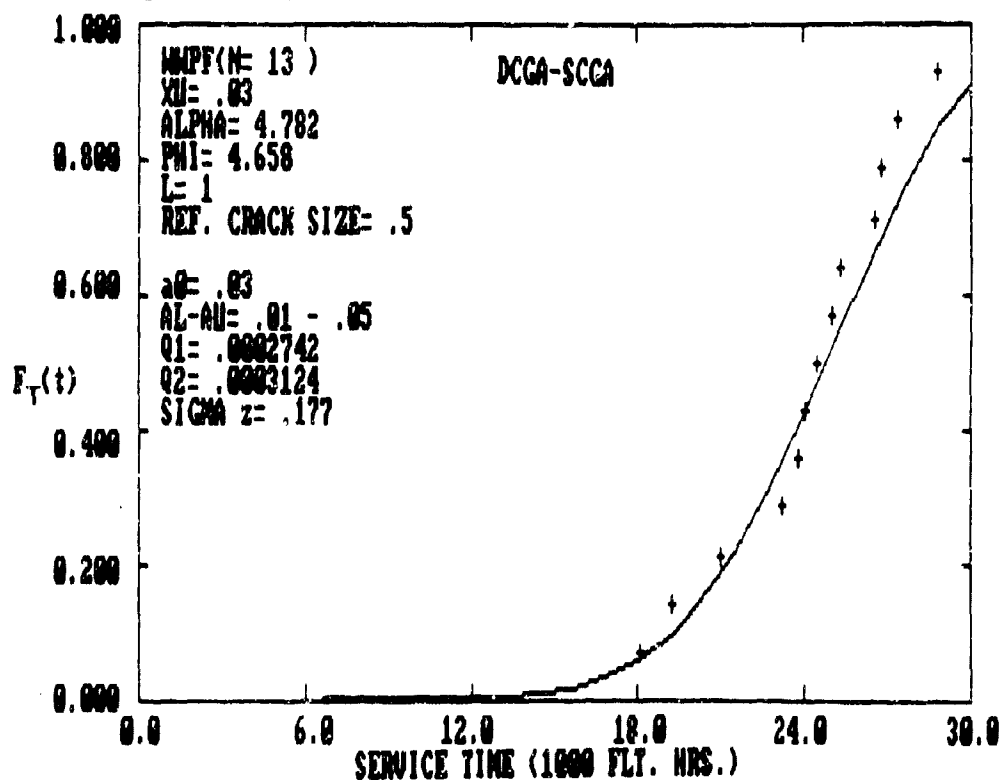


**Figure 59.** Correlations Between Theoretical Predictions and Experimental Results (WWPF Data Set) for Cumulative Distribution of Service Time to Reach Crack Size $x_1$ = 0.5" Based on DCGA-SCGA.

fects of scaling on the initial fatigue quality estimation and the accuracy for $p(i, \mathcal{T})$ and $F_{T(x_i)}(\mathcal{T})$ predictions.

3. Predictions for $p(i, \mathcal{T})$ and $F_{T(x_i)}(\mathcal{T})$ based on the DCGA-SCGA correlated slightly better than those based on the DCGA-DCGA, particularly in the large crack size region. Therefore, based on the results presented herein, the DCGA-SCGA is considered to be superior to the DCGA-DCGA.

### 4.4 DEMONSTRATION FOR THE F-16 LOWER WING SKINS

The two-segment DCGA-DCGA and DCGA-SCGA are demonstrated and evaluated in the following using the F-16 lower wing skin. Predictions will be correlated with results from the F-16 wing durability test articles. The F-16 wing box assembly is shown in Fig. 60 and stress regions for the lower wing skin are shown in Fig. 61.

A full-scale F-16 wing durability test was conducted using the F-16 1000 hour spectrum, consisting of two 500-hour blocks. After fatigue testing to 16,000 flight hours, a tear-down inspection was performed. All fastener holes in both lower wing skins (i.e., 3228 holes) were inspected using the eddy current technique. Each fastener hole with a crack indication was broken open and a fractographic analysis was performed. Tear-down inspection and fractographic results are documented in Ref. 4.

A durability analysis of the F-16 lower wing skins has been previously reported [8,9,11,20]. This analysis was concerned with relatively small fatigue cracks (e.g., $x_1 \leq 0.03"$) and reflected the one-segment DCGA [6,8].

The following procedures are used to demonstrate and
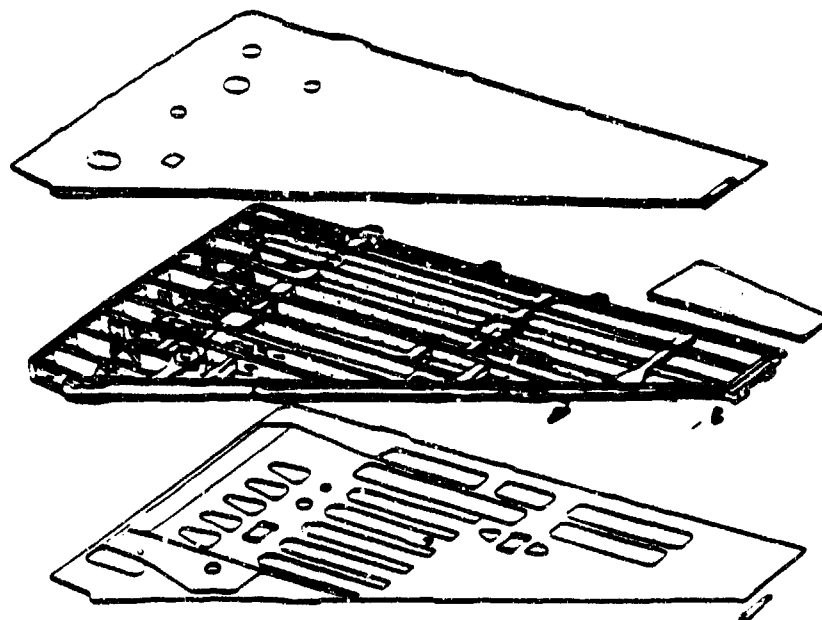
Figure 60.   F-16 Wing Box Assembly.
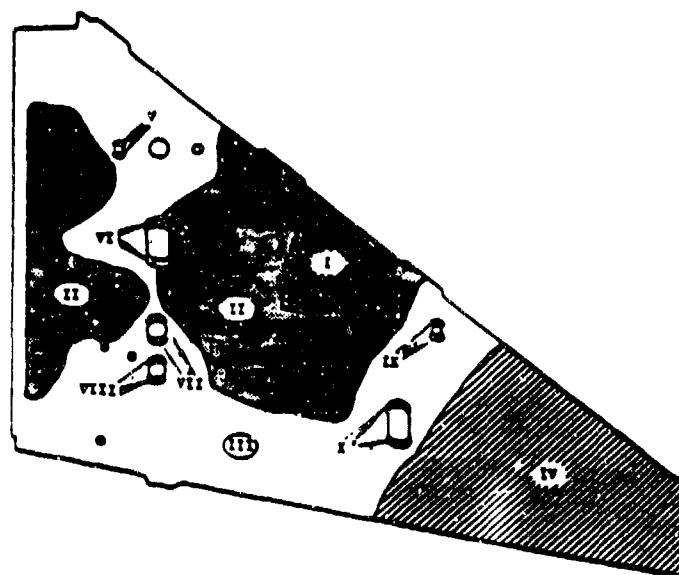


Figure 61.   Stress Regions for F-16 Lower Wing Skin.

evaluate the two-segment DCGA-DCGA and DCGA-SCGA using the F-16 lower wing skins.

1. The IFQ is based on the fractographic results from AFXLR4, AFXMR4 and AFXHR4 data sets. A data pooling procedure based on the CLSSA is used to estimate the Weibull compatible EIFSD parameters; with the results used: $x_u$ = 0.03", $\alpha$ = 1.716 and $\phi$ = 6.308, see Table 13. These EIFSD parameters, based on the AL-AU = 0.01" - 0.05" and $\ell$= 4 for each of the three data sets, characterize the distribution of EIFS for a single hole population.

2. The F-16 lower wing skin is divided into 10 stress regions as shown in Fig. 61. The stress level and the number of fastener holes in each stress region are shown in Table 15.

3. The crack growth rate parameter, $Q_1$ for segment 1, in each stress region are determined using (1) the available pooled Q values from the AFXLR4, AFXMR4 and AFXHR4 data sets (see Table 13; AL-AU = 0.01" - 0.05"), and (2) the model for Q as a function of stress given by Eq. 43. Results of the model parameters C and V in Eq. 43 obtained from three data sets (AFXLR4, AFXMR4 and AFXHR4) are shown in Figs. 47 and 62(a).

4. The crack growth rate parameters, $Q_2$, for segment 2 in each stress region are determined using available wide specimen fractographic results of WAFXMR4 and WAFXHR4 in $a_0$ - AU' = 0.05" - 0.5" along with Eq. 43. The model parameters C and V obtained from WAFXMR4 and WAFXHR4 data sets are shown in Fig 62(b).

5. Prediction for $p(i,T)$ in each stress region using the two-segment DCGA-DCGA is computed from Eqs 22 - 26. Equations 33 - 38 are used to compute $p(i,T)$ in each stress region using the DCGA-SCGA.

Table 15.  Stress Levels and Number of Fastener
Holes for F-16 Lower Wing Skin

| STRESS REGION | MAX. STRESS LEVEL (ksi) | NO. OF FASTENER HOLES |
|---|---|---|
| I | 28.3 | 59 |
| II | 27.0 | 320 |
| III | 24.3 | 680 |
| IV | 16.7 | 469 |
| V | 28.4 | 8 |
| VI | 29.2 | 30 |
| VII | 32.4 | 8 |
| VIII | 26.2 | 8 |
| IX | 26.2 | 12 |
| X | 25.7 | 20 |

1614

**ESTIMATE $Q_1$**

**A**

AL-AU = .01"-.05"

$\ln Q$

AFXHR4

AFXLR4

AFXMR4

$Q_1 \leftarrow$

$Q_1 = C\sigma^V$

$C = 4.829 \times 10^{-4}$
$V = 6.380$

$\sigma_1^*$

$\ln \sigma$

*For each of 10 stress regions

**ESTIMATE $Q_2$**

**B**

$a_0$-AU' = .05"-.5"

$Q_1 \leftarrow$

WAFXHR4

WAFXMR4

$\ln Q$

$Q_1 = C\sigma^V$

$C = 1.234 \times 10^{-6}$
$V = 1.549$

$\sigma_1^*$

$\ln \sigma$

*For each of 10 stress regions
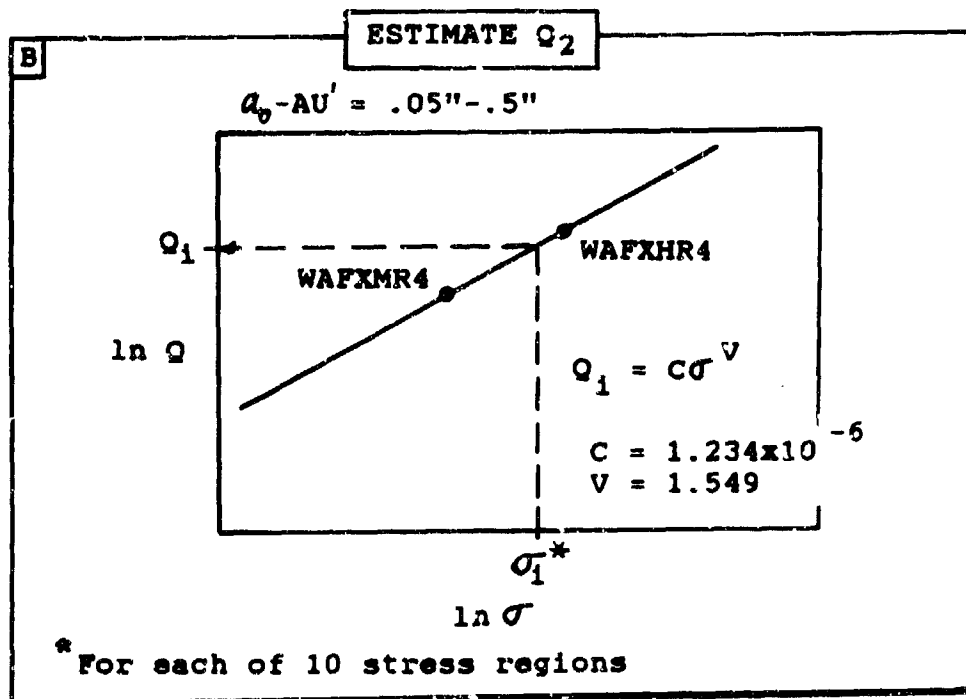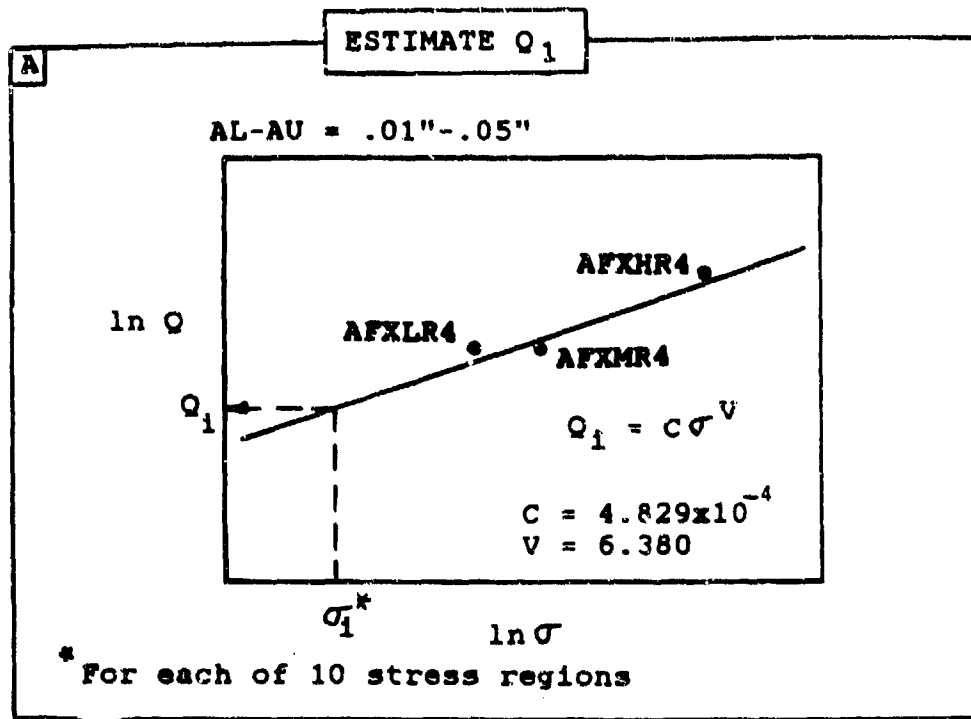
Figure 62. <u>General Approach for Estimating Service Crack
Growth Parameters $Q_1$ and $Q_2$</u>.

6. From the predicted crack exceedance probability, $p(i, \tau)$, and the number of fastener holes in each stress region, the statistics for the number of cracks exceeding some crack sizes in the entire lower wing skin are computed using the Binomial distribution, Eqs. 39 - 42.

7. Theoretical predictions will be correlated with actual test results from the F-16 durability test articles. Results will be plotted in a useful format for evaluating the two-segment DCGA-DCGA and the DCGA-SCGA for durability analysis.

The same three fractographic data sets, i.e. AFXLR4, AFXMR4 and AFXHR4, were used to determine the EIFSD parameters in the previous [8] and present durability analyses for F-16 lower wing skin. However, different $\alpha$ and $\phi$ values for $x_u = 0.03"$ are obtained in the present analysis due to different: (1) AL-AU ranges used, (2) fractographic data processing methods/screening considerations used. The resulting EIFSD parameter values are $x_u = 0.03"$, $\alpha = 1.716$ and $\phi = 6.308$ (see Table 13).

In the previous durability analysis [8], experimental terminal crack size dimensions in fastener holes were based on initial measurements of the fracture. In the present durability analysis, however, terminal crack sizes were based on the fractography. The final crack dimensions based on the fractography are more accurate than the initial fracture surface measurements. There are small differences between the initial crack size dimensions and those based on the fractography. As a result of these differences, the experimental results for the average number of fastener holes/skin (for both wing skins) with a crack size 0.03" is 14.5 holes (fractography) versus 16.5 holes (initial measurements).

Tho F-16 durability test article was fatigue tested to 16,000 flight hours using the F-16 1,000hour spactrum. This preliminary spectrum included two 500 hour blocks. The F-16 400 hour spectrum has been used extensively in recent years for General Dynamics IRAD and CRAD research programs. This spectrum is slightly more severe than the F-16 1,000-hour spectrum but it doesn't apply to F-16 production aircraft. It is assumed for durability analysis purposes that the coupon fractographic results (i.e., AFXLR4, AFXMR4, AFXHR4, WAFXMR4 and WAFXHR4) based on the F-16 400-hour spectrum directly can be applied to the prediction of the F-16 durability test article.

The F-16 lower wing skins contain several cutouts. However, the present durability analysis/correlation covers only fatigue cracks in fastener holes.

### 4.4.1 Estimation of Service Crack Growth Parameters

The service crack growth parameters $Q_1$ and $Q_2$ were estimated for the small (i.e., AL-AU =0.01" -0.05") and large crack size region (i.e., $a_0$ - AU$'$ = 0.05" - 0.5") for each of the ten stress regions. A general approach for estimating $Q_1$ and $Q_2$ is described in Fig. 62. In the small crack size region, $Q_1$ values for the AFXLR4, AFXMR4 and AFXHR4 data sets were obtained previously (Table 13 and Fig. 47). From these $Q_1$ values, the constants C and V in Eq. 43 were determined using a least-squares fit procedure (Fig. 47). Then, $Q_1$ values in each of the ten stress regions are computed from Eq. 43, and the results are shown in Table 16.

A similar approach to that described above was used for the large crack size region to estimate $Q_2$ for each of the ten stress regions. In this case, fractographic results of the WAFXMR4 and WAFXHR4 data sets (see Table 12) were used to

estimate the constants C and V in Eq. 43. Results are shown in Table 16 and in Fig. 63.

In practice, suitable fractographic data may not be available to estimate $Q_1$ and $Q_2$. In such cases, an analytical crack growth program [e.g., 18,19] can be used to estimate the crack size versus time information needed to establish $Q_1$ and $Q_2$ for given durability analysis conditions (e.g., stress level, load spectrum, % bolt load transfer, etc.). (Refer to Vol. I [1] and the durability design handbook (2nd Edition) [21] for guidelines and procedures).

### 4.4.2 Theoretical/Experimental Correlations

Probability of crack exceedance predictions $p(i, \mathcal{T})$ at $\mathcal{T} = 16,000$ flight hours for five different crack sizes (i.e., $x_1 = 0.03"$, $0.05"$, $0.1"$, $0.2"$ and $0.3"$) are shown in Tables 17 and 18 for the two-segment DCGA-DCGA and the DCGA-SCGA, respectively. The average number of fastener holes in each stress region, $\bar{N}(i, \mathcal{T})$ with a crack size greater than $x_1$ at $\mathcal{T} = 16,000$ flight hours is also shown in these two tables. The analysis for the DCGA-SCGA was conducted using $\sigma_z = 0.3$ (natural log basis), which is quite reasonable for countersunk fastener holes in 7475-T7351 aluminum [21].

Predictions for the average number of fastener holes in the entire lower wing skin with a crack size $> x_1$ at $16,000$ flight hours, $\bar{L}(\mathcal{T})$, and the standard deviation, $\sigma_L(\mathcal{T})$, are shown in Table 19 for both the DCGA-DCGA and the DCGA-SCGA. $\bar{L}(\mathcal{T})$ and $\sigma_L(\mathcal{T})$ values are computed based on the Binomial distribution, Eqs. 39 and 40. The tear-down inspection results based on the average of two lower wing skins are shown in the same table for comparison.

Theoretical predictions for the average number of fastener holes with a crack size $> x_1$ at $\mathcal{T} = 16,000$ flight hours

**Table 16.  Summary of Crack Growth Rate Parameters for Each Stress Region.**

| STRESS REGION | MAX. STRESS LEVEL (ksi) | NO. OF FASTENER HOLES | $Q_1 \times 10^4$ (1) (1/HR.) | $Q_2 \times 10^4$ (2) (1/HR.) |
|---|---|---|---|---|
| 1 | 28.3 | 59 | 0.884 | 2.187 |
| 2 | 27.0 | 320 | 0.655 | 2.033 |
| 3 | 24.3 | 680 | 0.334 | 1.727 |
| 4 | 16.7 | 469 | 0.030 | 0.966 |
| 5 | 28.4 | 8 | 0.904 | 2.199 |
| 6 | 29.2 | 30 | 1.080 | 2.296 |
| 7 | 32.4 | 8 | 2.097 | 2.697 |
| 8 | 26.2 | 8 | 0.541 | 1.941 |
| 9 | 26.2 | 12 | 0.541 | 1.941 |
| 10 | 25.7 | 20 | 0.478 | 1.884 |
| | | 1614 | | |

Notes: (1) Segment 1: AL-AU = .01"–.05"
$C_1 = 4.829 \times 10^{-14}$; $V_1 = 6.380$
(2) Segment 2: AL-AU = .05"–.5"
$C_2 = 1.234 \times 10^{-6}$ ; $V_2 = 1.549$
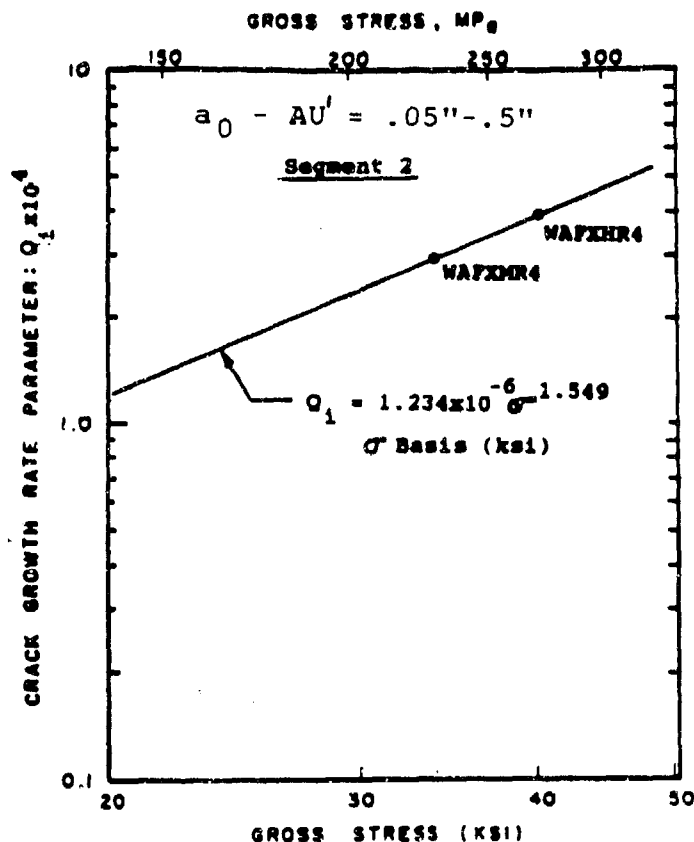


Figure 63.  Crack Growth Rate Parameter Q Versus Gross Stress for Wide Specimen Data Sets (WAFXMR4 and WAFXHR4).

**Table 17.** Crack Exceedance Probability and Average Number of Fastener Holes with Crack Size Exceeding $x_i$ at $T$ = 16000 Flight Hours in Each Stress Region Based on DCGA-DCGA

| STRESS REGION | $x_i = 0.03"$ | | $x_i = 0.05"$ | | $x_i = 0.1"$ | | $x_i = 0.2"$ | | $x_i = 0.3"$ | |
|---|---|---|---|---|---|---|---|---|---|---|
| | $p(i,T)$ | $N(i,T)$ | $p(i,T)$ | $N(i,T)$ | $p(i,T)$ | $N(i,T)$ | $p(i,T)$ | $N(i,T)$ | $p(i,T)$ | $N(i,T)$ |
| 1 | .0739 | 4.36 | .035 | 2.07 | .018 | 1.05 | .00674 | .39 | .00222 | .13 |
| 2 | .0449 | 14.37 | .0145 | 4.64 | .0056 | 1.81 | .000687 | .22 | --- | --- |
| 3 | .0144 | 9.79 | .0000683 | 0.05 | --- | -- | --- | -- | --- | -- |
| 4 | .00023 | 0.11 | .0000065 | 0.00 | --- | -- | --- | -- | --- | -- |
| 5 | .0768 | 0.61 | .0371 | 0.29 | .020 | .16 | .00752 | .06 | .00265 | .02 |
| 6 | .1027 | 3.08 | .0576 | 1.73 | .034 | 1.02 | .0158 | .47 | .00782 | .23 |
| 7 | .2871 | 2.29 | .2250 | 1.80 | .16 | 1.28 | .1065 | .85 | .0772 | .62 |
| 8 | .0326 | 0.26 | .00714 | 0.06 | .0019 | .01 | --- | -- | --- | -- |
| 9 | .0326 | 0.39 | .00714 | 0.09 | .0019 | .02 | --- | -- | --- | -- |
| 10 | .0264 | 0.53 | .00403 | 0.08 | .0005 | .01 | --- | -- | --- | -- |
| | | 35.79 | | 10.81 | | 5.37 | | 1.99 | | 1.00 |

**Table 18.** Crack Exceedance Probability and Average Number of Fastener Holes with Crack Size Exceeding $x_1$ at $\mathcal{T}$ = 16000 Flight Hours in Each Stress Region Based on DCGA-SCGA.

| STRESS REGION | $x_1 = 0.03"$ p(i,$\mathcal{T}$) | $x_1 = 0.03"$ N(i,$\mathcal{T}$) | $x_1 = 0.05"$ p(i,$\mathcal{T}$) | $x_1 = 0.05"$ N(i,$\mathcal{T}$) | $x_1 = 0.1"$ p(i,$\mathcal{T}$) | $x_1 = 0.1"$ N(i,$\mathcal{T}$) | $x_1 = 0.2"$ p(i,$\mathcal{T}$) | $x_1 = 0.2"$ N(i,$\mathcal{T}$) | $x_1 = 0.3"$ p(i,$\mathcal{T}$) | $x_1 = 0.3"$ N(i,$\mathcal{T}$) |
|---|---|---|---|---|---|---|---|---|---|---|
| 1 | .0739 | 4.36 | .0350 | 2.07 | .0183 | 1.08 | .0071 | .42 | .00348 | .20 |
| 2 | .0449 | 14.37 | .0145 | 4.64 | .00566 | 1.81 | .00126 | .40 | .000419 | .13 |
| 3 | .0144 | 9.79 | .0000683 | .05 | .0000066 | .004 | .0000066 | .004 | .0000066 | .004 |
| 4 | .000239 | .11 | .00 | .00 | .0000066 | .003 | .0000066 | .003 | .0000066 | .003 |
| 5 | .0768 | .61 | .0371 | .29 | .0196 | .16 | .00783 | .06 | .00392 | .03 |
| 6 | .103 | 3.09 | .0577 | 1.73 | .0335 | 1.00 | .0158 | .47 | .00894 | .27 |
| 7 | .287 | 2.29 | .225 | 1.80 | .160 | 1.28 | .104 | .83 | .0756 | .60 |
| 8 | .0326 | .26 | .00714 | .06 | .00187 | .01 | .000196 | .002 | .0000451 | .00 |
| 9 | .0326 | .39 | .00714 | .09 | .00187 | .02 | .000196 | .002 | .0000451 | .00 |
| 10 | .0264 | .53 | .00403 | .08 | .000621 | .01 | .000031 | .001 | .0000096 | .00 |
| | | 35.80 | | 10.81 | | 5.377 | | 2.192 | | 1.237 |

Table 19.  Statistics for Number of Fastener Holes
with Crack Size Exceeding $x_1$ in F-16
Lower Wing Skin for Both DCGA-DCGA and
DCGA-SCGA.

| $x_1$ (IN.) | DCGA-DCGA | | DCGA-SCGA | | EXPERIMENTAL RESULTS (AVE.) |
|---|---|---|---|---|---|
| | $\overline{L}(\mathcal{T})$ | $\sigma_L(\mathcal{T})$ | $\overline{L}(\mathcal{T})$ | $\sigma_L(\mathcal{T})$ | |
| 0.03 | 35.80 | 5.800 | 35.80 | 5.800 | 14.5 |
| 0.05 | 10.81 | 3.185 | 10.81 | 3.185 | 9.5 |
| 0.1 | 5.37 | 2.258 | 5.38 | 2.262 | 7.0 |
| 0.2 | 1.99 | 1.379 | 2.19 | 1.450 | 1.0 |
| 0.3 | 1.00 | 0.977 | 1.24 | 1.097 | 0.5 |

in the entire lower wing skin are plotted in Fig. 64 for both of the two-segment crack growth approaches. In this figure, the results for the DCGA-DCGA and the DCGA-SCGA are depicted by a solid curve and a dashed curve, respectively. Results for both approaches are identical for the crack size $x_1 \leq$ 0.05" in the first crack growth segment. The tear-down inspection results are shown in Fig. 64 as solid circles for comparison. These results reflect the average extent of damage for a lower wing skin based on the total extent of damage for both lower wing skins combined.

The extent of damage estimate for an exceedance probability of P = 0.05 is also plotted in Fig. 64 as a solid-dashed-solid curve (— — —). This curve represents the estimated upper bound limit for extent of damage for P = 0.05. It is computed from $\bar{L}(\mathcal{T})$ + 1.65 $\sigma_L(\mathcal{T})$ where $\bar{L}(\mathcal{T})$ and $\sigma_L(\mathcal{T})$ values are shown in Table 19 for the DCGA-SCGA. Since the number of details in each stress region is large, it is reasonable to approximate the binomial distribution by the normal distribution. Hence, the predicted mean extent of damage, $\bar{L}(\mathcal{T})$, corresponds to an exceedance probability of P = 0.5.

To illustrate the usefulness of the extent of damage concept consider, for example, the extent of damage at $x_1$ = 0.3" in Fig. 64. The (predicted) probability is 50% (i.e., P = 0.5) that 1.24 fastener holes will have a crack size exceeding $x_1$ = 0.03"; whereas, the probability is 5% (i.e., P = 0.05) that 3.05 fastener holes will have a crack size larger than $x_1$ = 0.03" at $\mathcal{T}$ = 16,000 flight hours. Therefore, the durability analysis provides quantitative estimates of the extent of damage mean and upper bound limit. This type of information provides a physical description of the state of damage for a durability-critical component and a logical basis for estimating structural maintenance/repair requirements and costs.

CRACK SIZE, mm
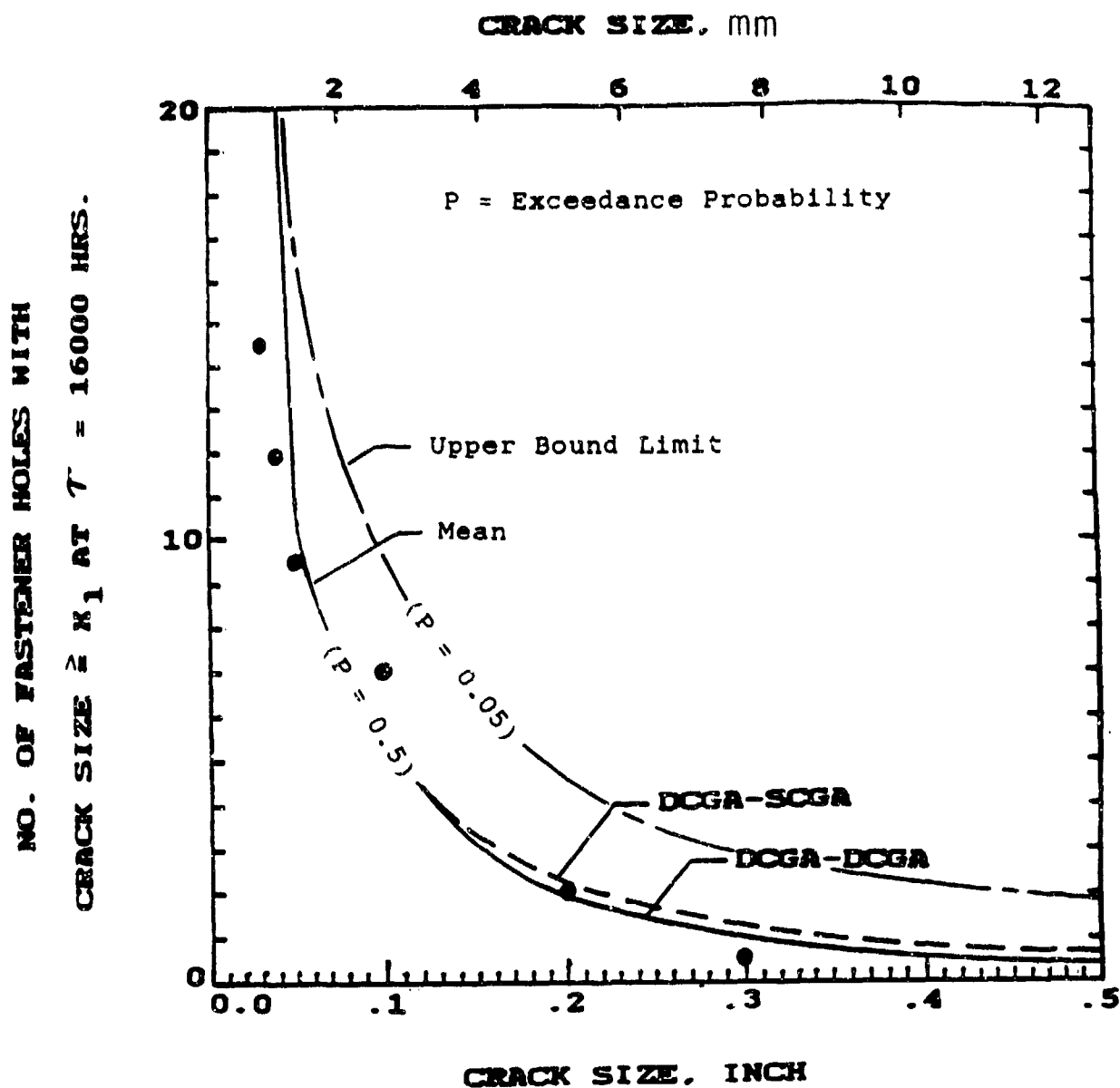


Figure 64. Correlations between Theoretical Predictions and Experimental Results for Fighter Lower Wing Skin for Extent of Damage at $\mathcal{T}$ = 16000 Flight Hours.

### 4.4.3   Discussion of Results

Two different two-segment approaches (i.e., DCGA-DCGA and DCGA-SCGA) have been demonstrated and evaluated using fractographic results for both coupon specimens and lower wing skins from a fighter aircraft. Straight bore and countersunk fastener holes with clearance-fit fasteners were considered. Results for both two-segment approaches were compared for the lower wing skin demonstration. Both approaches are considered reasonable for evaluating functional impairment due to fuel leakage/ligament breakage in metallic aircraft structures. However, the DCGA-SCGA is recommended for durability analysis because predictions are more accurate and slightly more conservative than those based on the DCGA-DCGA.

The stress level for each stress region is important for crack growth predictions. Therefore, the stress analysis for durability-critical components should reflect appropriate finite element model grid sizes to obtain the desired stress analysis accuracy for each stress region.

# SECTION V

## DURABILITY ANALYSIS STUDIES

Numerous studies were conducted during this program to evaluate and refine durability analysis and data processing methods. These studies are documented in Appendices B-J. A brief description of the durability analysis software developed for this program is presented in Appendix A. A software user's guide is provided in Volume V [5].

# SECTION VI

## CONCLUSIONS AND RECOMMENDATIONS

### 6.1 CONCLUSIONS

1. A comprehensive probabilistic durability analysis approach has been developed for metallic aircraft structures. It applies to the crack growth accumulation in any type of structural detail (e.g., fastener holes, cutouts, fillets, etc.). The approach has been verified for clearance-fit fastener holes in 7475-T7351 aluminum at two levels: (1) coupon specimens and (2) full-scale aircraft structure. Very reasonable durability analysis results have been obtained, including damages due to both small cracks (e.g., $\leq 0.05$") and large through-the-thickness cracks (e.g., $\geq 0.5$").

2. It has been shown that the initial fatigue quality (IFQ) of both straight-bore and countersunk fastener holes with clearance-fit fasteners can be reasonably estimated using fractographic results from coupon specimens and that the IFQ can be represented by an equivalent initial flaw size distribution (EIFSD). Furthermore, it has been demonstrated that the IFQ of fastener holes in full-scale structures can be defined using coupon specimens.

3. The probabilistic durability analysis approach developed can be used to "quantify" structural durability in meaningful terms, such as: (1) probability of crack exceedance at any service time, (2) probability of functional impairment at any service time, (3) cumulative distribution of service time to reach any given crack size, (4) extent of damage and (5) structural wearout rate. Since the probabilistic approach developed accounts for the fatigue crack growth accumulation in each structural detail susceptible to fatigue cracking in service, it is referred to as a "quanti-

tative durability analysis approach." The extent of damage prediction at a given service time is defined by the statistics, such as the average and standard deviation, of the number of structural details expected to exceed functional impairment crack size limits. This quantitative prediction provides an effective basis for evaluating functional impairment, economic life and structural wearout, and trade-offs as a function of the design and service variables.

4. The probabilistic durability analysis approach is a powerful "durability design tool." It gives the user new durability analysis capabilities and features not provided by the existing deterministic crack growth approach based on the "worst case" detail within a group of details. The probabilistic durability analysis method is not intended to completely replace the deterministic crack growth approach in the durability design process. The deterministic crack growth approach will continue to be a valuable tool for durability analysis - primarily during the preliminary design process. Since a deterministic crack growth analysis provides information only for the "worst case" detail within a group of details, it cannot provide the "extent of damage" type information for the entire population of structural details.

5. Actual initial flaws in the bore of manufactured fastener holes in metallic aircraft structures usually consist of random scratches, burrs, microscopic imperfections, etc. Such flaws, except for gross manufacturing defects, cannot be reliably detected and quantified by NDE for production aircraft structures. In reality, the actual initial flaws in fastener holes produced by manufacturing and assembly are not physical "cracks" in the usual sense associated with the linear elastic fracture mechanics approach. Whatever the source of fatigue cracking may be, a practical method for representing the reality of the as-manufactured condition is needed for durability

110

analysis. This is taken care of by the equivalent initial flaw concept.

6. An equivalent initial flaw size (EIFS) is an artificial crack size which results in an actual crack size at an actual point in time when the equivalent initial flaw is grown forward. It is determined by back-extrapolating fractographic results and has the following characteristics: (1) An EIFS is an artificial crack assumed to represent the initial fatigue quality of a structural detail in the as-manufactured condition whatever the source of fatigue cracking may be, (2) no direct relationship to actual initial flaws in fastener holes such as scratches, burrs, microdefects, etc., and it cannot be verified by NDI, (3) it has a universal crack shape in which the crack size is measured in the direction of crack propagation, (4) EIFSs are in a fracture mechanics format but they are not subject to such laws and limitations as the "short crack effect," (5) it depends on the fractographic data used, the fractographic crack size range for the back-extrapolation and the crack growth rate model used, (6) it must be grown forward in a manner consistent with the basis for the EIFS, and (7) EIFSs are not unique - a different set is obtained for each crack growth law used for the back-extrapolation.

7. Equivalent initial flaw sizes (EIFSs) are determined by back-extrapolating fractographic results. Since the fractographic data depends on the testing conditions (e.g., load spectrum, fastener holes, cutout, etc.), EIFSs are not strictly "generic." However, EIFSD parameters can be estimated for different fractographic data sets using the data pooling and statistical scaling procedures. It has been conclusively shown that the EIFSD based on given fractographic data sets can be used to obtain very reasonable durability analysis predictions for the other data sets and full-scale aircraft structure for clearance-fit fastener holes (both

straight-bore and countersunk) in 7475-T7351 aluminum. It should be clear that an EIFSD does not necessarily contain the "rogue flaw."

8. When an EIFSD is grown forward to a selected service time, the service crack growth should be consistent with the "basis" for the EIFSs. Therefore, the analytical crack growth program used [e.g., 18,19] should be "tuned" or "curve fitted" to the EIFS master curves reflected in the EIFSD.

9. Probabilistic-based durability analysis methods [1, 14,16] are now sufficiently developed and demonstrated for immediate applications to metallic airframes. An updated durability design handbook [21] and software for an IBM or IBM-compatible PC are available for implementing the advanced durability analysis [5].

10. A "natural fatigue crack" data base for estimating the initial fatigue quality of structural details can be acquired as a part of the Aircraft Structural Integrity Program (ASIP) test plan. For example, by not preflawing structural details in test specimens, "natural fatigue crack" data can be obtained--thereby satisfying data requirements for both durability and damage tolerance. Additional testing and fractographic evaluations, beyond the normal ASIP effort, may be needed to define IFQ, depending on the desired confidence level and circumstances. IFQ data requirements can be readily incorporated into the ASIP test plan to minimize the cost and time for acquiring the requisite data base.

11. The stress level for each stress region is important for crack growth predictions. Therefore, the stress analysis for durability-critical components should reflect appropriate finite element grid sizes to obtain the desired stress analysis accuracy.

12. Probabilistic durability analysis methodologies developed can be extended to establish the optimal inspection/repair/replacement/proof test maintenance for life management of metallic aircraft structure. The extension can be made based on some fundamental research efforts appearing in the literature [e.g., 43-53].

## 6.2 RECOMMENDATIONS

1. The advanced durability analysis method developed under this program should be used for future durability analyses for metallic airframes. Structural durability can now be quantitatively accounted for in the durability design process.

2. Recommendations for durability analysis are as follows: (1) define the equivalent initial flaw size distribution (EIFSD) using fractographic data in the small crack size region (e.g., 0.01"-0.05"), (2) use fractographic data pooling procedure and statistical scaling technique to estimate the EIFSD parameters in a "global sense" for a "single hole population" basis, and (3) use the two-segment deterministic-stochastic crack growth approach (DCGA-SCGA) to predict the extent of damage in the entire durability critical component; the two-segment deterministic crack growth approach (DCGA-DCGA) is also reasonable but it is slightly less conservative than the DCGA-SCGA.

3. The recommended changes in Air Force philosophy and durability design requirements described in Volume IV [54] should be adopted. This will allow the full potential of the probabilistic durability analysis approach to be utilized in the design and analysis of future metallic aircraft structures.

4. The advanced durability analysis approach developed

under this program should be investigated for other structural details and considerations. For example, the life enhancement effects of fastener hole cold working, interference fit fasteners, press fit bushings, etc., on initial fatigue quality should be investigated. Similarly, the initial fatigue quality of structural details, such as cutouts, lugs, fillets, etc., should be investigated. Suitable test specimens should be developed and standardized for acquiring initial fatigue quality data for the key structural details to be included in the durability analysis.

5. Future ASIP test plans should be designed to provide data for initial fatigue quality, durability and damage tolerance. Selected fatigue tests should be conducted using specimens without intentional preflaws so that "natural fatigue crack" data can be obtained. This approach should be used to minimize cost and time for acquiring the requisite IFQ data base.

6. The meaning and limitations of EIFSs and an EIFSD must be emphasized. In particular, all EIFSs should be grown forward consistent with the basis for the EIFSD. The EIFSD should not be grown forward using an analytical crack growth program without tuning and considering the basis for the EIFS.

7. All aerospace contractors should use the same method to define EIFSs for different materials and structural details so that compatible EIFSs can be obtained. The "Qa(t) model" reflected in Eq. 4 is reasonable for determining EIFSs. This model or some other suitable model should be used to standardize the way EIFSs are determined. Then, for a given fractographic data set, fractographic crack size range (AL-AU) and the same analysis procedure, all contractors will obtain the same EIFSs. By standardizing the way EIFSs are determined, EIFSs from various sources can be di-

rectly compared -- thereby providing a means for cataloging and utilizing existing data from various sources to estimate the initial fatigue quality of structural details.

8. Initial fatigue quality should not be represented by the identical initial flaw size distribution irrespective of material, type of fastener hole, structural details, manufacturing processes, etc. For example, the statistical dispersion of EIFSD for countersunk holes is significantly larger than that of the EIFSD for straight-bore holes for clearance-fit fasteners in the same material in which the holes were drilled using comparable methods. Thus, if a single initial flaw size is selected for a given probability or percentile (e.g., 1/1000), and the deterministic approach is used for durability analysis, the initial flaw size for a countersunk fastener hole should be larger than that for a straight-bore fastener hole based on our investigation.

9. The probabilistic durability analysis approach should be investigated for discriminating "quality" at three levels: (1) material, (2) manufactured detail, and (3) component. Of particular interest is the following question: "How does improvement in initial material quality translate into improvement in life of actual aircraft components?" This research can be built on the advancements made under this program and the work conducted by ALCOA [e.g., 55,56].

# REFERENCES

1.  Manning, S. D., and Yang, J. N., "Advanced Durability Analysis, Volume I - Analytical Methods" AFWAL-TR-86-3017, Air Force Wright Aeronautical Laboratories, Wright-Patterson Air Force Base, OH, July 1987.

2.  Gordon, D. E., et al, "Advanced Durability Analysis, Volume III - Fractographic Test Data," AFWAL-TR-86-3017, Air Force Wright Aeronautical Laboratories, Wright-Patterson Air Force Base, OH, August 1987.

3.  Noronha, P. J., et al, "Fastener Hole Quality," AFFDL-TR-78-206, Vols. I and II, Dec. 1978.

4.  Speaker, S. M., et al , "Durability Methods Development - Vol. VIII - Test and Fractography Data," AFFDL-TR-79-3118, Air Force Flight Dynamics Laboratory, Wright-Patterson Air Force Base, OH, Nov. 1982.

5.  Manning, S. D., and Yang, J. N., "Advanced Durability Analysis, Volume V - Durability Analysis Software User's Guide," AFWAL-TR-86-3017, Air Force Wright Aeronautical Laboratories, Wright-Patterson Air Force Base, OH, August 1987.

6.  Yang, J. N., Manning, S. D., and Garver, W. R., "Durability Methods Development, Vol. V - Durability Analysis Methodology, AFFDL-TR-79-3118, Air Force Flight Dynamics Lab., Wright-Patterson Air Force Base, OH, Sept. 1979.

7.  Yang, J. N., and Manning, S. D., "Distribution of Equivalent Initial Flaw Size," 1980 Proceedings, Annual Reliability and Maintainability Symposium, San Francisco, CA, 22-24 Jan. 1980, pp. 112-120.

8.  Manning, S. D., and Yang, J. N., "USAF Durability Design Handbook: Guidelines for the Analysis and Design of Durable Aircraft Structures," AFWAL-TR-83-3027, Air Force Wright Aeronautical Laboratories, Wright-Patterson Air Force Base, OH, Jan. 1984.

9.  Rudd, J. L., Yang, J. N., Manning, S. D., and Yee, B. G. W., Probabilistic Fracture Mechanics Analysis Method for Structural Durability," Proceedings, Conference on the Behavior of Short Cracks in Airframe Components, AGARD-CP-328, Toronto, Canada, Sept. 1982, pp. 10-1 through 10-23.

10. Rudd, J. L., Yang, J. N., Manning, S. D., and Yee, B. G. W., "Damage Assessment of Mechanically Fastened Joints in the Small Crack Size Range," Proceedings on the Ninth U. S. National Congress of Applied Mechanics, 1982, pp. 329-338.

11. Manning, S. D., Yang, J. N., and Rudd, J. L., "Durability of Aircraft Structures," Probabilistic Fracture Mechanics and Reliability, Edited by J. W. Proven, Martinus Nijhoff Publishers, The Netherlands, 1987, pp. 213-268.

12. Yang, J. N., Manning S. D., Rudd, J. L., and Hsi, W. H., "Stochastic Crack Propagation in Fastener Holes," Journal of Aircraft, Vol. 22, No. 9, Sept. 1985, pp. 810-817.

13. Yang, J. N., Manning, S. D., and Rudd, J. L., "Evaluation of a Stochastic Initial Fatigue Quality Model for Fastener Holes," Fatigue in Mechanically Fastened Composite and Metallic Joints, ASTM STP 927, John M. Potter, Ed., American Society for Testing and Materials, Philadelphia, 1986, pp. 118-149.

14. Yang, J. N., Manning, S. D., Rudd, J. L., and Artley, M. E., "Probabilistic Durability Analysis Methods for Metallic Airframes," Journal of Probabilistic Engineering Mechanics, Vol. 1, No. 4, Dec. 1986.

15. Yang, J. N., Manning, S. D., Rudd, J. L., Artley, M. E., and Lincoln, J. W., "Stochastic Approach for Predicting Functional Impairment of Metallic Airframes," Proceedings of the 28th AIAA/ASME/ASCE/AHS Structures, Structural Dynamics and Materials Conference, Paper No. AIAA-87-0752-CP, Monterey, CA, April 1987.

16. Yang, J. N., Manning, S.D., Akbarpour, A. and Artley, M. E., "Demonstration of Probabilistic-Based Durability Analysis Method for Metallic Airframes," AIAA Paper No. 88-2421, Paper presented at the 29th AIAA/ASME/ASCE/AHS Structure, Structural Dynamics and Materials Conference, Williamsburg, VA, 18-20 April 1988.

17. Yang, J. N., Hsi, W. H., Manning, S. D., and Rudd, J. L., "Stochastic Crack Growth Models for Application to Aircraft Structures," Chapter IV, Probabilistic Fracture Mechanics and Reliability, Edited by J. W. Provan, Martinus Nijhoff Publishers, The Netherlands, 1987, pp. 171-211.

18. Roach, G. R., McComb, T. H., and Chung, J. H., "ADAMSys Users Manual," Structures and Design Department, General Dynamics, Fort Worth Division, July 1987.

19. Engle, R. M., and Wead, J. A., "CRACKS-PD, A Computer Program for Crack Growth Analysis Using the Tektronix 4051 Graphics System," Air Force Flight Dynamics Laboratory, Wright-Patterson AFB, OH, AFFDL-TM-79-63-FBE, June 1979.

20. Manning, S. D., Yang, J. N., Shinozuka, M., Gordon, D. E., and Speaker, S. M., "Durability Methods Development - Vol. VII - Phase II Documentation," AFFDL-TR-79-3118, Air Force Flight Dynamics Lab., Wright-Patterson Air Force Base, OH, Nov. 1982.

21. Manning, S. D., and Yang, J. N., "USAF Durability Design Handbook: Guidelines for the Analysis and Design of Durable Aircraft Structures," AFWAL-TR-83-3027, Second Edition, Air Force Wright Aeronautical Laboratories, WrightPatterson Air Force Base, OH, August 1988.

22. Benjamin, J. R., and Cornell, C. A., _Probability, Statistics and Decision of Civil Engineers_, New York: McGraw-Hill Book Company, 1970.

23. Rudd, J. L., Yang, J. N., Manning, S. D., and Garver, W. R., "Durability Design Requirements and Analysis for Metallic Airframe," _Design of Fatigue and Fracture Resistant Structures_, ASTM STP 761, P. R. Abelkis and C. M. Hudson, Eds., American Society for Testing and Materials, 1982, pp. 133-151.

24. Forness, S. D., "Fracture Mechanics Methodology Update," General Dynamics, Fort Worth Division, Report ERR-FW2219 (Proprietary), Dec. 1981.

25. Walker, K., "The Effects of Stress Ratio During Crack Propagation and Fatigue for 2024-T3 and 7075-T6 Aluminum," _Effects of Environment and Complex Load History on Fatigue Life_, ASTM-STP 462, American Society for Testing and Materials, 1970, pp. 1-14.

26. Gallagher, J. P., and Huges, T. F., "Influence of Yield Strength on Overload Affected Fatigue Crack Growth Behavior in 4340 Steel," AFFDL-TR-74-27, Air Force Flight Dynamics Laboratory, Wright-Patterson Air Force Base, OH, July 1974.

27. Virkler, D.A., Hillberry, B. M., and Goel, P. K., "The Statistical Nature of Fatigue Crack Propagation," AFFDL-TR-78-43, Air Force Flight Dynamics Laboratory, April 1978.

28. "Standard Test Method for Measurement of Fatigue Crack Growth Rates," ASTM Standard E647-86a, _1987 Annual Book of ASTM Standards_, Section 3, "Metals Test Methods and Analytical Procedures," pp. 899-926.

29. Ostergaard, D. F., Thomas, J. R., and Hillberry, B. M., "Effect of a-Increment on Calculating da/dN from a versus N Data," *Fatigue Crack Growth Measurement and Data Analysis*, ASTM-STP 738, S. J. Hodak, Jr., and R. J. Bucci, Eds., American Society for Testing and Materials, 1981, pp. 194-204.

30. Fong, J. T., and Dowling, N. E., "Analysis of Fatigue Crack Growth Rate Data from Different Laboratories," *Fatigue Crack Growth Measurement and Data Analysis*, ASTM-STP 738, S. J. Hudak, Jr., and R. J. Bucci, Eds., American Society for Testing and Materials, 1981, pp. 171-193.

31. Anon., "Military Specification Aircraft Structures General Specification For," MIL-A-87221 (USAF), Air Force Aeronautical Systems Division, Wright-Patterson Air Force Base, OH, Feb. 28, 1985.

32. Pearson, S., "Initiation of Fatigue Cracks in Commercial Aluminum Alloys and the Subsequent Propagation of Very Short Cracks," *Engineering Fracture Mechanics*, Vol. 7, 1975, pp. 235-247.

33. Cruse, T. A., "Fracture Mechanics Problems for Gas Turbine Engine Structures," *Fracture Mechanics*, Proceedings of the 2nd International Symposium on Fracture Mechanics, the University Press of Virginia, Sept. 1978, pp. 399-420.

34. Hudak, S. J., "Small Crack Behavior and the Prediction of Fatigue Life", *Journal of Engineering Materials and Technology*, Vol. 103, 1981, pp. 26-35.

35. Lankford, J., "The Growth of Small Fatigue Cracks in 7075-T6 Aluminum," *Fatigue Eng. Mat. Struct.*, Vol. 5, 1982, pp. 233-248.

36. Miller, K. J., "The Short Crack Problem," *Fatigue of Engineering Materials and Structures*, Vol. 5, No. 3, 1982, pp. 223-232.

37. Smith, R. A., "Short Fatigue Cracks," *Fatigue Mechanisms: Advances in Quantitative Measurement of Physical Damage*, American Society for Testing and Materials, ASTM STP 811, 1983, pp. 269-279.

38. Chan, K. S., Lankford, J., and Davidson, D. L., "A Comparison of Crack-Tip Field Parameters for Large and Small Fatigue Cracks," *Transactions of the ASME*, Journal of Engineering Materials and Technology, Vol. 10B, July 1986, pp. 206-213.

39. Yang, J. N., and Donath, R. C., "Statistical Fatigue Crack Propagation in Fastener Holes Under Spectrum Loading," Journal of Aircraft, AIAA, Vol. 20, No. 12, Dec. 1983, pp. 1028-1032.

40. Yang, J. N., Salivar, G. C., and Annis, C. G., "Statistical Modeling of Fatigue Crack Growth in a Nickel-Based Superalloy," Journal of Engineering Fracture Mechanics, Vol. 18, No. 2, June 1983, pp. 257-270.

41. Yang, J. N., "Statistical Estimation of Service Cracks and Maintenance Costs for Aircraft Structures," Journal of Aircraft, AIAA, Vol. 13, No. 12, Dec. 1976, pp. 929-937.

42. Manning, S. D. and Yang, J. N., Unpublished Research, 1984-1987.

43. Yang, J. N., "Statistical Estimation of Economic Life for Aircraft Structures," Proc. AIAA/ASME/ASCE/AHS 20th Structures, Structural Dynamics, and Materials Conference, April 4-6, 1979, St. Louis, Mo., pp. 240-248; Journal of Aircraft, AIAA, Vol. 17, No. 7, 1980, pp. 528-535.

44. Yang, J. N., and Chen, S., "Fatigue Reliability of Gas Turbine Engine Components Under Schedule Inspection Maintenance," Journal of Aircraft, AIAA, Vol. 22, No. 5, May 1985, pp. 415-422.

45. Yang, J. N., and Chen, S., "An Exploratory Study of Retirement-for-Cause for Gas Turbine Engine Components," Journal of Propulsion and Power, AIAA, Vol. 2, No. 1, January 1986, pp. 38-49.

46. Yang, J. N., and Trapp, W. J., "Reliability Analysis of Fatigue-Sensitive Aircraft Structures Under Random Loading and Periodic Inspection," Air Force Materials Laboratory Technical Report, AFML-TR-74-2, Wright-Patterson Air Force Base, February 1974.

47. Yang, J. N., and Trapp, W. J., "Reliability Analysis of Aircraft Structures Under Random Loading and Periodic Inspection," AIAA Journal, Vol. 12, No. 12, 1974, pp. 1623-1630.

48. Yang, J. N., and Trapp, W. J., "Inspection Frequency Optimization for Aircraft Structures Based on Reliability Analysis," Journal of Aircraft, AIAA, Vol. 12, No. 5, 1975, pp. 494-496.

49. Yang, J. N., "Reliability Analysis of Structures Under Periodic Proof Test In Service," AIAA Journal, Vol. 14, No. 9, Sept. 1976, pp. 1225-1234.

50. Yang, J. N., "Optimal Periodic Proof Test Based on Cost-Effective and Reliability Criteria," AIAA Journal, Vol. 15, No. 3, March 1977, pp. 402-409.

51. Yang, J. N., and Chen, S., "Fatigue Reliability of Structural Components Under Scheduled Inspection and Repair Maintenance," Probabilistic Methods in Mechanics of Solids and Structures, edited by S. Eggwertz and N. C. Lind, Springer-Verlag, Berlin, Jan. 1985, pp. 559-568.

52. Heer, E., and Yang, J. N., "Structural Optimization Based on Fracture Mechanics and Reliability Criteria," AIAA Journal, Vol. 9, No. 5, April 1971, pp. 621-628.

53. Lincoln, J. W., "Risk Assessment of an Aging Military Aircraft," J. Aircraft, Vol. 22, No. 9, Aug. 1985, pp. 687-691.

54. Manning, S. D. and Yang, J. N., "Advanced Durability Analysis, Volume IV - Executive Summary," AFWAL-TR-86-3017, Air Force Wright Aeronautical Laboratories, Wright-Patterson Air Force Base, OH, September 1987.

55. Bucci, R. J, Brazill, R. L., and Brockenbrough, J. R., "Assessing Growth of Small Flaws from Residual Strength Data," Small Fatigue Cracks, Edited by R. O. Ritchie and J. Lankford, The Metallurgical Society of AIME, 1986, pp. 541-556.

56. Owen, C. R., Bucci, R. J., and Kegarise, R. J., "An Aluminum Quality Breakthrough for Aircraft Structural Reliability," Alcoa Laboratories Technical Report No. 57-87-20, October 19, 1987.

# DEFINITIONS

The technical terms defined herein supercede those given in Volume I [1]. New terms have been added and selected Volume I terms have been revised. Should any questions arise, the definitions herein should be used.

## DEFINITIONS

1. **Combined Least Square Sums Approach (CLSSA)** - the least square sums for individual fractographic data sets are combined to estimate the EIFSD parameters in a "global sense." This approach is used in conjunction with the data pooling philosophy.

2. **Compatible Equivalent Initial Flaw Size Distribution Function** - this is a distribution function for equivalent initial flaw sizes (EIFS) which is derived using a physically meaningful cumulative distribution of time-to-crack initiation (TTCI) function and a suitable deterministic crack growth law.

3. **Crack Size** - is the length of a crack in a structural detail in the direction of crack propagation.

4. **Cumulative Distribution of Service Time $(F_{T(x_1)}(T))$** - is defined as the probability that the service time $T(x_1)$ to reach a crack size $x_1$ is shorter than $T$. It is equal to the probability that the crack size $a(T)$ at service life $T$ will exceed $x_1$, which is simply the probability of crack exceedance, i.e.,

$$F_{T(x_i)}(T) = P[T(x_i) \leq T] = P[a(T) \leq x_i] = p(i, T)$$

5. **Data Pooling** - is a concept for estimating the EIFSD parameters using one or more fractographic data sets in a "global sense." A data pooling procedure is used to increase the sample size for determining the EIFSD parameters.

6.  **Deterministic Crack Growth Approach (DCGA)** -- Crack growth parameters are treated as deterministic values resulting in a single value prediction for crack length.

7.  **Durability** - is a quantitative measure of the structural resistance to fatigue cracking under specified service conditions. Structural durability is concerned with the prevention of functional impairments due to (1) excessive cracking and (2) fuel leakage/ligament breakage. Excessive cracking is concerned with relatively small subcritical crack sizes (e.g., $\leq 0.05"$) which affect functional impairment, structural maintenance requirement and life-cycle-costs. Such cracks may not pose an immediate safety problem. However, if the structural details containing such cracks are not repaired, economical repairs cannot be made when these cracks exceed a limiting crack size. Functional impairment due to fuel leakage/ligament breakage is typically concerned with large through-the-thickness cracks (e.g., $0.50"-0.75"$). Although such cracks are usually subcritical, they affect the residual strength, fleet readiness, and may require increased maintenance action.

8.  **Durability Analysis** - is concerned with quantifying the extent of structural damage due to fatigue cracking for structural details (e.g., fastener hole, fillet, cutout, lug, etc.) as a function of service time. Results are used to ensure design compliance with Air Force's durability design requirements.

9.  **Economic Life** - is that point in time when an aircraft structure's damage state due to fatigue, accidental damage and/or environmental deterioration reaches a point where operational readiness goals cannot be preserved by economically acceptable maintenance action.

10.  Economic Life Criteria - are guidelines and formats
for defining quantitative economic life requirements for air-
craft  structure to satisfy U. S. Air Force Durability design
requirements.  The economic life criterion provides the basis
for analytically and experimentally ensuring  design  compli-
ance  of  aircraft  structure with durability design require-
ments.  Two recommended formats for  economic  life  criteria
are:

      o  probability of crack exceedance

      o  cost ratio:  repair cost/replacement cost

11.  Economic  Repair Limit - is the maximum damage size
that can be economically repaired (e.g.,  repair  0.03"-0.05"
radial crack in fastener holes by reaming hole to next size).

12.  Equivalent Initial Flaw Size (EIFS) - is an artifi-
cial  crack  size which results in an actual crack size at an
actual point in time when the initial flaw is grown  forward.
It is determined by back-extrapolating fractographic results.
It  has the following characteristics:  (1) an EIFS is an ar-
tificial crack assumed to represent the initial fatigue qual-
ity of a structural detail in the  as-manufactured  condition
whatever the source of fatigue cracking may be, (2) no direct
relationship  to  actual initial flaws in fastener holes such
as scratches, burrs, microdefects, etc.,  and  it  cannot  be
verified  by  NDI,  (3)  a universal crack shape in which the
crack size is measured in the direction of crack propagation,
(4) it's in a fracture mechanics format  but  EIFSs  are  not
subject  to  linear elastic fracture mechanics (LEFM) laws or
limitations, such as the "short crack effect" [e.g.,  32-38],
(5)  it  depends on the fractographic data, the fractographic
crack size range for the back extrapolation,  and  the  crack

125

growth rate model used, (6) it must be grown forward in a manner consistent with the basis for the EIFS, and (7) EIFSs are not unique - a different set is obtained for each crack growth law used for the back- extrapolation.

13. **Equivalent Initial Flaw Size Distribution (EIFSD)** - is used to represent the initial fatigue quality variation of a structural detail. An EIFS is a random variable, and the EIFSD statistically describes the EIFS population. The EIFSD does not necessarily contain the "rogue flaw."

14. **EIFS Master Curve** - is a curve (e.g., equation, tabulation of a(t) vs. t or curve without prescribed functional form) used to determine the EIFS value at t=0 corresponding to a given TTCI value at a specified crack size. Such a curve is needed to determine the EIFS distribution. The EIFS master curve depends on several factors, such as the fractographic data base, the fractographic crack size range used, the functional form of the crack growth equation used in the curve fit, etc. (Ref. EIFS).

15. **Extent of Damage** - is a quantitative measure of structural durability at a given service time. For example, the number of structural details (e.g., fastener holes, cutouts, fillets, etc.) or percentage of details exceeding specified crack size limits with a certain probability. Crack length is the fundamental measure for structural damage. The predicted extent of damage is compared with the specified economic life criterion for ensuring design compliance with U. S. Air Force durability requirements.

16. __Generic EIFS Distribution__ - An EIFS distribution is "generic" if it depends only on the material and manufacturing/fabrication processes. An EIFSD is not strictly "generic" because it is based on fractographic results which reflect given conditions (e.g., load spectra). For durability analysis, an EIFSD is established using the fractographic results for one or more data sets, and the resulting EIFSD is justified for a different set of conditions.

17. __Initial Fatigue Quality (IFQ)__ - characterizes the initial manufactured state of a structural detail or details with respect to initial flaws in a part, component, or airframe prior to service. Actual initial flaws in a fastener hole are typically random scratches, burrs, microscopic imperfections, etc. Such flaws are not cracks per se like those associated with linear elastic fracture mechanics. The IFQ is represented by an equivalent initial flaw size distribution (EIFSD).

18. __Probability of Crack Exceedance $(p(i, \mathcal{T}))$__ - refers to the probability that a crack in the ith stress region will exceed a specified crack size, $x_1$, at a given service time, $\mathcal{T}$. It can be used to quantify the extent of damage due to fatigue cracking in fastener holes, cutouts, fillets, lugs, etc.

19. __Reference Crack Size $(a_0)$__ - This is the specified crack size in a detail used to reference TTCIs.

20. **Service Crack Growth Master Curve (SCGMC)** - SCGMC is a curve, expressed by equation or tabulation of $a(t)$ versus $t$, used to grow EIFSs forward in order to determine the crack size distribution at any service time. The SCGMC must be consistent with the basis for the EIFS distribution.

21. **Service Time to Reach Any Crack Size $x_1$** - This term describes the time, $T(x_1)$, to reach any specified crack size $x_1$. In this context, the crack size $x_1$ can be associated with either the "crack initiation" or the "crack propagation" process. The time-to-crack-initiation (TTCI) term is restricted to crack sizes associated with the crack initiation process, where $x_1 = a_0$ (reference crack size for TTCIs).

22. **Statistical Scaling** - is used to account for the inhomogeneous fractographic data, in particular fractographic data associated with the largest flaw per specimen with $\ell$ holes.

23. **Stochastic Crack Growth Approach (SCGA)** - an approach which directly accounts for the crack growth rate dispersion in the durability analysis.

24. **Structural Detail** - is any element in a metallic structure susceptible to fatigue cracking (e.g., fastener hole, fillet, cutout, lug, etc.).

25. **Time-To-Crack-Initiation (TTCI)** - is the time or service hours required to initiate a specified (observable) fatigue crack size, $a_0$, in a structural detail (with no initial flaws intentionally introduced).

26.  <u>TTCI Lower Bound Limit $(\epsilon)$</u> - is  a  minimum  value
for  time-to-crack initiation with a reference crack size $a_0$.
It depends on the reference crck size $a_0$ for TTCI; the larger
$a_0$, the larger $\epsilon$.

.

.

.

.

27.  <u>Upper  Bound EIFS Limit $(x_u)$</u> - defines the largest
EIFS in  the  initial  fatigue  quality  distribution.   Con-
straints on $x_u$ for fatigue holes:   largest EIFS in data set $\leq$
$x_u$ (e.g., 0.03"-0.05").

.

.

.

.

## ACRONYMS

| | | |
|---|---|---|
| ADA | = | Advanced Durability Analysis |
| ASIP | = | Aircraft Structural Integrity Program |
| CLSSA | = | Combined Least Square Sums Approach |
| DADTA | = | Durability and Damage Tolerance Assessment |
| DCGA | = | Deterministic Crack Growth Approach |
| EIFS | = | Equivalent Initial Flaw Size |
| EIFSD | = | Equivalent Initial Flaw Size Distribution |
| FHQ | = | Fastener Hole Quality |
| HEIFS | = | Homogeneous EIFS |
| IFQ | = | Initial Fatigue Quality |
| LEFM | = | Linear Elastic Fracture Mechanics |
| LT | = | Load Transfer Through the Fastener |
| MM | = | Method of Moments |
| NDE | = | Non Destructive Evaluation |
| NDI | = | Non Destructive Inspection |
| NLT | = | No Load Transfer Through the Fastener |
| SCGA | = | Stochastic Crack Growth Approach |
| SCGMC | = | Service crack growth master curve |
| SSE | = | Sum Squared Error |
| TSE | = | Total Standard Error |
| TTCI | = | Time-to-Crack Initiation |

a       = Crack Size

$a_0$       = Reference crack size for given TTCIs

a(0)       = EIFS - Crack size at t=0

a(t)       = Crack size at any service time t

$a(t)$, $a(t_1)$, $a(t_2)$ = Crack size at time t, $t_1$ and $t_2$, respectively

a(T)       = Crack size at service time T

$a(\tau)$       = Crack size at any service time $\tau$

AL, AU       = Lower and upper bound fractographic crack size, respectively, used to define the EIFSD parameters. Also used in conjunction with the SCGMC to define crack size limits for the small crack size region.

$AU'$       = Upper bound crack size limit for the large crack size region

b, Q       = Crack growth parameters in the equation $\frac{da(t)}{dt} = Q[a(t)]^b$. Used in conjunction with the IFQ model.

$b_1, Q_2$       = Service crack growth rate parameters in the equation $da/dt = Q_1(a)^{b_1}$ associated with the one-segment DCGA or 1st segment of the two-segment approach.

131

$b_2, Q_2$ — Service crack growth rate parameters in the equation $da/dt = Q_2(a)^{b_2}$ for segment two of the two-segment DCGA.

$c$ — $b - 1$; Used in conjunction with the IFQ model when the crack growth law, $\frac{da(t)}{dt} = Q[a(t)]^b$ is used and $b > 1.0$.

$\frac{da(t)}{dt}$ — Crack growth rate as a function of time

$f_X(u)$ — Probability density function of X.

$F_{a(0)}(x)$ — EIFS cumulative distribution function for a "single hole population."

$F_{a_\ell(0)}(x)$ — Cumulative distribution of EIFS based on the largest fatigue crack per test specimen with $\ell$ holes.

$F_{a_{\ell_i}(0)}(x_{ij})$ — Subscripted notation used for $F_{a_\ell(0)}(x)$ in conjunction with data pooling, where: j denotes the jth crack in the ith data set.

$F_{a(t)}(x)$ — Cumulative distribution of crack size $a(t)$ at any service time t.

$F_{a_\ell(t)}(x)$ — Cumulative distribution of crack size $a_\ell(t)$ at any service time t for the largest fatigue crack per test specimen with $\ell$ holes.

132

$F_T(t)$      =    TTCI cumulative distribution function

$F_{T_{\ell_i}}(t)$     =    Cumulative distribution of minimum TTCIs based on the largest fatigue crack par test specimen with $\ell_i$ holes.

$F_{T_{\ell_i}}(t_{ij})$    =    Subscripted notation used for $F_{T_\ell}(t)$ in conjunction with data pooling, where: j = jth TTCI value in the ith data set.

$F_{T(x_1)}(\mathcal{T})$    =    Cumulative Distribution of service time $T(x_1)$ to reach a crack size $x_1$.

$G(x_1; \mathcal{T} | X=u)$    =    Initial flaw size corresponding to crack size $x_1$ at time $\mathcal{T}$ with X = u.

$\ell$      =    No. of fastener holes per test specimen.

$L(\mathcal{T})$, $\bar{L}(\mathcal{T})$    =    Total and average number of details, respectively, in the entire component having a crack size $\geq x_1$ at any service time $\mathcal{T}$.

LT     =    Load transfer through the fastener.

m     =    Number of stress regions (or total number of fatigue cracks in a data set, Eqs. 3-33, 3-34).

M     =    Total number of EIFS data sets used to estimate the EIFSD parameters.

$N_i$     =    Number of TTCI or EIFS values for the ith data set used in conjunction with the combined least square sums approach.

133

| | | |
|---|---|---|
| $N(i,T)$, $\bar{N}(i,T)$ | = | Total and average number of details, respectively, having a crack size exceeding $x_1$ at any service time $T$ |
| $p(i,T)$ | = | Probability that a detail in the ith stress region will have a crack size $>x_1$ at the service time $T$ |
| $Q_i$ | = | Crack growth rate parameter (see Eq. 3-6) for the ith fractographic data set or "pooled Q" value. It is used to determine EIFSs. |
| $Q_j$ | = | Crack growth rate parameter (see Eq. 3-5) for the jth fatigue crack in a fractographic data set. |
| $t$, $t_1$, $t_2$ | = | Flight hours at $t$, $t_1$, $t_2$, respectively. |
| $T$, TTCI | = | Time-to-crack-initiation |
| $T(x_1)$ | = | Service time to reach any crack size $x_1$. |
| $u$ | = | A particular value of X (lognormal random variable). |
| $x$ | = | Crack size |
| $x_1$ | = | Crack size used for $p(i,T)$ predictions or reference crack size for $F_{T(x_1)}(T)$ predictions. |

134

$x_u$ = Upper bound limit for EIFS

$x$ = Lognormal random variable with a median of 1.0.

$x_{ij}$ = ln ln$(x_u/x_{ij})$

$Y_{1i}(\mathcal{T})$ = An EIFS value in the EIFSD corresponding to a crack size $x_1$ at time $\mathcal{T}$ in the ith stress region.

$Y_{ij}$ = $\ln\left\{-(1/b_i)\ln\left[\frac{i}{N_i \tau_i}\right]\right\}$

$Z$ = Log X

$\Gamma(\ )$ = Gamma function

$C, V$ = Empirical constants in the equation: $Q_i = C\sigma_i^V$, where $\sigma_i$ = stress

$\sigma_Z$ = Standard deviation of Z = Log X.

$\mathcal{T}$ = A particular service time

$\alpha, \phi$ = Weibull compatible shape and scale EIFSD parameters, respectively

$\gamma$ = $Q_i/Q_2$

# APPENDIX A
## DURABILITY ANALYSIS SOFTWARE

Software is available for implementing the advanced dur-
ability analysis method described in this Volume (II) and in
Volume I [1]. A comprehensive software user's guide is given
in Volume V [5].

## A.1  SOFTWARE DESCRIPTION

The advanced durability analysis software includes six
programs in "GWBASIC". The purpose of each program is des-
cribed in Table A.1. All programs can be implemented on an
IBM or IBM-compatible personal computer.

Software is available for plotting the fractographic
data for any crack size or time range and/or durability an-
alysis results for $F_{T(x_i)}(T)$, $p(i,T)$ or $F_{a(t)}(x)$. A plotting
capability is available for the following durability analysis
options:  (1)  DCGA, (2) DCGA-DCGA and (3) DCGA-SCGA. Plots
can be obtained with or without correlating data. Typical
example plots are shown in Fig. A.1

## A.2  SYSTEM REQUIREMENTS

Minimum system requirements are as follows:

Memory:                  640K RAM
Operating System:        MS-DOS Version 2.0 or Later
Graphics Monitor:        Monochrome or Color
Disk Drive:              1 Double Sided Disk Drive
Printer:                 IBM or IBM-Compatible Graphics
                         Printer
Graphics Program:        Need Special "GRAPHICS" Program
                         for Doing Screen Prints of
                         Graphic Display

TABLE A.1.   Description of Durability Analysis Software.

| PROGRAM FILENAME | PURPOSE |
|---|---|
| "FRACT" | Save or read/print out fractographic data on 5 1/4" floppy disk |
| "SCREEN" | Study the character and quality of a fractographic data set (tabulate data and plot fractography) |
| "QSZAT" | Compute pooled Q and $\bar{G}$ for a given fractographic data set |
| "WCIFQ" | Estimate EIFSD parameters for Weibull compatible distribution function |
| "PLOT" | Plot fractographic data and/or durability analysis results |
| "AHAL" | Make durability analysis predictions |
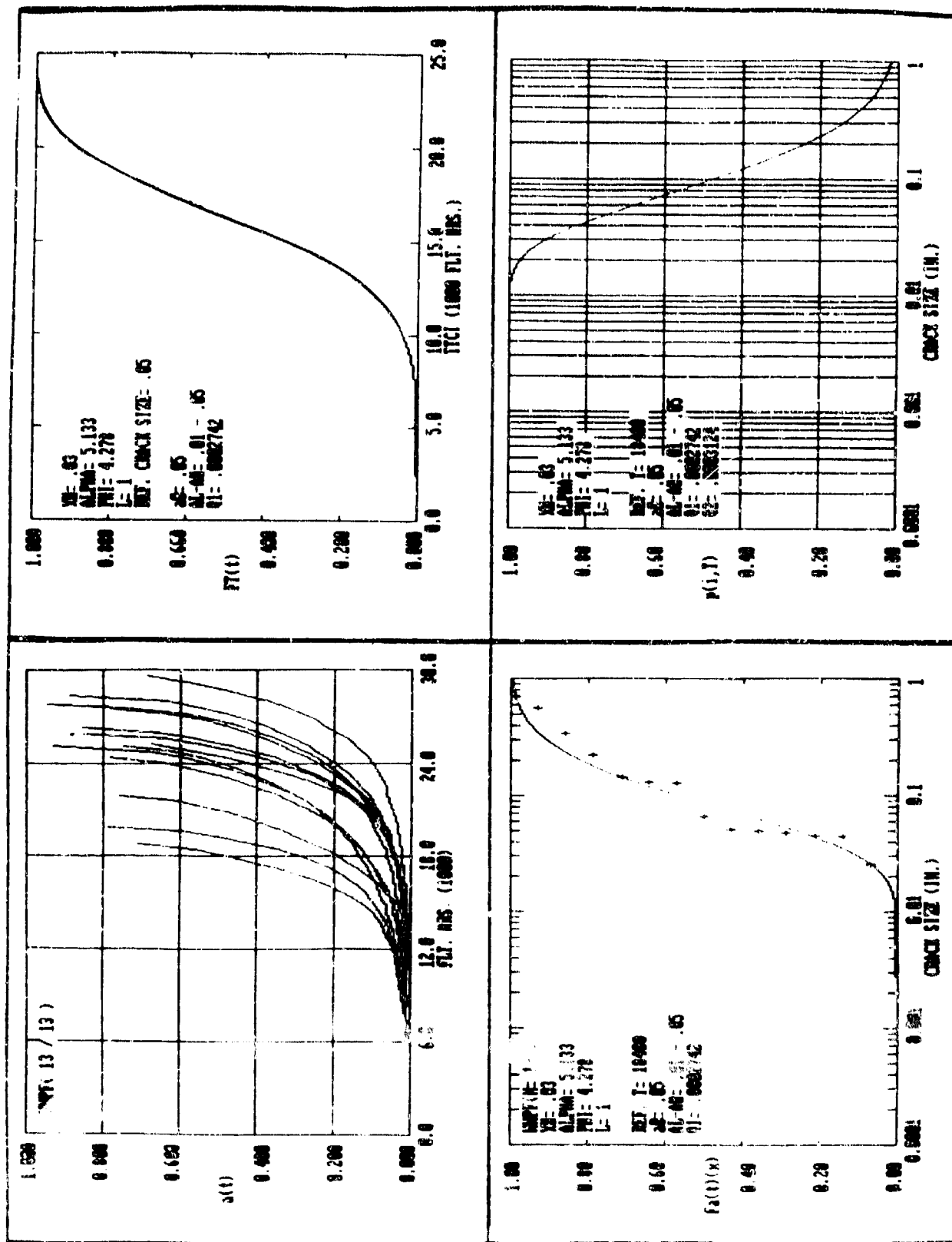
Figure A.1. Example Plots for Durability Analysis Software "PLOT".

# APPENDIX B

## FRACTOGRAPHIC DATA SCREENING/PROCESSING

### B.1 INTRODUCTION

The purpose of this section is to review fractographic data screening and processing considerations for durability analysis. This aspect is particularly important because fractographic data is used to determine (1) pooled Q values for individual data sets, (2) the initial fatigue quality (IFQ) or EIFSD parameters for fastener holes, (3) the TTCIs for a given reference crack size ($a_0$), and (4) the crack sizes, a(t), at a given reference time. Fractographic data considerations, data screening and plotting are considered in the following.

### B.2 FRACTOGRAPHIC DATA CONSIDERATIONS

Fractographic data are used to estimate the IFQ of structural details for the durability analysis. The IFQ depends on the fractographic data and crack size range, AL-AU, used. Ideally, the fractographic data should be homogeneous and cover the desired AL-AU range (i.e., AL $\leq$ a(t) $\leq$ AU) for defining the EIFSD parameters. Realistically, the fractographic data may not be perfectly homogeneous.

The following fractographic data considerations will be made: (1) data sparsity, (2) fatigue crack origins, (3) extrapolations, and (4) survivors/failures.

"Data sparsity" occurs when all the fractographic data in a data set do not uniformly cover the desired AL-AU range that is to be used to define the IFQ. For example, there may be little data (i.e., a(t) versus t) in the desired AL-AU range for a particular crack. Hence, some data may have to be extrapolated to "cover" the AL-AU range. If extrapolations

are made care should be taken for extrapolations far beyond the limits of the actual (a(t), t) data.

Fastener holes in durability test specimens are not intentionally preflawed so that natural fatigue cracks can occur. Fatigue cracks usually originate in the bore of the hole. There may be multiple crack origins and crack branching in the microstructure. Eventually, the individual microcracks tend to merge into a single crack front. Microcracking is a very complex process. Sometimes, for various reasons, fatigue cracks may originate on the surface of mating parts instead of the bore of the hole. Pooled Q, $\sigma_z$ and the EIFSD parameters should be defined using fractographic data for similar crack origins. For example, don't mix cracks with origins in the bore of the hole with those with origins on the surface.

The fractographic data may be based on fatigue tests to a specified time or failure - whichever comes first. Specimens tested to failure are called "failures;" otherwise, specimens are called "runouts" or "survivors." The fractographic data processing and data rankings for a given data set should recognize whether a specimen is a failure or a runout.

B.3  FRACTOGRAPHIC DATA SCREENING AND PLOTTING

Fractographic data should be screened and plotted before using it for any durability analysis purpose. Software for an IBM or IBM-compatible PC is available in Volume V [5] for screening and plotting fractographic data. Screening involves a physical description of fractographic data limits and a display of the actual fractographic data for visual observation.

A physical survey of each fractographic data set acquired under this program is given in Tables B.1 through B.11. Survey results for data sets AFXHR4, AFXLR4 and AFXMR4 [4] are shown

in Tables B.12, B.13, and B.14, respectively. These tables provide the following information for each crack in the data set: (1) crack I.D., (2) minimum and maximum a(t), (3) minimum and maximum TTCI, (4) number of (a(t), t) fractographic readings, and (5) type of data (i.e., F = failure and S = survivor). Also, the minimum critical crack size, largest initial time fractography reading, minimum time to failure, and the common crack size range, AL-AU, for all cracks are defined for each data set. The above information provides an overall description of the fractographic data.

Plots of the fractographic data (i.e., a(t) versus t) are given in Figs. B.1 through B.18 for selected data sets from the current program. Other plots are also shown for AFXLR4, AFXMR4 or AFXHR4 in Figs. B.21 through B.24. Two crack size ranges are plotted: (1) full range (use all the data) and (2) AL-AU = 0 - 0.5" range. Such plots are convenient for assessing data sparsity, variability and abnormal crack growth behavior. For example, in Fig. B.19 the abnormal crack growth behavior of crack number 8 is observed. Also note in Fig. B.20 that some cracks cover the AL-AU = .01" - .05" range; whereas others do not.

# TABLE B.1  FRACTOGRAPHIC DATA SURVEY FOR WWPF DATA SET

| CRACK I.D. | a(t) MIN. | MAX. | TTCI MIN. | MAX. | NC(I) | TYPE |
|---|---|---|---|---|---|---|
| 1 | .0035 | .69 | 12000 | 29616 | 46 | F |
| 2 | .0069 | .712 | 6000 | 18806 | 33 | F |
| 3 | .0154 | .78 | 10000 | 24435 | 37 | F |
| 4 | .0037 | .678 | 10800 | 25232 | 37 | F |
| 5 | .0089 | .65 | 10000 | 25931 | 41 | F |
| 6 | .0058 | .85 | 11600 | 26336 | 38 | F |
| 7 | .0094 | .78 | 12000 | 27551 | 40 | F |
| 8 | .0095 | .89 | 12400 | 28355 | 41 | F |
| 9 | .0104 | .79 | 6000 | 19884 | 36 | F |
| 10 | 8.999999E-03 | .76 | 10800 | 21880 | 29 | F |
| 11 | .0098 | .95 | 11600 | 27827 | 42 | F |
| 12 | .0073 | .93 | 8400 | 25120 | 43 | F |
| 13 | 8.0C0001E-03 | .75 | 7200 | 25150 | 46 | F |

CONSTRAINTS DUE TO FAILURE(S) IN DATA SET

MAX. AO(REF.)= .678      MAX. TAU= 18806

LARGEST INITIAL TIME/DATA SET= 12400

LARGEST COMMON CRACK SIZE RANGE/DATA SET= .0154 - .678


# TABLE B.2  FRACTOGRAPHIC DATA SURVEY FOR WWPB DATA SET

| CRACK I.D. | a(t) MIN. | MAX. | TTCI MIN. | MAX. | NC(I) | TYPE |
|---|---|---|---|---|---|---|
| 1 | .0018 | .8316 | 12656 | 29858 | 18 | F |
| 2 | .0071 | .8050001 | 10547 | 34869 | 25 | F |
| 3 | .0028 | .8499999 | 10547 | 34910 | 25 | F |
| 4 | .0057 | .69 | 18773 | 39856 | 21 | F |
| 5 | .0018 | .7909 | 21937 | 36492 | 15 | F |
| 6 | .0019 | .9080999 | 10547 | 28051 | 18 | F |
| 7 | 9.599999E-03 | .6737 | 27000 | 38596 | 12 | F |
| 8 | .0036 | .8043 | 28055 | 40494 | 13 | F |
| 9 | .0087 | .8474999 | 21937 | 35432 | 14 | F |
| 10 | .0069 | .6365 | 27000 | 38596 | 12 | F |
| 11 | .0037 | .8091 | 26156 | 43664 | 18 | F |
| 12 | .0052 | .7839 | 25101 | 40494 | 16 | F |

CONSTRAINTS DUE TO FAILURE(S) IN DATA SET

MAX. AO(REF.)= .6737      MAX. TAU= 28051

LARGEST INITIAL TIME/DATA SET= 28055

LARGEST COMMON CRACK SIZE RANGE/DATA SET= 9.599999E-03 - .6737

## TABLE B.3 FRACTOGRAPHIC DATA SURVEY FOR WAFXMR4 DATA SET

| CRACK | a(t) | | TTCI | | | |
| I.D. | MIN. | MAX. | MIN. | MAX. | NC(I) | TYPE |
|---|---|---|---|---|---|---|
| 1 | .0016 | .915 | 12800 | 21208 | 22 | F |
| 2 | .0064 | .8337 | 14800 | 28436 | 35 | F |
| 3 | .1475 | .758 | 20800 | 33208 | 32 | F |
| 4 | .0086 | .7855 | 10000 | 22836 | 33 | F |
| 5 | .0262 | .7388 | 7200 | 17236 | 26 | F |
| 6 | .0156 | .9895 | 4400 | 11608 | 19 | F |
| 7 | .0019 | .7915 | 3200 | 19637 | 43 | F |
| 8 | .0054 | .7677 | 14800 | 30036 | 39 | F |
| 9 | .0136 | .9341 | 3600 | 12808 | 24 | F |
| 10 | .0046 | .9875 | 6800 | 15208 | 22 | F |
| 11 | .0028 | .7304 | 8000 | 18436 | 27 | F |
| 12 | .0114 | 1.2975 | 14800 | 21792 | 19 | F |
| 13 | 8.999999E-03 | .9037 | 10800 | 15304 | 13 | F |
| 14 | .0199 | .8949 | 24400 | 31636 | 19 | F |

CONSTRAINTS DUE TO FAILURE(S) IN DATA SET

MAX. A0(REF.)= .7304     MAX. TAU= 11608

LARGEST INITIAL TIME/DATA SET= 24400

LARGEST COMMON CRACK SIZE RANGE/DATA SET= .1475 - .7304

## TABLE B.4 FRACTOGRAPHIC DATA SURVEY FOR WAFXMR4 DATA SET

| CRACK | a(t) | | TTCI | | | |
| I.D. | MIN. | MAX. | MIN. | MAX. | NC(I) | TYPE |
|---|---|---|---|---|---|---|
| 1 | .0048 | .76 | 2000 | 7297 | 14 | F |
| 2 | .0092 | .85 | 1600 | 5616 | 12 | F |
| 3 | .0051 | .79 | 4800 | 12968 | 22 | F |
| 4 | .0086 | .79 | 1200 | 9323 | 22 | F |
| 5 | .0089 | .68 | 400 | 8108 | 21 | F |
| 6 | 8.000001E-03 | .65 | 4400 | 14589 | 27 | F |
| 7 | .0067 | .88 | 2000 | 13649 | 31 | F |
| 8 | 9.100001E-03 | .63 | 800 | 10567 | 26 | F |
| 9 | .0132 | .88 | 1200 | 9537 | 22 | F |
| 10 | .0097 | .59 | 2000 | 10973 | 24 | F |
| 11 | .0123 | .678 | 1200 | 12592 | 30 | F |
| 12 | .0031 | .72 | 2000 | 16643 | 38 | F |
| 13 | .0149 | .6137 | 1600 | 7732 | 17 | F |

CONSTRAINTS DUE TO FAILURE(S) IN DATA SET

MAX. A0(REF.)= .59     MAX. TAU= 5616

LARGEST INITIAL TIME/DATA SET= 4800

LARGEST COMMON CRACK SIZE RANGE/DATA SET= .0149 - .59

B-5

## TABLE B.5  FRACTOGRAPHIC DATA SURVEY FOR WWPCL DATA SET

| CRACK I.D. | a(t) MIN. | a(t) MAX. | TTCI MIN. | TTCI MAX. | NC(I) | TYPE |
|---|---|---|---|---|---|---|
| 1 | .0033 | .9115 | 36400 | 55192 | 48 | F |
| 2 | .0697 | .9866999 | 40800 | 59252 | 48 | F |
| 3 | .0129 | 1.0224 | 30800 | 45992 | 39 | F |
| 4 | .0158 | .7356 | 28000 | 38792 | 28 | F |

CONSTRAINTS DUE TO FAILURE(S) IN DATA SET

MAX. A0(REF.)= .7356      MAX. TAU= 38792

LARGEST INITIAL TIME/DATA SET= 40800

LARGEST COMMON CRACK SIZE RANGE/DATA SET= .0697 - .7356


## TABLE B.6  FRACTOGRAPHIC DATA SURVEY FOR WWPCH DATA SET

| CRACK I.D. | a(t) MIN. | a(t) MAX. | TTCI MIN. | TTCI MAX. | NC(I) | TYPE |
|---|---|---|---|---|---|---|
| 1 | .0127 | .7144 | 24800 | 33652 | 24 | F |
| 2 | .0106 | .9641999 | 12000 | 21112 | 24 | F |
| 3 | .0119 | .9281 | 18800 | 24700 | 16 | F |
| 4 | .1449 | .9522999 | 18400 | 24980 | 18 | F |
| 5 | 8.599998E-03 | .7561 | 24000 | 31252 | 20 | F |
| 6 | .0087 | .8176 | 15600 | 24924 | 24 | F |

CONSTRAINTS DUE TO FAILURE(S) IN DATA SET

MAX. A0(REF.)= .7144      MAX. TAU= 21112

LARGEST INITIAL TIME/DATA SET= 24800

LARGEST COMMON CRACK SIZE RANGE/DATA SET= .1449 - .7144

## TABLE B.7  FRACTOGRAPHIC DATA SURVEY FOR WFI DATA SET

| CRACK | a(t) | | TTCI | | | |
|---|---|---|---|---|---|---|
| I.D. | MIN. | MAX. | MIN. | MAX. | NC(I) | TYPE |
| 1 | .0072 | .77 | 12400 | 31200 | 48 | F |
| 2 | .0087 | .72 | 8000 | 27200 | 49 | F |
| 3 | .0061 | .7820001 | 3600 | 23600 | 51 | F |
| 4 | .003 | .7454 | 6000 | 30400 | 62 | F |
| 5 | .0044 | .71 | 11200 | 30800 | 50 | F |
| 6 | .0087 | .71 | 5600 | 17600 | 31 | F |
| 7 | 8.999999E-03 | .94 | 2400 | 16400 | 36 | F |
| 8 | .0089 | 1.02 | 8400 | 28000 | 50 | F |
| 9 | 9.599999E-03 | 1.06 | 12000 | 36480 | 63 | F |
| 10 | .0079 | .823 | 6800 | 30000 | 59 | F |
| 11 | .0087 | .8599999 | 6800 | 20400 | 35 | F |
| 12 | .0088 | .8560001 | 11200 | 32400 | 54 | F |
| 13 | .0093 | 1.03 | 5600 | 29360 | 61 | F |
| 14 | .0094 | .758 | 12800 | 33600 | 53 | F |

CONSTRAINTS DUE TO FAILURE(S) IN DATA SET

MAX. A0(REF.)= .71          MAX. TAU= 16400

LARGEST INITIAL TIME/DATA SET= 12800

LARGEST COMMON CRACK SIZE RANGE/DATA SET= 9.599999E-03 - .71

## TABLE B.8  FRACTOGRAPHIC DATA SURVEY FOR WBI DATA SET

| CRACK | a(t) | | TTCI | | | |
|---|---|---|---|---|---|---|
| I.D. | MIN. | MAX. | MIN. | MAX. | NC(I) | TYPE |
| 1 | .0197 | .8264 | 28055 | 41449 | 14 | F |
| 2 | .0102 | .0858 | 39656 | 44739 | 6 | S |
| 3 | .0134 | .8983999 | 31219 | 43200 | 13 | F |
| 4 | .0103 | .7704 | 45773 | 58050 | 13 | F |
| 5 | .0075 | .7159 | 35437 | 51975 | 17 | F |
| 6 | .0046 | .891 | 37547 | 54601 | 18 | F |
| 7 | .0083 | .7161 | 26156 | 37979 | 13 | F |
| 8 | .0084 | .9030999 | 46828 | 53020 | 13 | F |
| 9 | 8.499999E-03 | .743 | 25101 | 39129 | 15 | F |
| 10 | .0103 | .8015 | 25101 | 40078 | 16 | F |
| 11 | .0067 | .2611 | 51047 | 57659 | 8 | S |
| 12 | .012 | .8764 | 32273 | 49855 | 18 | F |

CONSTRAINTS DUE TO FAILURE(S) IN DATA SET

MAX. A0(REF.)= .7159          MAX. TAU= 37979

LARGEST INITIAL TIME/DATA SET= 51047

LARGEST COMMON CRACK SIZE RANGE/DATA SET= .0197 - .0858

## TABLE B.9 FRACTOGRAPHIC DATA SURVEY FOR WXWPB DATA SET

| CRACK I.D. | a(t) MIN. | a(t) MAX. | TTCI MIN. | TTCI MAX. | NC(I) | TYPE |
|---|---|---|---|---|---|---|
| 1 | .0003 | .9745999 | 15609 | 27830 | 13 | F |
| 2 | .0043 | .8178 | 19828 | 39644 | 20 | F |
| 3 | .0045 | .8427999 | 14555 | 30470 | 17 | F |
| 4 | .0057 | .919 | 18773 | 42595 | 24 | F |
| 5 | .0098 | .9224999 | 24047 | 40698 | 18 | F |
| 6 | .0081 | .7423 | 25101 | 42595 | 18 | F |
| 7 | .0044 | 1 | 33328 | 55677 | 23 | F |
| 8 | .0147 | 1.1 | 18773 | 40784 | 23 | F |
| 9 | .0037 | 1.0614 | 30164 | 51352 | 22 | F |
| 10 | .0076 | .8990999 | 27000 | 55571 | 29 | F |
| 11 | .0179 | .95 | 18773 | 36743 | 19 | F |
| 12 | 9.099999E-03 | 1.0249 | 19828 | 47870 | 28 | F |
| 13 | .0041 | .9048999 | 17719 | 38798 | 22 | F |
| 14 | .0036 | 1.1447 | 27000 | 53832 | 27 | F |
| 15 | .0013 | .9501999 | 25101 | 46815 | 22 | F |

CONSTRAINTS DUE TO FAILURE(S) IN DATA SET

MAX. A0(REF.)= .7423        MAX. TAU= 27830

LARGEST INITIAL TIME/DATA SET= 33328

LARGEST COMMON CRACK SIZE RANGE/DATA SET= .0179 - .7423

## TABLE B.10 FRACTOGRAPHIC DATA SURVEY FOR WABXHR4 DATA SET

| CRACK I.D. | a(t) MIN. | a(t) MAX. | TTCI MIN. | TTCI MAX. | NC(I) | TYPE |
|---|---|---|---|---|---|---|
| 1 | .01 | .6935 | 2109 | 15385 | 14 | F |
| 2 | .0035 | .9138999 | 2109 | 17389 | 16 | F |
| 3 | .0091 | .5828 | 4219 | 19815 | 16 | F |
| 4 | .006 | .739 | 1055 | 12644 | 12 | F |
| 5 | .004 | .8008 | 2109 | 16650 | 15 | F |
| 6 | .007 | .6531 | 2109 | 19815 | 18 | F |
| 7 | .005 | .4411 | 1055 | 12643 | 12 | F |
| 8 | .015 | .5523 | 4219 | 11583 | 8 | F |
| 9 | .005 | .8328 | 3164 | 15808 | 14 | F |
| 10 | .0088 | .5702 | 5273 | 15595 | 11 | F |
| 11 | .0060 | .9536 | 1055 | 11875 | 12 | F |
| 12 | .004 | .7463 | 4219 | 13700 | 11 | F |
| 13 | .007 | .7026 | 2109 | 14540 | 13 | F |
| 14 | .0069 | .7616 | 3164 | 13277 | 11 | F |
| 15 | .0084 | .8211 | 2109 | 11486 | 10 | F |

CONSTRAINTS DUE TO FAILURE(S) IN DATA SET

MAX. A0(REF.)= .4411        MAX. TAU= 11486

LARGEST INITIAL TIME/DATA SET= 5273

LARGEST COMMON CRACK SIZE RANGE/DATA SET= .0156 - .4411

## TABLE B.11 FRACTOGRAPHIC DATA SURVEY FOR WWPFO DATA SET

| CRACK I.D. | a(t) MIN. | a(t) MAX. | TTCI MIN. | TTCI MAX. | NC(I) | TYPE |
|---|---|---|---|---|---|---|
| 1 | .0068 | .8882 | 14800 | 22348 | 20 | F |
| 2 | .0057 | .8552 | 3600 | 15478 | 31 | F |
| 3 | 0.499999E-03 | .6317 | 14000 | 19635 | 15 | F |
| 4 | .004 | .7789 | 15200 | 24406 | 24 | F |
| 5 | .0125 | .7558 | 15600 | 26806 | 29 | F |
| 6 | .0046 | .9410001 | 16800 | 26006 | 24 | F |
| 7 | .0043 | .7726 | 16400 | 27235 | 28 | F |
| 8 | .0074 | .8193 | 14800 | 22806 | 21 | F |
| 9 | .0026 | .7831 | 12000 | 23606 | 30 | F |
| 10 | .004 | .6601 | 11200 | 20435 | 24 | F |
| 11 | .006 | .6979 | 15200 | 23606 | 22 | F |
| 12 | .0032 | .8523 | 12800 | 24000 | 29 | F |
| 13 | .0064 | .6854 | 10800 | 20035 | 24 | F |
| 14 | .0057 | .7966 | 8000 | 21206 | 34 | F |

CONSTRAINTS DUE TO FAILURE(S) IN DATA SET

MAX. A0(REF.)= .6317          MAX. TAU= 15478

LARGEST INITIAL TIME/DATA SET= 16800

LARGEST COMMON CRACK SIZE RANGE/DATA SET= .0125 - .6317

## TABLE B.12 FRACTOGRAPHIC DATA SURVEY FOR AFXHR4 DATA SET

| CRACK I.D. | a(t) MIN. | a(t) MAX. | TTCI MIN. | TTCI MAX. | NC(I) | TYPE |
|---|---|---|---|---|---|---|
| 1 | .0125 | .4681 | 1200 | 9871 | 23 | F |
| 2 | .0158 | .3527 | 4800 | 13073 | 21 | F |
| 3 | .014 | .3087 | 4800 | 12806 | 21 | F |
| 4 | .0084 | .2664 | 2400 | 6900 | 13 | F |
| 5 | .0093 | .2543 | 6400 | 16000 | 25 | S |
| 6 | .0339 | .3091 | 4000 | 8035 | 12 | F |
| 7 | .0252 | .274 | 2000 | 4807 | 9 | F |
| 8 | .0187 | .3254 | 2000 | 5206 | 10 | F |
| 9 | .0181 | .3292 | 6000 | 12435 | 18 | F |
| 10 | .0155 | .5777 | 1600 | 7075 | 15 | F |

CONSTRAINTS DUE TO FAILURE(S) IN DATA SET

MAX. A0(REF.)= .2664          MAX. TAU= 4807

LARGEST INITIAL TIME/DATA SET= 6400

LARGEST COMMON CRACK SIZE RANGE/DATA SET= .0339 - .2543

## TABLE B.13  FRACTOGRAPHIC DATA SURVEY FOR AFXLR4 DATA SET

| CRACK I.D. | a(t) MIN. | a(t) MAX. | TTCI MIN. | TTCI MAX. | NC(I) | TYPE |
|---|---|---|---|---|---|---|
| 1 | .0166 | .1821 | 8000 | 16000 | 21 | S |
| 2 | .0245 | .4332 | 4000 | 10407 | 18 | F |
| 3 | .0296 | .437 | 12000 | 25235 | 35 | F |
| 4 | .0205 | .4008 | 5200 | 23235 | 46 | F |
| 5 | .0089 | .4616 | 6800 | 24806 | 47 | F |
| 6 | .0191 | .1343 | 9600 | 31606 | 56 | F |
| 7 | .0097 | .1817 | 10000 | 32000 | 55 | S |
| 8 | .0698 | .1335 | 11600 | 32000 | 52 | S |
| 9 | .0177 | .199 | 20000 | 30808 | 28 | F |
| 10 | .0299 | .1801 | 8800 | 19206 | 27 | F |
| 11 | .015 | .4324 | 5600 | 11606 | 17 | F |

CONSTRAINTS DUE TO FAILURE(S) IN DATA SET

MAX. A0(REF.)= .1343        MAX. TAU= 10407

LARGEST INITIAL TIME/DATA SET= 20000

LARGEST COMMON CRACK SIZE RANGE/DATA SET= .0698 - .1335

## TABLE B.14  FRACTOGRAPHIC DATA SURVEY FOR AFXMR4 DATA SET

| CRACK I.D. | a(t) MIN. | a(t) MAX. | TTCI MIN. | TTCI MAX. | NC(I) | TYPE |
|---|---|---|---|---|---|---|
| 1 | .0229 | .0709 | 4000 | 16000 | 31 | S |
| 2 | .0099 | .3526 | 3600 | 11255 | 20 | F |
| 3 | .0017 | .0764 | 6000 | 16000 | 26 | S |
| 4 | .0223 | .0777 | 7200 | 16000 | 23 | S |
| 5 | .0239 | .3008 | 4000 | 16000 | 31 | S |
| 6 | .0217 | .5372 | 4400 | 12806 | 22 | F |
| 7 | .0041 | .0504 | 6800 | 16000 | 24 | S |
| 8 | .0312 | .5572 | 5200 | 16000 | 28 | S |
| 9 | .0181 | .3786 | 2400 | 6006 | 11 | F |

CONSTRAINTS DUE TO FAILURE(S) IN DATA SET

MAX. A0(REF.)= .3526        MAX. TAU= 6006

LARGEST INITIAL TIME/DATA SET= 7200

LARGEST COMMON CRACK SIZE RANGE/DATA SET= .0312 - .0504
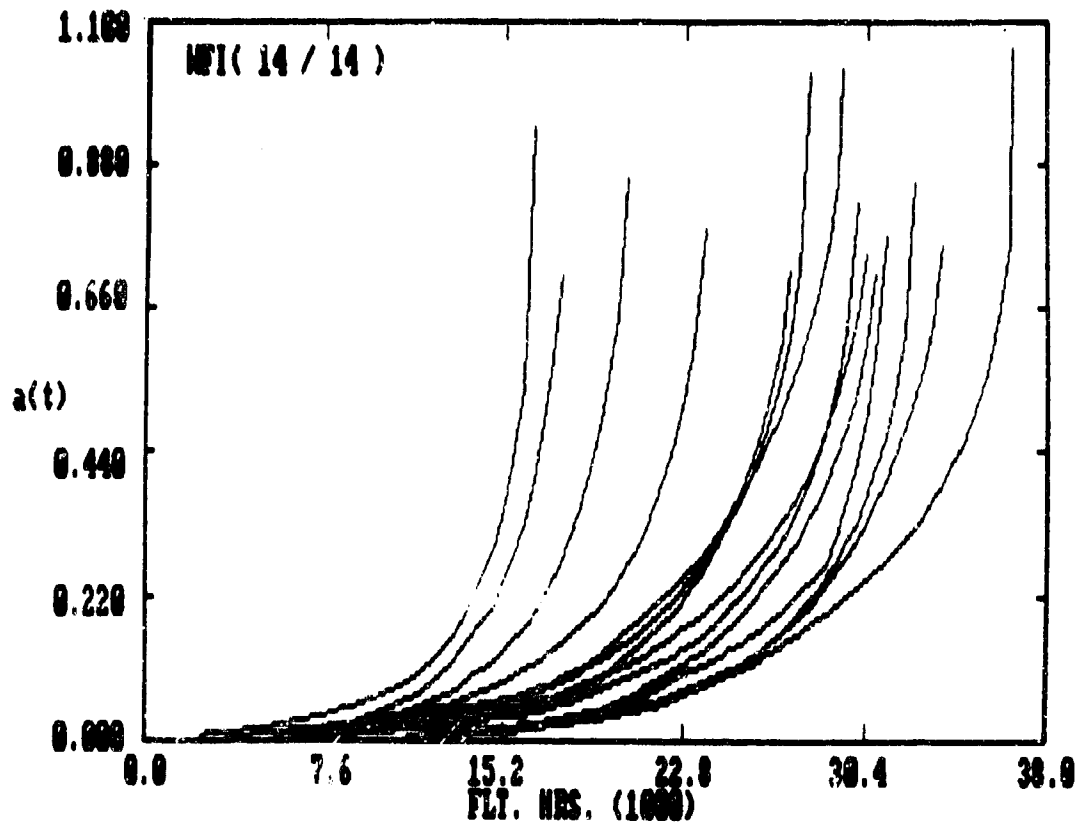
Figure B.1. a(t) VERSUS t FRACTOGRAPHIC DATA FOR WFI
DATA SET (FULL RANGE).
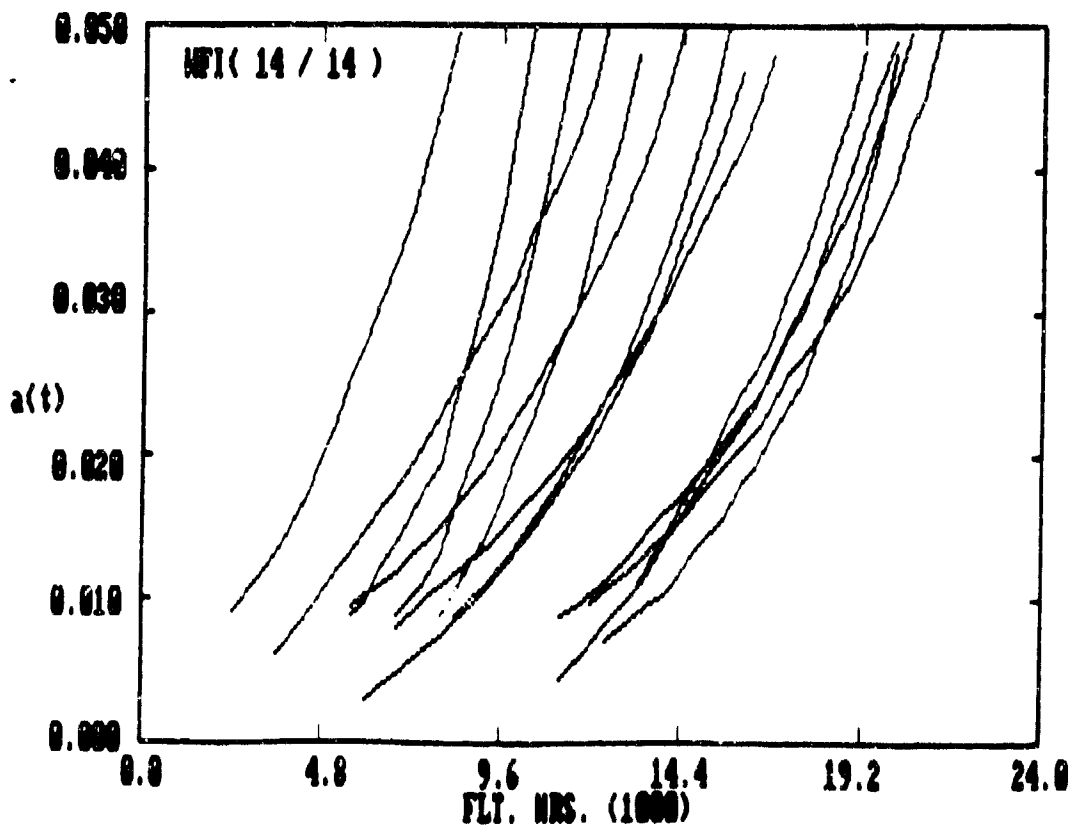


Figure B.2. a(t) VERSUS t FRACTOGRAPHIC DATA FOR WFI
DATA SET (AL-AU = 0 - .05").

B-11
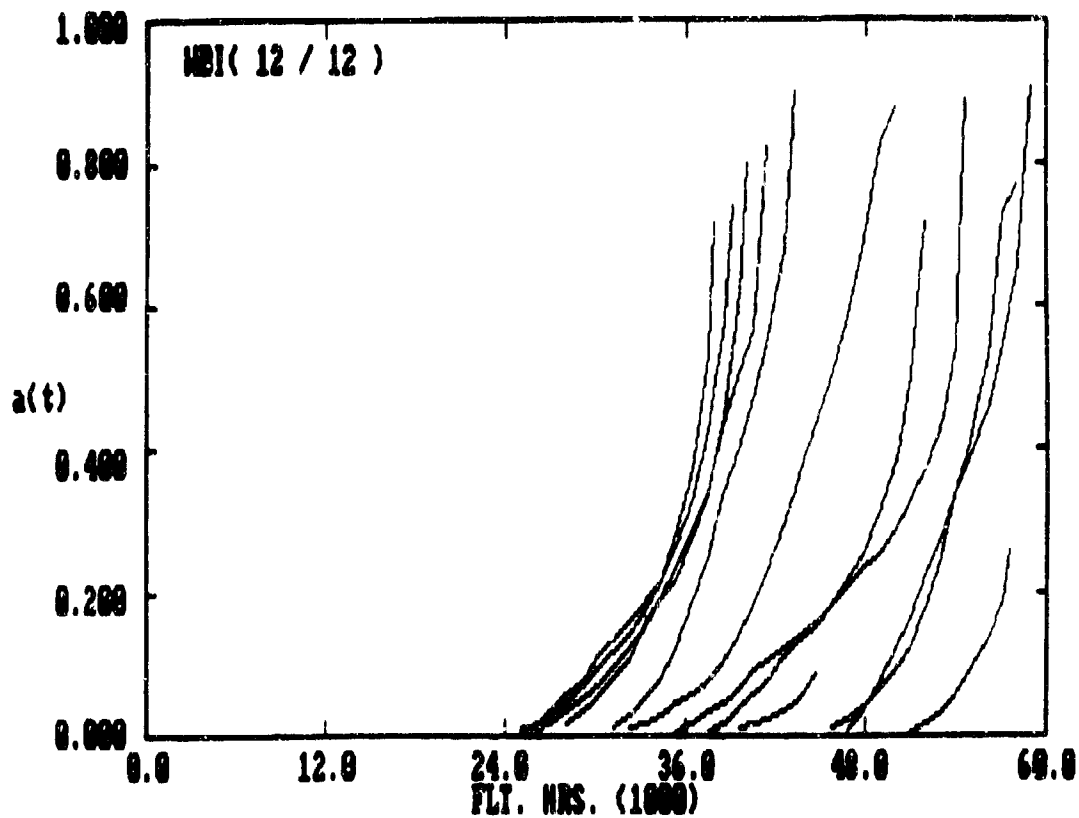
Figure B.3.   a(t) VERSUS t FRACTOGRAPHIC DATA FOR WBI
DATA SET (FULL RANGE).
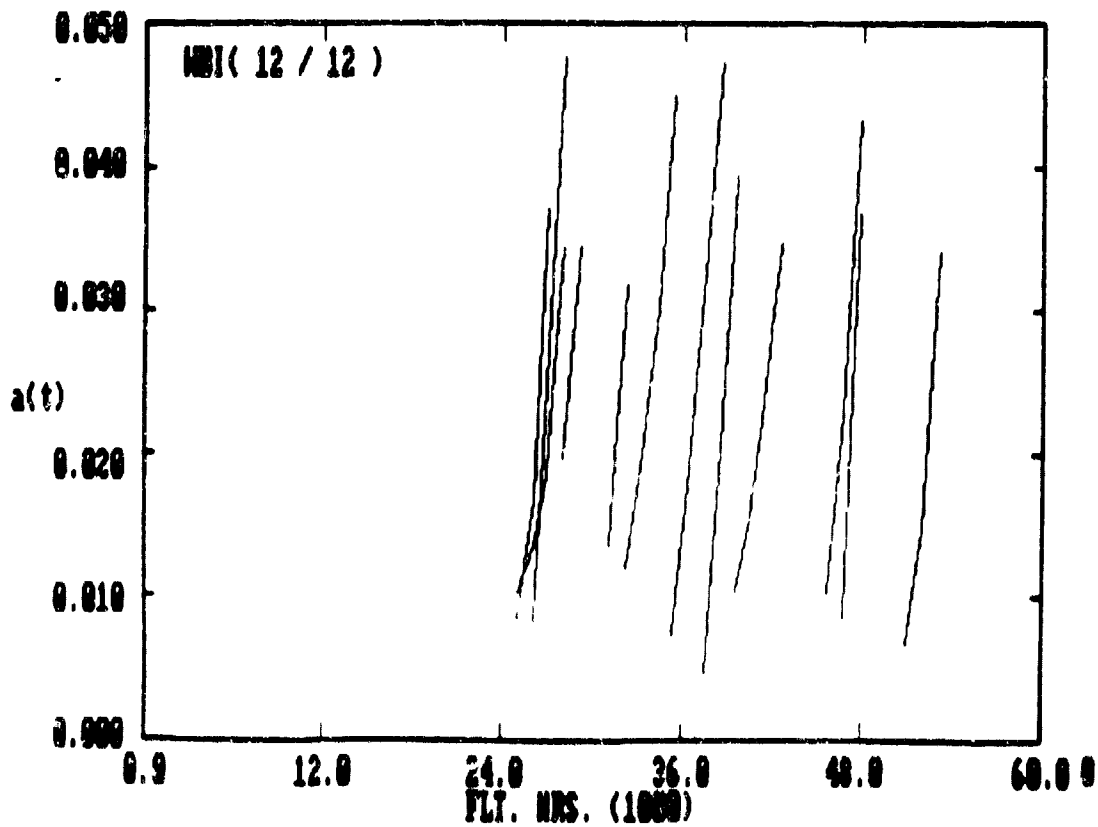


Figure B.4.   a(t) VERSUS t FRACTOGRAPHIC DATA FOR WBI
DATA SET (AL-AU = 0 -.05")
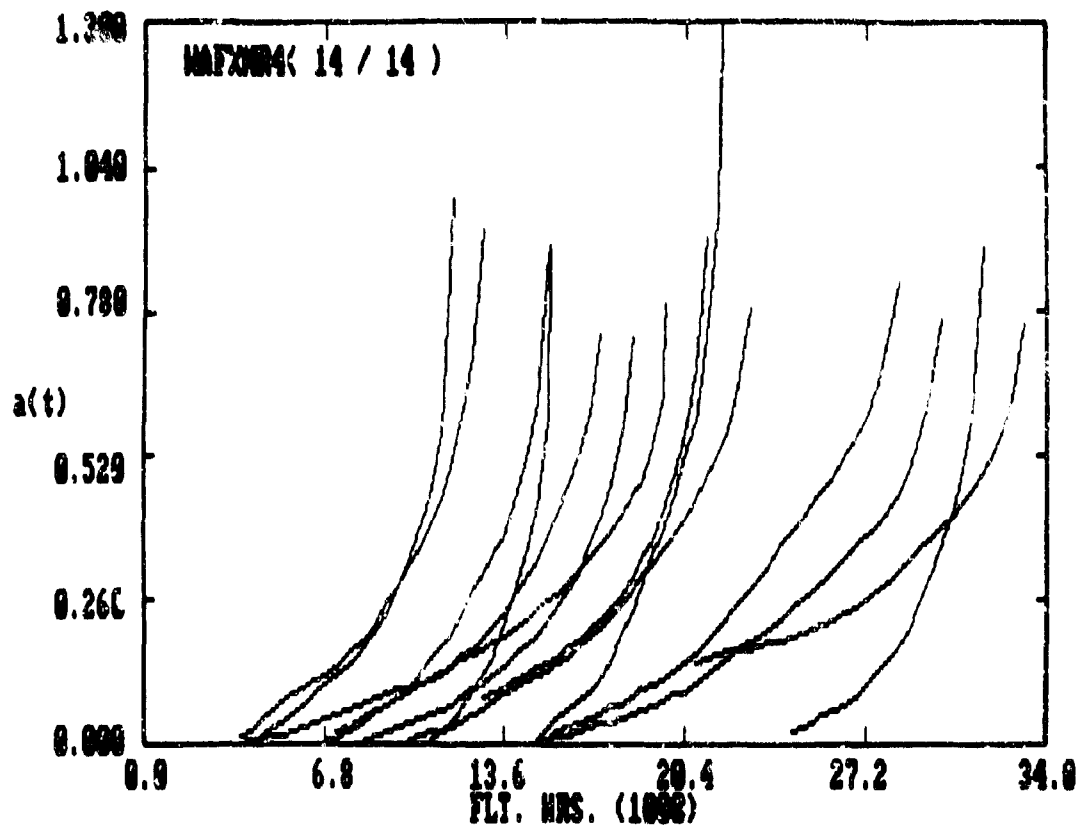
Figure B.5.    a(t) VERSUS t FRACTOGRAPHIC DATA FOR WAFXMR4
DATA SET (FULL RANGE).
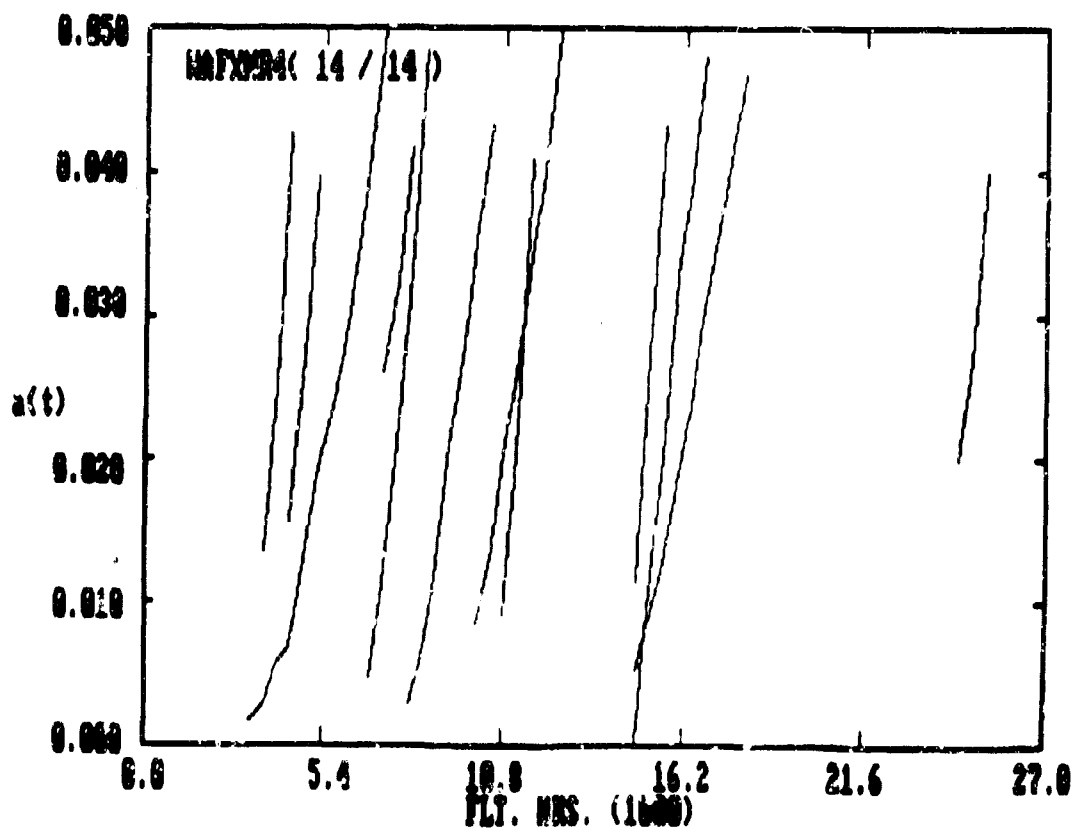


Figure B.6.    a(t) VERSUS t FRACTOGRAPHIC DATA FOR WAFXMR4
DATA SET (AL-AU = 0 - .05").
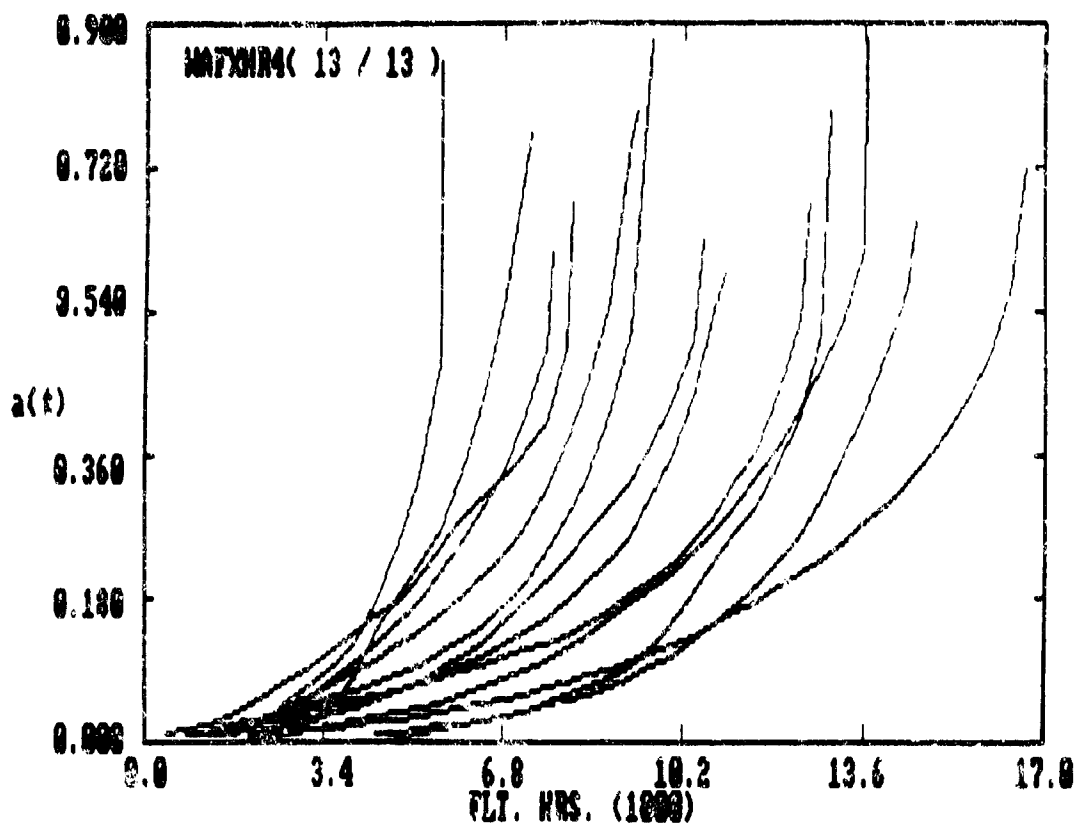
Figure B.7.  a(t) VERSUS t FRACTOGRAPHIC DATA FOR WAFXHR4
DATA SET (FULL RANGE).
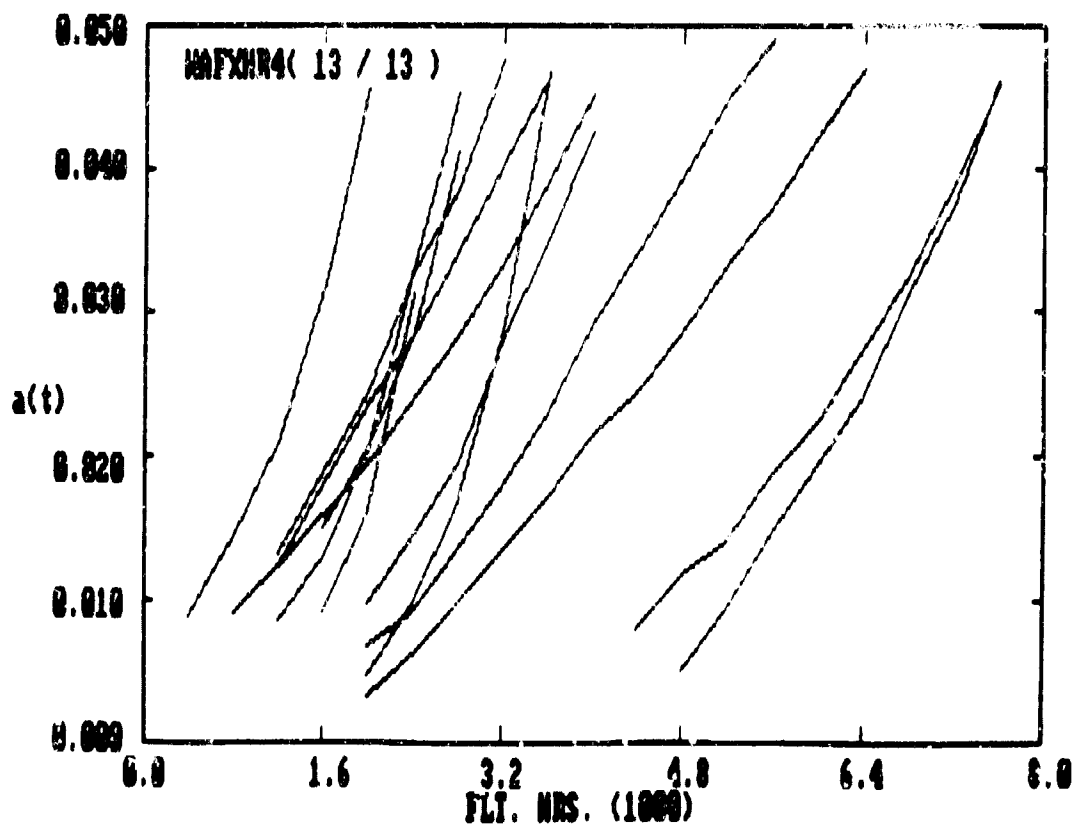


Figure B.8.  a(t) VERSUS t FRACTOGRAPHIC DATA FOR WAFXHR4
DATA SET (AL-AU = 0 - .05")
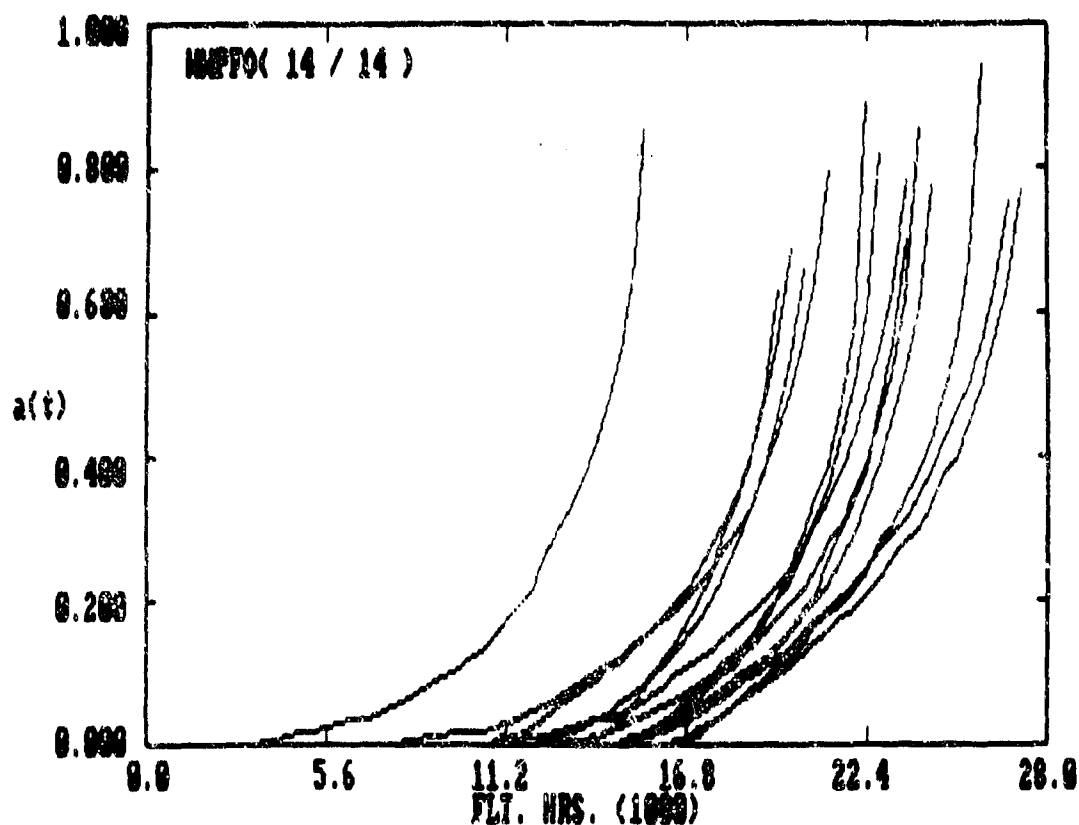
Figure B.9.    a(t) VERSUS t FRACTOGRAPHIC DATA FOR WWPFO
               DATA SET (FULL RANGE).
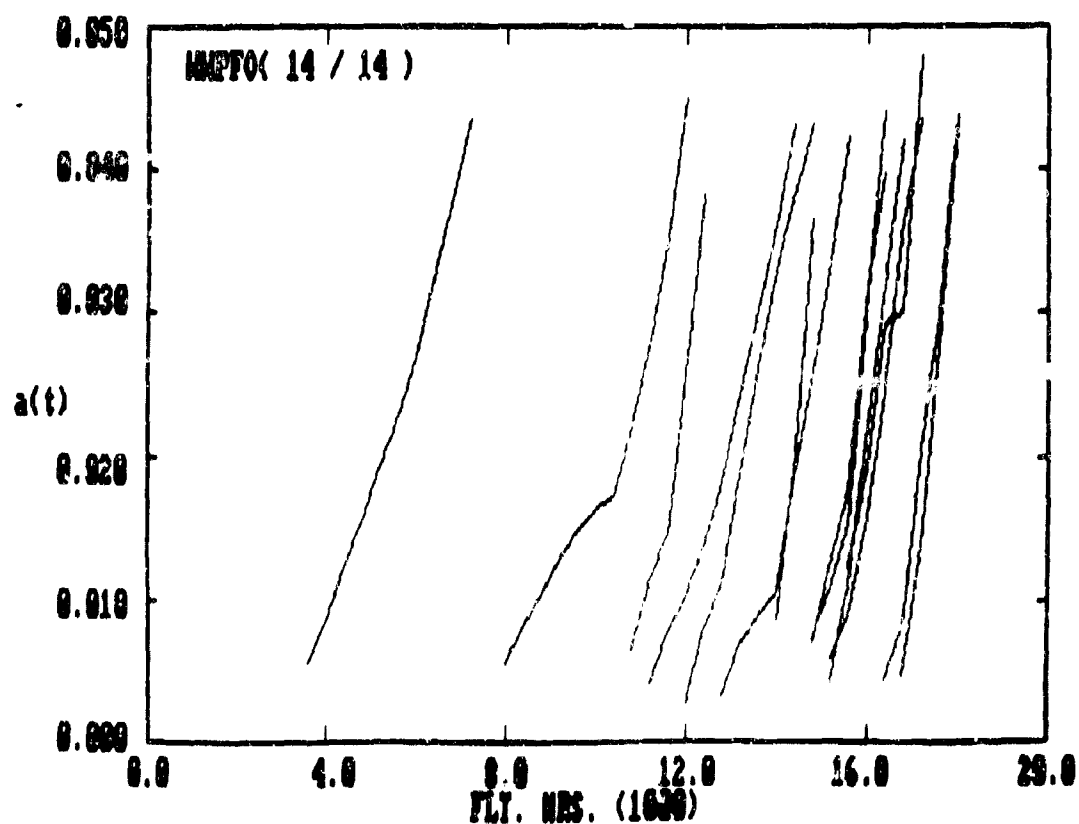


Figure B.10.   a(t) VERSUS t FRACTOGRAPHIC DATA FOR WWPFO          B-15
               DATA SET (AL-AU = 0 - .05").
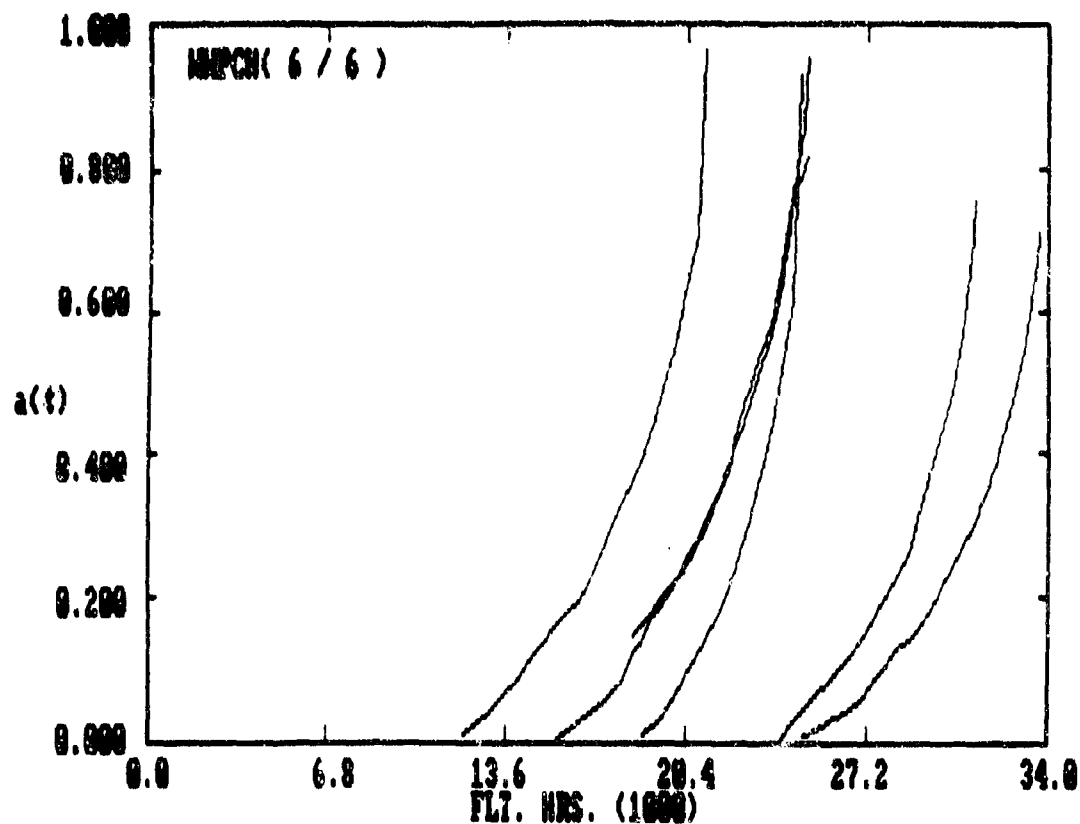
Figure B.11.   a(t) VERSUS t FRACTOGRAPHIC DATA FOR WWPCH
DATA SET (FULL RANGE).
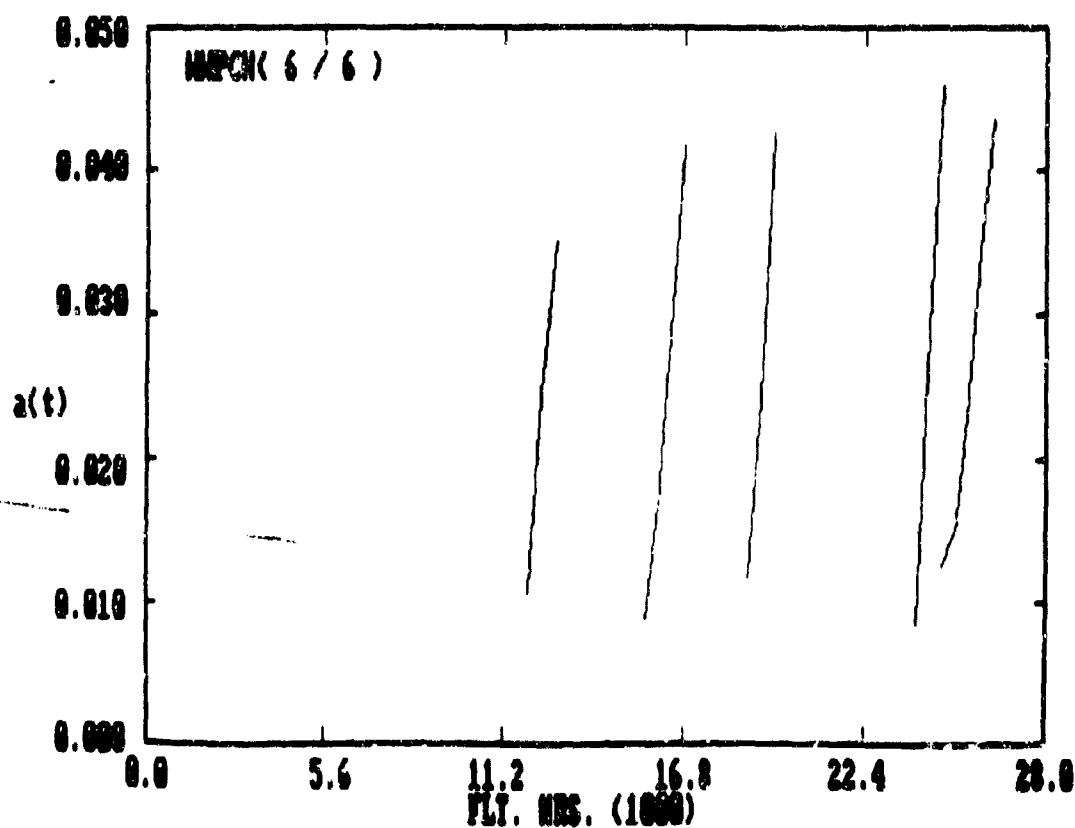


Figure B.12.   a(t) VERSUS t FRACTOGRAPHIC DATA FOR WWPCH     B-16
DATA SET (AL-AU = 0 - .05").
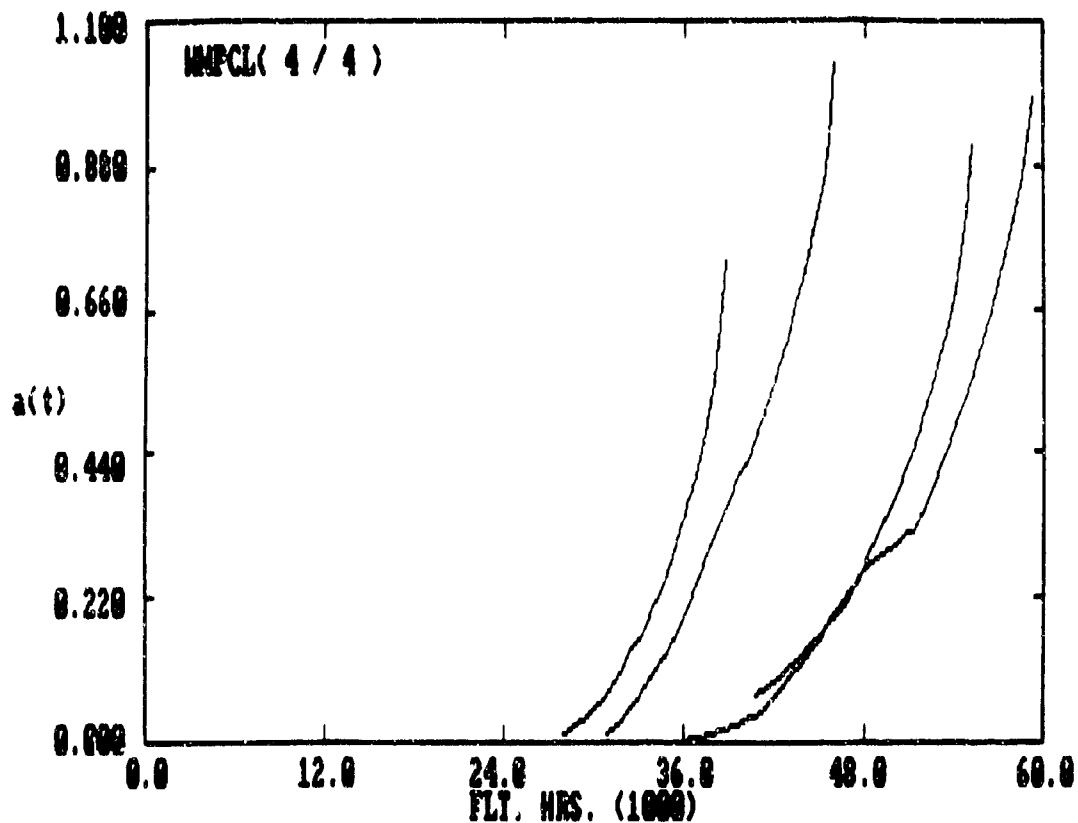
Figure B.13.   a(t) VERSUS t FRACTOGRAPHIC DATA FOR WWPCL
DATA SET (FULL RANGE).
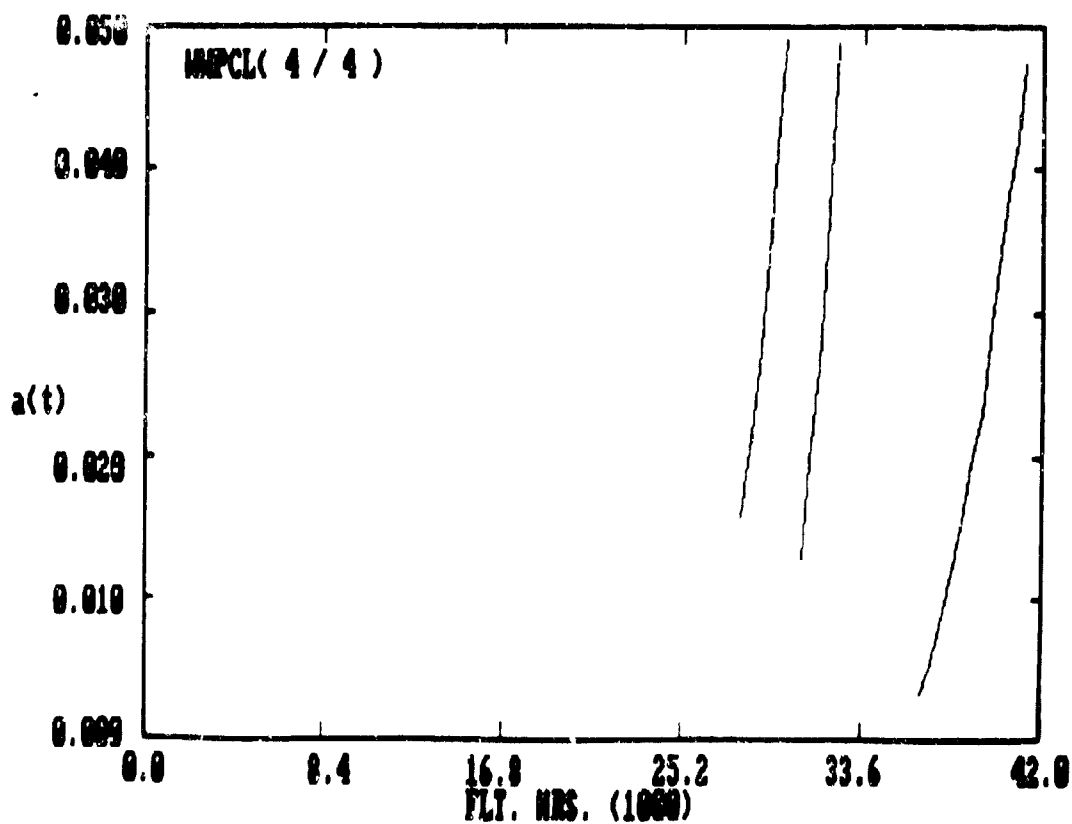


Figure B.14.   a(t) VERSUS t FRACTOGRAPHIC DATA FOR WWPCL
DATA SET (AL-AU = 0 - .05").

B-17
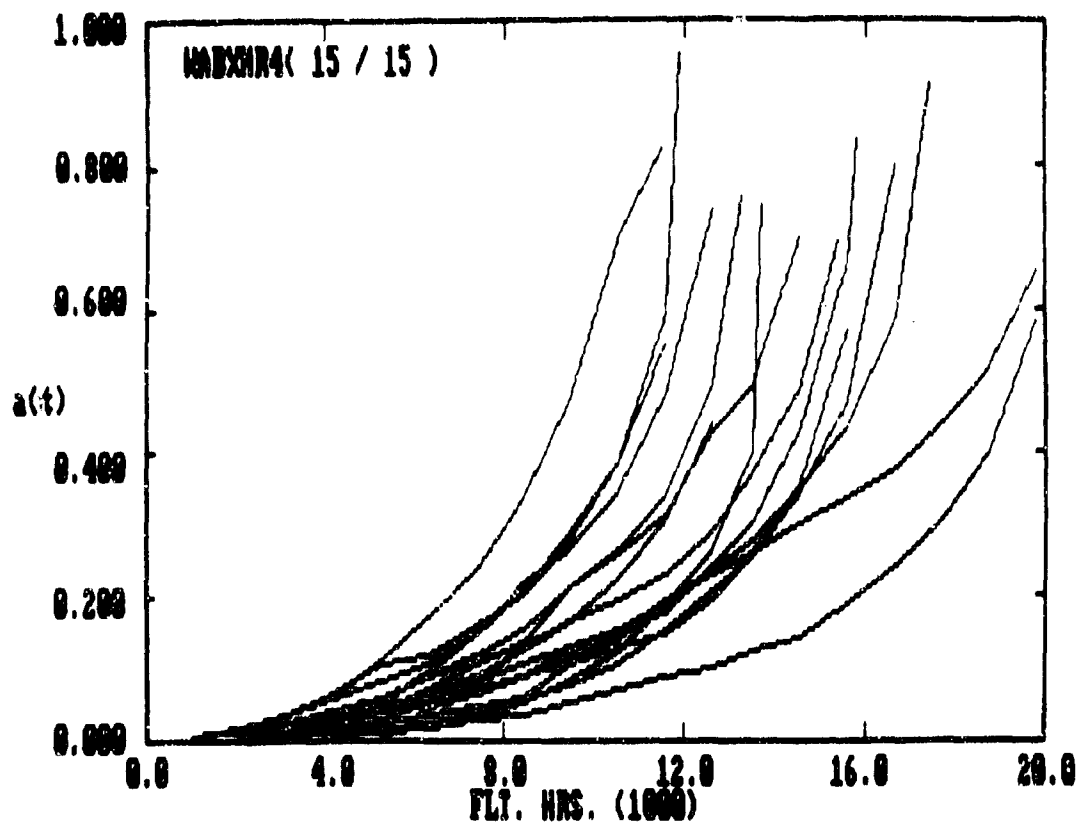
Figure B.15. a(t) VERSUS t FRACTOGRAPHIC DATA FOR WABXHR4 DATA SET (FULL RANGE)
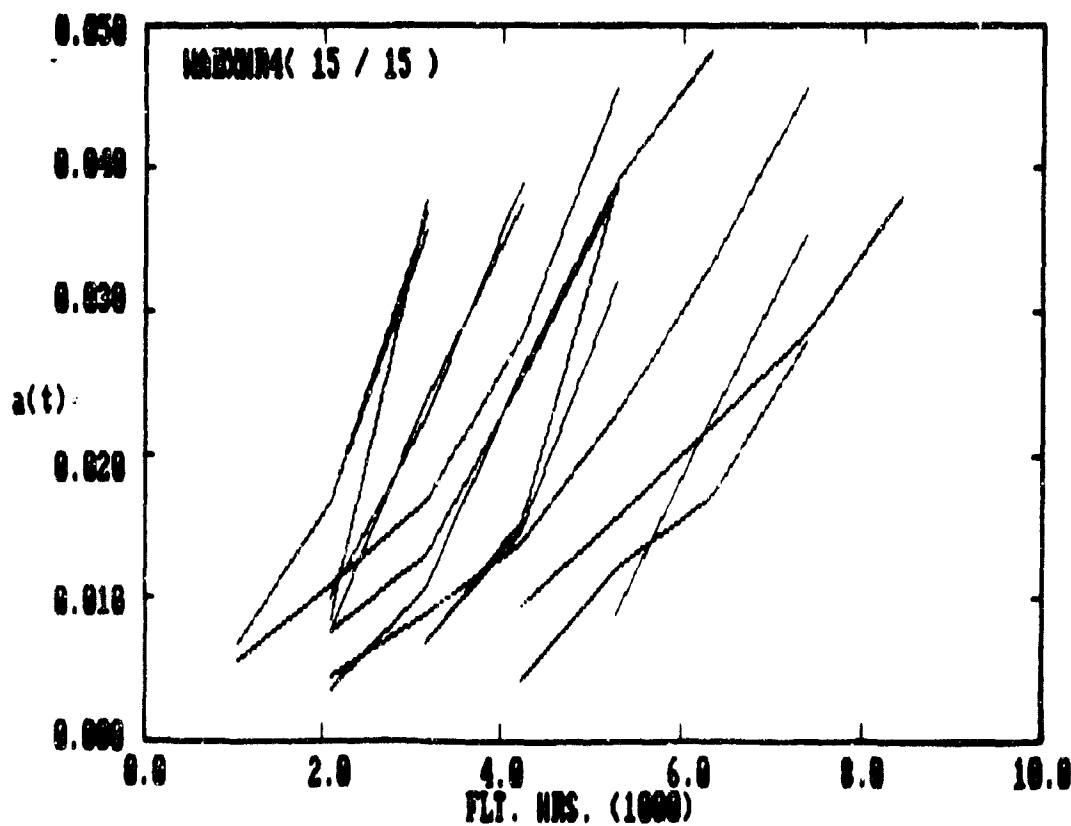


Figure B.16. a(t) VERSUS t FRACTOGRAPHIC DATA FOR WABXHR4 DATA SET (AL-AU = 0 - .05")

B 18
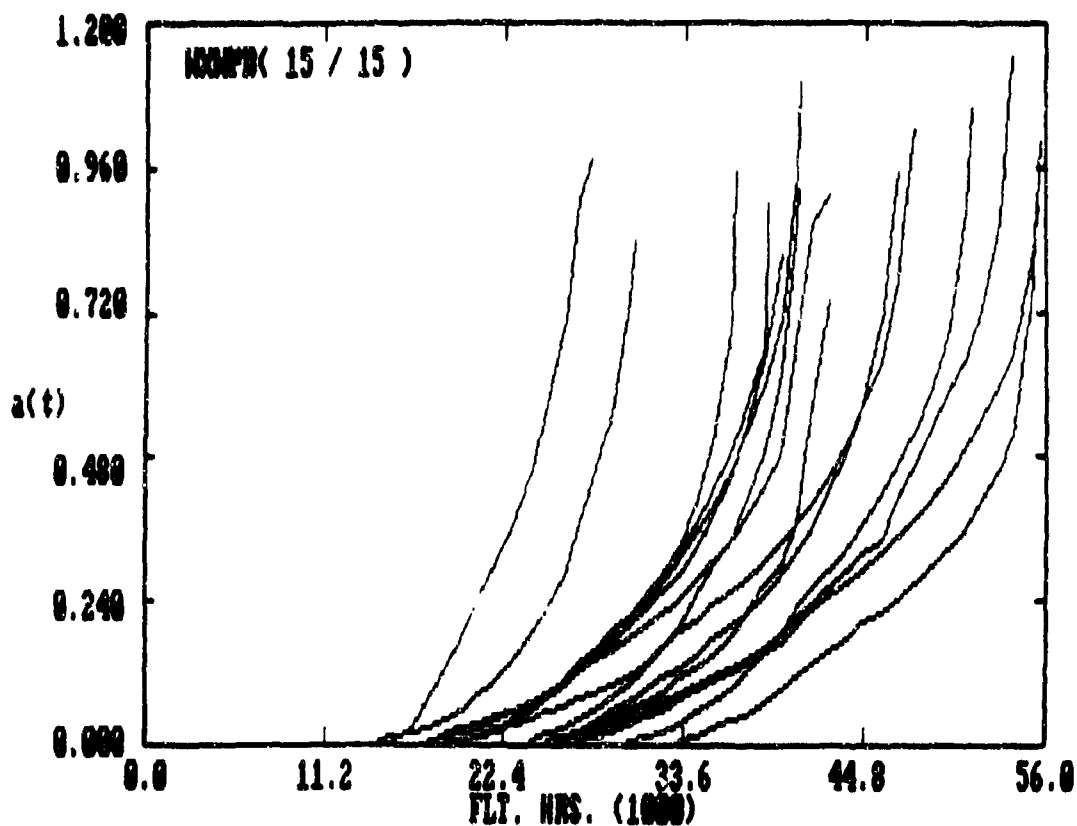
Figure B.17.   a(t) VERSUS t FRACTOGRAPHIC DATA FOR WXWPB
DATA SET (FULL RANGE).
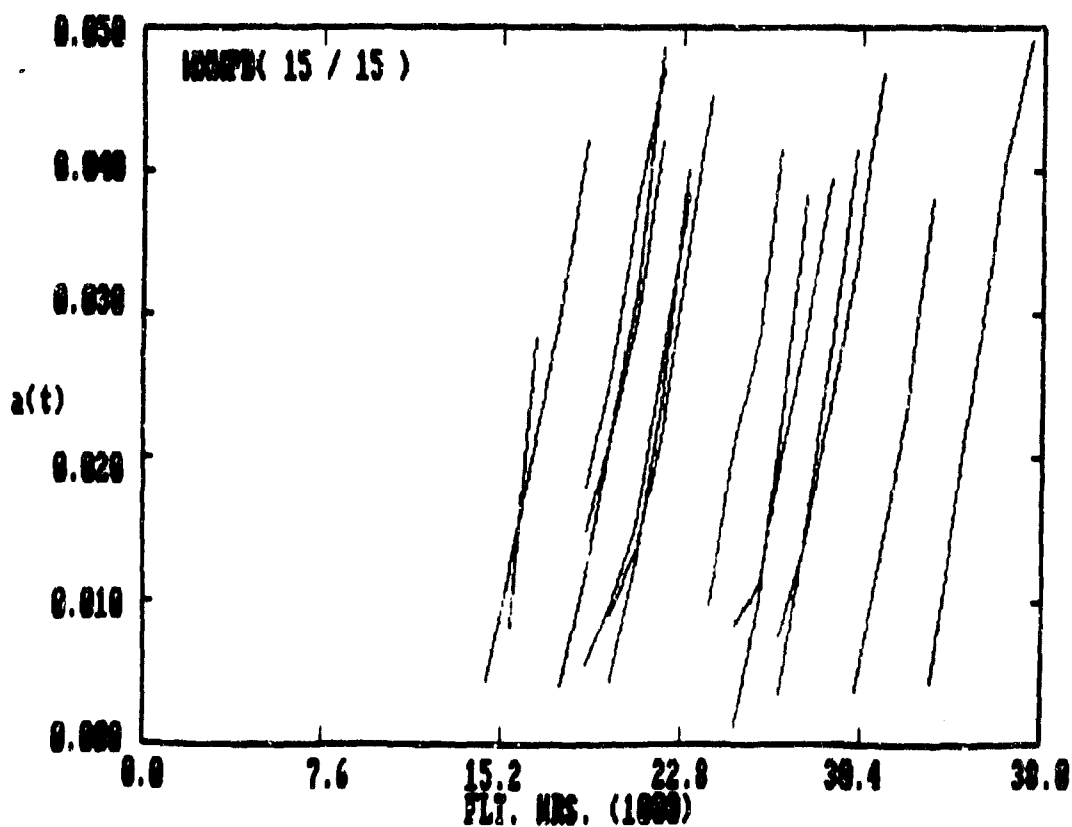


Figure B.18.   a(t) VERSUS t FRACTOGRAPHIC DATA FOR WXWPB       B-19
DATA SET (AL-AU = 0 - .05").
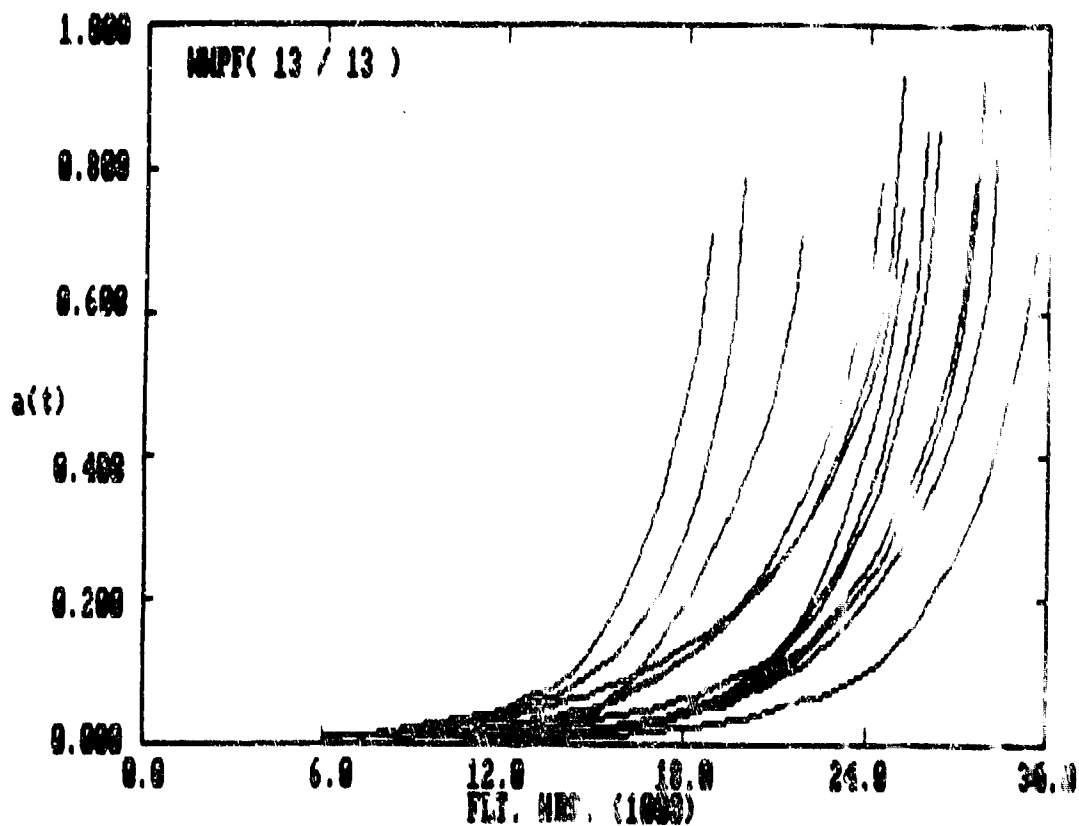
Figure B.19. a(t) VERSUS t FRACTOGRAPHIC DATA FOR WWPF
DATA SET (FULL RANGE)
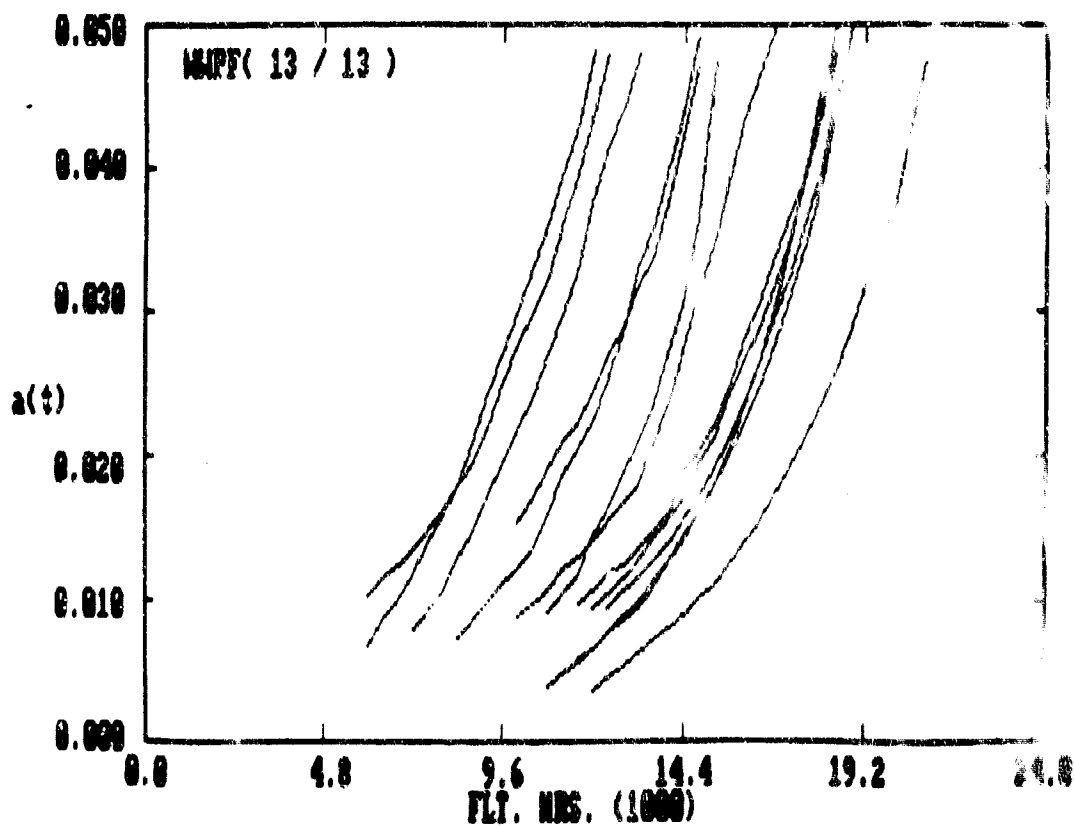


Figure B.20. a(t) VERSUS t FRACTOGRAPHIC DATA FOR WWPF
DATA SET (AL-AU = 0 - .05")
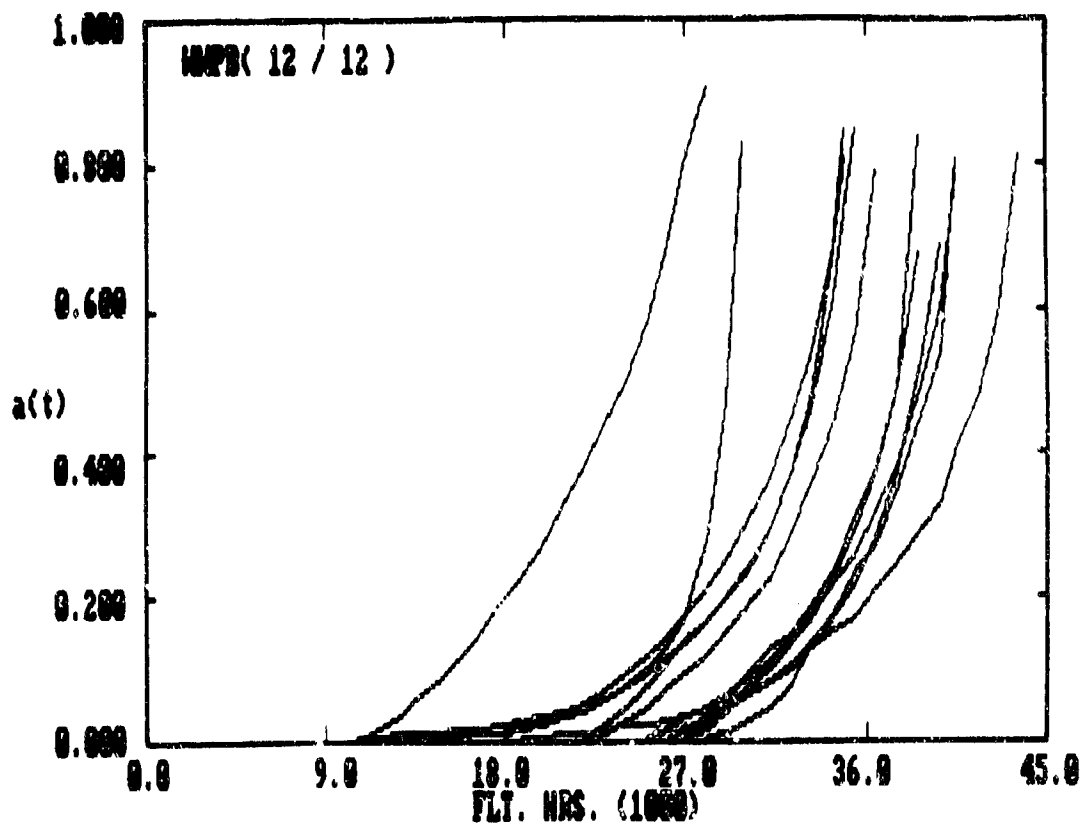
Figure B.21.    a(t) VERSUS t FRACTOGRAPHIC DATA FOR WWPB
                DATA SET (FULL RANGE).
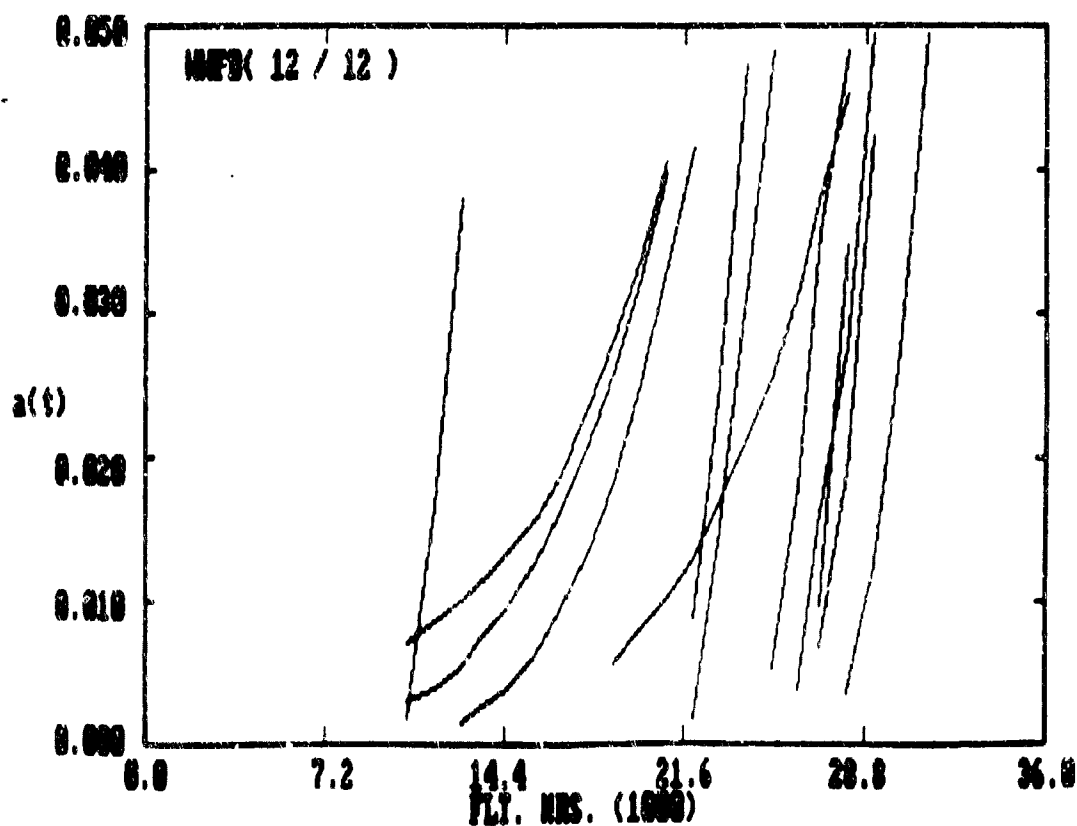


Figure B.22.    a(t) VERSUS t FRACTOGRAPHIC DATA FOR  WWPB
                DATA SET (AL-AU = 0 - .05").
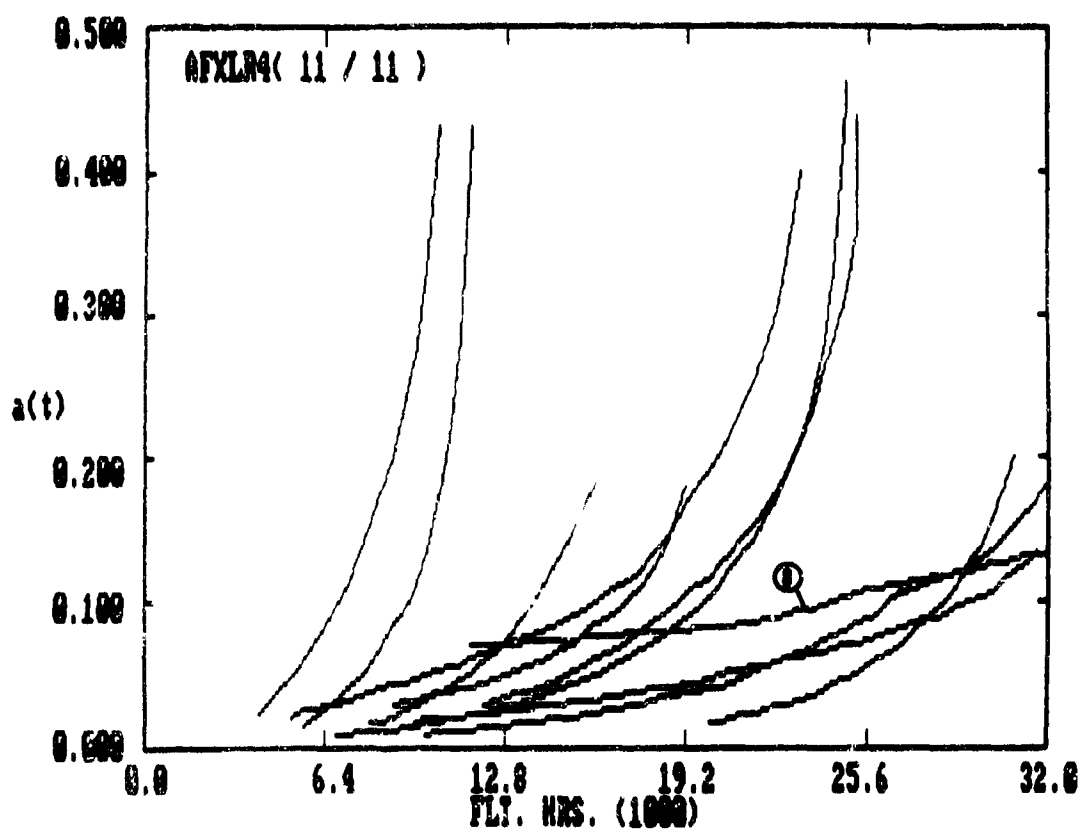
Figure B.23.  a(t) VERSUS t FRACTOGRAPHIC DATA FOR AFXLR4
DATA SET (FULL RANGE).
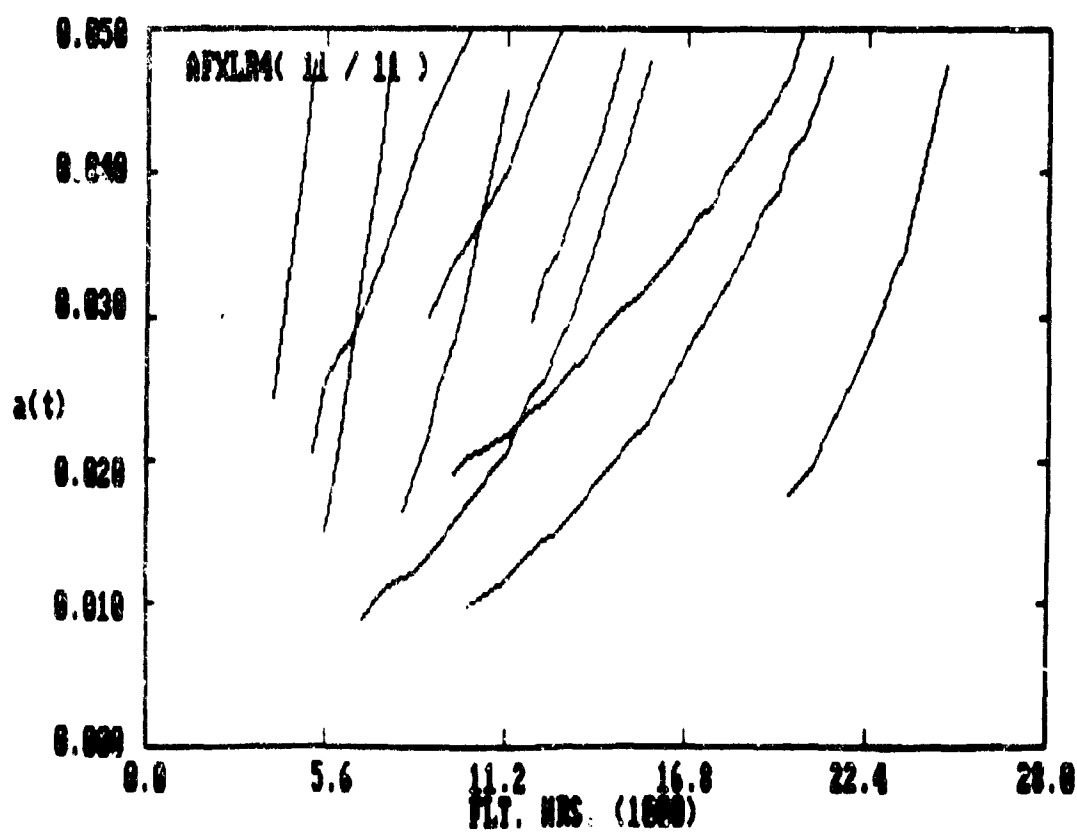


Figure B.24.  a(t) VERSUS t FRACTOGRAPHIC DATA FOR AFXLR4
DATA SET (AL-AU = 0 - .05").
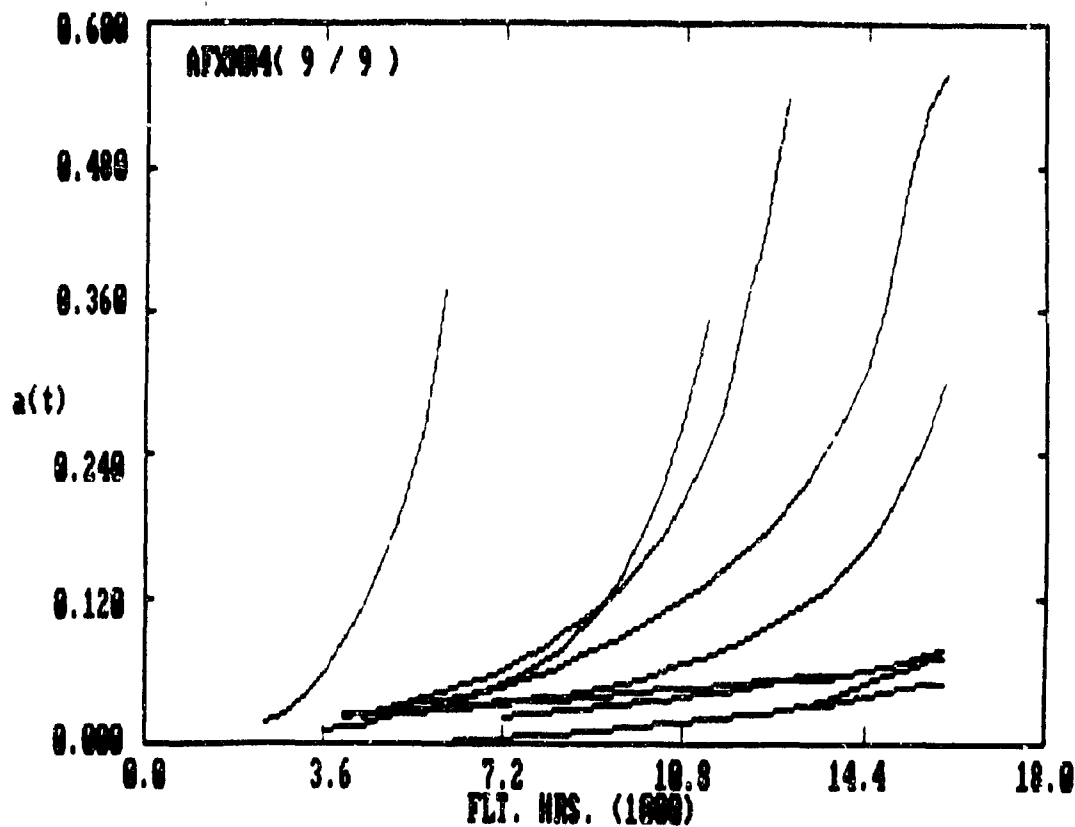
Figure B.25. a(t) VERSUS t FRACTOGRAPHIC DATA FOR AFXMR4 DATA SET (FULL RANGE).
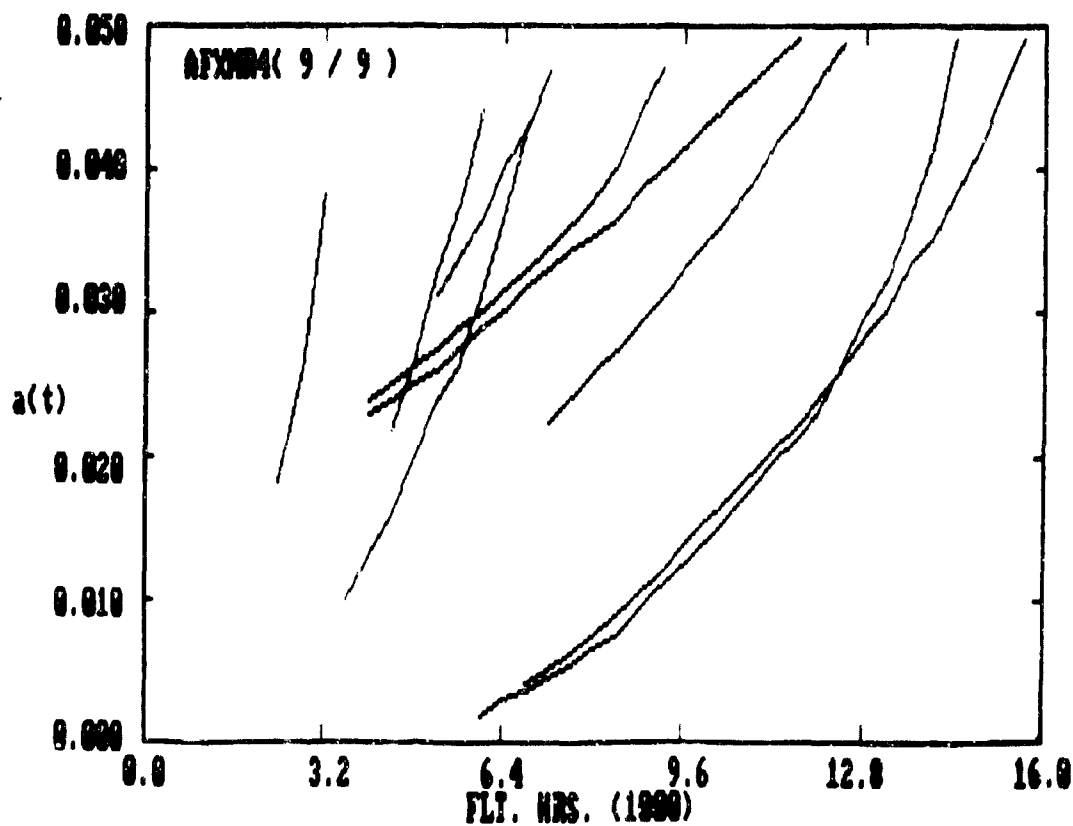


Figure B.26. a(t) VERSUS t FRACTOGRAPHIC DATA FOR AFXMR4 DATA SET (AL-AU = 0 - .05").
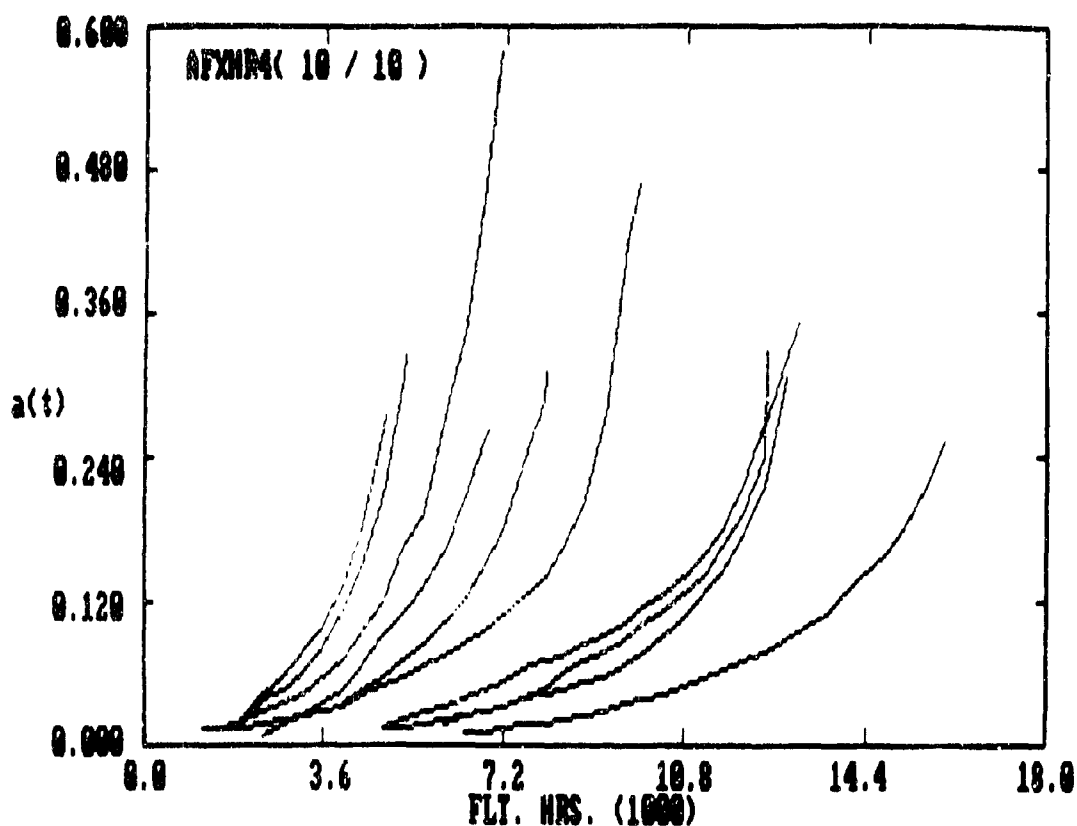
Figure B.27.  a(t) VERSUS t FRACTOGRAPHIC DATA FOR AFXHR4
DATA SET (FULL RANGE).
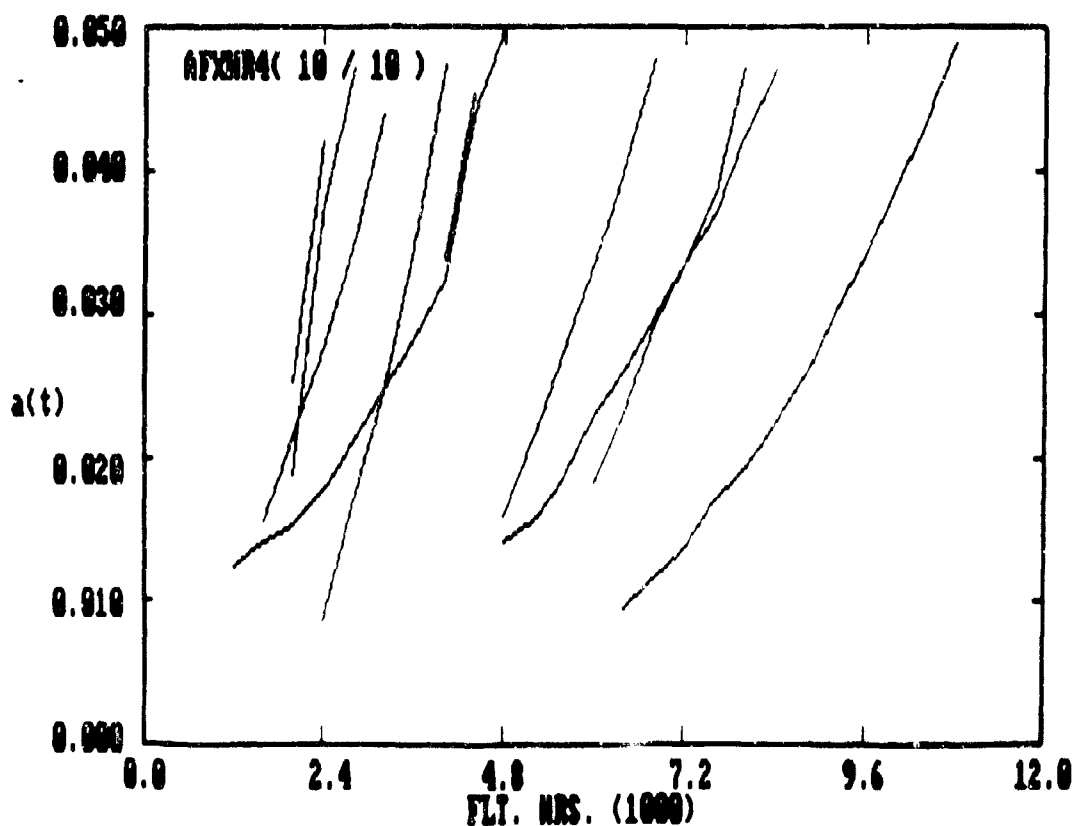


Figure B.28.  a(t) VERSUS t FRACTOGRAPHIC DATA FOR AFXHR4
DATA SET (AL-AU = 0 - .05")

# APPENDIX C
## EVALUATION OF STATISTICAL SCALING METHOD

### C.1 INTRODUCTION

The purpose of this section is to evaluate the statistical scaling method described in Volume I [1]. This method can be applied to obtain the EIFSD for fastener holes on a "single hole basis" using only the fractographic data for the largest crack in $l$ holes per specimen. Fractographic results from Volume III [2] will be used.

The initial fatigue quality of fastener holes is
"single hole population basis." This means that the fatigue cracking resistance of each fastener hole in each specimen should be accounted for. If fractographic readings are available for the largest fatigue crack in each hole of each specimen, and these results are used to define the IFQ, the resulting IFQ will automatically reflect a single hole population basis. However, if fractographic results are available only for the largest fatigue crack per specimen with $l$ holes, a method is needed for "scaling" the fractographic results to obtain the EIFD on a single hole population basis. Such a method has been developed in Volume I [1].

### C.2 EVALUATION PLAN

The plan for evaluating the statistical scaling method described in Volume I [1] is conceptually described in Fig. C.1. A brief overview of the plan is described below and details are provided later.

1. The statistical scaling method is evaluated using the durability analysis methods developed in Volume I [1] and the "WFI" fractographic data set from Volume III [3]. The
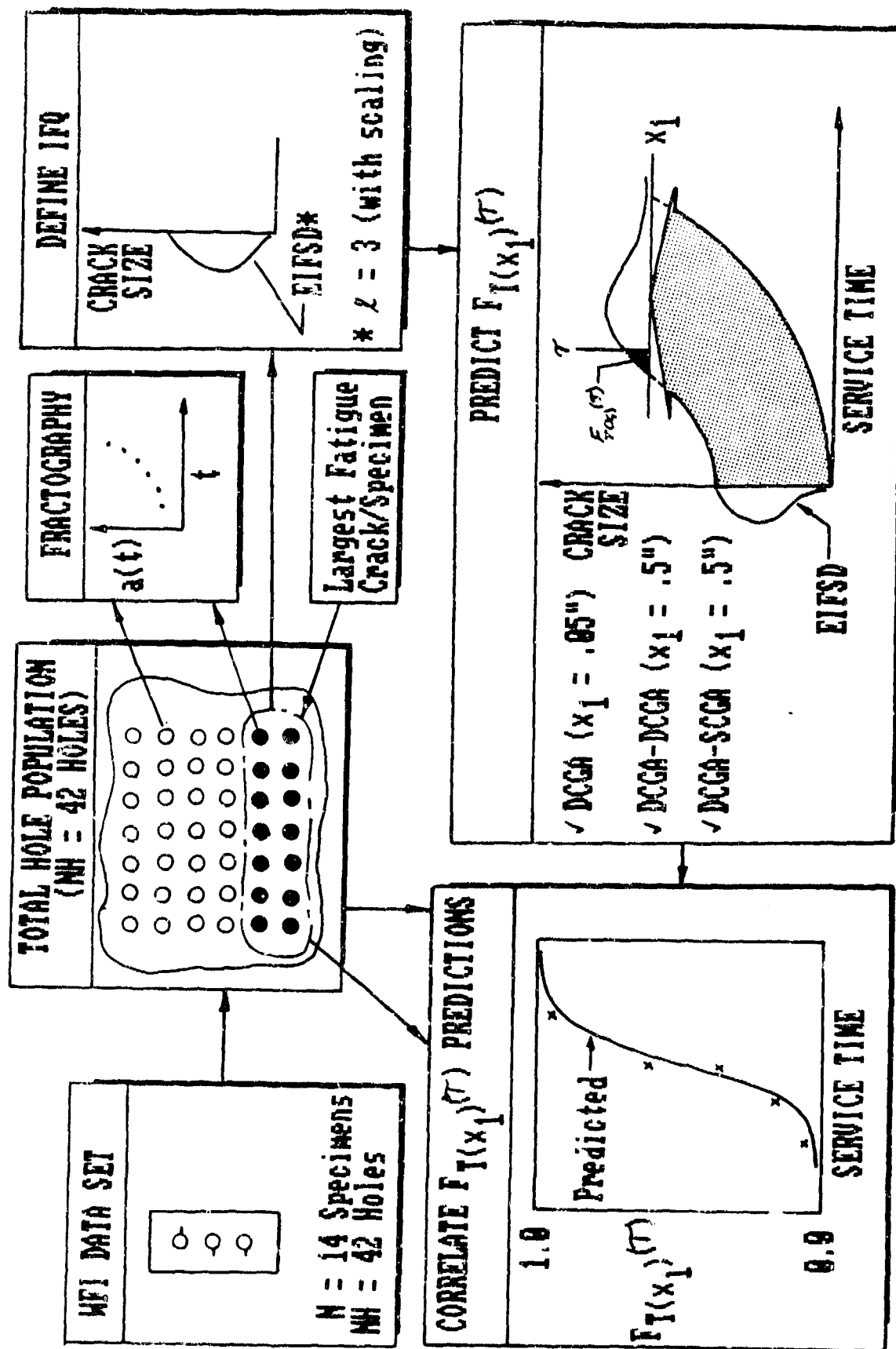
Figure C.1. Study Plan for Evaluating Statistical Scaling Method.

WFI data set is described in Table C.1 and specimen details are shown in Fig. 1.

2.  The initial fatigue quality of the 42 fastener holes in the WFI data set is estimated using (1) fractographic results for only 14 fastener holes (i.e., the largest fatigue crack in each of 14 specimens), (2) the Weibull compatible distribution function (Eq. 1), (3) statistical scaling, (4) combined least square sums approach (CLSSA), and (5) an "EIFS fit   A fractographic crack size range of AL-AU = .01"-.05" and $x_u$ = .03" is used to estimate the EIFSD parameters (i.e.,$\alpha$ and $\phi$). The EIFSD parameter $\phi$ is also estimated using $\ell$ = 1 (no scaling) and $\ell$ = 3 (with scaling) for later evaluation and comparison.

3.  Predictions for the cumulative distribution of service time, $F_{T(x_i)}(T)$, to reach $x_1$ = .05" based on the one segment DCGA, are correlated with experimental results for WFI data set. Results are evaluated for the following:  (1) largest fatigue crack per specimen (NH = 14), (2) total fastener hole population (NH = 42 fastener holes).

4.  Statistical scaling is also evaluated for $F_{T(x_1)}(T)$ predictions in the large crack size region (e.g., $x_1$ = .5"). In this case two different two-segment crack growth approaches are considered (i.e., DCGA-DCGA and DCGA-SCGA). The IFQ based on $\ell$ = 3 is used to make $F_{T(x_T)}(T)$ predictions for $x_1$ = .5". Predictions are correlated with experimental results for the WFI data set (i.e., largest fatigue crack per specimen data).

C.3  WFI DATA SET DETAILS/DATA

The WFI data set, described in Table C.1 and in Fig. 1, includes 15 specimens fatigue tested to failure. Fracto-graphic results for only 14 specimens are used in the

C-3

TABLE C.1   Description of WFI Data Set

Material:   7475-T7351 Aluminum (1/2" plate)

No. Specimens:   14

Fastener Type:   MS-90353-08 (1/4") Blind Pull Through
                 Rivet (csk)

Specimen With:   3.00"

Test Spectrum:   F-16 400 Hour

Maximum Gross Stress:   34 ksi

No. of Holes/Specimen:   3

Percent of Load Transfer:   0%

evaluation herein because specimen WFI-12 was not tested properly. Each specimen in the WFI data set included 3 countersunk fastener holes with no load transfer and MS90353 rivets installed. Therefore, there are 42 fastener holes in the 14 specimens from the WFI data set.

The time-to-failure (TTF) for each specimen in the WFI data set and the service time to reach a crack size $x_1$ = .05" are summarized in Table C.2. Fastener holes are identified as "A", "B", and "C". Fractographic results were acquired [3] for the largest fatigue crack per specimen. Where possible, fractographic results were also acquired for the largest fatigue crack in the other two holes. In some cases, fractographic results could not be acquired for some fastener holes for various reasons (e.g., cracks too small and complex, damaged fracture surfaces, etc.). For ranking purposes, service times to reach a crack size $x_1$ = .05" in some fastener holes are shown as less than or greater than the TTF in Table C.2.

Service times for the largest fatigue crack per specimen (NH = 14 holes) to reach $x_1$ = .05" are summarized in Table C.3 for the WFI data set. These results are used later to correlate $F_{T(x_1)}(T)$ predictions.

Ranked service times to reach $x_1$ = .05" and .5" are summarized in Table C.4 for the WFI data set total hole population (i.e., NH = 42 holes). These results are used later to evaluate $F_{T(x_1)}(T)$ predictions.

### C.4    COMPUTATION OF Q AND $\sigma_z$

The crack growth rate parameter Q in Eq. 10 and the standard deviation $\sigma_z$ in Eq. 30 are needed to conduct the analysis described in Fig. C.1 and they are estimated using the fractographic results for the largest fatigue crack per specimen (NH = 14 holes) in the WFI data set. Pooled Q are obtained (i.e., AL-AU = .01"-.05" and .05"-.5") using Eqs. 4 and

Table C.2.  Summary of Service Times to Reach $x_i$ = .05" for Each Hole in Each Specimen of the WFI Data Set.

| WFI HOLE I.D. (1) | TTF (FLT. HRS.) (2) | | SERVICE TIME (FLT. HRS.) (7) | |
|---|---|---|---|---|
| | | A | B | C |
| -1 | 31200 | >31200 | 20191 | 28200 |
| -2 | 27200 | 22776 | 17867 | 13451 |
| -3 | 23600 (3) | 12747 | 12411 | <23600 |
| -4 | 30400 | 16302 | 22540 | 25167 |
| -5 | 30800 | 19376 | >30800 | 21892 |
| -6 | 17600 | 10400 | >17600 | 16428 |
| -7 | 16400 | 8445 | 12092 | >16400 |
| -8 | 28000 | >28000 | 15634 | <28000 |
| -9 | 36480 | 21235 | (30800) | 27843 |
| -10 | 30000 | 19200 | 22000 | 17000 |
| -11 | 20400 | 11617 | 16989 | <20400 |
| -12 | 30240 (4) | <30240 | 24240 | <30240 |
| -13 | 32400 | <32400 | 20218 | >32400 |
| -14 | 29360 | 17421 | 14440 | 25512 |
| -15 | 33600 | 20472 | >33600 | >33600 |

NOTES:  (1)  Material: 7475-T7351 Aluminum; Ref. Fig. 1
        (2)  TTF = Time-To-Failure
        (3)  Specimen failed when disk drive was disconnected from computer system
        (4)  Specimen bent in compression due to load cell malfunction
        (5)

        A
        B
        C
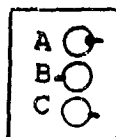
        (6)  (xxx) = Value extrapolated from fractographic results
        (7)  Ref. 2

Table C.3.  Summary of Service Times to Reach $x_1$  for
Largest Fatigue Crack/Specimen Basis (NH=14).

| I | SERVICE TIME (FLT. HRS.) | |
|---|---|---|
| | ($x_1$ = .05") | ($x_1$ = .50") |
| 1 | 8445 | 15860 |
| 2 | 10400 | 16938 |
| 3 | 11617 | 19342 |
| 4 | 12411 | 22683 |
| 5 | 13451 | 26255 |
| 6 | 14440 | 26509 |
| 7 | 15634 | 26864 |
| 8 | 16302 | 28939 |
| 9 | 17000 | 28994 |
| 10 | 19376 | 29782 |
| 11 | 20191 | 30445 |
| 12 | 20218 | 31423 |
| 13 | 20472 | 32230 |
| 14 | 21235 | 34950 |

Table C.4.  Summary of Ranked Service Times for Lower
Tail for WFI Data Set.

| I | I/(N+1) | SERVICE TIME (FLT. HRS.) | |
|---|---|---|---|
| | | ($x_1$ = .05") | ($x_1$ = .5") |
| 1 | .023 | 8445 | 15860 |
| 2 | .047 | 10400 | 16400 |
| 3 | .069 | 11617 | >16400 |
| 4 | .093 | 12092 | |
| 5 | .116 | 12411 | |
| 6 | .139 | 12747 | |
| 7 | .163 | 13451 | |
| 8 | .186 | 14440 | |
| 9 | .209 | >14440 | |
| 42 | .977 | >14400 | >16400 |

32, respectively. The IBM-compatible software of Volume V [5] and filename = "QSZAT" were used to determine pooled Q and $\sigma_Z$ values. Results are summarized in Table C.5.

## C.5    ESTIMATE EIFSD PARAMETERS

EIFSD parameters for the Weibull compatible distribution function, Eq. 1, were estimated for $x_u = .03''$ using: (1) fractographic results for the largest fatigue crack per specimen in the WFI data set, (2) the CLSSA, (3) an "EIFS fit", and (4) statistical scaling (i.e., $\ell = 1$ (no scaling) and $\ell = 3$ (with scaling)). IBM-compatible PC software from Volume V [5] and filename = "WCIFQ" were used. The resulting EIFSD parameters without scaling ($\ell = 1$) and with scaling ($\ell = 3$) are summarized in Table C.6.

## C.6    $F_{T(x_1)}(T)$ PREDICTIONS AND CORRELATIONS

$F_{T(x_1)}(T)$ predictions for $x_1 = .05''$ based on the one segment DCGA, are correlated with experimental results for the WFI data set in Figs. C.2 through C.4.

In Fig. C.2, predicted service times to reach $x_1 = 0.05''$, $F_{T(x_1)}(T)$, for the largest fatigue crack per specimen (NH = 14) in the WFI data set, based on the EIFSD established with scaling ($\ell = 3$), are plotted as a solid curve. The experimental results are shown in the figure as a plus sign (+) for comparison. The same predictions and correlations are displayed in Fig. C.3 when the EIFSD is established without scaling ($\ell = 1$).

Theoretical predictions for $F_{T(x_1)}(T)$ for the total hole population (NH = 42) of the WFI data set, based on the EIFSD established without scaling ($\ell = 1$), are displayed in Fig. C.4 as a solid curve. The ranked experimental results for the 8 smallest values out of 42 holes are shown as a plus sign (+) for comparison. Similar predictions and correlations are given in Fig. C.4 when the EIFSD is established with scaling

Table C.5.  Summary of Pooled Q and $\sigma_z$ Values for Different Crack Size Ranges for WFI Data Set.

| CRACK SIZE RANGE | $Qx10^4$ (1/HR.) | $\sigma_z$ |
|---|---|---|
| .01" – .05" | 2.329 | .247 |
| .05" – .5" | 2.114 | .212 |

Table C.6. Summary of EIFSD Parameters for Weibull Compatible Distribution Function for WFI Data Set.

| CASE | AL – AU | $Qx10^4$ | $a_0$ | $\ell$ | $x_u$ | $\alpha$ | $\phi$ |
|---|---|---|---|---|---|---|---|
| I | .01" – .05" | 2.329 | .05" | 1 | .03" | 3.045 | 3.565 |
| II | .01" – .05" | 2.329 | .05 | 3 | .03" | 3.045 | 5.113 |
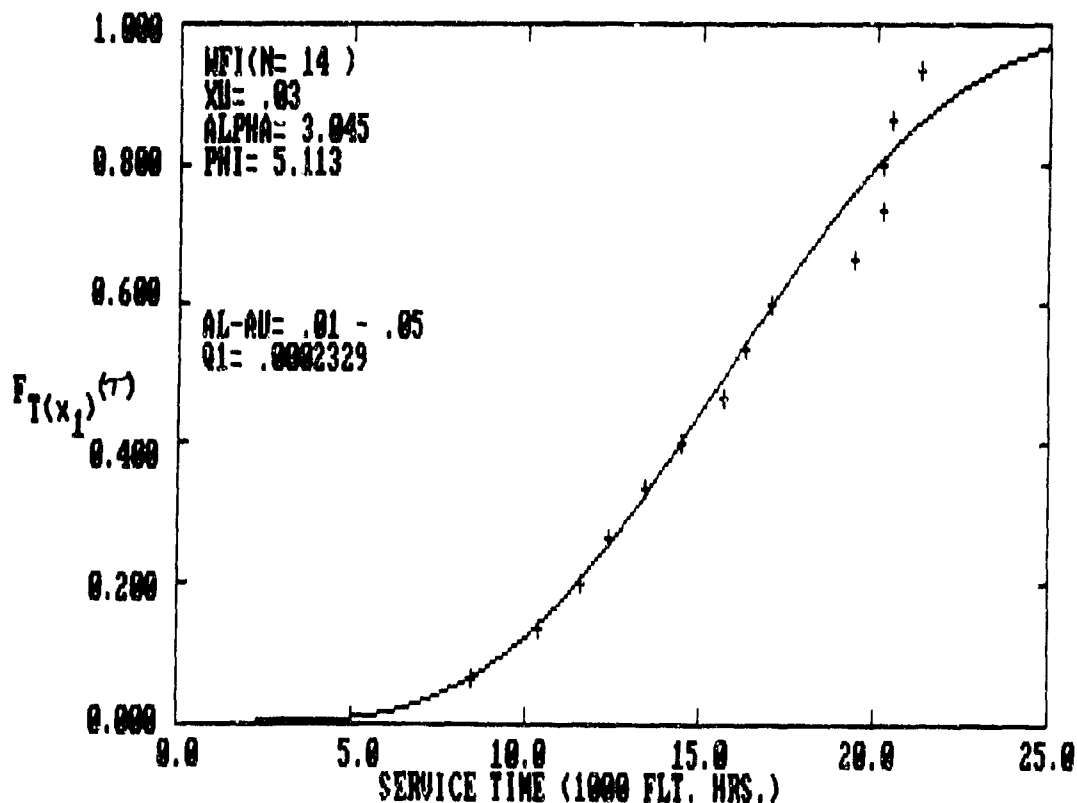
Figure C.2.    Predicted Service Time to Reach $x_1$ = .05" for the
Largest Fatigue Crack Per Specimen (NH = 14) in the
WFI Data Set Based on EIFSD With Scaling ($\ell$ = 3).
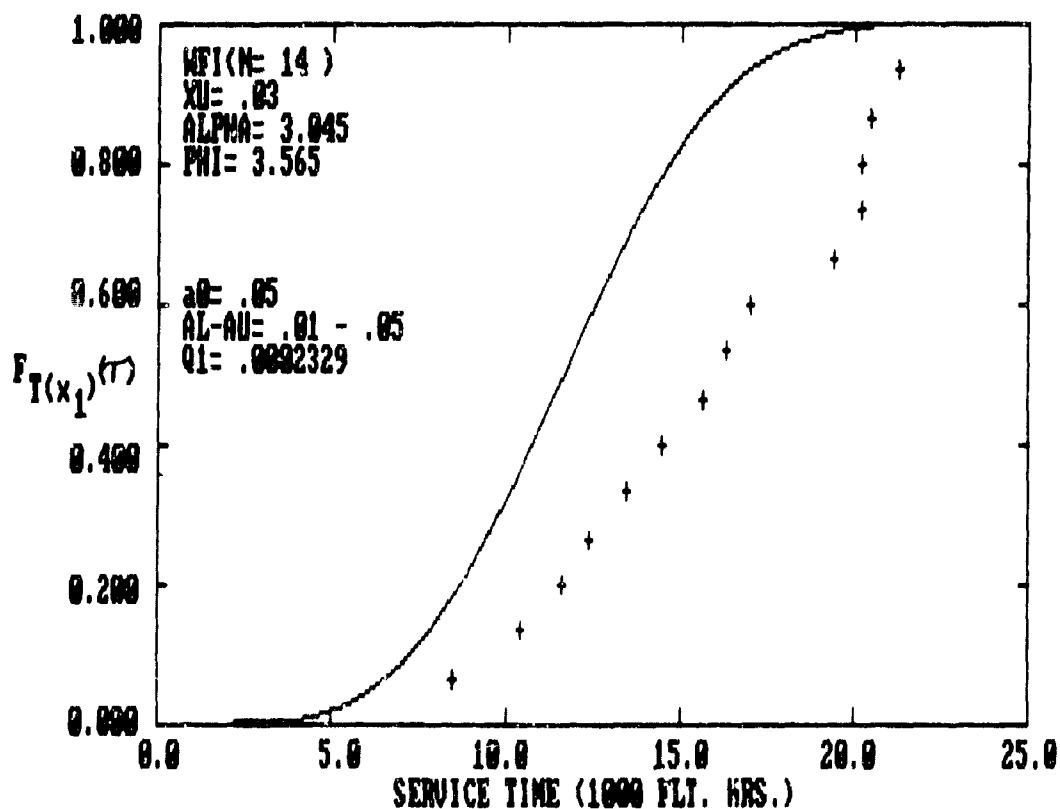


Figure C.3.    Predicted Service Time to Reach $x_1$ = .05" for the
Largest Fatigue Crack Per Specimen (NH = 14) in the
WFI Data Set Based on EIFSD Without Scaling ($\ell$ = 1).

($\ell$ = 3). The ranked service times for $x_1$ = .05" reflected in Figs. C.2 through C.5 are shown in Tables C.3 and C.4.

Data for the service time to reach a large crack size of $x_1$ = 0.5" for the total hole population can not be analyzed and ranked meaningfully. This is because when a specimen fails, most of the cracks in the other two holes have not reached 0.5" yet. However, service data to reach $x_1$ = 0.5" for the crack population consisting of the largest fatigue crack per specimen (NH = 14) are available. Consequently, correlations and predictions will be made for such a crack population using EIFSD established with ($\ell$ = 3) and without ($\ell$ = 1) scaling. $F_{T(x_1)}(T)$ predictions for $x_1$ = 0.5" using the two-segment DCGA-DCGA are plotted as a solid curve in Fig. C.6. The predicted results are based on the EIFSD with scaling of $\ell$ = 3. For comparison, the ranked test results are depicted as a plus sign (+) in the same figure. Similar predictions and correlations are displayed in Fig. C.7 using the two-segment DCGA-SCGA.

## C.7    DISCUSSIONS AND CONCLUSIONS

The statistical scaling technique developed in Volume I [1] has been evaluated herein using fractographic results for coupon specimens containing three fastener holes per specimen. Theoretical predictions for $F_{T(x_1)}(T)$ at $x_1$ = .05", based on the one-segment DCGA and $\ell$ = 3, correlated very well with ranked service times for NH = 14 holes (Fig. C.2) and NH = 42 holes (Fig. C.5). The effects of "scaling" can be clearly shown by comparing the results of Fig. C.2 ($\ell$ = 1) with Fig. C.3 ($\ell$ = 3) as well as the results of Fig. C.4 ($\ell$ = 1) with Fig. C.5 ($\ell$ = 3). It is clear that the fatigue cracking resistance of each fastener hole in a test specimen should be accounted for when defining the IFQ of fastener holes.

$F_{T(x_1)}(T)$ predictions for the largest fatigue crack per specimen (NH = 14) with $x_1$ = .5", based on the DCGA-DCGA and the DCGA-SCGA, are shown in Figs. C.6 and C.7, respectively.
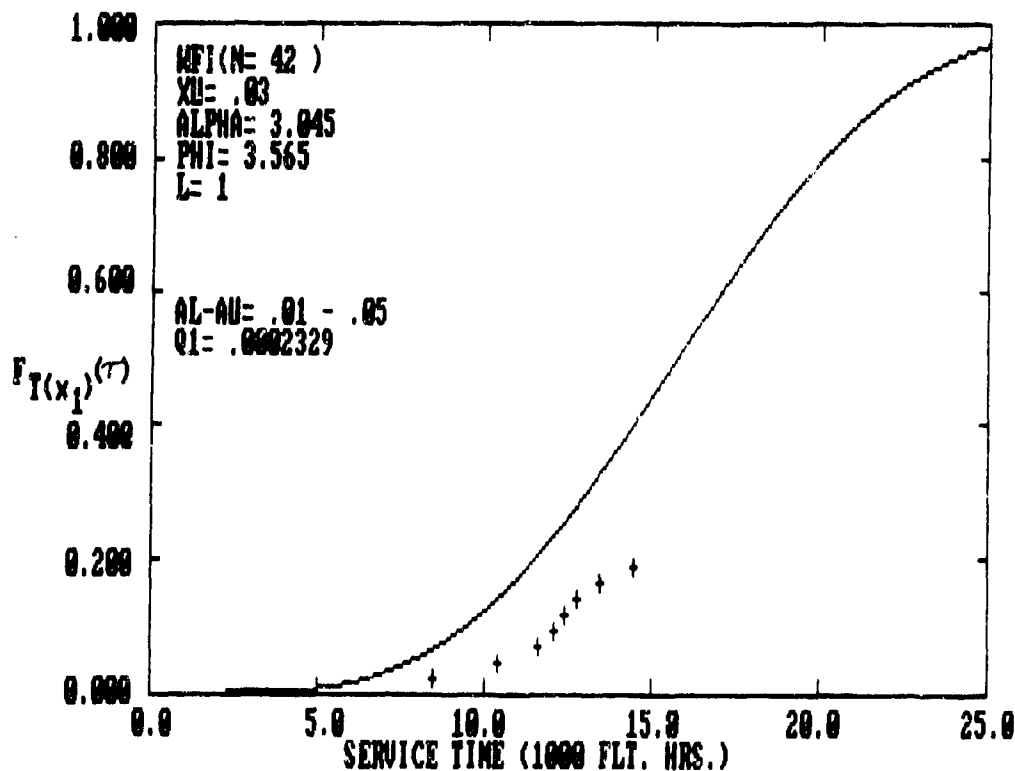
Figure C.4. **Predicted Service Time to Reach** $x_1$ **= .05" for the Total Hole Population (NH = 42) of the WFI Data Set Based on EIFSD Parameters With No Scaling ($\ell$ = 1).**
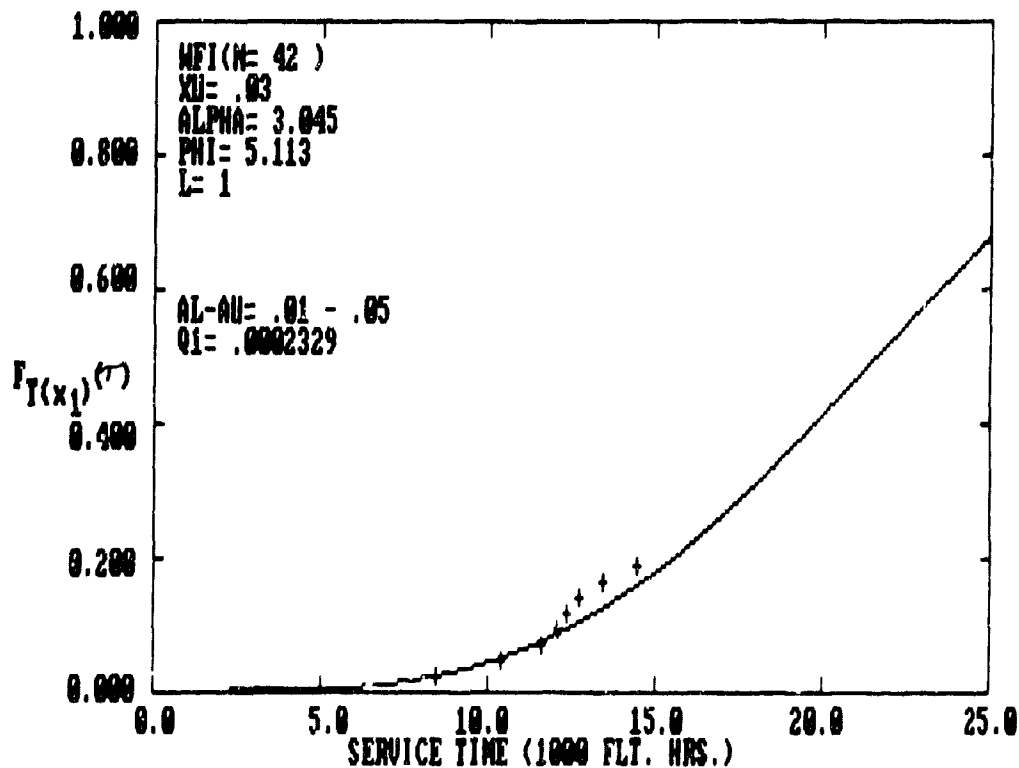


Figure C.5. **Predicted Service Time to Reach** $x_1$ **= .05" for the Total Hole Population (NH = 42) of the WFI Data Set Based on EIFSD Parameters With Scaling ($\ell$ = 3).**
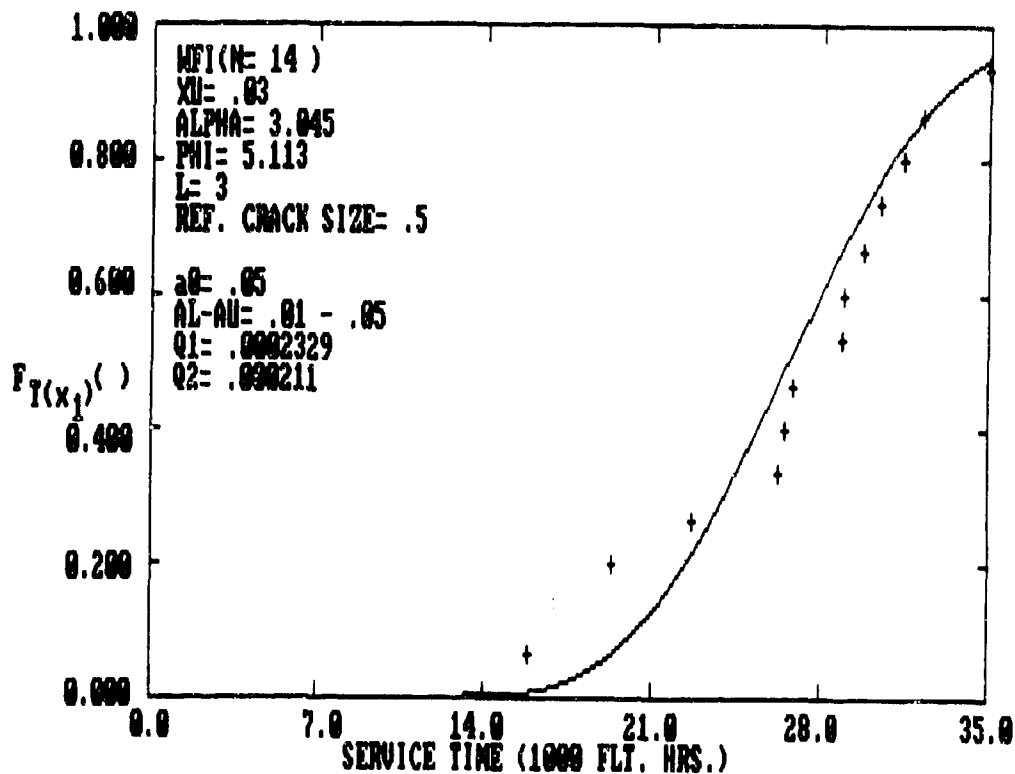
Figure C.6. Predicted Service Time to Reach $x_1$ = .5" for the Largest Fatigue Crack Per Specimen (NH = 14) in the WFI Data Set Based on EIFSD Parameters With Scaling ($\ell$ = 3); DCGA-DCGA.
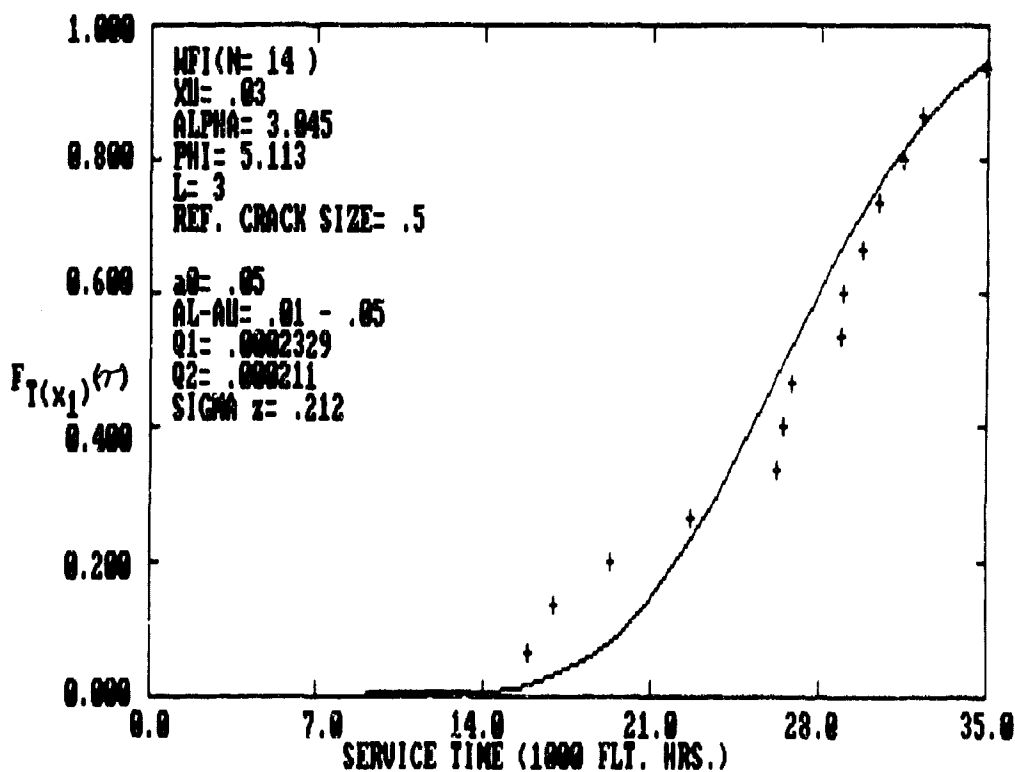


Figure C.7. Predicted Service Time to Reach $x_1$ = .5" for the Largest Fatigue Crack Per Specimen (NH = 14) in the WFI Data Set Based on EIFSD Parameters With Scaling ($\ell$ = 3); DCGA-SCGA.

These results reflect a scaling factor of $\ell = 3$ used for establishing EIFSD. Theoretical predictions in both cases correlated reasonably well with ranked service times to reach $x_1 = .5"$. No significant difference in the theoretical predictions for either the DCGA-DCGA or the DCGA-SCGA were observed in this case.

The statistical scaling technique has also been demonstrated using the F-16 lower wing skins in Section 4.4 of this volume (II). Very reasonable durability analysis predictions were obtained using the statistical scaling technique developed.

# APPENDIX D
## SERVICE CRACK GROWTH MASTER CURVE
## TUNING STUDY

### D.1 INTRODUCTION

A service crack growth master curve (SCGMC) and an equivalent initial flaw size distribution (EIFSD) are needed to predict the probability of crack exceedance at any service time for desired service conditions (e.g., load spectrum, stress level, % bolt load transfer, etc.). SCGMCs can be determined using either fractographic results (if available) or a suitable LEFM analytical crack growth program [e.g., 24]. For consistent durability analysis, the SCGMC should be compatible with the basis for EIFSD. When a LEFM analytical crack growth program is used to define the SCGMC, the crack growth program should be "tuned" or "curve fitted" to the EIFSD data base.

A study was performed to illustrate how SCGMCs can be determined by "curve fitting" an analytical crack growth program to the EIFSD data base. Details of the study, including methods, results and conclusions are presented in this section.

### D.2 DETAILS OF THE SCGMC TUNING STUDY

A SCGMC tuning study was performed using eight fractographic data sets from the "Fastener Hole Quality" program [3]. The data sets used are described in Table D.1.

Based on Eq. D-1, an EIFS master curve was defined for each fractographic data set.

$$a(0) = a(t) \exp(-Qt) \qquad \text{(D-1)}$$

Table D.1  Description of Fractographic Data Sets Used in the
SCGMC Study

| Fractographic Data Set [3] | Material | % Bolt Load Transfer | Load Specrum | Max. Stress (Gross) (ksi) | Fastener I.D. |
|---|---|---|---|---|---|
| WPF | 7475-T7351 | 0 | F-16 400 Hrs | 34 | *NAS-6402 (1/4" Dia) |
| XWPF | | 15 | | 34 | |
| HYWPF | | 15 | | 40.8 | |
| LYWPF | | 15 | | 30.6 | |
| WPB | | 0 | B-1 Bomber | 34 | |
| XWPB | | 15 | | 34 | |
| HYWPB | | 15 | | 40.8 | |
| LYWPB | | 15 | | 30.6 | |

*Straight shank fastener installed in a straignt-bore hole drilled with
a Modified Winslow Specematic drill.

in which a(0) = EIFS, a(t) = crack size at time t, and Q = "pooled Q" value for a data set. Equation D-1 is based on the crack growth rate model of Eq. D-2 (Refer to Volume I for details [1]).

$$da(t)/dt = Q*a(t) \qquad (D-2)$$

Pooled Q values for each of the eight fractographic data sets were determined using a fractographic crack size range of AL-AU = 0.01" - 0.05". Results are summarized in Table D.2. The pooled Q values are based on a preliminary method developed early in the program. For example, Q values were based directly on Eq. D-2 instead of Eq. D-1, that is now recommended for use. Also, this study was conducted without any prior screening or plotting of the fractographic data. Fractographic results for a few surface cracks were combined with results for fatigue cracking in the bore of the fastener hole. The pooled Q values used in this study, however, have the same order of magnitude as those values based on the refined method. For illustrative purposes, it is not critical if the pooled Q values used are identical to those based on the refined methods with fractographic data screening. The main goal of this section is to illustrate "curve fitting" the analytical crack growth program to the EIFSD data base in order to obtain the desired SCGMC(s).

The SCGMC tuning study was based on the following: (1) RXN analytical crack growth program [24], (2) Walker- ΔK crack growth rate model [25], and (3) Modified Willenborg retardation model [26]. Different parameter values were used in the SCGMC tuning study (see Table D.3 for summary).

The Walker ΔK equation [25], given in Eq. D-3, was used to model the crack growth rate in the RXN analytical crack growth program. In Eq. D-3, a = half crack length, N =

Table D.2  Summary of EIFS Master Curve Parameters Used in the SCGMC Tuning Study

| Fractographic Data Set [3] | Load Spectrum | Crack Size Range Used | $Q_i * \times 10^4$ (1HR) | $a(0)*$ (In) |
|---|---|---|---|---|
| WPF | F-16 400 Hr | 0.01"-0.05" | 2.731 | 0.005" |
| XWPF | | | 3.437 | |
| HYWPF | | | 8.316 | |
| LYWPF | ↓ | | 2.210 | ↓ |
| WPB | B-1 Bomber | | 1.258 | |
| XWPB | | | 2.368 | |
| HYWPB | | | 4.375 | |
| LYWPB | ↓ | ↓ | 1.550 | ↓ |

*Initial flaw size at t= 0

TABLE D.3  Summary of Parameters Used in The SCCHC Tuning Study

| FRACTOGRAPHIC DATA SET [3] | LOAD SPECTRUM | WALKER-ΔK PARAMETERS (1) | | | GENERALIZED WILLENBORG | | RXH CRACK GROWTH ANALYSIS INPUT | | | | | |
|---|---|---|---|---|---|---|---|---|---|---|---|---|
| | | $C \times 10^{10}$ | M | N | $(K_{max})_{TH}$ (2) | S (3) | $K_{Ic}$ (ksi-$\sqrt{in}$) | YIELD STR. (ksi) | HOLE DIA. (In) | STRESS LEVEL (ksi) | % LT (5) | INITIAL FLAW SIZE (4) |
| MPF | F-16 400 HR | 9.3 | 3.543 | 0.60 | 1.50 | 2.00 | 35 | 59.5 | 0.25 | 34 | 0 | 0.005 |
| | | | | | | 2.50 | | | | | 0 | |
| XMPF | | | | | | 2.55 | | | | | 3.0 | |
| | | | | | | 2.65 | | | | | 4.0 | |
| | | | | | | 3.00 | | | | | 5.0 | |
| HYWPF | | | | | | 2.55 | | | | 40.8 | 7.0 | |
| | | | | | | | | | | | 3.0 | |
| LYWPF | | | | | | | | | | 30.6 | 4.0 | |
| | | | | | | | | | | | 5.0 | |
| | | | | | | | | | | | 7.0 | |
| | | | | | | | | | | | 5.0 | |
| MFB | B-1 Bomber | | | | | 2.00 | | | | 34 | 0 | |
| | | | | | | 2.65 | | | | | 4.0 | |
| XMPB | | | | | | 3.00 | | | | | 5.0 | |
| | | | | | | 4.00 | | | | | 6.0 | |
| | | | | | | 4.75 | | | | | 7.0 | |
| | | | | | | 5.00 | | | | | 8.0 | |
| HYWPB | | | | | | 5.25 | | | | 40.8 | 6.0 | |
| LMYPB | | | | | | 4.75 | | | | 30.6 | 6.0 | |

Notes:  (1) Based on GD/FWD Data for 7475-T7351 Aluminum
(2) Threshold Max. Stress-Intensity Factor
(3) Overload Shutoff Ratio
(4) Corner Flaw
(5) % Bolt Load Transfer

D-5

number of cycles of loading, $\Delta K$ = stress intensity factor range, R = stress ratio, and C, m and n = empirical constants. The constants C, m and n were determined using GD/FWD data for 7475-T7351 aluminum.

$$da/dN = C \left[ \frac{\Delta K}{(1-R)^{1-m}} \right]^n \qquad (D-3)$$

For reference purposes, the key equations of the Generalized Willenborg retardation model [26] are summarized below ( D-4 through D-10).

$$(\Delta K)_{eff} = (K_{max})_{eff} - (K_{min})_{eff} \qquad (D-4)$$

$$R_{eff} = \frac{(K_{min})_{eff}}{(K_{max})_{eff}} \qquad (D-5)$$

The effective values of $K_{max}$ and $K_{min}$ are defined in the following manner:

$$(K_{max})_{eff} = (K_{max})_\infty - \phi \left[ K_{max}{}^{OL} \left[ 1 - \frac{\Delta a}{Z_{OL}} \right]^{1/2} - (K_{max})_\infty \right] \qquad (D-6)$$

$$(K_{min})_{eff} = (K_{min})_\infty - \phi \left[ K_{max}{}^{OL} \left[ 1 - \frac{\Delta a}{Z_{OL}} \right]^{1/2} - (K_{max})_\infty \right] \qquad (D-7)$$

in which

$$\phi = \frac{1 - [(K_{max})_{TH}/(K_{max})_\infty]}{S - 1} \qquad (D-8)$$

$$S = \frac{K_{max}{}^{OL}}{(K_{max})_\infty} \qquad (D-9)$$

$$Z_{OL} = \frac{1}{2\pi} \left[ \frac{(K_{max}{}^{OL})_\infty}{\sigma_{ty}} \right]^2 \quad \text{(plane stress)} \qquad (D-10)$$

where

$(K_{max})$ = maximum remote stress-intensity factor of current cycle,

$K_{max}^{OL}$ = maximum remote stress-intensity factor of overload cycle,

a = incremental growth following overload,

$Z_{OL}$ = load interaction zone size created by overload,

$(K_{min})$ = minimum remote stress-intensity factor of current cycle,

$(K_{max})_{TH}$ = threshold maximum stress-intensity factor for no fatigue growth at R = 0,

S = overload shut-off ratio that produced no fatigue growth, and

$_{ty}$ = tensile yield strength.

The three-step procedure below was used to "tune" the RXN analytical crack growth program [24] to the selected fractographic data sets:

1. Select a baseline fractographic data set with no bolt load transfer to perform the initial tuning (e.g., WPF and/or WPB in Table D.1).

2. For a given maximum stress intensity threshold, $(K_{max})_{TH}$, determine by trial and error, using the RXN program, the corresponding overload shutoff ratio (S) that will give a reasonable "curve fit" to the EIFS master curve for the baseline specimen geometry/configuration. In our case we used $(K_{max})_{TH}$=1.5 ksi-$\sqrt{in}$. and varied S as indicated in Table D.3.

3. The overload shutoff ratio (S) and corresponding $(K_{max})_{TH}$ for the baseline specimen geometry/configuration was then used to "curve fit" the EIFS master curve for a bolt load transfer case. By trial and error, the % bolt load

transfer was varied in the RXN program to accomplish the curve fitting. The bolt load transfer specimen used (e.g., XWPF), a double- reversed dog-bone specimen, was designed for a particular % bolt load transfer, but due to the clearance fit between the fasteners and holes, the actual % bolt load transfer varies depending on applied load level to the specimen. A strain survey is presented in Appendix G. This step is important because a "transfer function" is developed for scaling the % load transfer in the crack growth analysis to the % load transfer data base.

Once the theoretical-to-test % load transfer relationship has been determined, the crack growth analysis parameter developed in steps 1-3 (i.e., S, $(K_{max})_{TH}$ and % bolt load transfer) can be used to obtain SCGMCs for other % bolt load transfers and stress levels.

### D.3  RESULTS

Results of the SCGMC tuning study are shown in Figs. D.1 - D.8 for the eight data sets shown in Table D.1. Figs. D.1 and D.5 show step one of the procedure while Figs. D.2 and D.6 show step two. The remaining figures are representative of step three. For both the fighter and bomber load spectra, approximately a 6% bolt load transfer was required to obtain a reasonable "curve fit" for the "15% bolt load transfer" cases. The 6% bolt load transfer agrees very well with the results from the strain survey at the 100% load level (see Appendix G).

### D.4  CONCLUSIONS

The conclusions of this study are:

1.  The procedure illustrated in this study for tuning the analytical crack growth program to the EIFSD data base is reasonable for determining the SCGMC needed for durability analysis.
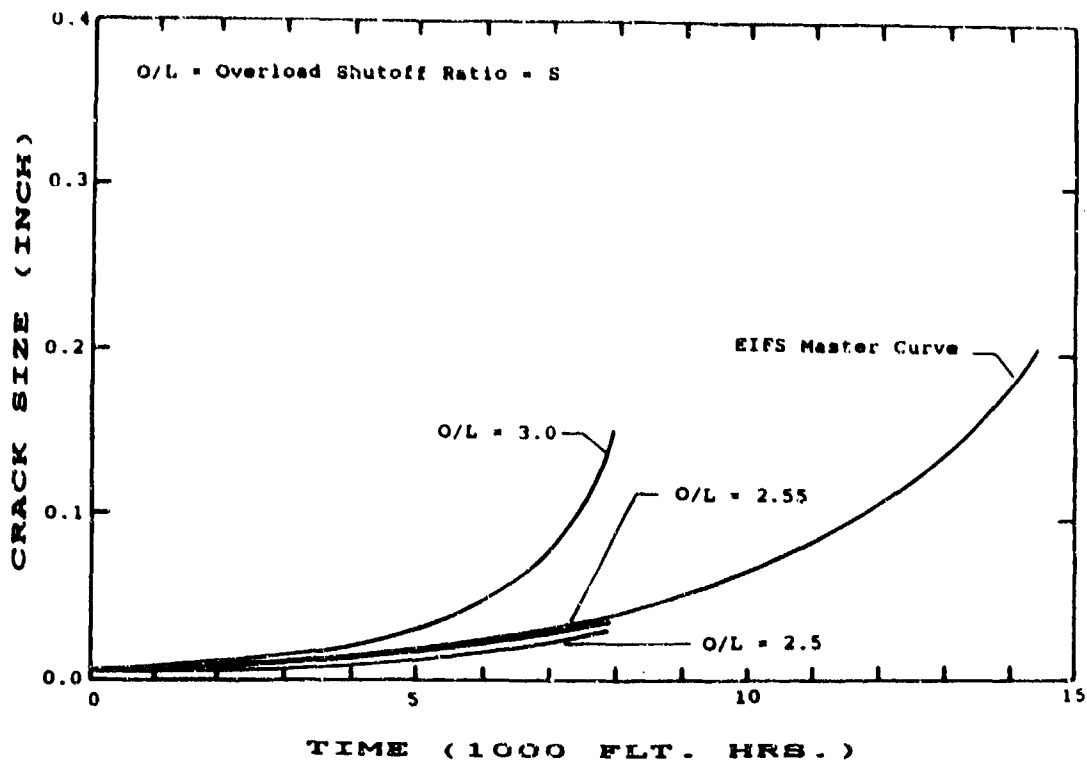
Figure D.1. __Tuning the SCGMC to the WPF Data Set__ $((K_{max})_{TH}$ __= 1.5 ksi-__$\sqrt{in.}$ __Vary S).__
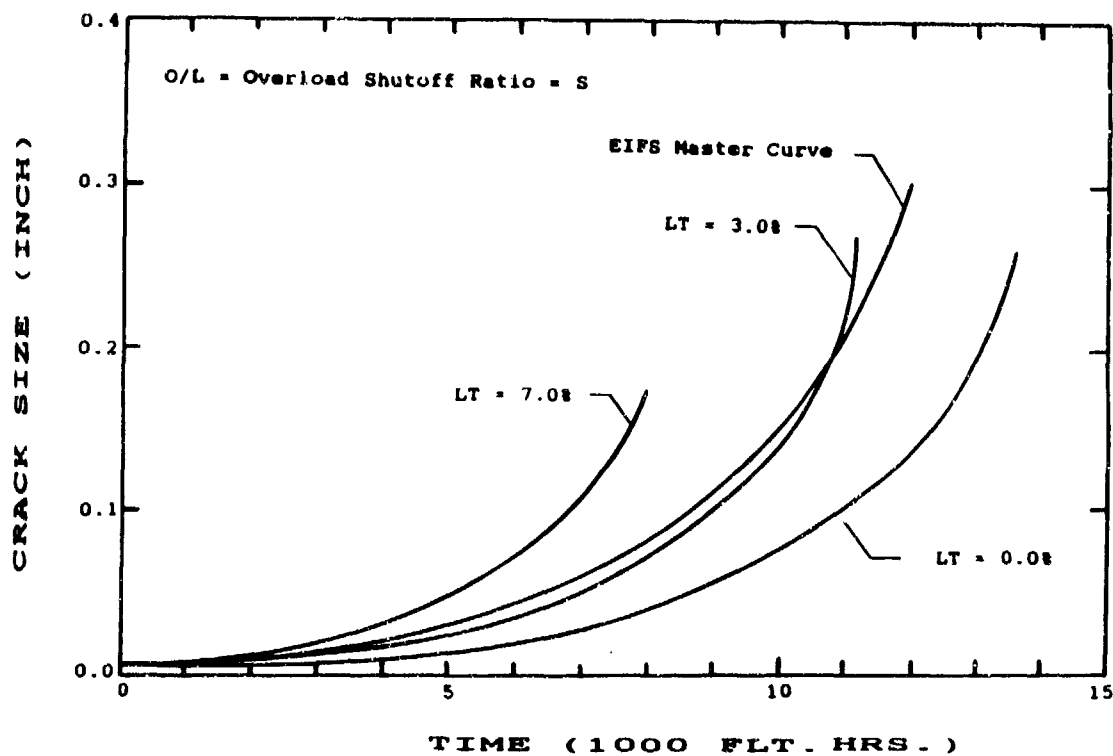


Figure D.2. __Tuning the SCGMC to the XWPF Data Set__ $((K_{max})_{TH}$ __= 1.5 ksi-__$\sqrt{in.}$ __S = 2.55; Vary % Load Transfer).__

D-9
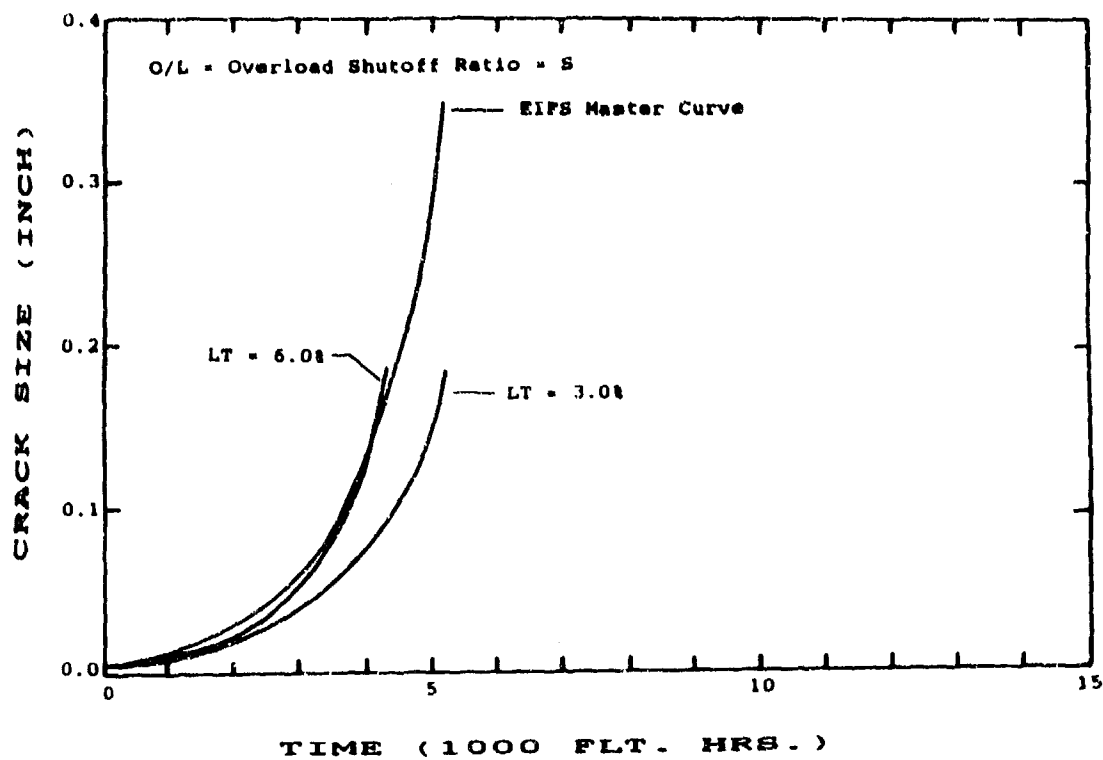
Figure D.3. Tuning the SCGMC to the HYWPF Data Set $((K_{max})_{TH} = 1.5$ ksi-$\sqrt{in.}$, $S = 2.55$; Vary % Load Transfer).
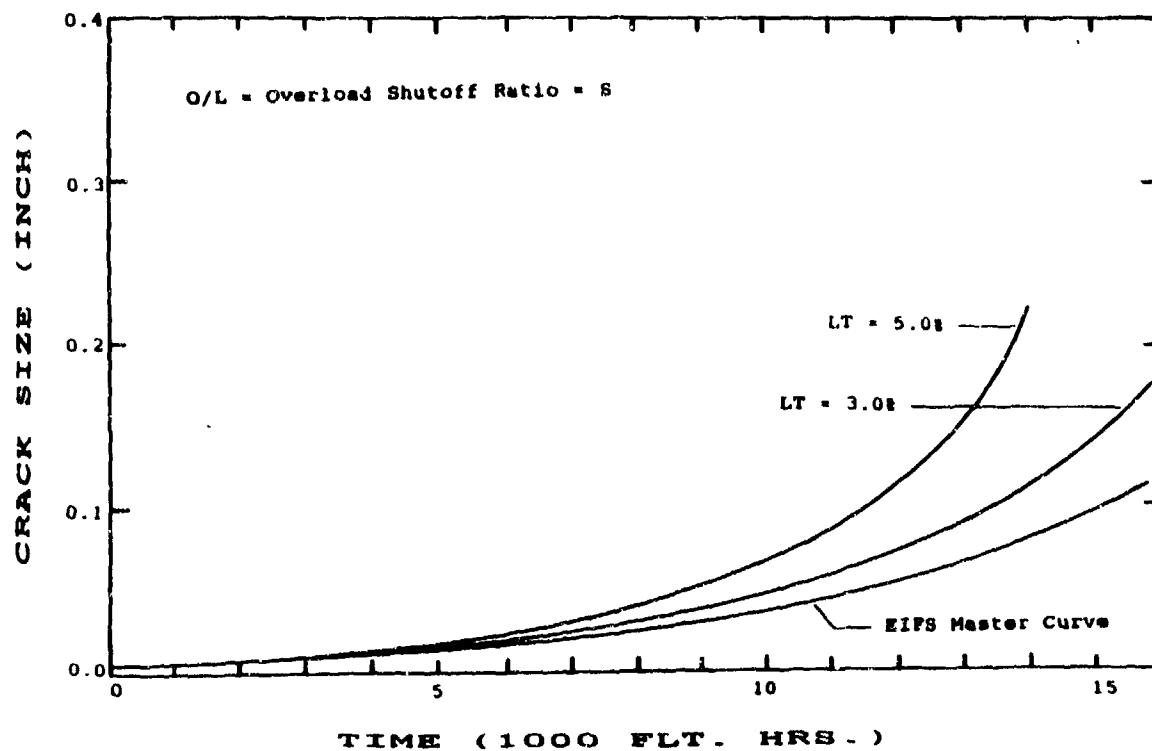


Figure D.4. Tuning the SCGMC to the LYWPF Data Set $((K_{max})_{TH} = 1.5$ ksi-$\sqrt{in.}$, $S = 2.55$; Vary % Load Transfer).

D-10
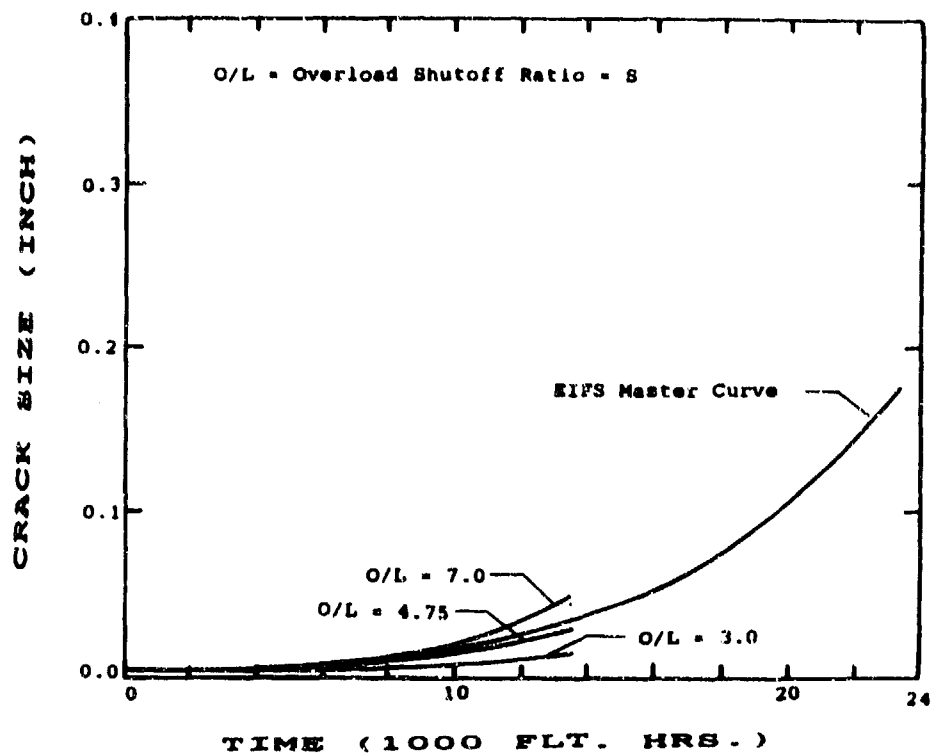
Figure D.5. Tuning the SCGMC to the WPB Data Set ($(K_{max})_{TH}$ = 1.5 ksi-$\sqrt{in.}$, Vary S).
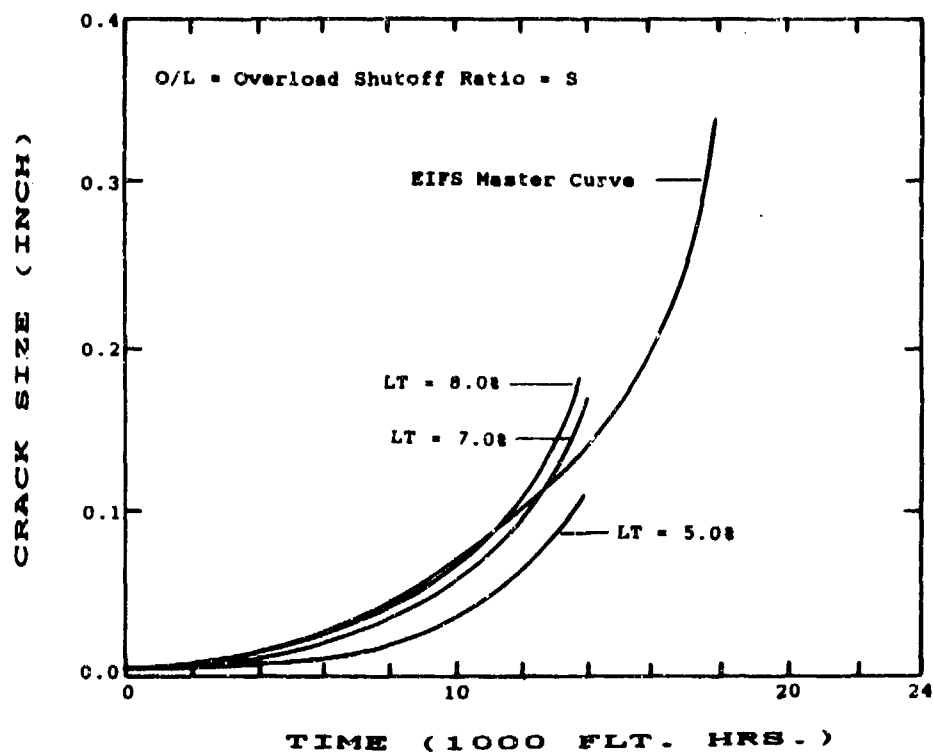


Figure D.6. Tuning the SCGMC to the XWPB Data Set ($(K_{max})_{TH}$ = 1.5 ksi-$\sqrt{in.}$, S = 4.75; Vary % Load Transfer).
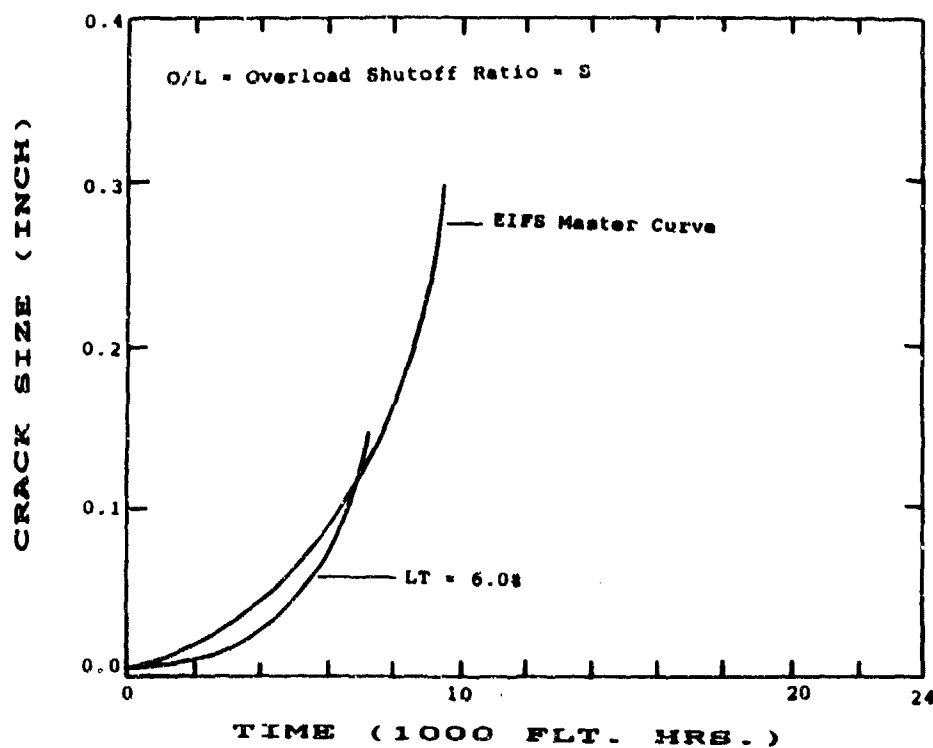
Figure D.7. **Tuning the SCGMC to the HYWPB Data Set ($(K_{max})_{TH} = 1.5$ ksi-$\sqrt{in}$, S = 4.75; Vary % Load Transfer).**
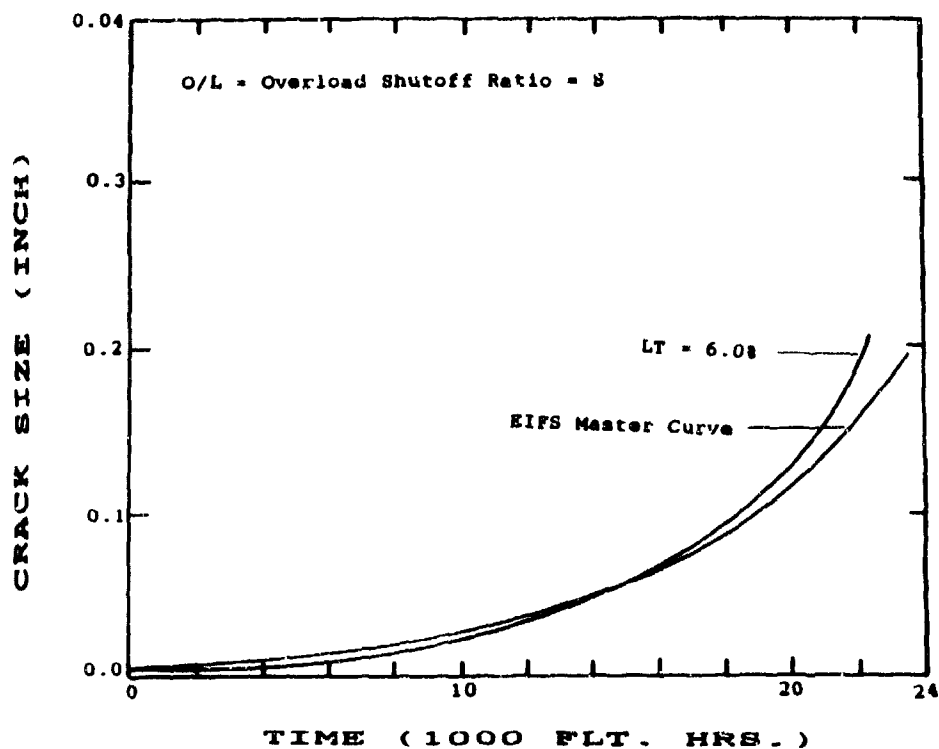


Figure D.8. **Tuning the SCGMC to the LYWPB Data Set ($(K_{max})_{TH} = 1.5$ ksi-$\sqrt{in}$, s = 4.75; Vary % Load Transfer).**

2. When applicable fractographic data is limited or not available for a direct determination of the SCGMC, an analytical crack growth program can be used to estimate the SCGMC. In this case, the user has to make assumptions, judgements and adapt available data to the crack growth conditions. This situation is no different than a "damage tolerance" type crack growth analysis required for specified conditions (e.g., material load spectrum, stress level, percent bolt load transfer, flaw shape and geometry).

3. An initial flaw size of $a(0) = 0.005"$ was used to plot the baseline EIFS master curves used in this investigation. The maximum crack size reflected in the EIFS master curve plot was arbitrarily selected. Also, the analytical crack growth program was loosely "curve fitted" to an unspecified crack size range. In practice, the analytical crack growth program should be "curve fitted" to the same AL-AU crack size range (e.g., 0.01" - 0.05") that is used to define the EIFSD parameters.

4. One or more crack growth segments may be required to define a SCGMC for durability analysis in the large crack size region (e.g., crack size > 0.50"). The same curve fitting concept used in this section can also be used to determine the SCGMC for desired AL-AU ranges. In any case, the SCGMC is determined for a specified AL-AU crack size range. A two-segment SCGMC is discussed in Volume I [1].

5. A SCGMC can be determined for the small crack size region without violating LEFM principles. For example, the analytical crack growth program is curve fitted to the EIFS master curve for a crack size range of AL-AU = 0.01" - 0.05". Since the analytical crack growth program is used as a "curve fitting tool" and is limited to a minimum crack size of AL = 0.01". LEFM principles apply and "short crack effects" do not have to be accounted for.

# APPENDIX E

## INITIAL FATIGUE QUALITY STUDIES FOR FASTENER
## HOLES IN 7475-T7351 ALUMINUM

### E.1  INTRODUCTION

A comprehensive investigation was conducted to evaluate and refine the initial fatigue quality methods developed under this program. Also, the sensitivity of various factors on the initial fatigue quality (IFQ) results was investigated. This effort was extensive but the results are too voluminous to present herein [42]. The purpose of this section is to briefly describe the overall investigation conducted, to discuss the key issues and to summarize our overall conclusions and recommendations. The studies described herein were a part of the "learning process" for developing and refining the methods and procedures for defining IFQ. Durability analysis methods and equations are developed in Volume I [1].

### E.2  INVESTIGATION SUMMARY

The investigation included numerous studies with overlapping aspects. These studies are loosely grouped into four parts as follows:  (1) evaluation of methods for determining Q, (2) evaluation of EIFSD parameters, (3) sensitivity of IFQ parameters, and (4) estimation of initial flaw sizes. All studies were conducted using fractographic data for fastener holes in dog-bone specimens of 7475-T7351 aluminum [2-4]. Both straight-bore and countersunk fastener holes (clearance-fit) were considered. Studies are briefly described in the following and sample results are presented.

#### E.2.1  Evaluation of Methods for Determining Q

The crack growth rate parameter Q in Eq. 2 for a data set, referred to as the pooled Q is needed to implement the durability

analysis method developed. Pooled $Q$ for a given fractographic data set can be estimated using either Eq. 2 or Eq. 3 and a least squares fit procedure as follows. Suppose the ith fractographic data set contains a total of m fatigue cracks, where each fatigue crack is denoted by $j = 1,2,\ldots,m$. The jth fatigue crack has a total of $N_j$ pairs of fractographic data in the AL-AU crack size range. $Q$ can be determined from Eq. 2 using the following least squares fit expression,

$$Q = exp\left\{\frac{\sum_{j=1}^{m}\sum_{k=1}^{N_j} ln\,(da(t)/dt)_{jk} - \sum_{j=1}^{m}\sum_{k=1}^{N_j} ln\,a_j(t_k)}{\sum_{j=1}^{m} N_j}\right\} \qquad (E\text{-}1)$$

where, $N_j$ = number of pairs of $[(da(t)/dt)_{jk}, a_j(t_k)]$ values in the AL-AU range (i.e., $k = 1,2,\ldots,N_j$) and $(da(t)/dt)_{jk}$ = kth crack growth rate for the jth fatigue crack at service time $t_k$, denoted by $a_j(t_k)$. $Q$ can also be determined from Eq. 3 using the least squares fit expression as follows,

$$Q = \frac{N\sum_{j=1}^{m}\sum_{k=1}^{N_j} X_{jk} Y_{jk} - \left(\sum_{j=1}^{m}\sum_{k=1}^{N_j} X_{jk}\right)\left(\sum_{j=1}^{m}\sum_{k=1}^{N_j} Y_{jk}\right)}{\sum_{j=1}^{m}\sum_{k=1}^{N_j} X_{jk}^2 - \left(\sum_{j=1}^{m}\sum_{k=1}^{N_j} X_{jk}\right)^2} \qquad (E\text{-}2)$$

where, $X_{jk} = t_{jk}$ (i.e., kth service time for the jth fatigue crack denoted by $a_j(t_k)$), $Y_{jk} = ln\,a_j(t_k)$ and $N$ = total number of $[X_{jk}, Y_{jk}]$ pairs in the AL-AU range $= \sum_{j=1}^{m} N_j$. Eqs. E-1 and E-2 were derived in Volume I [1].

Studies were conducted to evaluate pooled Q based on Eq. E-1 and E-2. Various data processing methods for computing pooled Q using fractographic results for both straight-bore and countersunk fastener holes were investigated. The modified secant method [27] and the five-point incremental polynomial method [28] were used to estimate $(da(t)/dt)_{jk}$ values for computing pooled Q values based on Eq. E-1.

The following effects on pooled Q values were also investigated: (1) fractographic crack size range (i.e., AL-AU), (2) equalizing or not equalizing the number of a(t)s for each fatigue crack in the selected AL-AU range, and (3) fractographic data censoring.

Pooled Q value for each data set results from the study, based on Eqs. E-1 and E-2, are shown in Table E.1 for three different fractographic data sets. These results were based on fractographic data for straight-bore fastener holes with clearance-fit fasteners.

### E.2.2 Evaluation of EIFSD Parameters

Three different distribution functions were considered for representing the EIFSD: (1) Weibull compatible distribution proposed by Yang and Manning [6,7], (2) two-parameter Weibull, and (3) lognormal. Both the homogeneous EIFS approach (HEIFS) and the combined least square sums approach (CLSSA) for estimating the EIFSD parameters were investigated. These approaches are described in Volume I [1].

EIFSD parameters were also determined using the data pooling procedure and statistical scaling technique described in Volume I. The CLSSA for estimating EIFSD parameters was evaluated using a "EIFS fit" [1] and a "TTCI fit" [1]. The following methods for estimating the EIFSD parameters were also considered: (1) non-linear least squares fit [1], (2) method of moments, and (3) maximum likelihood estmation (MLE). Single and double precision accuracy were considered in the evaluation of the linear and non linear least square fit methods.

Sample results from this study are shown in Table E.2 for selected fractographic data sets. These data sets were used to demonstrate and evaluate the durability analysis extension given in Section IV of this Volume (II). Similar results were obtained for numerous other data sets and for different fractographic data pooling combinations.

Table E.1. SUMMARY OF COMPUTED Q VALUES FOR SELECTED FRACTOGRAPHIC DATA SETS

| DATA SET (1) | No. Cracks Used | LT | GROSS STRESS (KSI) | TEST SPECTRUM | AL-AU (7) | $Q \times 10^4$ (1/HR) | | |
| --- | --- | --- | --- | --- | --- | --- | --- | --- |
| | | | | | | MS (5) | SPP (6) | Eq. E-2 |
| WPF (2) | 31/33 | 0 | 34 | F-16 400 HR | .01"-.05" | 2.394 | 2.397 | 2.393 |
| WWPF (3) | 13/13 | 0 | 34 | F-16 400 HR | .01"-.05" | 2.739 | 2.742 | 2.742 |
| XWPF (4) | 33/33 | 15 | 34 | F-16 400 hr | .01"-.05" | 3.812 | 3.816 | 3.851 |

NOTES:  (1)  Specimen Material:  7475-T7351 Aluminum

(2)  Ref. Fig. 4

(3)  Ref. Fig. 2

(4)  Ref. Fig. 5

(5)  MS - Modified Secant Method [27]

(6)  SPP = Five point incremental polynomial [28]

(7)  AL-AU = Fractographic crack size range used

Table E.2. Summary of EIFSD Parameters and Initial Flaw Size Percentile
Results for Weibull-Compatible Distribution Function for
Countersunk and Straight-Bore Fastener Holes.

| DATA SET (1) | TYPE HOLE | σ (ksi) | Cracks Used | AL-AU | Pooled Q×10⁻⁴ | $x_u$ | $\alpha$ | $\beta$ | $\ell$ | INITIAL FLAW SIZE (7) a(1/1000) | a(1/10000) | Approach |
|---|---|---|---|---|---|---|---|---|---|---|---|---|
| AFXLR4 (2) | CSK (6) | 32 | 10/11 | .01"-.05" | 2.101 | .03" | 1.960 | 5.708 | 4 | .0254" | .0285" | CLSSA |
|  |  |  |  |  |  | .05" | 2.450 | 5.918 | 4 | .0351" | .0436" | CLSSA |
| AFXMR4 (2) |  | 34 | 9/9 |  | 2.514 | .03" | 1.960 | 4.355 | 4 | .0264" | .0288" | CLSSA |
|  |  |  |  |  |  | .05" | 2.545 | 4.646 | 4 | .0368" | .0441" | CLSSA |
| AFXHR4 (2) |  | 38 | 10/10 |  | 6.062 | .03" | 1.870 | 6.857 | 4 | .0253" | .0285" | CLSSA |
|  |  |  |  |  |  | .05" | 2.240 | 7.108 | 4 | .0361" | .0455" | CLSSA |
| AFXLR4 AFXMR4 (3) AFXHR4 |  | {32 34 38} | {10/11 9/9 10/10} |  | {2.101 2.514 6.062} | .03" | 1.716 | 6.308 | {4 4 4} | .0268" | .0291" | CLSSA |
|  |  |  |  |  |  | .05" | 2.132 | 6.453 |  | .0388" | .0459" | CLSSA |
|  |  |  |  |  |  |  |  |  |  |  |  | CLSSA |
| WPF (4) | SB (6) | 34 | 31/33 | .01"-.05" | 2.329 | .03" | 6.920 | 3.808 | 1 | .0074" | .0109" | CLSSA |
| XWPF (5) |  | 34 | 31/33 |  | 3.671 | .03" | 5.136 | 5.440 | 4 | .0073" | .0121" | CLSSA |
| WPF XWPF (3) |  | {34 34} | {31/33 31/33} |  | {2.329 3.671} |  | 4.782 | 4.658 | {1 4} | .0099" | .0152" | CLSSA |
|  |  |  |  |  |  |  |  |  |  |  |  | CLSSA |
| WPF WJPF (3) |  | {34 34} | {31/33 13/13} |  | {2.329 2.742} | .03" | 6.390 | 3.954 | {1 1} | .0079" | .0117" | HEIFS |
|  |  |  |  |  |  | .03" | 5.740 | 3.990 |  | .0091" | .0135" | CLSSA |
|  |  |  |  |  |  | .05" | 7.280 | 4.480 |  | .0088" | .0141" | HEIFS |
|  |  |  |  |  |  | .05" | 6.536 | 4.507 |  | .0104" | .0166" | CLSSA |

NOTES:
(1) Specimen material: 7475-T7351 aluminum
(2) Individual data set; Ref. 6 for specimen geometry
(3) Pooled fractographic data sets
(4) Individual data set; Ref. 4 for specimen geometry
(5) Individual data set; Ref. 5 for specimen geometry
(6) CSK = countersunk; SB = straight bore
(7) a(1/1000), a(1/10000) = Initial flaw size for upper percentiles
    P = .001 and P = .0001, respectively

E-5

In Table E.2, the bracketed ( ) data sets indicate that the data pooling procedure with statistical scaling [1] was used. The sample results in Table E.2 are for the Weibull compatible EIFSD function. Parameters $\alpha$ and $\phi$, for a given $x_u$ (i.e., 0.03" or 0.05"), are based on an "EIFS fit" and either the CLSSA or the HEIFS approach. Initial flaw sizes for 0.1 and 0.01 percentiles are shown in Table E.2 for each EIFSD case.

## E.2.3 Sensitivity of Initial Fatigue Quality Parameters

The effects and sensitivity of various factors on the resulting IFQ of fastener holes were evaluated. For example, the effects of the following factors on IFQ were investigated: (1) fractographic crack size range used (i.e., AL-AU), (2) fractographic data censoring, (3) fractographic data pooling and statistical scaling, and (4) EIFS upper bound limit $(x_u)$. Typical results for this investigation, shown in Table E.2, will be discussed later.

## E.2.4 EIFS UPPER TAIL FIT

The EIFSD is established previously by fitting the distribution function to all EIFS values computed from available fractographic results. This procedure is referred to as the "total EIFS population fit". When the crack exceedance probability of practical concern is small, the upper tail portion of the EIFSD is critical to the prediction. Hence, the upper tail portion of the EIFSD should be determined with sufficient accuracy. For the total EIFS population fit, however, the EIFSD tends to fit the majority of EIFS values in the central portion, thus sacrificing the accuracy of fitting the upper tail. To overcome such a difficulty, the EIFSD may be established by fitting the distribution function to only upper q% of EIFS values, e.g., upper 30% of EIFS values. Such a procedure is referred to as the "upper tail fit".

EIFSD parameters will be obtained based on both the "total EIFS population fit" and the "upper tail fit". These parameters will be compared and evaluated. Both the Weibull compatible and two-parameter Weibull distribution functions will be considered for EIFDS. In the case of the upper tail fit, only the upper 30% of EIFS values will be used.

The Weibull compatible and two-parameter Weibull distribution functions are shown in Eq. 1 and E-3, respectively.

$$F_{a(o)}(x) = 1 - exp\left\{-(x/\beta)^{\alpha}\right\}; \quad x \geq 0 \tag{E-3}$$

In Eq. E-3, $\alpha$ and $\beta$ are the Weibull shape and scale parameters, respectively.

Equations 1 and E-3 can be transformed into a linear least squares fit form as shown in Eqs. E-4 and E-5 respectively.

$$\ln\left\{-\ln F_{a(o)}(x)\right\} = \alpha \ln \ln (x_u/x) - \alpha \ln \phi \tag{E-4}$$

$$\ln\left\{-\ln[1 - F_{a(o)}(x)]\right\} = \alpha \ln x - \alpha \ln \beta \tag{E-5}$$

In Fig. E.1, the ranked EIFS values $x_j$ ($j = 1, 2, \ldots, N$) for WPF data set are plotted in terms of $\ln(-\ln F_{a(o)}(x_j)$ versus $\ln(\ln(x_u/x))$ with $x_u = 0.03"$, where $F_{a(o)}(x_j) = j/(N+1)$. The least square fit line for the total EIFS population fit is shown in Fig. E.1 by a solid line whereas the result from the upper tail fit is denoted by a semi-dashed line. A similar plot for the two-parameter Weibull distribution is shown in Fig. E.2. the EIFSD parameters thus obtained are summarized in Table E.3.
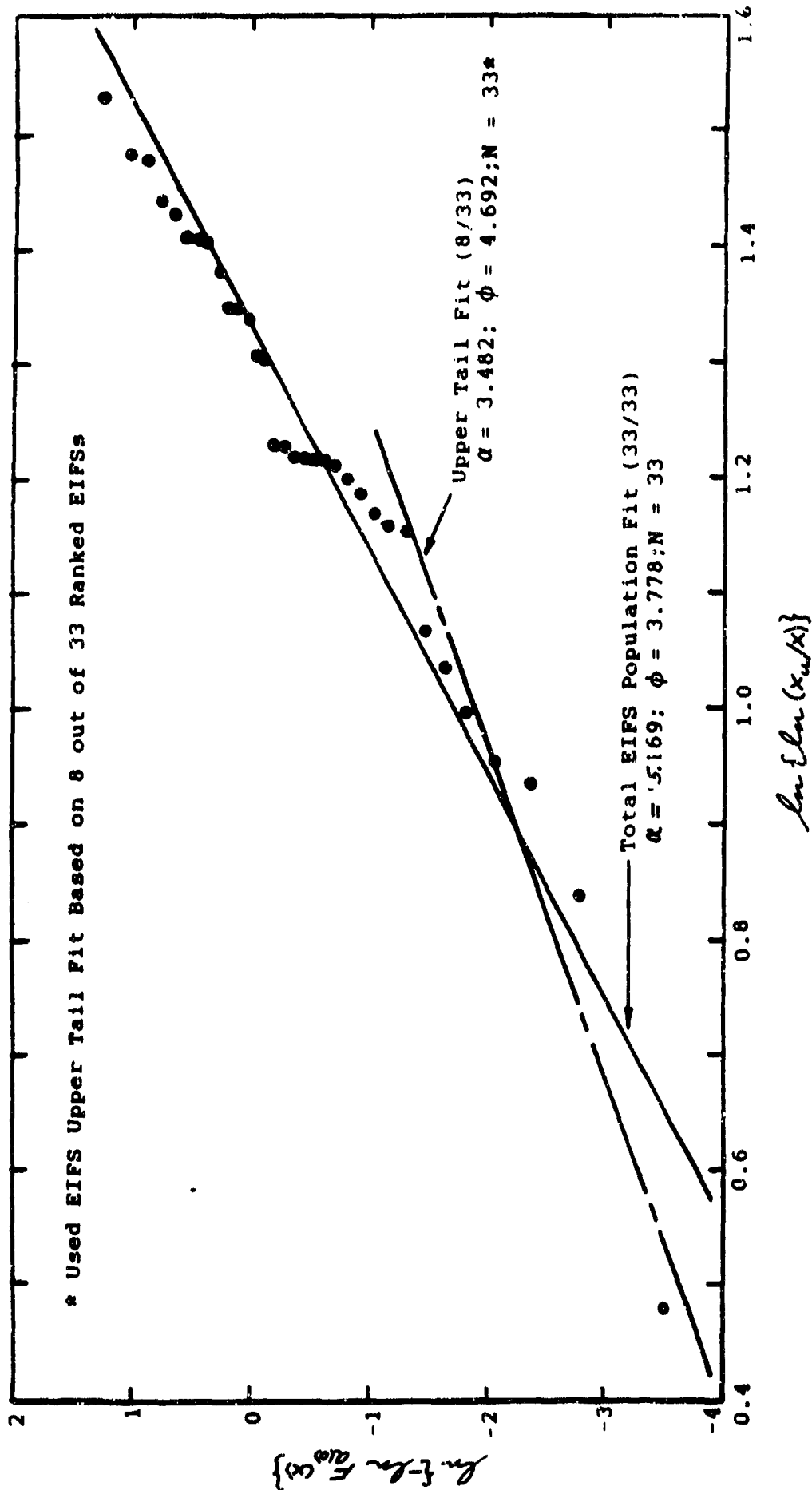
Figure E.1. $\ln\{-\ln F_{a(0)}(x)\}$ versus $\ln\{\ln(x_u/x)\}$ for WPF Data Set and Weibull Compatible Fit for EIFSD Parameters.

* Used EIFS Upper Tail Fit Based on 8 out of 33 Ranked EIFSs

Upper Tail Fit (8/33)
$\alpha = 3.482$; $\phi = 4.692$; $N = 33*$

Total EIFS Population Fit (33/33)
$\alpha = 5.169$; $\phi = 3.778$; $N = 33$
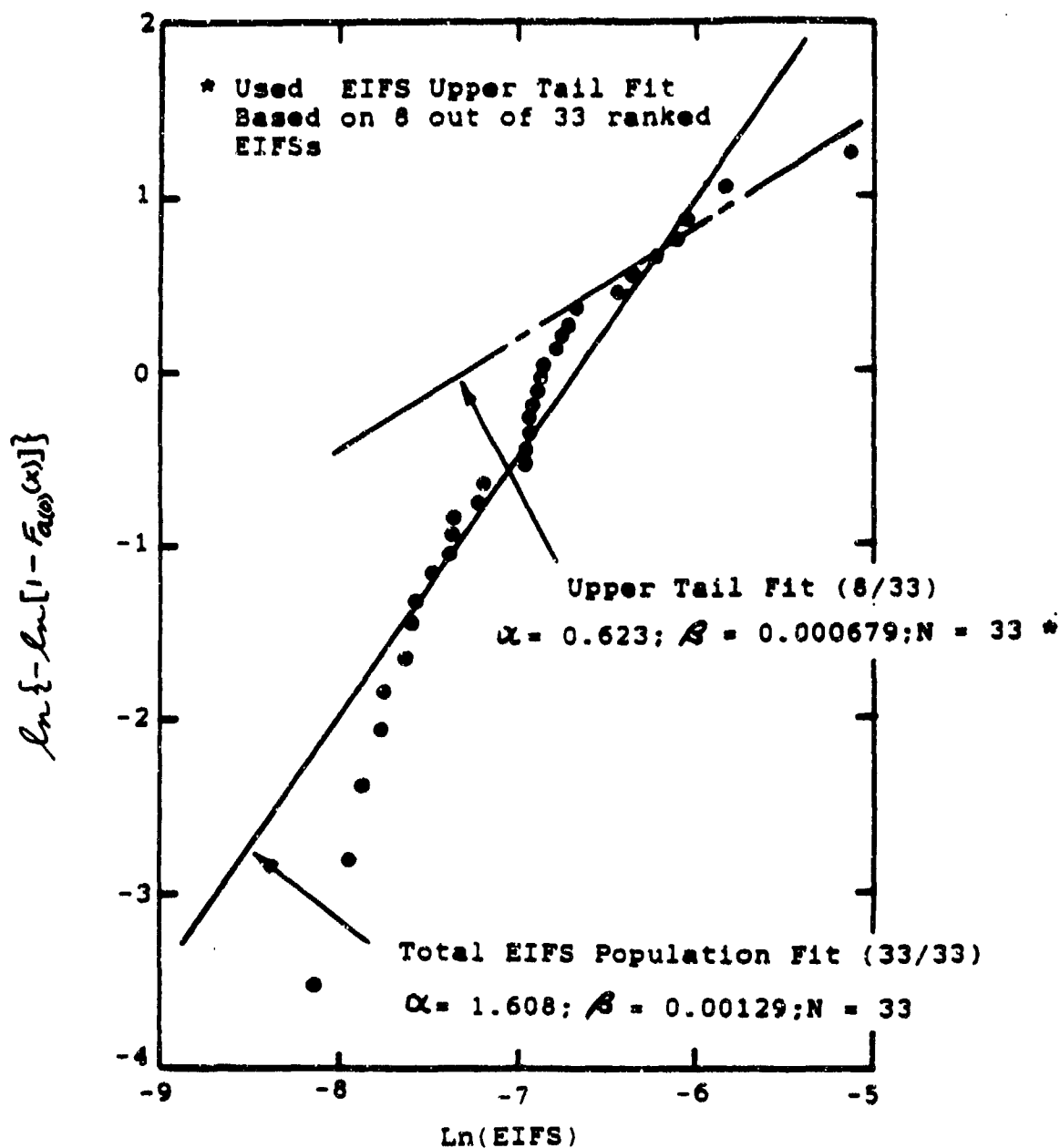
Figure E.2. $ln\{-ln[1-F_{a_{(0)}}(x)]\}$ Versus Ln(EIFS) for WPF Data Set and Two-Parameter Weibull Fit for EIFSD Parameters.

The figure contains the following annotations:

* Used EIFS Upper Tail Fit Based on 8 out of 33 ranked EIFSs

Upper Tail Fit (8/33)
$\alpha = 0.623$; $\beta = 0.000679$; $N = 33$ *

Total EIFS Population Fit (33/33)
$\alpha = 1.608$; $\beta = 0.00129$; $N = 33$

Y-axis: $ln\{-ln[1-F_{a_{(0)}}(x)]\}$ ranging from $-4$ to $2$

X-axis: Ln(EIFS) ranging from $-9$ to $-5$

**Table E.3.** Comparison of EIFSD Parameters for the Weibull-Compatible and Two-Parameter Weibull Distribution Functions Based on Total Population Fit and Upper Tail Fit (WPF Data Set).

| DISTRIBUTION FUNCTION | EIFSD PARAMETERS (2) | |
| --- | --- | --- |
| | TOTAL POP. FIT | UPPER TAIL FIT |
| Weibull-Compatible | $x_u = 0.03"$ | $x_u = 0.03"$ |
| | $\alpha = 5.169$ | $\alpha = 3.482$ |
| | $\phi = 3.778$ | $\phi = 4.692$ |
| Two Parameter Weibull | $\alpha = 1.608$ | $\alpha = 0.623$ |
| | $\beta = 0.00129$ | $\beta = 0.000679$ |

NOTES: (1) 7475-T7351 aluminum; straight-bore fastener holes with NAS 6204-08 bolt installed (clearance-fit)
(2) Least squares fit; 50% confidence

The $\alpha$ value in both the Weibull compatible and two-parameter the statistical variability. On the other hand, $\beta$ and $\phi$ in the respective EIFS distribution function denote the central tendency of the EIFS. For the Weibull compatible distribution function the average EIFS decreases as $\phi$ increases; whereas for the two parameter Weibull distribution function the average EIFS increases as $\beta$ increases. It is observed from Table E.3 that with the upper tail fit, the $\alpha$ value decreases indicating that the statistical dispersion increases. However, $\phi$ increases for the Weibull compatible distribution whereas $\beta$ decreases for the two-parameter Weibull distribution.

## E.3  CONCLUSIONS AND RECOMMENDATIONS

1.   As shown in Table E.1., the pooled Q values can be determined using either Eq. E-1 or E-2. Also, no significant differences in the pooled Q values were found using either the modified secant or the five-point incremental polynomial method.   Therefore, since Eqs. E-1 and E-2 yield the same pooled Q value, Eq. E-2 is recommended for durability analysis because it is simpler to implement.

2.   The value of the crack growth rate parameter Q (pooled) in Eq. 2 depends on the fractographic data used as well as the fractographic crack size range (i.e., AL-AU) used.

3.   All fractographic data should be screened and censored for any durability analysis purpose. In particular, data sparsity should be examined (i.e. scrutinize data outside the desired AL-AU range for the durability analysis). Screening can be accomplished using the durability analysis software of Volume V [5].

4.   EIFSD parameters based on the Weibull compatible distribution function are shown in Table E.2 for selected data sets. The following conclusions and recommendations are based on the extensive investigation conducted [42]:

(1)   The CLSSA is effective for estimating the EIFSD parameters for individual or pooled fractographic data sets.   It provides a rational approach for statistically scaling fractographic results to a common baseline.

(2)   It is interesting to note in Table E.2 that $\alpha$ values for a given $x_u$ based on the HEIFS approach are slightly larger than those based on the CLSSA.   The same $\phi$ value, however, is obtained using either approach.

(3)   $\alpha$ for the Weibull compatible EIFSD increases as $x_u$ increases.   The $\alpha$ value characterizes the variability of the EIFSD.   For example, the variability decreases as $\alpha$ increases.   It is observed that higher $\alpha$ values were obtained for straight-bore fastener holes than for countersunk fastener holes.

(4)   The Weibull compatible distribution function or other suitable "compatible type" distribution functions (e.g., lognormal compatible, etc.) are recommended for defining IFQ.   With a compatible type EIFSD function an upper bound EIFS limit is imposed (refer to Vol. I [1], Section H.3).   The selected upper bound limit, $x_u$, involves a subjective decision.   However, reasonable limits can be selected based on considerations for the economical repair limit and/or NDI.   For fastener holes an upper bound limit of $x_u = 0.03" - 0.05"$ is recommended.

(5)   Initial flaw sizes for different upper percentiles (i.e., P = .001 and P = .0001) are shown in Table E.2. It is seen that the upper percentile initial flaw size values for the countersunk and straight-bore fastener hole data sets are very consistent for individual and/or pooled data sets.

(6) Larger upper percentile initial flaw sizes were obtained for countersunk fastener holes than are currently used for a deterministic-based durability analysis. For example, in Table E.2 for (AFXLR4+AFXMR4+AFXHR4) and $x_u$ = .03" the initial flaw sizes are .0268" and .0291" for P = .001 and .0001, respectively. For $x_u$ = .05", the initial flaw sizes are .0388" and .0459", for P = .001 and .0001, respectively. If an EIFS is selected from the EIFSD for a given upper percentile, the resulting EIFS should be grown forward consistent with the basis for the EIFS distribution (see Vol. I [1]).

(7) A fractographic crack size range of AL-AU = .0" - .05" is considered reasonable for determining the EIFSD parameters for clearance-fit fastener holes. In any case, all durability analysis applications should be consistent with the basis for the IFQ results. For example, fatigue cracks should be grown backwards and forwards in a consistent manner.

(8) The reference crack size, $a_0$, should fall within the AL-AU range used (e.g., AL $\geq a_0 \geq$ AU). $a_0$ = AU is recommended for clearance-fit fastener holes.

(9) EIFSD parameters for the Weibull compatible distribution function were estimated using linear and nonlinear least square fit methods [42]. For a given $x_u$, no significant differences in $\alpha$ and $\phi$ were observed using either approach. Therefore, the linear least square fit method, reflected in the CLSSA, is recommended for estimating EIFSD parameters.

5. EIFS values, based on the total EIFS population fit and the upper tail fit are shown in Table E.3 for the Weibull compatible and two-parameter Weibull distribution functions. In this case, the initial flaw size values are of the same order of magnitude. Note that larger initial flaw sizes are obtained using the upper tail fit than the total population

fit.  For durability analysis, initial flaw size should be based on a total EIFS population fit since we are concerned with the total flaw population - not just the extreme values.  For damage tolerance analysis, however, the upper tail fit is considered reasonable.  Once again, we emphasize the importance of growing EIFSs forward in the same manner as EIFSs were defined.

# APPENDIX F

## EVALUATION AND SENSITIVITY OF Q AND $\sigma_Z$ FOR STRAIGHT-BORE AND COUNTERSUNK FASTENER HOLES IN 7475-T7351 ALUMINUM

### F.1    INTRODUCTION

The objectives of this section are to   (1) evaluate and compare preliminary and refined methods for computing the crack growth parameter, Q, and the standard deviation, $\sigma_Z$ of Z = lnX using fractographic data, (2) evaluate the sensitivity of Q, and   $\sigma_Z$ with respect to various analysis considerations (e.g., data processing, fractographic crack size range (AL-AU, data censoring, etc.).

This investigation was divided into two parts as follows.  Part I was concerned with the determination of Q,  and $\sigma_Z$ for selected uncensored fractographic data sets and the sensitivity of the results with respect to:  (1) fractographic crack size range (AL-AU), (2) equalizing or not equalizing the number of data points in the selected AL-AU range,  and (3) method  for computing crack growth rate, (i.e., modified secant [27] and five-point incremental polynomial [28]).   In Part II we investigated  the effects of fractographic data censoring, crack size range, and/or fractographic  extrapolations, on Q, $\sigma_Z$ mean TTCI and mean EIFS.

Both straight-bore  and countersunk fastener hole data sets were considered in Part I.  Fractograhic data sets  from the  "Fastener Hole Quality" (FHQ) [3] and the "Advanced Durability Analysis" (ADA) programs [2] were utilized.   Only straight-bore fastener hole fractograpnic data sets were considered  in Part II.  All the fractographic data sets used in this investigation are  described  in  Tables  F.1  and  F.2. Specimen details  are shown in Figs. 1-5. Details of the investigation, including  methods,  results,  observations  and

TABLE F.1. Description of Fastener Hole Quality (FHQ) Fractographic Data Sets.

| (1) DATA SET | NO. SPECIMEN | % LT | (KSI) (2) | WIDTH (IN.) | LOAD SPECTRUM | TYPE HOLE | SPECIMEN DETAILS |
|---|---|---|---|---|---|---|---|
| WPF | 33 | 0 | 34 | 1.5 | F-16 400 HR. | SB(3) | Fig. 4 |
| LYWPF | 7 | 15 | 30.6 | | | | Fig. 5 |
| XWPF | 33 | 15 | 34 | | | | |
| HYWPF | 10 | 15 | 40.8 | | | | |
| WPB | 32 | 0 | 33 | | B-1 BOMBER | | Fig. 4 |
| LYWPB | 10 | 15 | 29.7 | | | | Fig. 5 |
| XWPB | 31 | 15 | 33 | | | | |
| HYWPB | 10 | 15 | 39.6 | | | | |

Notes:
(1) 7475-T7351 Aluminum
(2) Maximum gross stress due to peak load in spectrum
(3) SB = straight-bore; NAS6204-0P(1/4" Dia.)
(4) FHQ fractographic data in Ref. 3

TABLE F.2.  Description of Advanced Durability Analysis (ADA) Fractographic Data Sets.

| (1) DATA SET | NO. SPECIMEN | % LT | $\sigma$ (KSI) (2) | WIDTH (IN.) | LOAD SPECTRUM | TYPE HOLE | SPECIMEN DETAILS |
|---|---|---|---|---|---|---|---|
| WWPF | 13 | 0 | 34 | 3.0 | F-16 400 HR. | SB(3) | Fig. 2 |
| WWPB | 12 | 0 | 34 | | B-1 Bomber | | |
| WWPCL | 4 | 0 | 34 | | F-16 C/D | | |
| WWPCH | 5 | 0 | 40.8 | | F-15 C/D | | |
| WWPTO | 14 | 0 | 34 | | F-16 400 HR. | (6) | |
| WPF | 15 | 15 | 34 | | F-16 400 HR. | CSK(4) | Fig.1 |
| WB | 13 | 15 | 36 | | B-1 BOMBER | | |
| WAFXHR4 | 14 | 15 | 34 | | F-16 400 HR. | | Fig.3 |
| WAFXHR4 | 14 | 15 | 40.8 | | F-16 400 HR. | | |
| WRWPB | 15 | 15 | 34 | | B-1 BOMBER | | |

Notes:  (1)  7475-T7351 Aluminum
        (2)  Maximum gross stress due to peak load in spectrum
        (3)  SB = straight-bore; NAS6204-08(1/4" Dia.)
        (4)  MS 90353-08 Pull-Through Rivet
        (5)  ADA fractographic data in Volume III [ 3]
        (6)  Open hole

conclusions, are presented in the following.

## F.2 PART I - EVALUATION OF PRELIMINARY AND REFINED METHODS USING UNCENSORED DATA SETS

Fractographic data for selected data sets in Tables F.1 and F.2 were used to evaluate Q, and $\sigma_z$. Preliminary and refined methods for computing Q and $\sigma_z$ are documented in Volume I [1]. The preliminary method for computing Q and $\sigma_z$ was thoroughly evaluated and refined to obtain the recommended method. This was definitely a "learning process" in which many variations in data processing and analysis were considered. Applicable equations for computing Q and $\sigma_z$ for the preliminary and refined methods are summarized in the following.

The simple crack growth rate model given in Eq. F-1 is useful for representing one segment of the service crack growth master curve (SCGMC).

$$da(t)/dt = Qa(t) \tag{F-1}$$

In Eq. F-1, da(t)/dt = crack growth rate, Q = crack growth rate parameter, and a(t) = crack size at any time t. The Q in Eq. F-1 can be determined for a single fatigue crack or pooled fatigue cracks. For a single fatigue crack, Eq. F-1 is rewritten as

$$da(t)/dt = Q_j a(t) \tag{F-2}$$

where, $Q_j$ = crack growth rate constant for the jth fatigue crack in a fractographic data set and the other terms are the

same as those defined for Eq. F-1. For pooled fatigue
cracks, Q can be approximated by a lognormal random variable.
The Q value evaluated in Eqs. F-5 and F-8 represents the med-
ian value; whereas the standard deviation of lnQ, denoted by
$\sigma_z$, are evaluated in Eqs. F-7 and F-10. Note that the stoch-
astic crack growth rate equation presented in Vol. I is ex-
pressed as da(t)/dt = XQa(t), where X is a lognormal random
variable. The Q value in such an equation is also evaluated
from Eqs. F-5 and F-8; whereas the standard deviation of lnX
is equal to $\sigma_z$, that is determined from Eqs. F-7 and F-10.
In what follows, the Q values obtained from Eqs. F-5 and F-8
are referred to as the "pooled Q" values for a data set.

Equations F-1 and F-2 can be transformed into Eq. F-3
and F-4, respectively.

$$\ln da(t)/dt = \ln Q + \ln a(t) \qquad (F-3)$$

$$\ln da(t)/dt = \ln Q_j + \ln a(t) \qquad (F-4)$$

A preliminary method for determining pooled Q and $Q_j$,
based on a least square fit procedure using [da(t)/dt, a(t)] data
is described in Volume I [1]. A subscript "i" is added to Q
(i.e., $Q_i$) to denote the "pooled Q" value for the ith fracto-
graphic data set. In the following, either Q or $Q_i$ is used.
The resulting equations for $Q_i$ and $Q_j$ are shown in Eqs. F-5
and F-6, respectively.

$$Q = Q_i = \exp \left\{ \frac{\sum_{j=1}^{m} \sum_{k=1}^{N_j} \ln \left[ da(t)/dt \right]_{jk} - \sum_{j=1}^{m} \sum_{k=1}^{N_j} \ln a_j(t_k)}{\sum_{j=1}^{m} N_j} \right\} \qquad (F-5)$$

$$Q_j = \frac{N_j \sum_{k=1}^{N_j} X_k Y_k - \sum_{k=1}^{N_j} X_k \sum_{k=1}^{N_j} Y_k}{\sum_{k=1}^{N_j} X_k^2 - \left(\sum_{k=1}^{N_j} X_k\right)^2} \qquad (F\text{-}6)$$

In Eqs. F-5 and F-6, m = total number of fatigue cracks in the data set, $N_j$ = number of a(t)s for the jth fatigue crack, $[da(t)/dt]_{jk}$ = ith crack growth rate for the jth fatigue crack, and $a_j(t_k)$ = kth a(t) value for the jth fatigue crack. An expression for determining the standard deviation, $\sigma_z$, is given in Eq. F-7.

$$\sigma_z = \sqrt{\frac{\sum_{j=1}^{m} \sum_{k=1}^{N_j} \left\{ \ln[da(t)/dt]_{jk} - \ln Q - \ln a_j(t_k) \right\}^2}{\sum_{j=1}^{m} N_j}} \qquad (F\text{-}7)$$

All terms in Eq. F-7 have already been defined in Eq. F-5. $\sigma_z$ is needed to implement the stochastic crack growth approach (SCGA), but it is not needed for the deterministic crack growth approach (DCGA).

Two methods for determining $[da(t)/dt]_{jk}$ in Eqs. F-5 through F-7 were investigated: (1) modified secant method [27] and (2) five-point incremental polynomial method [28].

The refined method for computing pooled $Q_i$, $Q_j$ and $\sigma_z$ is described in Volume I [1]. Applicable expressions for pooled $Q_i$, $Q_j$ and $\sigma_z$ are given in Eqs. F-8, F-9, and F-10, respectively.

$$Q = Q_i = \exp\left\{ \frac{1}{m} \sum_{j=1}^{m} \ln Q_j \right\} \qquad (F\text{-}8)$$

$$Q_j = \frac{N_j \sum_{k=1}^{N_j} X_k Y_k - \sum_{k=1}^{N_j} X_k \sum_{k=1}^{N_j} Y_k}{N_j \sum_{k=1}^{N_j} X_k^2 - \left(\sum_{k=1}^{N_j} X_k\right)^2} \qquad (F\text{-}9)$$

$$\sigma_s = \sqrt{\frac{\sum\limits_{j=1}^{m} \left[ \ln(Q_j/Q) \right]^2}{m}} \qquad (F-10)$$

In Eqs. F-8 through F-10, $m$ = number of fatigue cracks in the data set, $N_j$ = number of $a(t)$s for the jth fatigue crack; $X_k$ and $Y_k$ are defined in Eq. F-11.

$$X_k = t_k$$
$$ \qquad (F-11)$$
$$Y_k = \ln a_j(t_k)$$

In Eq. F-11, $t_k$ = kth time for the jth fatigue crack and $a_j(t_k)$ = kth $a(t)$ value for the jth fatigue crack.

The primary objective of the Part I investigation was to justify the refined methods for computing pooled Q and $\sigma_z$ and to study the effects of various data processing considerations on the resulting pooled Q and $\sigma_z$ values.

Results for pooled Q and $\sigma_z$, based on the modified secant and five-point incremental polynomial method for computing the $da(t)/dt$s, are shown in Tables F.3 and F.4, respectively. These results were based on uncensored fractographic data sets. In this case, the effect of the following on pooled Q, and $\sigma_z$ values will be examined: (1) fractographic crack size range (AL-AU), (2) unequal number of $a(t)$s for each fatigue crack in the AL-AU range, and (3) modified secant versus five-point incremental polynomial method for computing $da(t)/dt$ data. The pooled Q and $\sigma_z$ values shown in Tables F.3 and F.4 were based on Eqs. F-5 and F-7, respectively. Two different fractographic crack size ranges were considered, i.e., AL-AU = 0.01"-0.05" and all the data with no AL-AU restriction.

TABLE F.3. Summary of Q and $\sigma_z$ Based on Modified Secant Method for da/dts (With and Without Equalizing the Number of a(t)s in AL-AU Range).

| (1) DATA SET | LOAD SPECTRUM | MAX (KSI) | NO. CRACKS (1) | AL-AU | da/dt FILE (3) | EQUALIZE NO. a(t)s? (7) | (5) $Q \times 10^4$ (1/HR) (4) | (6) $\sigma_z$ (4) |
|---|---|---|---|---|---|---|---|---|
| RPF | F16 -400 HR | 34 | 33 | .01"-.05" | "DAHFS" | YES / NO | 2.395 / 2.305 | 0.215 / 0.217 |
| | | | | ALL (2) | | YES / NO | 2.541 / 2.588 | 0.363 / 0.391 |
| XRPF | F16 -400 HR | 34 | 33 | .01"-.05" | "DAHFS" | YES / NO | 3.831 / 3.467 | 0.431 / 0.338 |
| | | | | ALL (2) | | YES / NO | 3.674 / 3.373 | 0.452 / 0.407 |
| LXRPF | F16 -400 HR | 36.6 | 7 | .01"-.05" | "DAHFS" | YES / NO | 2.257 / 2.172 | 0.383 / 0.203 |
| | | | | ALL (2) | | YES / NO | 2.103 / 2.177 | 0.367 / 0.383 |
| HXRPF | F16 -400 HR | 40.8 | 18 | .01"-.05" | "DAHFS" | YES / NO | 9.175 / 0.577 | 0.315 / 0.367 |
| | | | | ALL (2) | | YES / NO | 8.432 / 8.478 | 0.506 / 0.571 |

Notes:

(1) Uncensored data set

(2) Use all the a(t), ts with no AL-AU restriction

(3) Filename for da/dts

(4) Based on program filename = "EIFS17" (Digital "Rainbow" PC)

(5) "Pooled Q" for data set based on da/dt = Qa(t) fit; Ref. Eq. F-5

(6) Standard deviation: ln da/dt versus ln a(t); Ref. Eq. F-7

(7) Artifically equalized the number of a(t)s for each fatigue crack in the data set for selected AL-AU range (yes or no)

(8) Deterministic crack growth approach used

TABLE F.4. Summary of Q and $\sigma_Q$ Based on Five-Point Incremental Polynomial Method for da/dts (With and Without Equalizing the Number of a(t)s in AL-AU Range).

| DATA SET | LOAD SPECTRUM | MAX (KSI) | NO. CRACKS (1) | AL-AU | da/dt FILENAME (3) | EQUALIZE No. a(t)s ? (7) | (5) $\sigma \times 10^6$ (1/hr) | (6) $\sigma_Q$ (4) |
|---|---|---|---|---|---|---|---|---|
| WPF | F-16 400 | 34 | 33 | .01"-.05 | "DWPF" | YES | 2.398 | 0.212 |
|  |  |  |  |  |  | NO | 2.300 | 0.214 |
|  |  |  |  | ALL (2) |  | YES | 2.518 | 0.356 |
|  |  |  |  |  |  | NO | 2.520 | 0.345 |
| HWPF |  | 34 | 33 | .01"-.05 | "DHWPF" | YES | 3.837 | 0.427 |
|  |  |  |  |  |  | NO | 3.477 | 0.336 |
|  |  |  |  | ALL (2) |  | YES | 3.735 | 0.424 |
|  |  |  |  |  |  | NO | 3.374 | 0.393 |
| LYWPF |  | 30.6 | 7 | .01"-.05 | "DLYWPF" | YES | 2.260 | 0.301 |
|  |  |  |  |  |  | NO | 2.178 | 0.287 |
|  |  |  |  | ALL (2) |  | YES | 2.263 | 0.346 |
|  |  |  |  |  |  | NO | 2.185 | 0.366 |
| HYWPF |  | 40.8 | 10 | .01"-.05 | "DHYWPF" | YES | 9.224 | 0.316 |
|  |  |  |  |  |  | NO | 8.690 | 0.368 |
|  |  |  |  | ALL (2) |  | YES | 8.519 | 0.506 |
|  |  |  |  |  |  | NO | 8.569 | 0.573 |

Notes:
(1) Uncensored data set
(2) Use all the a(t), ts with no AL-AU restriction
(3) Filename for da/dts
(4) Based on program filename = "EIFS17" (Digital "Rainbow" PC)
(5) "Pooled Q" for data set based on da/dt = Qa(t) fit ;Ref. Eq. F-5
(6) Standard deviation; in da/dt versus in a(t):Ref. Eq. F-7
(7) Yes = a(t)s in AL-AU range artificially equalized for each fatigue crack in data set; No = actual a(t)s in AL-AU range used
(8) Deterministic crack growth approach used

F-9

Note that $Q_j$ varies from specimen (crack) to specimen (crack) in a data set. As a result, the mean value, standard deviation and coefficient of variation for $Q_j$ in a data set can be computed. These quantities are referred to as the $Q_j$ statistics.

The refined method was used to compute pooled Q, $\sigma_z$ and $Q_j$ statistics for selected FHQ program [3] and "Advanced Durability Analysis" (ADA) program [2] data sets. In this case, pooled Q and $\sigma_z$ values were determined using Eqs. F-8 and F-10, respectively. Different AL-AU ranges were considered. In some cases, crack growth data outside the given AL-AU range were used because some fatigue cracks either had no data or insufficient data in the AL-AU range to carry out the computations. A default crack size range, DL-DU was used only for those fatigue cracks with insufficient data in the AL-AU range. $Q_j$ values for individual fatigue cracks were determined using Eq. F-9. The mean, standard deviation and coefficient of variation for $Q_j$ was determined using standard statistical anlaysis methods [e.g., 22].

Pooled Q, $\sigma_z$ and $Q_j$ statistics for selected FHQ fighter and bomber load spectra data sets are shown in Tables F.5 and F.6, respectively. Results for the ADA data sets are shown for straight-bore and countersunk data sets in Table F.7 and F.8, respectively. These results are discussed in Section F.4.

F.3   PART II - STUDY OF REFINED METHOD AND EFFECTS OF
      DATA CENSORING ON POOLED Q, $\sigma_z$, MEAN TTCI AND MEAN EIFS

The purpose of the Part II study was to investigate the effects of fractographic data censoring, crack size range (AL-AU) and/or fractographic extrapolations on pooled Q, $\sigma_z$, mean TTCI and mean EIFS.

Table F.5.  Summary of Pooled Q, $\sigma_z$, and Q Statistics for Different AL-AU Crack SIZE Ranges Based on Recommended Methods (FHQ -- Fighter Data Sets)

| DATA SET (1) | LOAD SPECTRUM | $\sigma$ MAX. (ksi) (2) | NO. CRACKS (3) | AL-AU | DL-DU (4) | $Q \times 10^4$ (1/HR.) (5) | $\sigma_z$ (6) | $Q_j$ STATISTICS (MEAN)$\times 10^4$ (1/HR.) | STD. DEV. $\times 10^4$ | COV |
|---|---|---|---|---|---|---|---|---|---|---|
| WPF | F16 -430 PQP | 34 | 33 | .01"-.05" | AL-BU | 2.393 | 0.166 | 2.429 | 0.464 | 0.191 |
|  |  |  |  | .01"-.10" |  | 2.364 | 0.159 | 2.396 | 0.422 | 0.176 |
|  |  |  |  | .01"-1" |  | 2.364 | 0.162 | 2.398 | 0.440 | 0.183 |
|  |  |  |  | ALL |  | 2.528 | 0.150 | 2.559 | 0.420 | 0.164 |
| XWPF |  | 34 | 32 (8) | .01"-.05" |  | 3.651 | 0.262 | 3.776 | 0.962 | 0.255 |
|  |  |  |  | .01"-.10" |  | 3.387 | 0.280 | 3.521 | 0.978 | 0.278 |
|  |  |  |  | .01"-1" |  | 3.231 | 0.267 | 3.351 | 0.935 | 0.279 |
|  |  |  |  | ALL |  | 3.351 | 0.234 | 3.445 | 0.822 | 0.239 |
| LXWPF |  | 30.6 | 7 | .01"-.05" |  | 2.330 | 0.247 | 2.408 | 0.664 | 0.276 |
|  |  |  |  | .01"-.10" |  | 2.185 | 0.214 | 2.241 | 0.562 | 0.250 |
|  |  |  |  | .01"-1" |  | 2.120 | 0.176 | 2.156 | 0.429 | 0.199 |
|  |  |  |  | ALL |  | 2.253 | 0.249 | 2.322 | 0.555 | 0.239 |
| HYBP F |  | 40.8 | 10 | .01"-.05" | .005"-.2" | 9.304 | 0.293 | 9.682 | 2.529 | 0.251 |
|  |  |  |  | .01"-.10" | .005"-.2" | 8.452 | 0.254 | 8.721 | 2.144 | 0.246 |
|  |  |  |  | .01"-1" | .005"-.2" | 7.965 | 0.229 | 8.177 | 1.893 | 0.231 |
|  |  |  |  | ALL | AL-AU | 8.803 | 0.249 | 9.057 | 1.904 | 0.219 |

Notes:  (1)  7475-T7351 Al.; straight bore holes with NAS 6204-08 (1/4" Dia.) bolts installed

(2)  Maximum gross stress at peak spectrum load

(3)  Uncensored data set

(4)  Default range used when data does not exist or is insufficient in the AL-AU range for required computations

(5)  Ref. Eq. F-8

(6)  Ref. Eq. F-10

(7)  Deterministic crack growth approach used

(8)  One surface fatigue crack not used

Table F.6. Summary of Pooled Q, $\sigma_z$, and Q statistics for Different AL-AU Crack Size Ranges Based on Recommended Methods (FHQ -- Bomber Data Sets)

| DATA SET (1) | LOAD SPECTRUM | $\sigma$ MAX. (ksi) (2) | NO. CRACKS (3) | AL-AU | DL-DU (4) | Q×10^4 (1/HR.) (5) | $\sigma_z$ (6) | $Q_j$ STATISTICS (MEAN)×10^4 (1/HR.) | STD. DEV. ×10^4 | COV |
|---|---|---|---|---|---|---|---|---|---|---|
| WPB | B-1 Bomber | 33 | 32 | .01"-.05" | AL=AU | 1.401 | 0.139 | 1.415 | 0.197 | 0.139 |
| | | | | .01"-.10" | | 1.425 | 0.149 | 1.441 | 0.219 | 0.152 |
| | | | | .01"-1" | | 1.449 | 0.166 | 1.469 | 0.256 | 0.174 |
| | | | | ALL | | 1.509 | 0.141 | 1.524 | 0.218 | 0.143 |
| JWPB | | 33 | 31 | ALL | | 2.469 | 0.233 | 2.534 | 0.564 | 0.222 |
| | | | | .01"-.05" | | 2.464 | 0.225 | 2.525 | 0.544 | 0.215 |
| | | | | .01"-.10" | | 2.473 | 0.228 | 2.538 | 0.580 | 0.229 |
| | | | | .01"-1" | | 2.493 | 0.213 | 2.550 | 0.547 | 0.214 |
| LWPB | | 29.7 | 18 | ALL | | 1.596 | 0.240 | 1.647 | 0.423 | 0.256 |
| | | | | .01"-.05" | | 1.667 | 0.213 | 1.706 | 0.384 | 0.225 |
| | | | | .01"-.10" | | 1.724 | 0.202 | 1.760 | 0.371 | 0.210 |
| | | | | .01"-1" | | 1.562 | 0.150 | 1.579 | 0.231 | 0.146 |
| HWPB | | 39.6 | 18 | ALL | | 4.410 | 0.229 | 4.527 | 1.036 | 0.229 |
| | | | | .01"-.05" | | 4.226 | 0.216 | 4.328 | 0.974 | 0.225 |
| | | | | .01"-.10" | | 4.338 | 0.151 | 4.389 | 0.673 | 0.153 |
| | | | | .01"-1" | | 4.835 | 0.144 | 4.886 | 0.712 | 0.146 |
| | | | | ALL | | | | | | |

Notes: (1) 7475-T7351 Al.; straight bore holes with NAS 6204-03 (1/4" Dia.) bolts installed

(2) Maximum gross stress at peak spectrum load

(3) Uncensored data set

(4) DL-DU same as AL-AU range to compute the crack growth parameter Q for a give crack or cracks in the data set

(5) Ref. Eq. F-8

(6) Ref. Eq. F-10

(7) Deterministic crack growth approach used

Table F.7. Summary of Pooled Q, $\sigma_z$, and Q statistics for Straight-Bore Fastener Holes Based on Recommended Methods.

| (1) DATA SET | (2) σ MAX (ksi) | (3) NO. CRACKS | AL-AU | (4) DL-DU | (5) Qx10⁴ (1/HR) | (6) $\sigma_z$ | $Q_j$ (MEAN)x10⁴ (1/HR.) | STD. DEV. x10⁴ | COV |
|---|---|---|---|---|---|---|---|---|---|
| WWPF  F-16 400 HR | 34 | 13 | .01"-.05" | AL-AU | 2.742 | 0.119 | 2.762 | 0.340 | 0.123 |
| | | | .01"-.10" | ⟶ | 2.750 | 0.146 | 2.782 | 0.450 | 0.165 |
| | | | .01"-2" | | 2.924 | 0.153 | 2.959 | 0.479 | 0.162 |
| | | | .05"-2" | | 3.123 | 0.177 | 3.172 | 0.555 | 0.175 |
| | | | .10"-2" | | 3.248 | 0.185 | 3.300 | 0.599 | 0.181 |
| | | | ALL | | 2.918 | 0.147 | 2.951 | 0.462 | 0.156 |
| WWPB  B-1 BOMBER | 34 | 12 | .01"-.05" | .005"-.10" AL-AU | 4.458 | 0.538 | 5.054 | 2.228 | 0.452 |
| | | | .01"-.10" | ⟶ | 3.655 | 0.400 | 3.936 | 1.402 | 0.356 |
| | | | .01"-2" | | 2.452 | 0.176 | 2.492 | 0.452 | 0.182 |
| | | | .05"-2" | | 2.259 | 0.197 | 2.307 | 0.509 | 0.221 |
| | | | .10"-2" | | 2.240 | 0.246 | 2.317 | 0.684 | 0.295 |
| | | | ALL | | 2.733 | 0.201 | 2.789 | 0.553 | 0.198 |
| | | | | | 4.579 | 0.479 | 5.092 | 2.193 | 0.431 |
| WWPCL  F-16 C/D | 34 | 4 | .01"-.05" | .005"-.10" AL-AU | 4.178 | 0.411 | 4.520 | 1.667 | 0.373 |
| | | | .01"-.10" | ⟶ | 2.185 | 0.331 | 2.300 | 0.695 | 0.302 |
| | | | .01"-2" | | 1.879 | 0.271 | 1.950 | 0.535 | 0.274 |
| | | | .05"-2" | | 1.752 | 0.260 | 1.813 | 0.486 | 0.268 |
| | | | .10"-2" | | 2.239 | 0.337 | 2.359 | 0.700 | 0.297 |
| | | | ALL | | 9.638 | 0.556 | 10.884 | 4.723 | 0.434 |
| WWPCH | 40.8 | 6 | .01"-.05" | .005"-20" .005"-20" AL-AU | 7.387 | 0.442 | 8.039 | 3.227 | 0.401 |
| | | | .01"-.10" | ⟶ | 4.056 | 0.234 | 4.172 | 1.124 | 0.269 |
| | | | .01"-2" | | 3.526 | 0.187 | 3.591 | 0.793 | 0.221 |
| | | | .05"-2" | | 3.323 | 0.199 | 3.394 | 0.812 | 0.239 |
| | | | .10"-2" | | 4.192 | 0.239 | 4.312 | 1.129 | 0.262 |
| | | | ALL | | 8.506 | 0.379 | 9.213 | 3.431 | 0.372 |
| WWPFO  F-16 400 HR | 34 | 14 | .01"-.05" | AL-AU | 6.624 | 0.279 | 6.895 | 2.049 | 0.297 |
| | | | .01"-.10" | ⟶ | 3.994 | 0.197 | 4.075 | 0.836 | 0.205 |
| | | | .01"-2" | | 3.460 | 0.204 | 3.534 | 0.742 | 0.209 |
| | | | .05"-2" | | 3.388 | 0.208 | 3.462 | 0.724 | 0.209 |
| | | | .10"-2"  ALL | | 4.346 | 0.199 | 4.436 | 0.918 | 0.207 |

Ref. Table F.9 for notes.

F-13

Table F.8.    Summary of Pooled Q, $\sigma_z$, and Q Statistics for Countersunk Fastener Holes Based on Recommended Methods.

| DATA SET (1) | LOAD SPECTRUM | $\sigma$ MAX. (ksi) (2) | NO. CRACKS (3) | AL-AU | DL-DU (4) | $Q \times 10^4$ (1/HR.) (5) | $\sigma_z$ (6) | Qj STATISTICS (MEAN)$\times 10^4$ (1/HR) | STD. DEV. $\times 10^4$ | COV |
|---|---|---|---|---|---|---|---|---|---|---|
| WFI | F-16 400 HR | 34 | 14 | .01"-.05" | AL-AU | 2.329 | .247 | 2.404 | .654 | .272 |
| | | | | .01"-.10" | → | 2.228 | .221 | 2.287 | .576 | .252 |
| | | | | .01"-2" | | 2.187 | .205 | 2.237 | .531 | .237 |
| | | | | .05"-2" | | 2.216 | .224 | 2.276 | .583 | .256 |
| | | | | .10"-2" | | 2.334 | .262 | 2.421 | .731 | .302 |
| | | | | ALL | | 2.216 | .204 | 2.227 | .530 | .234 |
| MBi | B-1 BOMBER | 36 | 12 | .01"-.05" | .01"-.20" | 5.709 | .284 | 5.949 | 1.806 | .304 |
| | | | | .01"-.10" | AL-AU → | 4.699 | .206 | 4.803 | 1.082 | .225 |
| | | | | .01"-2" | | 2.747 | .268 | 2.852 | .863 | .302 |
| | | | | .05"-2" | .05"-2" | 2.402 | .288 | 2.519 | .837 | .332 |
| | | | | .10"-2" | AL-AU | 2.309 | .313 | 2.435 | .904 | .371 |
| | | | | ALL | | 2.941 | .248 | 3.039 | .866 | .291 |
| WRFXMR4 | F-16 400 HR | 34 | 14 | .01"-.05" | .01"-.20" | 6.955 | .825 | 6.835 | 5.066 | .573 |
| | | | | .01"-.10" | .01"-.20" | 5.108 | .706 | 6.135 | 3.159 | .515 |
| | | | | .01"-2" | AL-AU → | 3.335 | .449 | 3.679 | 1.716 | .467 |
| | | | | .05"-2" | | 2.970 | .441 | 3.274 | 1.551 | .474 |
| | | | | .10"-2" | | 2.906 | .446 | 3.209 | 1.538 | .479 |
| | | | | ALL | | 3.543 | .447 | 3.901 | 1.814 | .465 |
| WRFXME4 | | 40.8 | 13 | .01"-.05" | AL-AU | 6.980 | .429 | 7.698 | 3.791 | .492 |
| | | | | .01"-.10" | → | 5.804 | .427 | 6.393 | 3.109 | .486 |
| | | | | .01"-2" | | 4.446 | .347 | 4.743 | 1.933 | .407 |
| | | | | .05"-2" | | 4.018 | .328 | 4.259 | 1.673 | .393 |
| | | | | .10"-2" | | 4.087 | .343 | 4.369 | 1.928 | .441 |
| | | | | ALL | | 4.655 | .357 | 4.989 | 2.135 | .429 |
| WMMPB | B-1 BOMBER | 34 | 15 | .01"-.05" | .01"-.20" | 4.277 | 0.209 | 4.376 | 0.981 | 0.224 |
| | | | | .01"-.10" | AL-AU | 3.413 | 0.337 | 3.694 | 1.774 | 0.480 |
| | | | | .01"-2" | AL-AU | 1.799 | 0.228 | 1.848 | 0.434 | 0.235 |
| | | | | .05"-2" | | 1.553 | 0.245 | 1.601 | 0.406 | 0.254 |
| | | | | .10"-2" | | 1.487 | 0.259 | 1.539 | 0.425 | 0.276 |
| | | | | ALL | | 1.968 | 0.239 | 2.026 | 0.507 | 0.250 |

Ref. Table F.9 for notes.

**TABLE F.9.  Notes for Tables F.7 and F.8.**

Notes:  (1)  7475-T7351 Al.
        (2)  Maximum gross stress at peak spectrum load
        (3)  Uncensored data set
        (4)  Default range used when data does not exist or is
             insufficient in the AL-AU range for required com-
             putations
        (5)  Ref. Eq. F-8
        (6)  Ref. Eq. F-10
        (7)  Deterministic crack growth approach

The investigation was conducted as follows: Five fractographic data sets (straight-bore holes) from Tables F.1 and F.2 were used (i.e. WPF, XWPF, HYWPF, LYWPF, and WWPF). First, the fractographic results for the largest fatigue crack per specimen were screened. The number of fatigue cracks with factographic data covering selected AL-AU ranges was determined for each data set. Also, the maximum common Al-AU range for each data was determined. Some non typical fatigue cracks were deleted from the data set for analysis purposes. Results of this survey are shown in Table F.10.

Software is available for screening fractographic results for a given data set using an IBM or IBM-compatible PC [5]. This software can be used to plot the fractographic results for selected crack size ranges and/or flight hour ranges. Plots of the fractographic data (i.e. a(t) versus flight hours) for the five data sets considered in Part II are shown in Figs. F.1-F.10. Data for the full range as well as for AL-AU = 0.01" - 0.05" range are shown in these plots.

The following values were computed using censored and uncensored data sets: Pooled Q, $\sigma_z$, TTCI (mean and COV), and mean EIFS (two different methods). Results are summarized in Tables F.11 and F.12. In Table F.11 the TTCI values were determined for the reference crack size, $a_0$, that was selected so that all TTCIs could be determined by interpolation with no extrapolations. In Table F.11 two numbers are shown for the number of cracks used. The first number denotes the number of fatigue cracks used for the analysis and the second number, separated by a slash (/), denotes the total number of fatigue cracks (i.e. largest fatigue crack per specimen) in the data set.

Mean EIFS values, obtained with and without TTCI extrapolations, are summarized in Table F.12 for the same data

TABLE F.10.  Crack Size Range Survey for Straight-Bore Hole Data Sets.

| Data | No. Cracks in AL-AU Range | Common AL-AU Range | Remarks |
|---|---|---|---|
| WPF | 27 | .01"-.02" | Delete #6, 19, 20, 21, 23, 29 |
| | 21 | .01 - .03 | Delete #6, 13, 19, 20, 21, 23, 24, 29, 30, 31, 32, 33 |
| | 18 | .01 - .04 | Delete #6, 13, 17, 19, 20, 21, 22, 23, 24, 26, 29, 30, 31, 32, 33 |
| | 6 | .01 - .05 | Delete #5, 6, 7, 8, 9, 11, 12, 13, 15, 16, 17, 18, 19, 20, 21, 22, 23, 24, 25, 26-33 |
| | 33 | .0042-.0129 | Delete #6 |
| XWPF | 30 | .01"-.02" | Delete #2, 16, 31 |
| | 30 | .01-.03 | Delete #2, 16, 31 |
| | 30 | .01-.04 | Delete #2, 16, 31 |
| | 30 | .01-.05 | Delete #2, 16, 31 |
| | 22 | .0141"-.0299" | Delete #16 |
| HYWPF | 7 | .01"-.02" | Delete #5 |
| | 5 | .01-.03 | Delete #4, 5, 7 |
| | 5 | .01-.04 | Delete #4, 5, 7 |
| | 5 | .01-.05 | Delete #4, 5, 7 |
| | 8 | .0026-.0163 | Use all |
| LYWPF | 6 | .01"-.02" | Use all |
| | 5 | .01-.03 | Delete #1 |
| | 5 | .01-.04 | Delete #1 |
| | 5 | .01-.05 | Delete #1 |
| | 6 | .21005-.02181 | Use all |
| WWPF | 12 | .01"-.02" | Delete #3 |
| | 12 | .01-.03 | Delete #3 |
| | 12 | .01-.04 | Delete #3 |
| | 12 | .01-.05 | Delete #3 |
| | 13 | .0154-.078 | Use all |
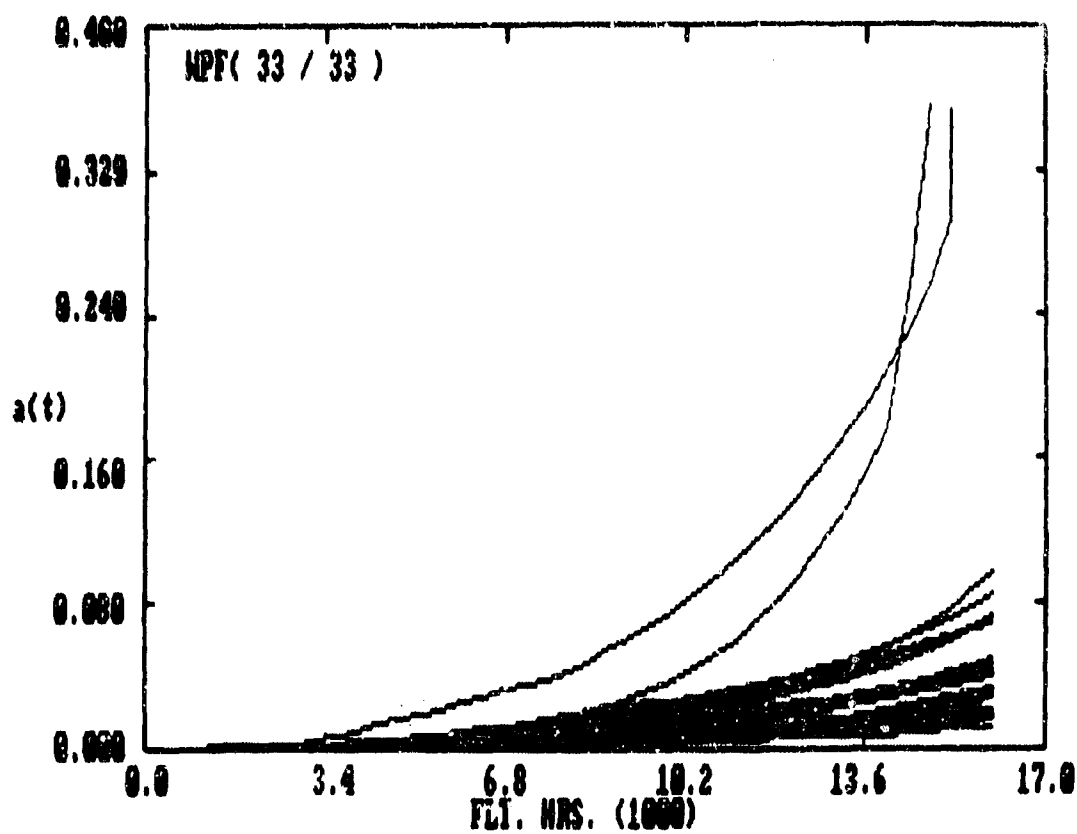
**Figure F.1.** a(t) Versus Flt. Hrs. for WPF Data Set (all the data).
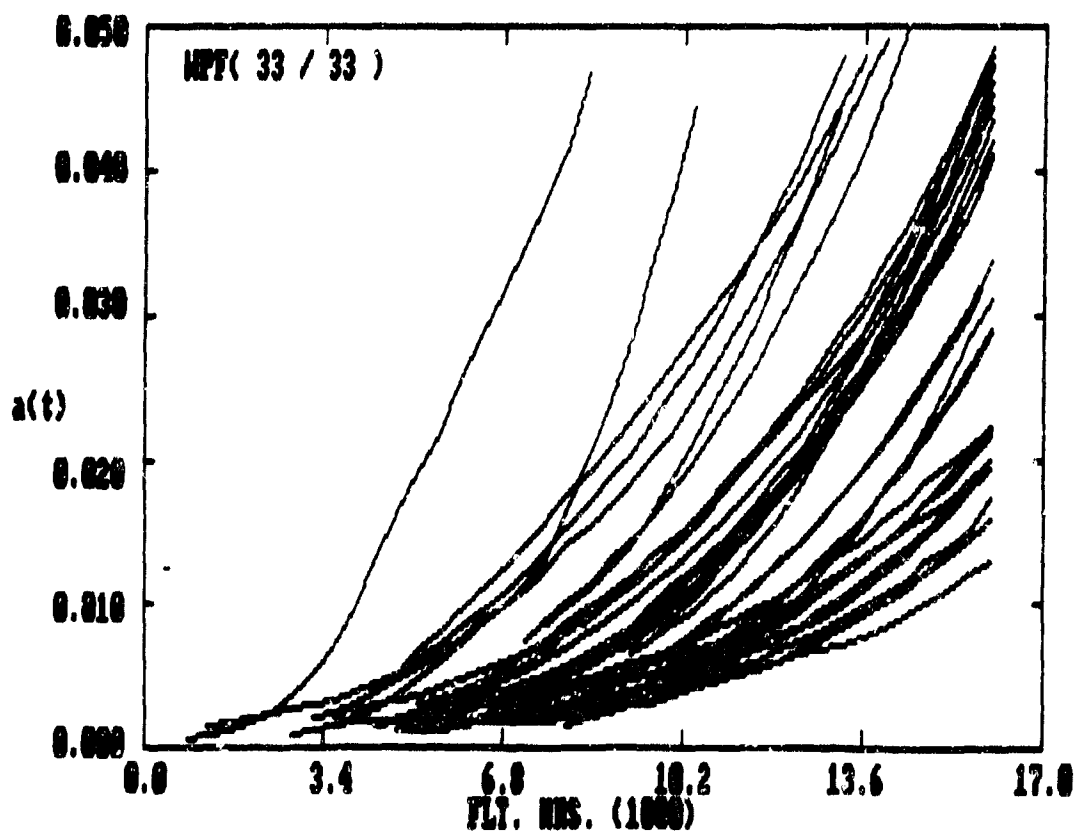


**Figure F.2.** a(t) Versus Flt. Hrs. for WPF Data Set (AL-AU = 0.0"-0.05").
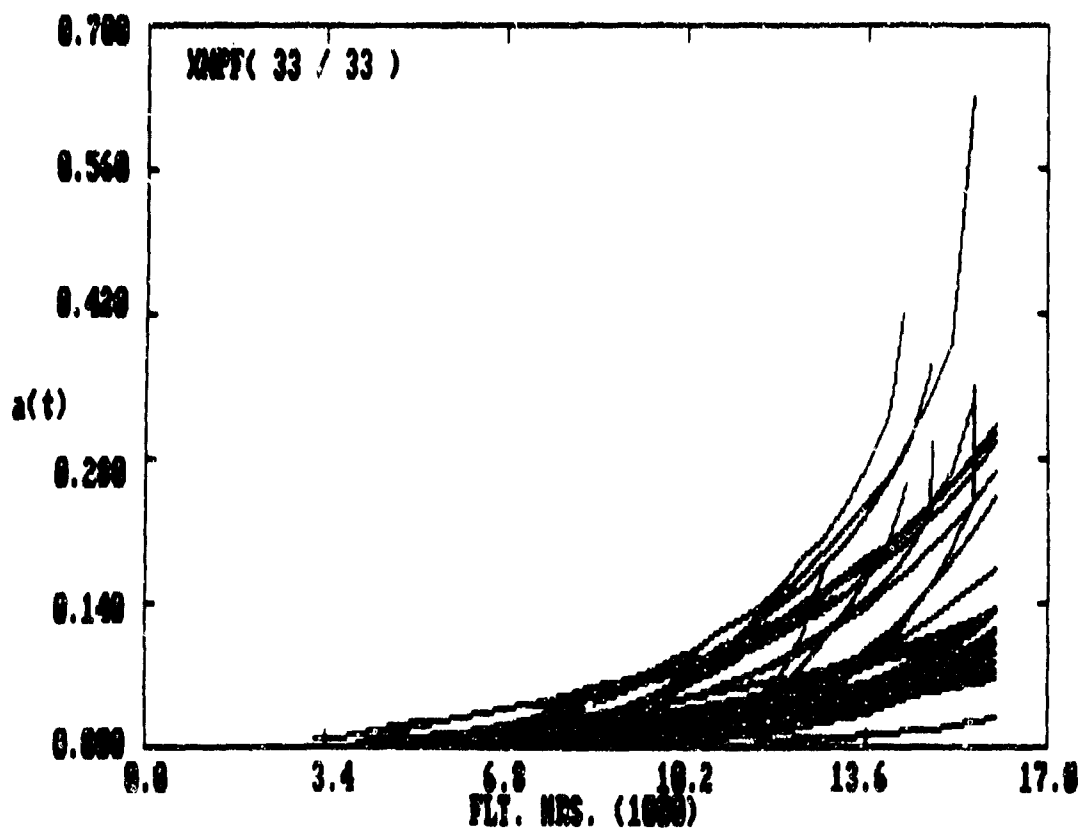
**Figure F.3.** a(t) Versus Flt. Hrs. for XWPF Data Set (all the data).
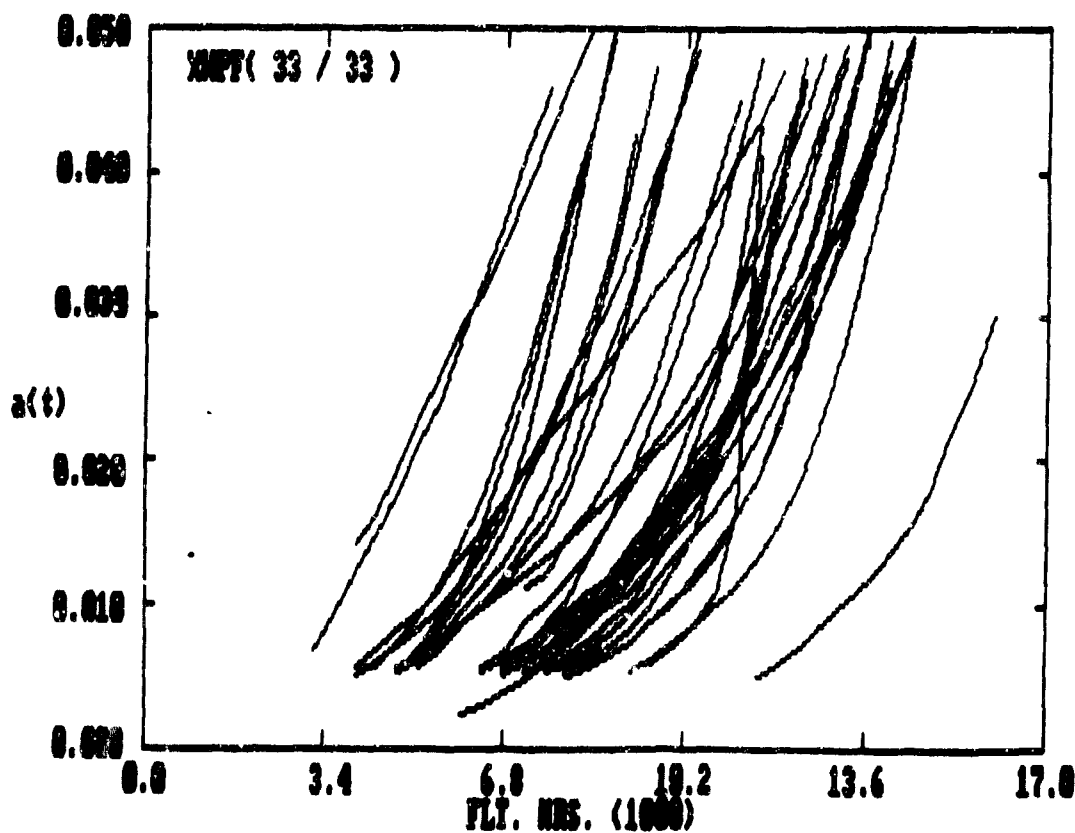


**Figure F.4.** a(t) Versus Flt. Hrs. for XWPF Data Set (AL-AU = 0.0"-0.05").
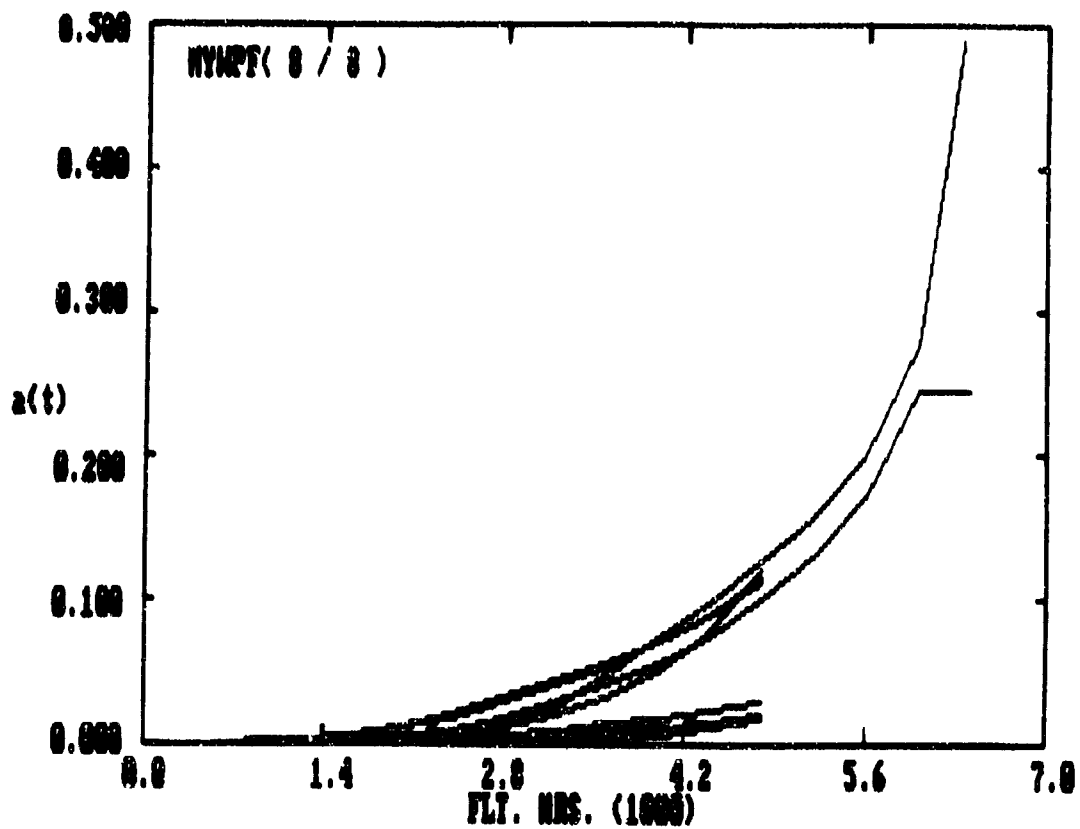
**Figure F.5.** a(t) Versus Flt. Hrs. for HYWPF Data Set (all the data).
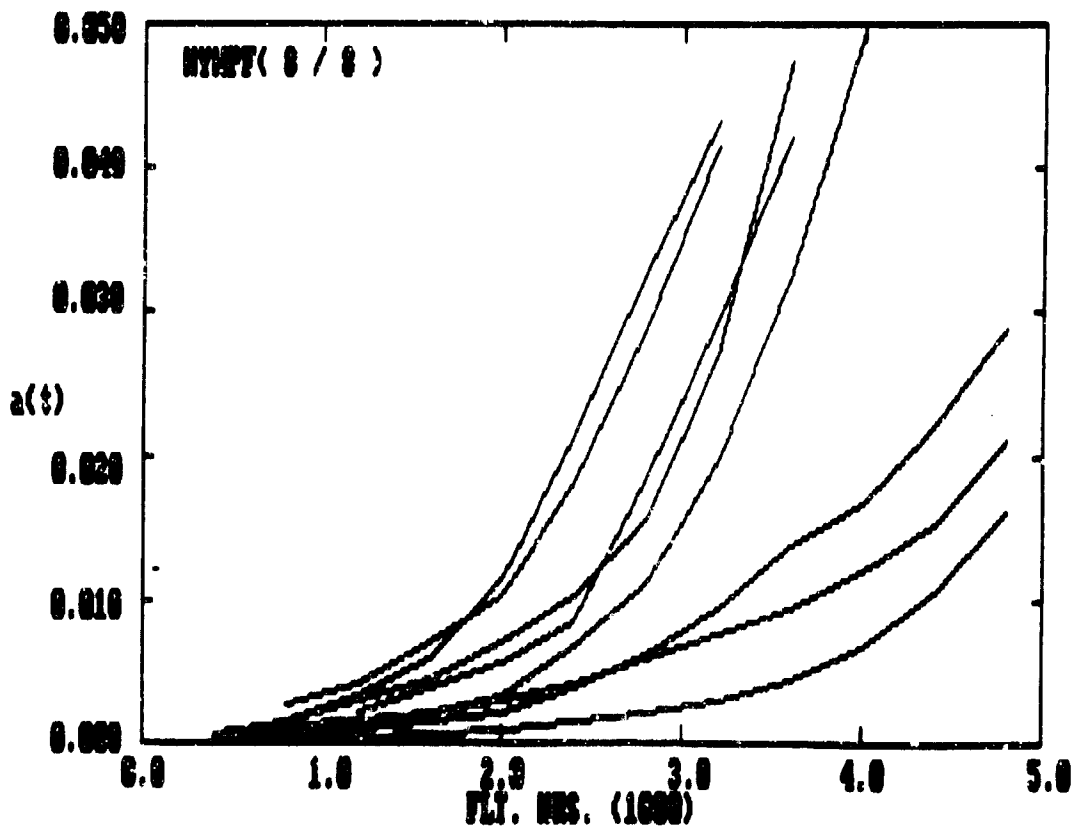


**Figure F.6.** a(t) Versus Flt. Hrs. for HYWPF Data Set (λL-λU = 0.0"-0.05").

F-20
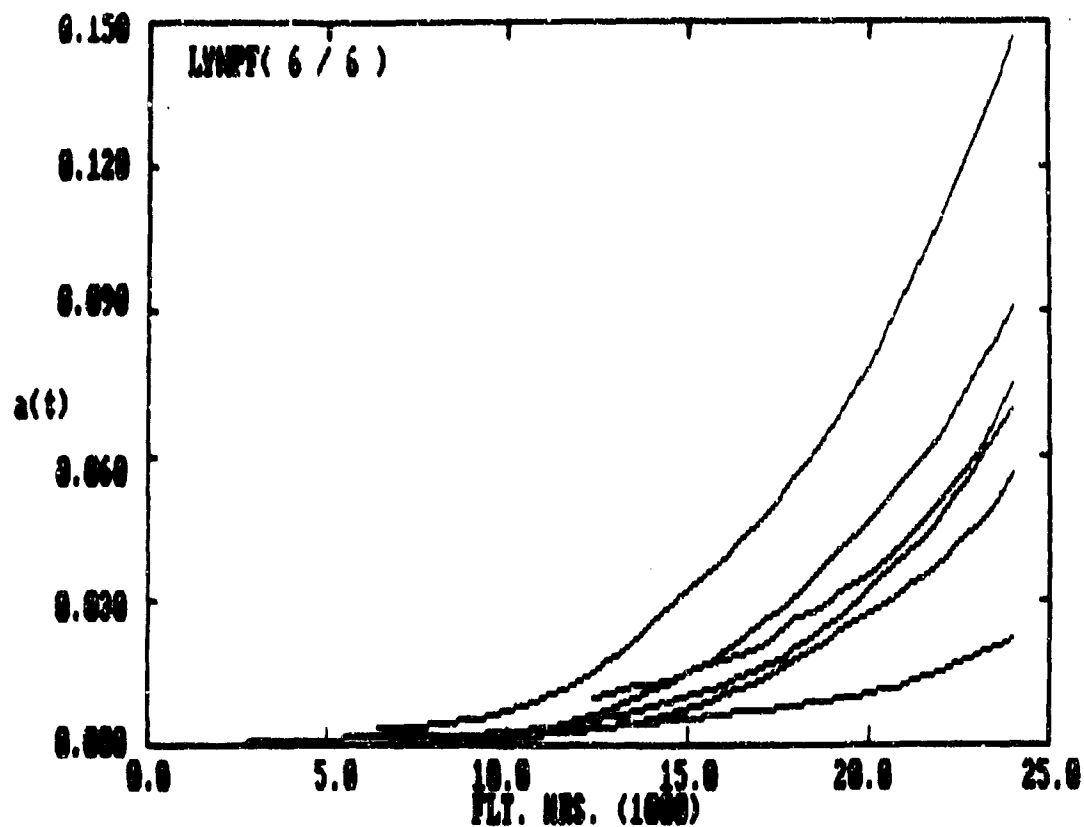
**Figure F.7.** a(t) Versus Flt. Hrs. for LYWPF Data Set (all the data).
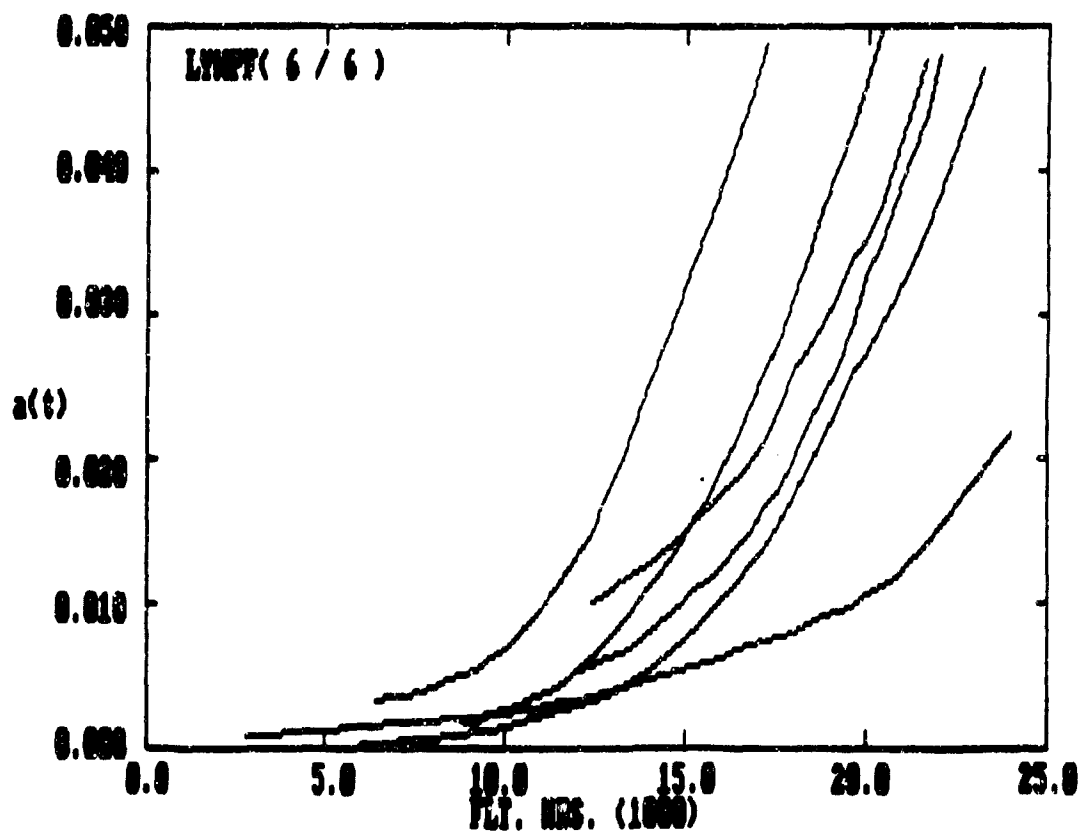


**Figure F.8.** a(t) Versus Flt. Hrs. for LYWPF Data Set (AL-AU = 0.0"-0.05").
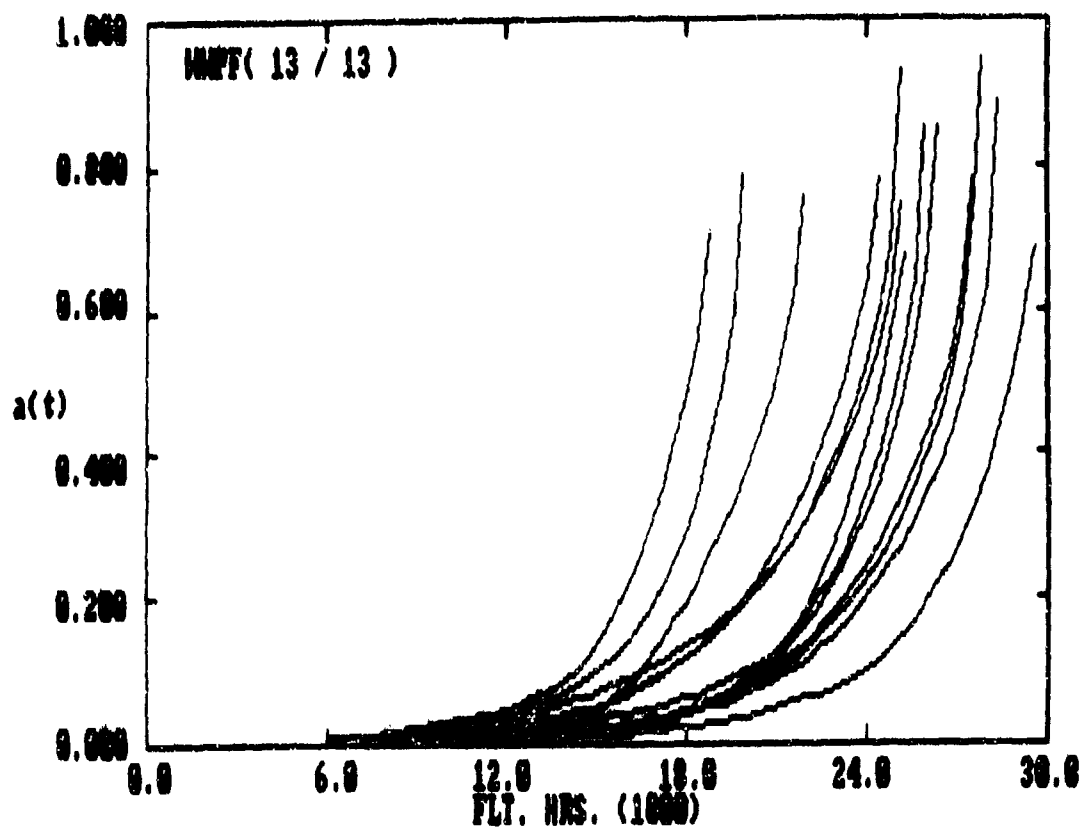
**Figure F.9.** <u>a(t) Versus Flt. Hrs. for WWPF Data Set</u>
<u>(all the data).</u>
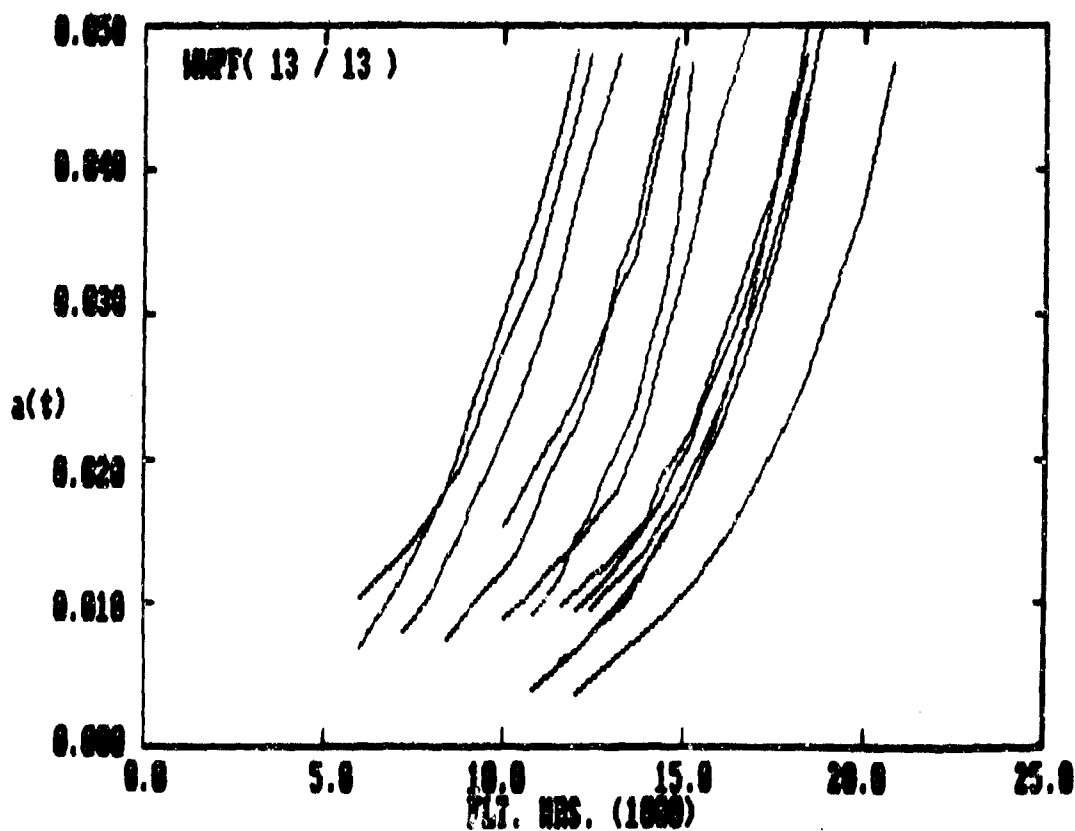


**Figure F.10.** <u>a(t) Versus Flt. Hrs. for WWPF Data Set</u>
<u>(AL-AU = 0.0"-0.05").</u>

Table F.11. Sensitivity of Pooled Q, $\sigma_z$, Mean TTCI and Mean EIFS to AL-AU Range and Censored Data.

TABLE F.12. Sensitivity of Mean EIFS to Data Censoring, AL-AU Range and Use of TTCI Extrapolations.

| Data Set | $\beta$ | No. Cracks Used | AL-AU | DL-DU | Pooled q x10 | $q_g$ | $q_g = .05^M$ Median EIFS x$10^4$ | $a_0$ | MEAN EIFS at $10^4$ | Crack No. Deleted |
|---|---|---|---|---|---|---|---|---|---|---|
| MFF | 1.0 | 32/33 | .0065-.0129 | AL-AU | 2.902 | .143 | 4.313 | .0129 | 5.997 | #6 |
| | | 32/33 | 0-.0129 | | 3.242 | .232 | 2.589 | | 4.309 | #6 |
| | | 27/33 | .01-.02 | | 2.731 | .182 | 6.396 | | 7.994 | #6, 19, 20, 21, 23, 29 |
| | | 20/33 | .01-.03 | | 2.642 | .178 | 8.930 | | 10.309 | #6, 13, 19, 20-24, 29-33 |
| | | 18/33 | .01-.04 | | 2.476 | .184 | 12.003 | | 12.709 | #6, 13, 17, 19-24, 26, 29-33 |
| | | 6/33 | .01-.05 | | 2.614 | .264 | 16.184 | | 36.774 | #5-9, 11-13, 15-33 |
| | | 32/33 | .01-.05 | | 2.376 | .164 | 9.699 | | 10.125 | #6 |
| RMFF | 1.0 | 32/33 | .0141-.0299 | .01-.03 | 3.947 | .337 | 6.215 | .0299 | 6.064 | #16 |
| | | 32/33 | 0-.0299 | AL-AU | 4.045 | .218 | 5.621 | | 6.305 | #16 |
| | | 30/33 | .01-.02 | | 4.017 | .279 | 5.432 | | 5.844 | #2, 16, 31 |
| | | 30/33 | .01-.03 | | 3.964 | .305 | 5.741 | | 6.130 | #2, 16, 31 |
| | | 30/33 | .01-.04 | | 3.985 | .342 | 6.406 | | 6.464 | #2, 16, 31 |
| | | 30/33 | .01-.05 | | 3.891 | .371 | 6.199 | | 6.547 | #2, 16, 31 |
| | | 32/33 | .01-.05 | | 3.848 | .363 | 6.681 | | 7.478 | #16 |
| GMFF | 1.0 | 13/13 | .0154-.03 | AL-AU | 2.795 | .165 | 6.622 | .03 | 6.919 | Use all |
| | | 13/13 | .0154-.04 | | 2.749 | .149 | 7.081 | | 7.329 | Use all |
| | | 13/13 | .0154-.05 | | 2.726 | .123 | 7.323 | | 7.544 | Use all |
| | | 13/13 | .01-.05 | | 2.742 | .119 | 7.154 | | 7.394 | Use all |
| | | 12/13 | .01-.02 | | 2.819 | .197 | 6.321 | | 6.625 | #3 |
| | | 12/13 | .01-.03 | | 2.812 | .124 | 6.335 | | 6.638 | #3 |
| | | 12/13 | .01-.04 | | 2.806 | .208 | 6.437 | | 6.729 | #3 |
| | | 12/13 | .01-.05 | | 2.787 | .109 | 6.617 | | 6.890 | #3 |
| | | 13/13 | .01-.05 | | 2.742 | .119 | 7.155 | | 7.395 | Use all |
| LYMFF | 1.0 | 6/6 | .0100-.02181 | AL-AU | 2.325 | .249 | 3.666 | .02181 | 4.066 | Use all |
| | | 6/6 | 0-.02181 | | 2.345 | .320 | 3.895 | | 3.982 | Use all |
| | | 6/6 | .01-.02 | | 2.331 | .252 | 3.595 | | 4.073 | Use all |
| | | 5/6 | .01-.03 | | 2.468 | .211 | 3.639 | | 3.207 | #1 |
| | | 5/6 | .01-.04 | | 2.393 | .175 | 4.638 | | 5.621 | #1 |
| | | 5/6 | .01-.05 | | 2.191 | .144 | 5.558 | | 5.910 | #1 |
| | | 6/6 | .01-.05 | | 2.140 | .162 | 5.287 | | 5.558 | Use all |
| RYMFF | 1.0 | 8/8 | .0026-.0163 | AL-AU | 10.991 | .244 | 5.994 | .0163 | 6.632 | Use all |
| | | 8/8 | 0-.0163 | | 12.157 | .210 | 3.833 | | 4.883 | Use all |
| | | 7/8 | .01-.02 | .01-.03 | 10.135 | .424 | 9.121 | | 9.336 | #5 |
| | | 5/8 | .01-.03 | AL-AU | 13.228 | .101 | 3.040 | | 5.595 | #4, 5, 7 |
| | | 5/8 | .01-.04 | | 12.625 | .0455 | 5.048 | | 6.500 | #4, 5, 7 |
| | | 5/8 | .01-.05 | | 11.626 | .074 | 7.244 | | 8.339 | #4, 5, 7 |
| | | 8/8 | .01-.05 | | 9.949 | .249 | 8.621 | | 8.705 | Use all |

F-24

sets and conditions shown in Table F.11. In one case, TTCI values were determined for $a_0 = 0.05"$ by either interpolation or extrapolation. In the other case, TTCI values were determined by interpolation for a selected reference crack size which "sliced through" all the data. Method 1, described in Fig. F.11, was used in this case.

The results for Part II are discussed in Section F.4, including comparisons with the results for Part I.

## F.4 DISCUSSION

1. There's no significant difference in the resulting pooled Q, $\sigma_z'$, and EIFS values based on either the modified secant or five-point incremental polynomial method for the uncensored FHQ data sets in the .01"-.05" crack size range considered, see results in Tables F.3 and F.4.

2. In most cases, equalizing or not equalizing the number of a(t)s in the AL-AU range does not significantly change the pooled Q and $\sigma_z$ values. Larger differences are noted when all the data are used, as observed from Tables F.3 and F.4.

3. The AL-AU crack size range affects the pooled Q and $\sigma_z$ values. For some data sets the effect of the AL-AU range on pooled Q and $\sigma_z$ seems to be greater than others. In any case pooled Q and $\sigma_z$ should be defined for a specified AL-AU range, see Table F.5.

4. Pooled Q and $\sigma_z$ values computed using the preliminary method (based on da(t)/dts) were approximately the same as those based on the refined methods. For example, compare the results in Tables F.3 and F.4 with those results for the same AL-AU range in Table F.5. Since the refined method is simpler and more straight forward than the preliminary method
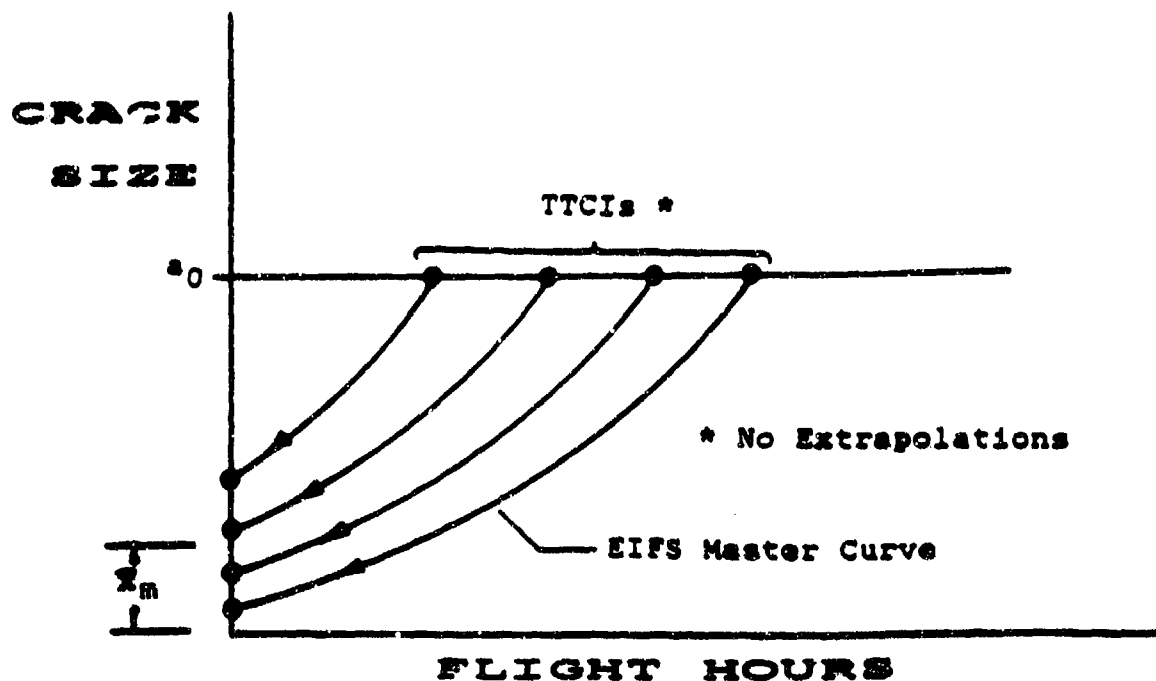
(a) Method 1--Use No TTCI Extrapolations and EIFS Master Curve
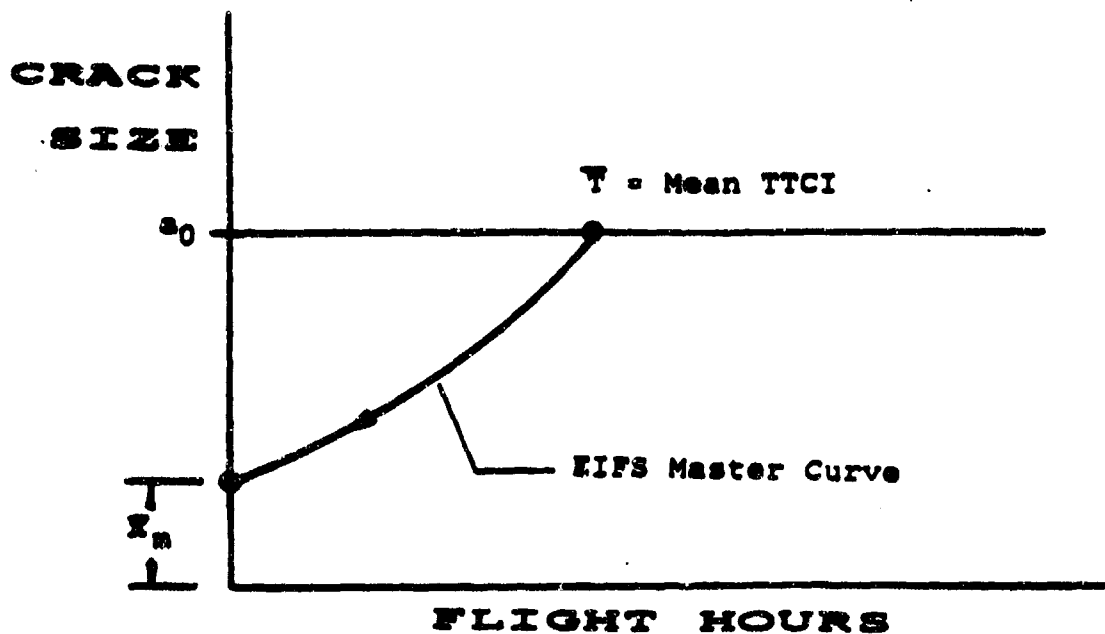


(b) Method 2--Use Mean TTCI and EIFS Master Curve

Figure F.11. Methods Considered for Determining the Mean EIFS for a Fractographic Data Set.

based on da(t)/dt data, it is recommended for durability analysis.

5. Pooled Q, $\sigma_z$, and $Q_j$ statistics are shown in Tables F.7 and F.8 for the ADA data sets. Pooled Q and $\sigma_z$ depend on the fractographic crack size range used. In particular, it appears that the AL-AU range has a bigger influence on $\sigma_z$ than on pooled Q.

6. In Table F.10 the five fractographic data sets were surveyed to determine which cracks covered the selected AL-AU ranges. By far, the WPF data set contained more specimens with cracks that did not cover the designated AL-AU range than any of the other four data sets. For example, the WPF data set had only 6 specimens out of 33 that "covered" the .01"-.05" crack size range (i.e. .01"< a(t) > .05"). The other four data sets had the following number of specimens that covered the AL-AU = range: XWPF (30 out of 33), HYWPF (5 out of 8), LYWPF (5 out of 6) and WWPF (12 out of 13).

7. The fractographic plots shown in Fig. F.1 and F.10 are useful for quickly examining the character or behavior of the fractographic data sets. The durability software filename = "PLOT" can be effectively used to "zoom in" and study the fractographic data in desired crack size ranges. This tool should be used to screen fractographic results before being used in the durability analysis. Further details about the plotting tool are given in Volume V [5].

8. Conclusions about the sensitivity study summarized in Tables F.11 and F.12 are (1) the fractographic crack size range used (i.e. AL-AU) affects significantly pooled Q and $\sigma_z$ values, (2) the variation in pooled Q and $\sigma_z$ for different AL-AU ranges was greatest for the WPF data set, followed by the HYWPF data set, (3) "mixing and matching"

interpolated and extrapolated fractographic data can have a significant effect on the mean EIFS for a given data set (e.g., refer to results for the WPF data set), and (4) deleting fractographic results for an "abnormal fatigue cracks" can affect pooled Q, and the mean EIFS for a data set. It is important not to accept all fractographic results for durability analysis without screening the data first.

9. Mean EIFS values obtained using two different methods are summarized in Table F.12 for selected crack size ranges for five data sets. Conclusions are (1) Methods 1 and 2 do not give the same mean EIFS, (2) in all cases, mean EIFS values based on Method 1 were larger than those based on Method 2, (3) the mean EIFS is sensitive to the AL-AU crack size range used, and (4) the coefficient of variation for TTCI is fairly consistent for the selected AL-AU range for all five data sets.

# APPENDIX G

## STRAIN SURVEY FOR EVALUATING % BOLT LOAD TRANSFER

A strain survey was performed to determine the % bolt load transfer as a function of % load level for a double-reverse, dog-bone specimen (Fig. G.1). Experimental results from the strain survey are presented, evaluated, and discussed in this section. Objectives of the survey were to (1) estimate the actual % bolt load transfer and variations for a so-called "15% load transfer test specimen" and (2) provide a basis for comparing the predicted % bolt load transfer based on the service crack growth master curve (SCGMC) tuning studies (see Appendix D).

Two axial-type strain gages were mounted on the outer surface of the dog-bone specimen (i.e., Durability specimen #120), as shown in Fig. G.1. Gage Number 1 was located on the surface along the centerline of the specimen on the "big lug side". In a similar manner, Gage Number 2 was located on the "small lug side". Durability Specimen #120 dimensions were: width = 3.0085 in and total thickness of specimen (two pieces) = 0.3912".

The strain survey was conducted using a maximum ram load of 45.9K (100% load). Strain readings were taken in 20% load increments, starting at 0% up to a 100% load level. Following the strain gage readings at the 100% load level, the ram load was reduced to zero and the strain gages were read. Strain gage readings are summarized in Table G.1.

The strain survey results were used to determine the amount of bolt load transfer -- defined as the ratio of the bolt load ($P_a$) and the input load to the joint. Using this definition, two different bolt load transfers can be obtained, depending on which side of the specimen is considered.

1.  Material:  7475-T7351 Aluminum
2.  Match drill holes using modified Winslow Spacematic drill
    without deburring
3.  Drill and install MS90353-08 rivets per M198.

Figure G.1.   Double-Reverse Dog-Bone Specimen (15% Bolt
              Load Transfer) with 3.00" Width.

**TABLE G.1.** Summary of Strain Survey Readings for Durability Specimen 120.

| % LOAD | STRAIN READINGS ($\mu$ IN.) | |
|:---:|:---:|:---:|
| | $\epsilon_1$ | $\epsilon_2$ |
| 0 | 0 | 0 |
| 20 | 845 | 594 |
| 40 | 1656 | 1228 |
| 60 | 2434 | 1910 |
| 80 | 3174 | 2620 |
| 100 | 3966 | 3417 |
| 0 | 0 | 0 |

For example, refer to the specimen freebodies shown in Fig. G.2 (detail "A" and "B"). For this reason, the amount of bolt load transfer was determined three ways: (1) based on detail "A" ($P_S/P_1$), (2) based on detail "B" ($2P_S/P_T$), and (3) based on results for detail "A" and "B".

Results of the bolt load transfer analysis, including the basic equations used, are summarized in Table G-2. Plots of the bolt load transfer variations as a function of the total applied load as shown in Fig. G.3. Three plots are shown in Fig. G.3, i.e., for the large and small lug side and the average result.

In Fig. G.3 it is interesting to note that the amount of bolt load transfer (based on the strain survey results): (1) varies depending on the total applied load to the specimen, (2) decreases as the total applied is increased, and (3) compares very well with the "15% LT specimen design" at the small % total specimen load level. Intuitively, it was expected, due to fastener hole-fit variations, that the amount of bolt load transfer would increase as the total applied load was increased.

The % bolt load transfer versus % total specimen load, shown in Fig. G.3, is based on a single specimen. To assess the variation in the % bolt load transfer, as a function of the % total specimen load, several "replicate specimens" would have to be tested. In any case, the % bolt load transfer for the "15% load transfer specimen" is expected to vary depending on fastener hole-fit, geometric variations and applied load level.
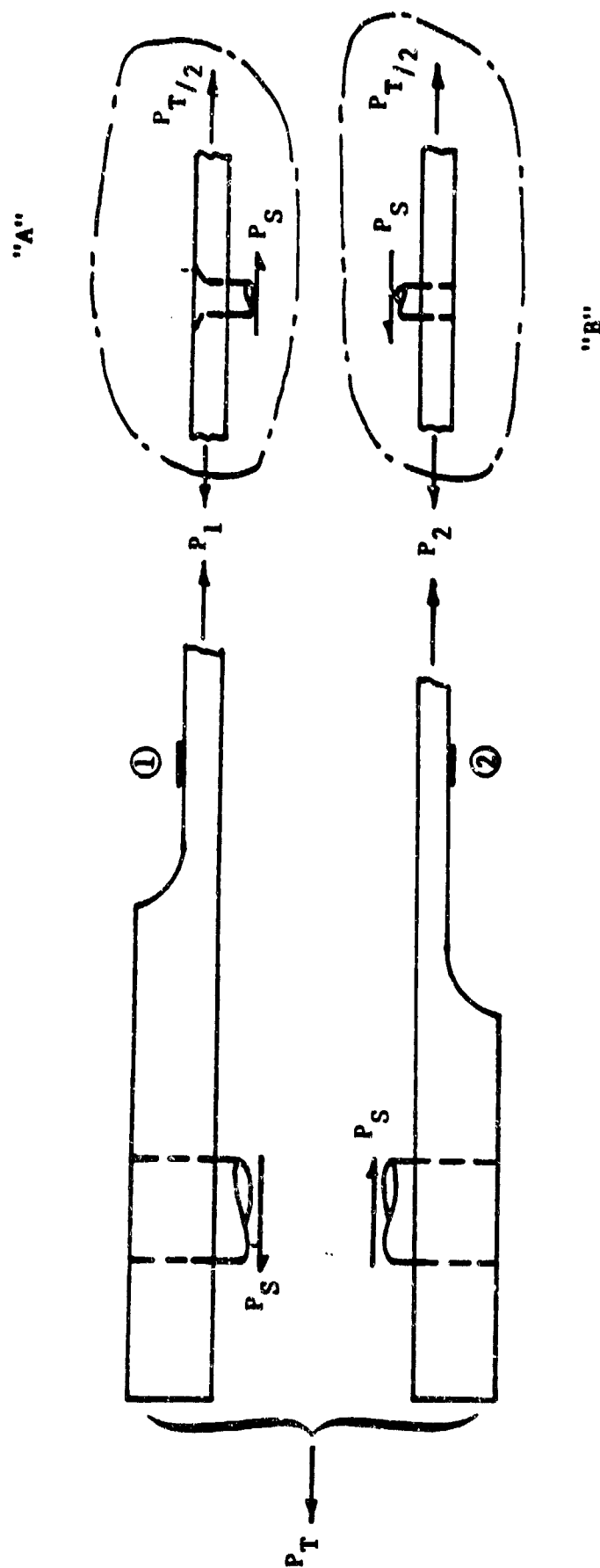
Figure G.2. **Freebodies for Double-Reverse Dog-Bone Type Specimen.**

TABLE G.2. Summary of Strain Survey Results and Evaluation of Bolt Load Transfer.

| Z LOAD | $\epsilon_1$ | $\epsilon_2$ | $P_T$ | $P_1$ (1) | $P_2$ (2) | $P_S$ (3) | $P_S/P_1$ (4) | $2P_S/P_T$ (5) | AVE LT (6) |
|---|---|---|---|---|---|---|---|---|---|
| | (μIN.) | | (KIPS) | | | | | | |
| 0 | 0 | 0 | 0 | 0 | 0 | 0 | — | — | — |
| 20 | 845 | 594 | 9.18 | 5.39 | 3.79 | + 0.8 ∓ | 0.148 | 0.174 | 0.161 |
| 40 | 1656 | 1228 | 18.36 | 10.54 | 7.82 | + 1.36 ∓ | 0.129 | 0.148 | 0.139 |
| 60 | 2434 | 1910 | 27.54 | 15.43 | 12.11 | + 1.66 ∓ | 0.108 | 0.120 | 0.114 |
| 80 | 3174 | 2620 | 36.72 | 20.12 | 16.60 | + 1.76 ∓ | 0.087 | 0.096 | 0.092 |
| 100 | 3968 | 3417 | 45.9 | 24.66 | 21.24 | + 1.71 ∓ | 0.069 | 0.074 | 0.072 |
| 0 | 0 | 0 | 0 | 0 | 0 | 0 | — | — | — |

Notes:

(1) $P_1 = P_T\left(\dfrac{\epsilon_1}{\epsilon_1 + \epsilon_2}\right)$

(2) $P_2 = P_T - P_1$

(3) $\left\{\begin{array}{l} P_S = P_1 - \dfrac{P_T}{2} = \dfrac{P_T}{2} - P_2 \\[2mm] P_S = \dfrac{P_T}{2}\left(\dfrac{\epsilon_1 - \epsilon_2}{\epsilon_1 + \epsilon_2}\right) \end{array}\right.$

(4) $P_S/P_1 = \dfrac{\epsilon_1 - \epsilon_2}{2\epsilon_1}$      (Ref. Fig. G.2: Detail "A")

(5) $2P_S/P_T = \dfrac{\epsilon_1 - \epsilon_2}{\epsilon_1 + \epsilon_2}$      (Ref. Fig. G.2: Detail "B")

(6) AVE LT $= \dfrac{1}{2}\left(P_S/P_1 + 2P_S/P_T\right) = P_S\dfrac{(P_T + 2P_1)/2P_1 \cdot P_T}{} = \dfrac{(\epsilon_1 - \epsilon_2)(3\epsilon_1 + \epsilon_2)}{4\epsilon_1(\epsilon_1 + \epsilon_2)}$

G-6
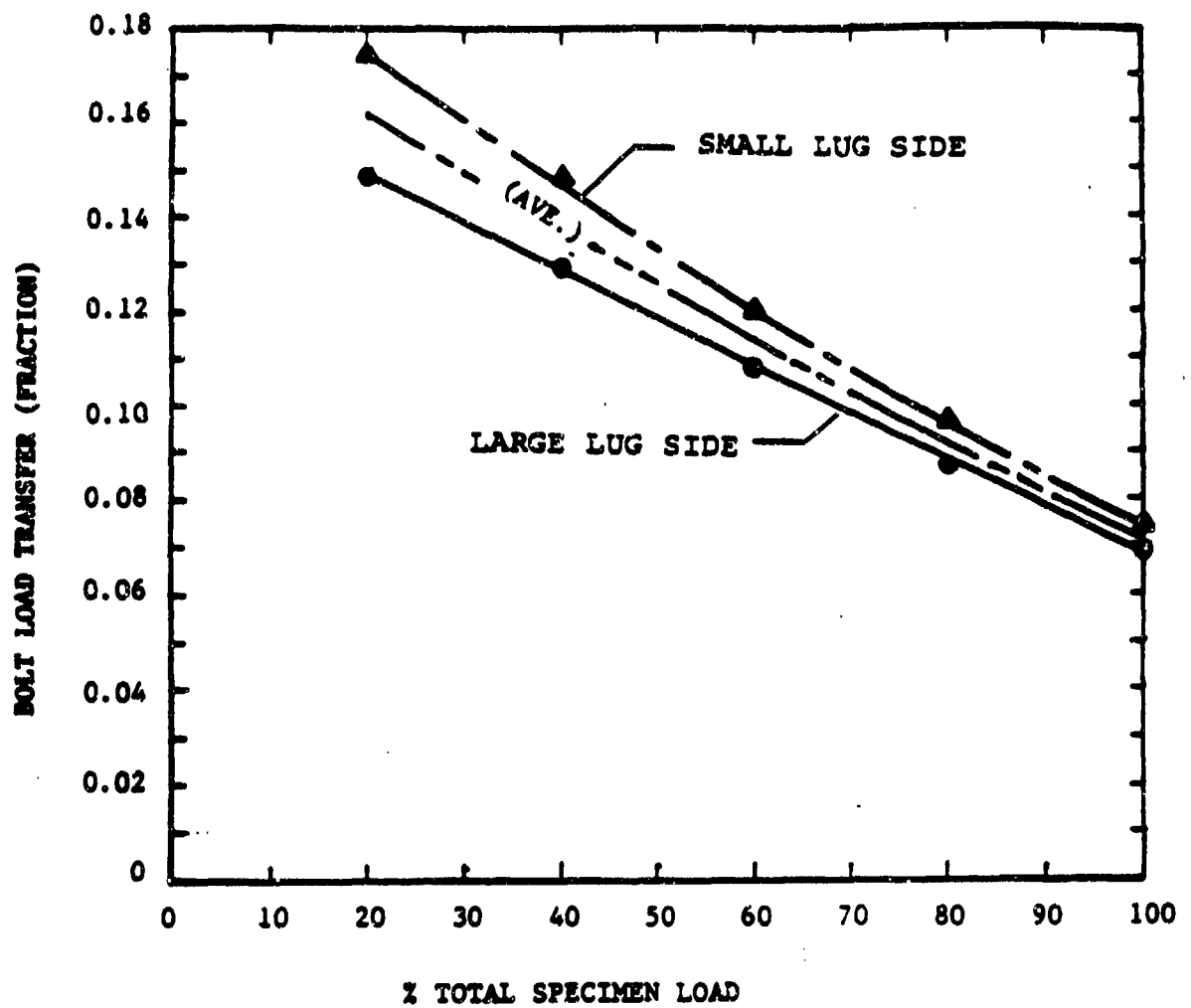
Figure G.3. <u>Bolt Load Transfer (Fraction) Versus Specimen % Load.</u>

# APPENDIX H

## TIME-TO-GIVEN-CRACK-SIZE (TTGCS) AND
## TIME-TO-FAILURE (TTF) STATISTICS

TTGSC and TTF statistics for the 3.0" wide specimens tested under this program (Volume III) are summarized in this section. All specimens considered were made from 7475-T7351 aluminum (1/2" plate).

The following information is presented for each data set:

- o  Mean
- o  Standard deviation
- o  Coefficient of variation
- o  Maximum and minimum values in data set
- o  No. specimen reflected in the analysis

TTGSC or TTF

The above statistics for TTGSC and TTF are summarized in Tables H.1 and H.2 for fighter and bomber load spectra, respectively. Given crack sizes of $x_1$ = 0.01", 0.03", 0.05", 0.1", 0.5", 0.75" and 1.0" are considered for the TTGSC.

The results shown in Tables H.1 and H.2 are based on the durability analysis software (filename = "QSZAT") documented in Volume V [5]. Fractographic data was extrapolated if necessary to obtain the TTGSC value for the selected given crack size, $x_1$. The fractographic data was not screened prior to the statistical analysis.

Coefficient of Variation (COV) values for comparable fighter and bomber data sets (i.e., same specimen configuration and type fastener hole) are summarized in H.3 for six data sets. COV values based on TTGCS for three different crack sizes (i.e., $x_1$ = 0.05", 0.1" and 0.5") are shown as

# Table H.1. Summary of TTGCS and TTF Statistics for Advanced Durability Data Sets (Fighter Load Spectra)

| DATA SETS | ITEM | TTGCS STATISTICS (4) GIVEN CRACK SIZE x, | | | | | | | (4),(5) TTF STATISTICS |
|---|---|---|---|---|---|---|---|---|---|
| | | .01" | .03" | .05" | .1" | .5" | .75" | 1.0" | |
| GGFT | MEAN (FLT. HRS) | 10580 | 14536 | 16452 | 18915 | 24143 | 25086 | 25691 | 25086 |
| | STD. DEV. | 2678 | 2745 | 2678 | 2768 | 3016 | 3079 | 3062 | 3092 |
| | COV | .253 | .189 | .163 | .146 | .125 | .123 | .119 | .123 |
| | MAX. (FLT. HRS) | 14800 | 18986 | 21058 | 24040 | 28825 | 29834 | 30546 | 29516 |
| | MIN. (FLT. HRS) | 5809 | 10000 | 12091 | 14372 | 18112 | 18869 | 19606 | 19884 |
| | NO. SPECIMEN | 13 | | | | | | | |
| WGFT | MEAN (FLT. HRS) | 31933 | 34412 | 35777 | 37702 | 46372 | 48773 | 50137 | 49007 |
| | STD. DEV. | 3714 | 4256 | 4679 | 5007 | 7017 | 7546 | 7781 | 7970 |
| | COV | .116 | .124 | .131 | .133 | .151 | .155 | .155 | .160 |
| | MAX. (FLT. HRS) | 37501 | 39734 | 41501 | 42886 | 54431 | 57403 | 59370 | 59137 |
| | MIN. (FLT. HRS) | 27274 | 28999 | 30018 | 31632 | 37760 | 38851 | 39466 | 38792 |
| | NO. SPECIMEN | 4 | | | | | | | |
| WGFH | MEAN (FLT. HRS) | 16365 | 17759 | 18579 | 19897 | 24510 | 25909 | 26230 | 25849 |
| | STD. DEV. | 6372 | 5983 | 5933 | 5870 | 6139 | 6205 | 6340 | 6123 |
| | COV | .393 | .337 | .319 | .295 | .250 | .242 | .239 | .237 |
| | MAX. (FLT. HRS) | 24605 | 25835 | 26677 | 27778 | 32910 | 33815 | 34455 | 33452 |
| | MIN. (FLT. HRS) | 5860 | 7683 | 8476 | 9780 | 13004 | 13602 | 14060 | 13800 |
| | NO. SPECIMEN | 8 | | | | | | | |
| WGFO | MEAN (FLT. HRS) | 13346 | 14539 | 15335 | 16912 | 21814 | 22712 | 23320 | 22666 |
| | STD. DEV. | 3381 | 2962 | 2805 | 2680 | 2926 | 2897 | 3059 | 3066 |
| | COV | .253 | .204 | .183 | .159 | .134 | .132 | .131 | .101 |
| | MAX. (FLT. HRS) | 17047 | 17661 | 18191 | 19773 | 26615 | 27173 | 27870 | 27235 |
| | MIN. (FLT. HRS) | 4146 | 6194 | 7490 | 9519 | 14540 | 15265 | 15863 | 15470 |
| | NO. SPECIMEN | 14 | | | | | | | |
| HF1 | MEAN (FLT. HRS) | 9401 | 13944 | 16365 | 19651 | 27464 | 28712 | 29450 | 27660 |
| | STD. DEV. | 3776 | 4204 | 4404 | 4624 | 6447 | 6924 | 7156 | 5906 |
| | COV | .402 | .302 | .269 | .235 | .235 | .241 | .246 | .213 |
| | MAX. (FLT. HRS) | 16836 | 21497 | 24242 | 27547 | 40645 | 44345 | 46597 | 36460 |
| | MIN. (FLT. HRS) | 2739 | 6275 | 8448 | 11503 | 15874 | 16303 | 16606 | 16400 |
| | NO. SPECIMEN | 15 | | | | | | | 13 (6) |
| WGFBA1 | MEAN (FLT. HRS) | (7) | 10723 | 13500 | 13977 | 20302 | 21288 | 21977 | 21385 |
| | STD. DEV. | (7) | 5577 | 5421 | 5523 | 6560 | 6773 | 6937 | 6768 |
| | COV | (7) | .520 | .456 | .395 | .323 | .318 | .317 | .317 |
| | MAX. (FLT. HRS) | (7) | 24854 | 25544 | 27065 | 31721 | 33195 | 34220 | 33208 |
| | MIN. (FLT. HRS) | (7) | 4107 | 4595 | 5957 | 10958 | 11613 | 11766 | 11556 |
| | NO. SPECIMEN | 14 | | | | | | | |
| WGFBA1 | MEAN (FLT. HRS) | (7) | 3349 | 4163 | 6047 | 10406 | 11006 | 11445 | 10788 |
| | STD. DEV. | (7) | 1883 | 1883 | 2100 | 2883 | 3002 | 3043 | 2861 |
| | COV | (7) | .473 | .452 | .347 | .277 | .273 | .266 | .276 |
| | MAX. (FLT. HRS) | (7) | 6721 | 7692 | 9781 | 16011 | 16896 | 17485 | 16643 |
| | MIN. (FLT. HRS) | (7) | 1554 | 1562 | 3283 | 5449 | 5763 | 5993 | 5516 |
| | NO. SPECIMEN | 14 | | | | | | | |

Notes:
(1) Data Sets described in Section II.
(2) 7475-T7351 aluminum
(3) Fractographic Data from Ref. 2.
(4) Fractographic results were extrapolated (where necessary to obtain TTGCS values for the selected crack size, $x_i$ . Such extrapolations were made without considering the time-to-failure (TTF) limitations.
(5) Some TTGCS statistics for larger $x_i$ values are not compatible with the TTF results because of (4).
(6) All specimens tested were used to obtain TTGCS statistics but two specimens in this data set were not tested to failure due to testing problems.
(7) Statistics not computed for this $x_i$
(8) Used fractographic results for the largest fatigue crack per specimen.

Table H.2.    Summary of TTGCS and TTF Statistics
for Advanced Durability Data Sets
(Bomber Load Spectra)

| DATA SET | ITEM | TTGCS STATISTICS (4) | | | | | | | TTF Statistics |
|---|---|---|---|---|---|---|---|---|---|
| | | GIVEN CRACK SIZE $x_1$ | | | | | | | |
| | | .01" | .03" | .05" | .1" | .5" | .75" | 1.0" | |
| MADB | MEAN (FLT. HRS) | 21347 | 23847 | 25328 | 27793 | 35154 | 36423 | 37740 | 36761 |
| | STD. DEV. | 5907 | 4972 | 4619 | 4798 | 4723 | 4428 | 4563 | 4410 |
| | COV | .276 | .209 | .190 | .173 | .134 | .128 | .121 | .117 |
| | MAX. (FLT. HRS) | 28916 | 30299 | 31248 | 32663 | 41924 | 43499 | 44826 | 43564 |
| | MIN. (FLT. HRS) | 11169 | 12291 | 13156 | 15241 | 24047 | 26512 | 28566 | 28051 |
| | NO. SPECIMEN | 12 | | | | | | | |
| MB1 | MEAN (FLT. HRS) | 33606 | 35899 | 37194 | 39445 | 47047 | 48662 | 49825 | 47242 |
| | STD. DEV. | 10101 | 9056 | 8685 | 8191 | 7495 | 7436 | 7511 | 7961 |
| | COV | .301 | .252 | .234 | .208 | .159 | .154 | .151 | .159 |
| | MAX. (FLT. HRS) | 51520 | 52584 | 53718 | 55217 | 59596 | 60667 | 61466 | 59076 |
| | MIN. (FLT. HRS) | 14386 | 23079 | 27158 | 29781 | 37410 | 38341 | 39153 | 36408 |
| | NO. SPECIMEN | 13 | | | | | | | |
| W04FB | MEAN (FLT. HRS) | 22654 | 24662 | 26335 | 29347 | 40517 | 42631 | 43776 | 43418 |
| | STD. DEV. | 5528 | 5363 | 5506 | 5684 | 7646 | 8126 | 8082 | 8194 |
| | COV | .244 | .216 | .209 | .194 | .189 | .191 | .185 | .189 |
| | MAX. (FLT. HRS) | 33822 | 35514 | 37608 | 39990 | 53773 | 55122 | 56302 | 55677 |
| | MIN. (FLT. HRS) | 15298 | 16698 | 17107 | 18130 | 26516 | 26119 | 27758 | 27930 |
| | NO. SPECIMEN | 15 | | | | | | | |
| MADB4RM | MEAN (FLT. HRS) | 3039 | 4802 | 5960 | 7940 | 10117 | 15246 | 16133 | 14614 |
| | STD. DEV. | 1167 | 1538 | 1670 | 1997 | 2635 | 2811 | 2942 | 2648 |
| | COV | .384 | .320 | .279 | .252 | .186 | .184 | .182 | .179 |
| | MAX. (FLT. HRS) | 5359 | 7580 | 9236 | 12475 | 19492 | 20863 | 22415 | 19815 |
| | MIN. (FLT. HRS) | 1425 | 2814 | 3764 | 5055 | 9550 | 10369 | 11956 | 11466 |
| | NO. SPECIMEN | 15 | | | | | | | |

NOTES:

(1) **Data sets described in Section II**

(2) 7475-T7351 Aluminum.

(3) Ref. AFWAL-TR-86-3017, Vol. III (Fractographic Test Data)

(4) Fractographic results were extrapolated (where necessary) to obtain TTCI Values for the selected ref. crack size, $a_0$. Such extrapolations were made without considering the time-to-failure (TTF) limitations.

(5) Some TTCI statistics for larger $a_0$ values are not compatible with the TTF results because of (4).

(6) All specimens tested were used to obtain TTCI statistics but 2 specimens in this data set were not tested to failure due to testing problems.

(7) Statistics not computed for this $a_0$.

(8) Used fractographic results for the largest fatigue crack per specimen.

TABLE H.3 Coefficient of Variation (COV) Comparisons for Fighter and Bomber Data Sets.

| DATA SET | NO. SPECIMENS | COEFFICIENT OF VARIATION (COV) | | | | FASTENER HOLE | $\sigma$ (ksi) | % LT |
|---|---|---|---|---|---|---|---|---|
| | | TTU | | | TTF | | | |
| | | $x_1 = .05"$ | $x_1 = .1"$ | $x_1 = .5"$ | | | | |
| WWPF | 13 | .163 | .146 | .125 | .123 | SB | 34 | 0 |
| WWPB | 12 | .190 | .173 | .134 | .117 | SB | 34 | 0 |
| WFI | 15 | .269 | .235 | .235 | .211 | CSK | 34 | 0 |
| WBI | 13 | .234 | .208 | .159 | .159 | CSK | 36 | 0 |
| WAFXHR4 | 14 | .452 | .347 | .277 | .276 | CSK | 40.8 | 15 |
| WABXHR4 | 15 | .279 | .252 | .186 | .179 | CSK | 40.8 | 15 |

well as COVs based on the time-to-failure (TTF). These results were obtained from Tables H.1 and H.2.

In Table H.3 it is interesting to note that (1) the COVs are very consistent for comparable fighter and bomber data sets for the same fastener hole type, (2) the COV values, based on TTGCS, decrease as $x_1$ increases, (3) as $x_1$ increases, the resulting COV values approach the COV values based on TTF, (4) COVs are smaller for straight-bore fastener holes than for countersunk fastener holes, (5) COVs are larger for 15% bolt load transfer specimens than for no load transfer type specimens, and (6) larger differences in the COVs are observed for the 15% bolt load transfer specimens for fighter and bomber data sets than for comparable no load transfer type specimens.

# APPENDIX I

## EVALUATION OF DETERMINISTIC AND STOCHASTIC-BASED
## EIFSs FOR STRAIGHT-BORE FASTENER HOLES

The purpose of this section is to (1) demonstrate three variations of a deterministic crack growth method and one stochastic crack growth method for determining EIFSs, (2) compute deterministic and stochastic-based EIFSs and EIFS statistics for a selected straight-bore hole fractographic data set, and (3) compare and discuss the EIFS results.

The investigation was conducted as follows: Fractographic results for the "WPF" data set from the "Fastener Hole Quality" (FHQ) program [3] was used to determine the deterministic and stochastic-based EIFSs. The WPF data set is described in Table F.1 and specimen details are shown in Fig. 4. Clearance-fit bolts (i.e., NAS 6204-08) were installed in the fastener hole of each specimen.

Methods for determining deterministic and/or stochastic-based EIFSs are given in Appendix E of Volume I [1]. Three methods for determining deterministic-based EIFSs are described in Fig. I.1. The method used to determine the stochastic-based EIFSs is conceptually described in Fig. I.2. Essential equations for computing EIFS, denoted by a(0), are summarized in the following.

Expressions for three different method variations for determining a deterministic-based EIFS for a given fatigue crack are given in Eqs. I-1 through I-3. The following notations are used: $a_j(0)$ = EIFS for the jth fatigue crack in a fractographic data set, $a_j(t_k)$ = kth crack size for the jth fatigue crack at service time $t_k$ in the AL-AU crack size range, Q = "pooled Q" or $Q_i$ value for the ith fractographic data set (see Eq. 6), $a_0$ = reference crack size for TTCIs, $\mathcal{T}$ = service time to reach crack size $a_0$, $X_k = t_k$, $Y_k = \ln a_j(t_k)$

● - Fractographic data point (a(t),t)
for a given fatigue crack
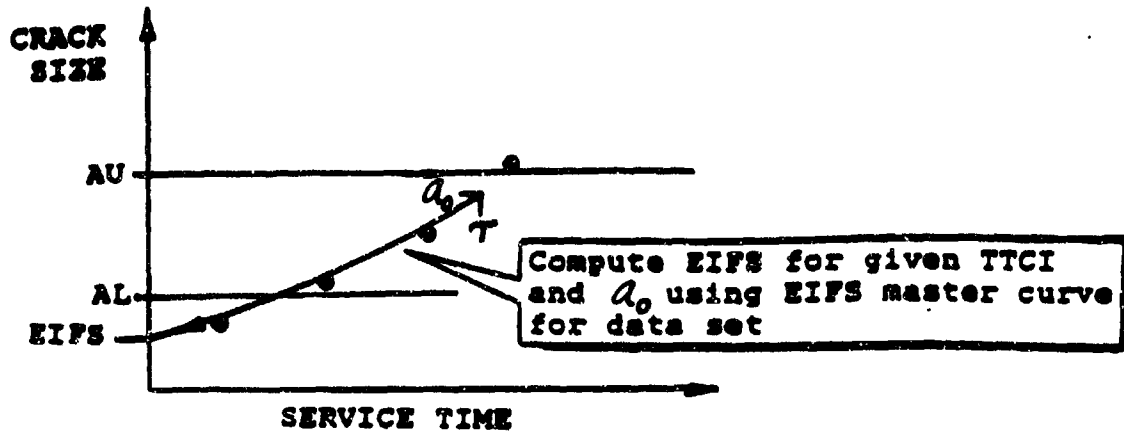


(c) Method 3 (TTCI at given $a_0$ )
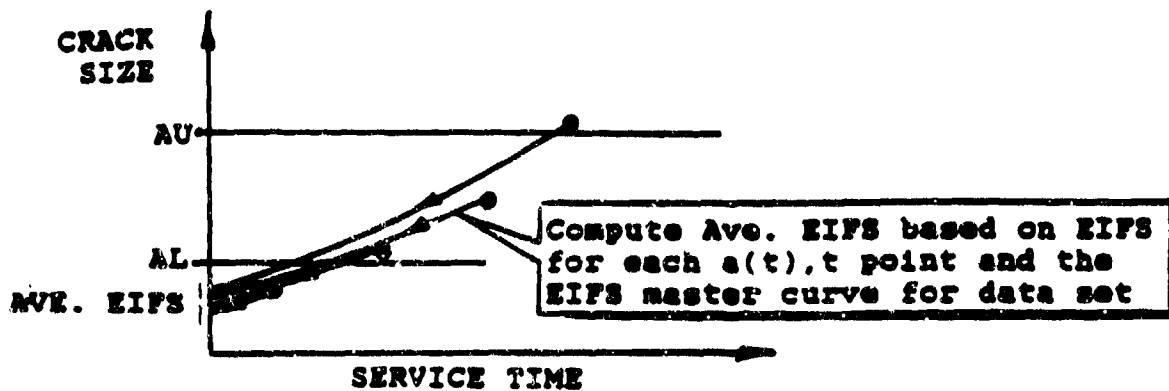


(b) Method 2 (Average EIFSs)
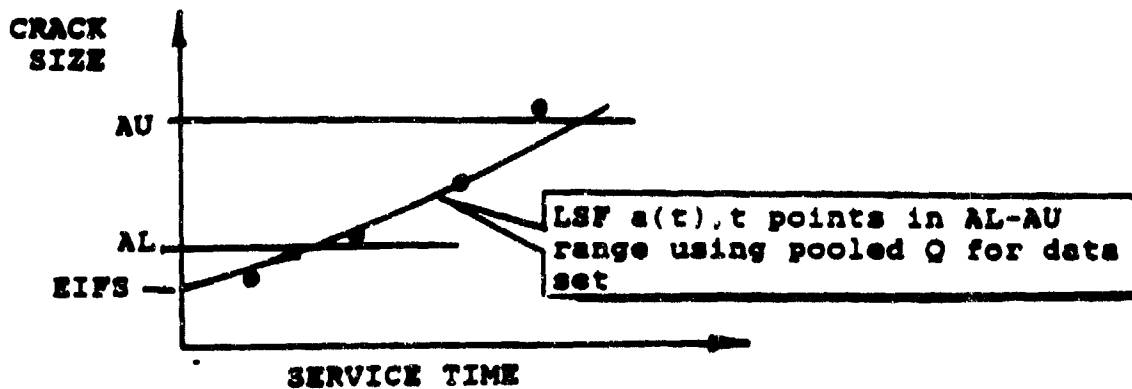


(a) Method 1 (Least Squares Fit)

Figure I.1. Different Methods for Computing
Deterministic-Based EIFSs.

I-2

● - Fractographic data for fatigue crack #1
▲ - Fractographic data for fatigue crack #2

Least squares fit individual fatigue crack

$$a(0) = a(t)\exp(-Q_f t)$$

CRACK SIZE

AU

AL

$a_2(0)$

$a_1(0)$

$a(0) = EIFS$

SERVICE TIME
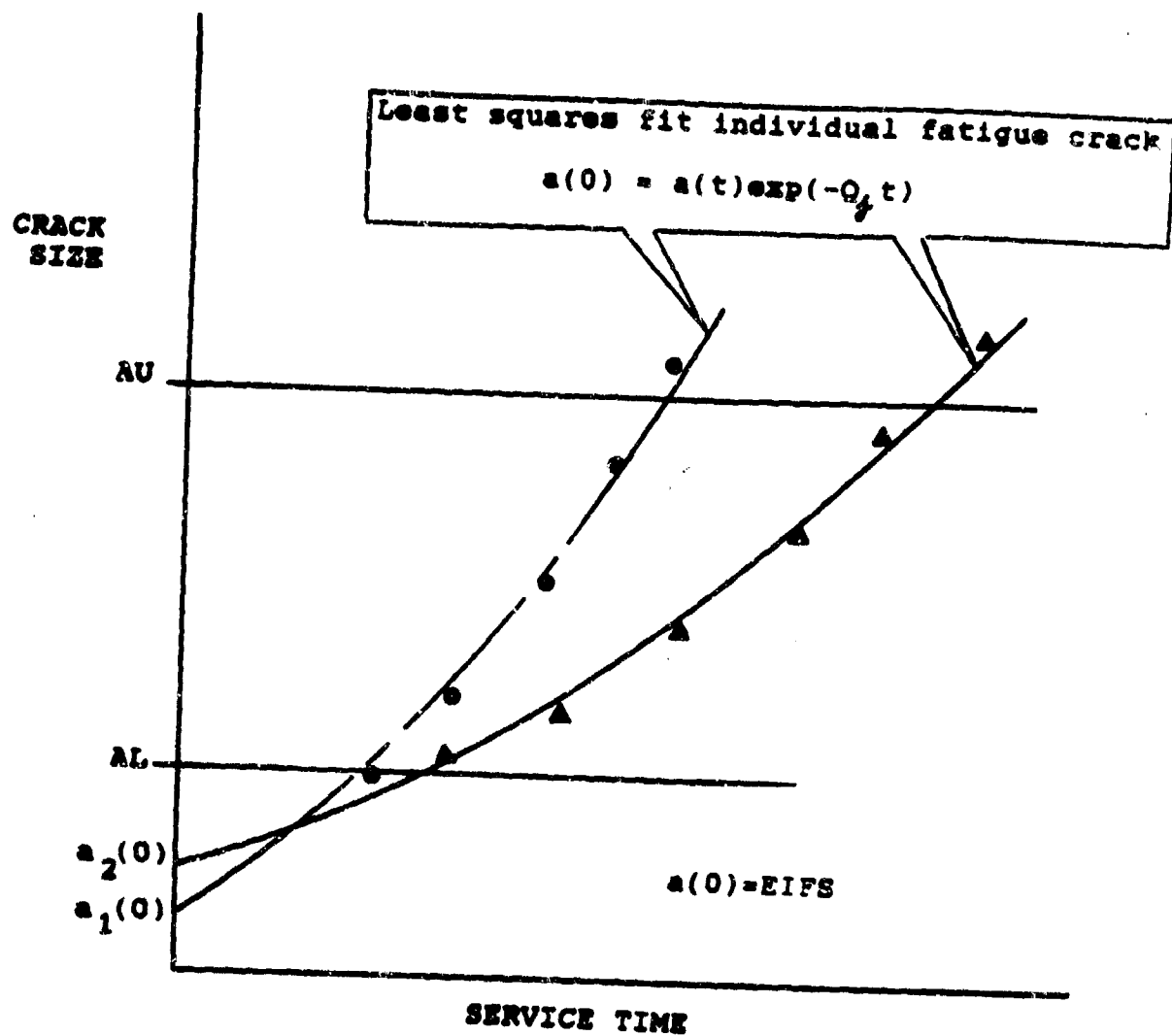
Figure I.2.   Method for Computing Stochastic-Based EIFSs.

and $N_j$ = number of pairs $[a_j(t_k), t_k]$ in the AL-AU range. These notations are slightly different than those used in the original derivation in Volume I [1]. Notations were changed herein to further clarify the terms used and to be consistent with the notations reflected in the durability design handbook [21].

## Method 1  (Least Squares Fit)

$$a_j(0) = EIFS = \exp\left\{ \frac{\sum_{k=1}^{N_j} Y_k - Q \sum_{k=1}^{N_j} X_k}{N_j} \right\} \qquad (I-1)$$

## Method 2  (Average EIFS)

$$a_j(0) = EIFS = \frac{1}{N_j} \sum_{k=1}^{N_j} a_j(t_k) \exp(-Q t_k) \qquad (I-2)$$

## Method 3  (TTCI at Given $a_0$)

$$a_j(0) = EIFS = a_0 \exp(-Q \mathcal{T}) \qquad (I-3)$$

## Stochastic-Based EIFS Method

An expression for determining stochastic-based EIFS is given in Eq. I-4 [1].

$$a_j(0) = EIFS = \exp\left\{ \frac{\sum_{k=1}^{N_j} Y_k - Q_j \sum_{k=1}^{N_j} X_k}{N_j} \right\} \qquad (I-4)$$

All terms in Eq. I-4 are the same as those defined in Eq. I-1 except $Q_j$ = crack growth rate parameter for the jth fatigue crack (see Eq. 5).

EIFS and EIFS statistics (mean, standard deviation and coefficient of variation) were determined for both the deterministic and stochastic crack growth approaches using the WPF data set (uncensored). Results are summarized in Table I.1. The deterministic-based EIFSs were determined using Eqs. I-1 through I-3. A "pooled Q" value of $2.379 \times 10^{-4}$ for the data set, based on Eq. F-5 and the modified secant method [27], was obtained using fractographic results in the AL-AU = 0.01" through 0.05" crack size region. The stochastic-based EIFSs were determined using Eq. I-4.

Fractographic results for 33 fatigue cracks were utilized for this investigation. EIFSs are ranked in descen      rder for the deterministic and stochastic approaches in Table I.1. Results are presented in a form for making direct comparisons. Similar EIFS studies have been reported for both straight-bore and counterbore fastener hole data sets [13-15].

The following conclusions are based on the results of Table I.1 and the experience gained during the course of this program.

1.    Either Method 1, 2, or 3 can be used to determine deterministic-based EIFSs. However, Method 3 (i.e., TTCI for given time) is recommended for durability analysis because it is simpler, more convenient to implement and has comparable accuracy (except COV is slightly higher than for Methods 1 and 2) with the other two methods.

**TABLE I.1.** Comparison of Deterministic and Stochastic Based EIFSs and Statistics for WPF Data Set.

| I | I/(N+1) | DETERMINISTIC-BASED EIFSs (IN.) METHOD 1 | METHOD 2 | METHOD 3 | SCGA EIFSs(IN.) |
|---|---------|---------|---------|---------|---------|
| 1 | .029 | .00596 | .00598 | .00655 | .00398 |
| 2 | .059 | .00295 | .00299 | .00389 | .00353 |
| 3 | .088 | .00234 | .00235 | .00206 | .00244 |
| 4 | .118 | .00223 | .00223 | .00198 | .00241 |
| 5 | .147 | .00199 | .00199 | .00185 | .00189 |
| 6 | .176 | .00179 | .00180 | .00175 | .00187 |
| 7 | .206 | .00164 | .00165 | .00163 | .00182 |
| 8 | .235 | .00125 | .00126 | .00108 | .00147 |
| 9 | .265 | .00123 | .00124 | .00107 | .00139 |
| 10 | .294 | .00118 | .00119 | .00106 | .00133 |
| 11 | .324 | .00113 | .00113 | .00104 | .00109 |
| 12 | .353 | .00107 | .00107 | .00104 | .00105 |
| 13 | .382 | .00103 | .00103 | .00101 | .00105 |
| 14 | .412 | .00102 | .00102 | .000985 | .00103 |
| 15 | .441 | .00100 | .00100 | .000958 | .00102 |
| 16 | .470 | .000997 | .000997 | .000954 | .00100 |
| 17 | .500 | .000994 | .000997 | .000908 | .000962 |
| 18 | .529 | .000975 | .000975 | .000889 | .000946 |
| 19 | .559 | .000974 | .000975 | .000866 | .000713 |
| 20 | .588 | .000751 | .000751 | .000751 | .000656 |
| 21 | .618 | .000743 | .000743 | .000744 | .000628 |
| 22 | .647 | .000639 | .000641 | .000732 | .000624 |
| 23 | .676 | .000633 | .000633 | .000653 | .000582 |
| 24 | .706 | .000629 | .000629 | .000649 | .000534 |
| 25 | .735 | .000558 | .000559 | .000455 | .000523 |
| 26 | .765 | .000509 | .000509 | .000439 | .000494 |
| 27 | .794 | .000501 | .000501 | .000418 | .000486 |
| 28 | .824 | .000493 | .000494 | .000389 | .000483 |
| 29 | .853 | .000448 | .000448 | .000387 | .000459 |
| 30 | .882 | .000434 | .000434 | .000349 | .000387 |
| 31 | .912 | .000374 | .000374 | .000335 | .000385 |
| 32 | .941 | .000356 | .000356 | .000330 | .000?? |
| 33 | .970 | .000293 | .000293 | .000259 | .000218 |
| Mean EIFS | | .00119 | .00119 | .00117 | .00115 |
| Std. Dev. EIFS | | .00106 | .00107 | .00119 | .000889 |
| COV EIFS | | .897 | .899 | 1.029 | .776 |

2.    The stochastic-based EIFSs had a slightly smaller
mean, standard deviation and COV than the comparable  results
for the deterministic-based EIFS.


3.    As a result of extensive investigations conducted
[12-15,17,42], the deterministic-based EIFS is recommended
for durability analysis.

# DEMONSTRATION OF PROBABILISTIC-BASED DURABILITY ANALYSIS METHOD FOR METALLIC AIRFRAMES

J. N. Yang[1], S. D Manning[2], A. Akbarpour[1], M. E. Artley[3]

## Abstract

A probabilistic-based durability analysis method for metallic airframes is demonstrated for clearance-fit countersunk fastener holes in 7475-T7351 aluminum. This method can be used to analytically predict the probability of functional impairment due to excessive cracking, fuel leaks or ligament breakage. The method accounts for the initial fatigue quality variation, crack growth damage accumulation in a population of structural details (e.g., fastener holes, lugs, fillets, cutouts, etc.), load spectra and material properties. The extent of damage (i.e., the number of structural details exceeding specified crack sizes) can be quantitatively estimated at any service time. Also, the cumulative distribution of service time at any crack size can be predicted. The probability of functional impairment is obtained by growing the equivalent initial flaw size distribution (EIFSD) forward to any service time using two different crack growth approaches. Both approaches, referred to as: (1) the "deterministic-deterministic crack growth approach" (DCGA-DCGA) and (2) the "deterministic-stochastic crack growth approach" (DCGA-SCGA), respectively, are evaluated and compared. Analytical predictions are compared with experimental results for dog-bone specimens and for a fighter lower wing skin. Good correlations are obtained using both crack growth approaches. However, the DCGA-SCGA was found to be more accurate and slightly more conservative than the DCGA-DCGA.

## Introduction

The fatigue crack growth accumulation in structural details (e.g., fastener holes, fillets, cutouts, etc.) affects structural integrity, reliability and maintainability requirements for metallic airframes. The U. S. Air Force has damage tolerance design specifications for ensuring structural safety [1-4], and durability design specifications [1,2,4] for minimizing functional impairment problems, such as excessive cracking (e.g., cracks < 2.54 mm), fuel leaks, and ligament breakage (e.g., cracks 12.7 mm - 19.0 mm). This paper is concerned with the structural durability problem which affects structural maintenance requirements, aircraft performance, and operational readiness.

Airframe manufacturers need effective analytical tools for ensuring structural safety and durability with a high degree of confidence. To effectively utilize existing aircraft fleets and limited resources (e.g., budget, manpower and facilities), the U. S. Air Force requires longer aircraft life, higher reliability, minimum maintenance requirements and an increased operational readiness. Hence, it is extremely important that effective analytical tools be used to accurately assess the expected extent of damage in a durability-critical aircraft component at any service time so that the liability and risks associated with a "structural warranty" can be quantified. The probabilistic-based durability analysis method described in this paper provides a powerful and comprehensive tool for quantitatively estimating the crack growth damage accumulation for a population of structural details.

A probabilistic-based durability analysis methodology has been developed and verified for full-scale aircraft structure for relatively small cracks (e.g., smaller than 2.54 mm) in fastener holes where excessive cracking is the issue [5-10]. This methodology has recently been extended to the large crack size region where functional impairment due to fuel leaks and ligament breakage are concerns [11-13]. Two different two-segment crack growth approaches have been developed for performing durability analysis in both the small and large crack size regions [11,12]. The two crack growth approaches are referred to as: (1) the "two-segment deterministic crack growth approach" or DCGA-DCGA and (2) the "two-segment deterministic-stochastic crack growth approach" or DCGA-SCGA.

Various deterministic and stochastic crack growth approaches have been developed for predicting the crack growth damage accumulation in a population of structural details [12]. These approaches have been evaluated for both small and large fatigue

1. School of Engineering and Applied Sciences, The George Washington University, Washington, D.C. 20052, Member AIAA.
2. General Dynamics, Fort Worth Division, P. O. Box 748, Fort Worth, TX 76101.
3. Air Force Wright Aeronautical Laboratories, Flight Dynamics Laboratory, AFWAL/FIBE, Wright-Patterson Air Force Base, OH 45433.

cracks in clearance-fit straight-bore and countersunk fastener holes in 7475-T7351 aluminum [13]. The one-segment deterministic crack growth approach (DCGA) and/or the one-segment stochastic crack growth approach (SCGA) have been previously evaluated using dog-bone specimens with clearance-fit fasteners [10].

The purpose of this paper is to compare, evaluate and demonstrate two different two-segment crack growth approaches for predicting statistically the extent of cracking in a durability-critical component associated with fuel leaks and ligament breakage (e.g., crack size 12.7 mm to 19.0 mm). Both approaches (i.e., DCGA-DCGA and DCGA-SCGA) are demonstrated using fractographic results for dog-bone specimens and for full-scale lower wing skins from a fighter aircraft. The demonstration is conducted using fractographic results for fatigue cracking in 7475-T7351 aluminum containing countersunk fastener holes and clearance fit fasteners. Good correlations are obtained between the analytical predictions and experimental results for both of the two-segment crack growth approaches in the large crack size region. However, based on the results presented the DCGA-SCGA is superior to the DCGA-DCGA.

## Technical Approach

### Initial Fatigue Quality

The initial fatigue quality (IFQ) defines the initially manufactured state of a structural detail or details with respect to initial flaws in a part, component, or airframe prior to service. The IFQ for a group of replicate details (e.g., fastener holes) is represented by an equivalent initial flaw size (EIFS) distribution. An equivalent initial flaw is an artificial initial crack size which results in an actual crack size at an actual point in time when the initial flaw is grown forward.

The Weibull compatible distribution function proposed by Yang and Manning [14, 15] has been found to be reasonable for representing the EIFS cumulative distribution [5-15]

$$F_{a(0)}(x) = \exp\left\{ -\left[ \frac{\ln(x_u/x)}{\phi} \right]^{\alpha} \right\} ; \quad 0 \le x \le x_u \quad (1)$$

$$= 1.0 \qquad ; \quad x > x_u$$

in which $x_u$ = EIFS upper bound limit; $\alpha$ and $\phi$ are empirical parameters.

An EIFS value for a fastener hole is determined by back-extrapolating fractographic data in a selected crack size range (AL-AU) using a simple but versatile deterministic crack growth rate model recommended by Yang and Manning [14,15],

$$da(t)/dt = Q[a(t)]^b \qquad (2)$$

where $da(t)/dt$ = crack growth rate, $a(t)$ = crack size at any time t in flight hours, and Q and b are empirical crack growth rate parameters. In this paper, the special case b = 1 is used.

After EIFS values, $a(0)$, are obtained from all available fractographic data, they are fitted by Eq. 1 to determine the EIFS distribution (EIFSD) parameters $x_u$, $\alpha$, and $\phi$. To predict the extent of cracking in service, the initial flaw size, $a(0)$, is grown forward, and the statistical distribution of the crack size $a(t)$ at any service time t can be derived from that of $a(0)$ given by Eq. 1. The EIFSD is grown forward to predict: (1) the probability that a crack in the ith stress region at any service time, $\tau$, will exceed any given crack size, $x_1$, denoted by $p(i,\tau)$, and (2) the cumulative distribution of service time, $F_{T(x_1)}(\tau)$, for a crack in the ith stress region to reach any given crack size $x_1$. $p(i,\tau)$ is referred to as the crack exceedance probability. Two different crack growth approaches are described below and in Fig. 1 for growing the EIFSD forward to predict $p(i,\tau)$ and/or $F_{T(x_1)}(\tau)$.
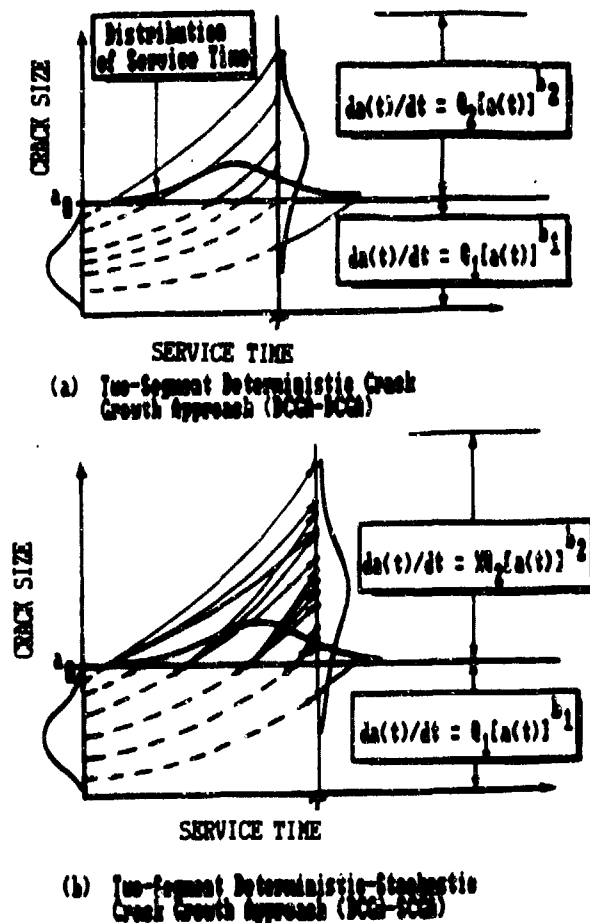


SERVICE TIME

(a) Two-Segment Deterministic Crack Growth Approach (DCGA-DCGA)

SERVICE TIME

(b) Two-Segment Deterministic-Stochastic Crack Growth Approach (DCGA-SCGA)

Fig. 1 Two-Segment Crack Growth Approaches for Durability Analysis

## Two-Segment Deterministic Crack Growth Approach (DCGA-DCGA)

The EIFSD given in Eq. 1 is grown forward using a service crack growth master curve (SCGMC) for a given stress region. To simplify the statistical analysis such a SCGMC can be fitted by an analytical crack growth rate equation. However, in some cases the SCGMC may not be fitted by a single equation, e.g., Eq. 2, with sufficient accuracy. Then, the SCGMC may be separated into two regions; one with the crack size smaller than the reference crack size, $a_0$, at crack initiation, and the other with crack size larger than $a_0$. The SCGMC can be represented in two regions using different crack growth rate equations or the same crack growth rate equation but with different crack growth rate parameters as follows:

$$da(t)/dt = Q_1 \left[a(t)\right]^{b_1} ; \quad a(t)<a_0 \qquad (3)$$

$$da(t)/dt = Q_2 \left[a(t)\right]^{b_2} ; \quad a(t)>a_0 \qquad (4)$$

The probability of crack exceedance, $p(i,\mathcal{T})$, can be derived by growing the initial flaw size distribution given in Eq. 1 using the crack growth rate equations given by Eqs. 3 and 4; with the results [see Refs. 11-12 for detailed derivations]

$$p(i,\tau) = P\left[a(\tau) \geq x_1\right] = 1 - F_{a(\tau)}(x_1) \qquad (5)$$

$$= 1 - F_{a(0)}\left[y(x_1; \tau)\right]$$

in which $F_{a(0)}(x)$ is the distribution function of EIFS given by Eq. 1, $F_{a(\mathcal{T})}(x)$ is the cumulative distribution of the crack size, $a(\mathcal{T})$, at service time $\mathcal{T}$, and $y(x_1; \mathcal{T})$ is defined in Eqs. 6 and 7 for $b_1 = b_2 = 1$

$$y(x_1;\tau) = x_1 \exp(-Q_1\tau); \quad x_1<a_0 \qquad (6)$$

$$y(x_1;\tau) = (x_1)^{Q_1/Q_2} \exp(\Lambda - Q_1\tau); \quad x_1>a_0 \qquad (7)$$

where

$$\Lambda = \left[1 - (Q_1/Q_2)\right] \ln a_0 \qquad (8)$$

Let $T(x_1)$ be the time for a crack to reach any given crack size $x_1$ and $F_{T(x_1)}(\mathcal{T})$ be the corresponding cumulative distribution function, i.e., $F_{T(x_1)}(\mathcal{T}) = P[T(x_1) \leq \mathcal{T}]$. The distribution function of $T(x_1)$ is the probability that the crack will reach a crack size $x_1$ before service time $\mathcal{T}$. Such a probability is equal to the probability that the crack size $a(\mathcal{T})$ at service time $\mathcal{T}$ will exceed $x_1$, which is simply the probability of crack exceedance. Hence,

$$F_{T(x_1)}(\tau) = P\left[T(x_1) \leq \tau\right] \qquad (9)$$

$$= P\left[a(\tau) \geq x_1\right] = p(i,\tau)$$

Consequently, $F_{T(x_1)}(\mathcal{T})$ is obtained for any given crack size $x_1$ by computing the crack exceedance probability, $p(i,\mathcal{T})$, at different values of service time $\mathcal{T}$.

## Deterministic-Stochastic Crack Growth Approach (DCGA-SCGA)

The crack growth damage accumulation is divided into two segments as shown in Fig. 1(b). For crack sizes < $a_0$, a deterministic crack growth rate model, Eq. 3, is used. The following stochastic crack growth rate model is used for crack sizes > $a_0$

$$da(t)/dt = X Q_2 \left[a(t)\right]^{b_2}; \quad a(t)>a_0 \qquad (10)$$

in which X is a lognormal random variable with a median of one; $Q_2$ and $b_2$ are crack growth rate parameters. Equation 10 accounts for the crack growth rate variability and is referred to as the "lognormal random variable model" proposed by Yang et al [16-21].

The probability density function of the lognormal random variable X with a median 1.0 is given by

$$f_X(u) = \frac{\log e}{\sqrt{2\pi}\, u\, \sigma_z} \exp\left\{-\frac{1}{2}\left[\frac{\log u}{\sigma_z}\right]^2\right\}; \quad u \geq 0 \qquad (11)$$

$$= 0 \qquad ; u < 0$$

in which $\sigma_z$ is the standard deviation of the normal random variable $Z = \log X$. Equation 11 is used when $\sigma_z$ is estimated using the log to base 10 form. If $\sigma_z$ is based on the natural log form, $f_X(u)$ given in Eq. 12 should be used.

$$f_X(u) = \frac{1}{\sqrt{2\pi}\, u\, \sigma_z} \exp\left\{-\frac{1}{2}\left[\frac{\ln u}{\sigma_z}\right]^2\right\}; \quad u \geq 0 \qquad (12)$$

$$= 0 \qquad ; u < 0$$

Note that $\sigma_z$ based on the log to base 10 is equal to that based on the natural log divided by the natural log of 10. Details for estimating $\sigma_z$ are given elsewhere [12, 13].

Let T be the time for an EIFS, $a(0)$, to reach the reference crack size $a_0$. Then, integrating Eq. 3 from $t = 0$ to $t = T$ for $b_1 = 1$, one obtains

$$T = Q_1^{-1} \ln\left[a_0/a(0)\right] \qquad (13)$$

in which it is understood that $a(T) = a_0$.

In the region where $a(\tau) > a_0$ (or $\tau > T$), Eq. 10 is integrated with $b_2 = 1$ from $t = T$ to $t = \tau$ (or from $a(T) = a_0$ to $a(t) = a(\tau)$), with the result

$$T = \tau \cdot (XQ_2)^{-1} \ln[a(\tau)/a_0] \; ; \; a(\tau) > a_0 \qquad (14)$$

Equating Eqs. 13 and 14 leads to the following relation between $a(\tau)$ and $a(0)$

$$a(0) = a_0 \exp(-Q_1 \tau)[a(\tau)/a_0]^{\gamma/X} \; ; \; a(\tau) > a_0 \qquad (15)$$

in which

$$\gamma = Q_1/Q_2 \qquad (16)$$

When the crack size, $a(\tau)$, at any service time $\tau$ is smaller than $a_0$, the relation between $a(\tau)$ and $a(0)$ is obtained by integrating Eq. 3 for $b_1 = 1$ from $t = 0$ to $t = \tau$ as follows:

$$a(0) = a(\tau)\exp(-Q_1 \tau) \; ; \; a(\tau) < a_0 \qquad (17)$$

Depending on the crack size of interest $x_1$, the crack exceedance probability, $p(i,\tau)$, can be derived in the following manner.

(1) When the crack size of interest $x_1$ is smaller than the reference crack size $a_0$, the distribution function $F_{a(\tau)}(x_1) = P[a(\tau) \leq x_1]$ of the crack size, $a(\tau)$, for $x_1 < a_0$ can be derived from the distribution function of $a(0)$ through the transformation of Eq. (17),

$$F_{a(\tau)}(x_1) = F_{a(0)}[y(x_1;\tau)] \qquad (18)$$

in which

$$y(x_1;\tau) = x_1 \exp(-Q_1 \tau) \qquad (19)$$

The crack exceedance probability, $p(i,\tau)$, is given by

$$p(i,\tau) = P[a(\tau) > x_1] = 1 - F_{a(\tau)}(x_1)$$
$$= 1 - F_{a(0)}[y(x_1,\tau)] \; ; \; x_1 \leq a_0 \qquad (20)$$

where $F_{a(0)}(x)$ is the distribution function of EIFS, $a(0)$, given by Eq. 1 or other suitable distribution functions.

(2) When the crack size of interest $x_1$ is larger than $a_0$, the conditional distribution function of $a(\tau)$ at any service time $\tau$, given $X=u$, can be derived from that of $a(0)$ through the transformation of Eq. 15. Then, the unconditional distribution function, $F_{a(\tau)}(x_1)$, of $a(\tau)$ can be obtained using the theorem of total probability with the result

$$F_{a(\tau)}(x_1) = \int_0^\infty F_{a(0)}[G(x_1;\tau|X=u)]f_X(u)\,du \qquad (21)$$

in which the lognormal probability density function $f_X(u)$ is given by Eq. 11 or 12 and

$$G(x_1;\tau|X=u) = a_0 \exp(Q_1 \tau) [x_1/a_0]^{\gamma/u} \qquad (22)$$

The crack exceedance probability, $p(i,\tau)$, for $x_1 > a_0$ is given by $p(i,\tau) = 1 - F_{a(\tau)}(x_1)$, i.e.,

$$p(i,\tau) = 1 - \int_0^\infty F_{a(0)}[G(x_1;\tau|X=u)]f_X(u)\,du \qquad (23)$$

When the Weibull compatible distribution, Eq. 1, is used for the EIFS the condition that $F_{a(0)}[G(x_1;\tau|X=u)] = 1$ or $G(x_1;\tau|X=u) > x_u$ should be selected in the computer program for computing the crack exceedance probability $p(i,\tau)$ Eq. 23.

The cumulative distribution of service time, $F_{T(x_1)}(\tau)$, for a crack to reach any given crack size $x_1$ is determined using Eq. 9. $F_{T(x_1)}(\tau)$ is obtained for $x_1 < a_0$ and for $x_1 > a_0$ by computing $p(i,\tau)$ at different service times $\tau$, using Eq. 20 and 23, respectively.

## Durability Analysis Procedures

Durability analysis procedures for implementing the two approaches (Fig. 1) described above and demonstrated elsewhere [12,14,22] are summarized in the following four steps.

(1) Select a reasonable EIFS distribution function, $F_{a(0)}(x)$, to represent the initial fatigue quality (IFQ) (e.g., Eq. 1), and suitable base-line fractographic data sets [e.g., 23,24]. For each base-line fractographic data set determine the EIFS master curve using (i) fractographic results in a selected crack size range AL-AU (e.g., 0.254 mm - 1.27 mm), (ii) the deterministic crack growth rate

model, Eqs. 2 or 3, and (iii) a least-squares fit procedure [12,13]. Select a reference crack size $a_0$ for $AL \leq a_0 \leq AU$ and determine the corresponding TTCI sample values for each data set. Then, for each data set the EIFS sample values are obtained by back-extrapolating the TTCI sample values at $a_0$ to time zero using the corresponding EIFS master curve [12, 13].

(2) Determine the IFQ or EIFSD for structural details in the durability critical components. Estimate/optimize the EIFSD parameters in Eq. 1 using: (i) the EIFS sample values from step (1), (ii) EIFS data pooling/global least squares fit procedures, and (iii) a statistical scaling technique [11-13]. Details of this step are given elsewhere [12,13]. The selected EIFSD is justified by checking the goodness-of-fit of crack exceedance predictions for $x_1 \leq AU$, Eq. 20 with $Q_1 = Q$, for the base-line fractographic data sets.

(3) The service crack growth master curve (SCGMC) in each stress region is determined by either available fractographic results or LEFM crack growth analysis. In the latter case, the LEFM crack growth computer program is "tuned" or "curve-fitted" to the EIFS master curve in the AL-AU crack size region where base-line fractographic data are available. Normal assumptions for the crack shape and geometry are reflected in the crack growth analysis. Then the SCGMC is fitted by Eqs. 3 and 4 for the DCGA-DCGA and by Eqs. 3 and 10 for the DCGA-SCGA using a least squares fit procedure [12, 13]. Equation 3 is used to obtain $Q_1$ for $a(t) < a_0$. For $a(t) > a_0$ Eq. 4 and 10 are used to estimate $Q_2$ for the DCGA-DCGA and the DCGA-SCGA, respectively. The standard deviation $\sigma_z$ in Eqs. 11 or 12 can be estimated using available fractographic data or based on past experience [12,13].

(4) The probability of crack exceedance, $p(i,T)$, at any service time, $T$, for each stress region, $i$, can be determined for the DCGA-DCGA and the DCGA-SCGA using Eqs. 5-8 and Eqs. 20-23, respectively. Then the statistics for the number of fastener holes that will have a crack size larger than $x_1$ in the entire durability critical component can be computed using the Binomial distribution [5,6,13].

The cumulative distribution of service time, $F_{T(x_1)}(T)$, to reach any given crack size, $x_1$, can be obtained using Eq. 9 and the applicable $p(i,T)$ expressions for the DCGA-DCGA and DCGA-SCGA, respectively.

Theoretical/Experimental Correlations

Theoretical and experimental correla-

tions for the DCGA-DCGA and the DCGA-SCGA were conducted for clearance-fit countersunk fasteners for both coupon specimens and full-scale lower wing skins from a fighter aircraft. There are several facets to the investigation conducted. Because of space limitations a brief description of the investigation and the pertinent results obtained are described in the following. Details are given elsewhere [12,13].

The initial fatigue quality of clearance-fit countersunk fasteners (MS 90353-08) in 7475-T7351 aluminum was determined using fractographic results for 38.1 mm wide double-reversed dog-bone specimens with a 15% bolt load transfer design (Fig. 2) tested under spectrum loading. Three
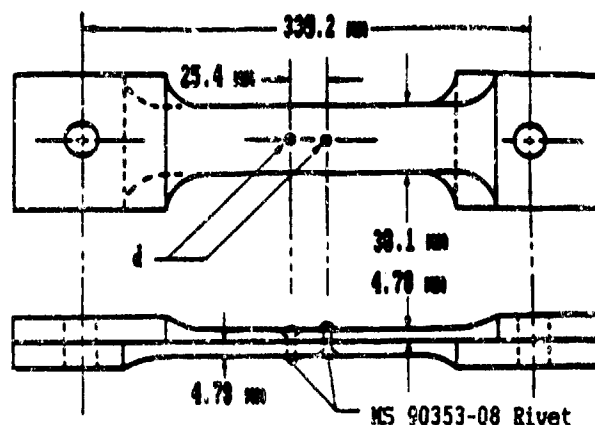
Fig. 2 Double Reversed Dog-Bone Specimen with 38.1 mm Width and 15% Load Transfer

different fractographic data sets (i.e., AFXLR4, AFXMR4 and AFXHR4) [23] were used to estimate the EIFSD parameters for the Weibull compatible distribution function given in Eq. 1. A statistical scaling technique and a data pooling procedure [12,13] were used to estimate the EIFSD parameters in a global sense. The resulting EIFSD parameters are summarized in Table 1, including the crack growth parameter $Q$ for each of the three data sets, Eq. 2.

The EIFSD defined by Eq. 1 and the parameters in Table 1 were then used to make $p(i,T)$ predictions for 76.2 mm wide double-reversed dog-bone specimens (Fig. 3) and for the full-scale lower wing skins of a fighter using both crack growth approaches (Fig. 1). Predictions for $F_{T(x_1)}(T)$ were also made for the 76.2 mm wide dog-bone specimens (Fig. 3). Analytical predictions and experimental correlations for coupon specimens and lower wing skin are described and discussed in the following.

| DATA SETS (1) | NO. SPEC. | $\sigma$ (MPa) | % BOLT LT | $\ell$ (2) | $x_u$ (mm) | $\alpha$ | $\phi$ | $Q \times 10^4$ (1/HR) (3) |
|---|---|---|---|---|---|---|---|---|
| AFXLR4 | 10 | 220.8 | 15 | 4 | .762 | 1.716 | 6.308 | 2.101 |
| AFXMR4 | 9 | 234.4 | | | | | | 2.514 |
| AFXHR4 | 10 | 261.9 | | | | | | 6.062 |

Notes:  (1)  Specimen details shown in Fig. 2
        (2)  Statistical scaling factor [13]
        (3)  Fractographic crack size range used:
             AL-AU = .254 mm - 1.27 mm

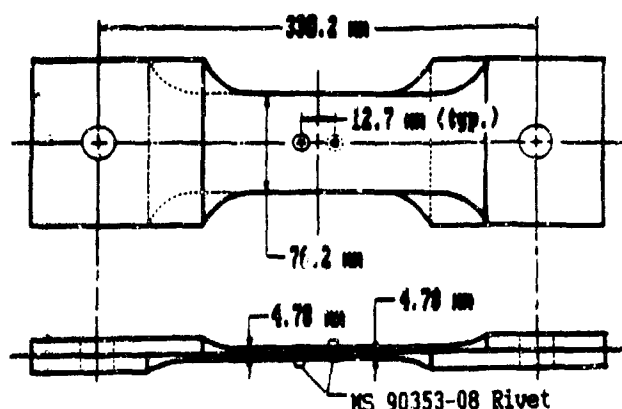

Fig. 3  Double Reversed Dog-Bone Specimen with 76.2 mm Width and 15% Bolt Load Transfer

## Coupon Specimens

Fractographic results were available for 76.2 mm wide double reversed dog-bone specimen (Fig. 3) fatigue tested to failure under a fighter load spectrum [24]. Two fractographic data sets (i.e. WAFXMR4 and WAFXHR4) were used. Except for the width, these specimens are identical to the 38.1 mm wide specimens shown in Fig. 2. Crack growth parameters $Q_1$ and $Q_2$ for two segments of crack growth (i.e., AL-AU = .254 mm - 1.27 mm and 1.27 mm - 12.7 mm) were determined using fractographic results. The standard deviation, $\sigma_z$, was

also determined for segment 2 (i.e., AL-AU = 1.27 mm - 12.7 mm) for implementing the DCGA-SCGA. Parameter results are summarized in Table 2. If applicable fractographic results are not available, $Q_1$ and $Q_2$ can be determined from the SCGMC based on a suitable analytical crack growth computer program.

Analytical predictions for the probability of crack exceedance, $p(i, \mathcal{T})$, for both crack growth approaches (Fig. 1) are correlated with experimental test results for the WAFXMR4 and WAFXHR4 data sets in Figs. 4 and 5, respectively. Predicted
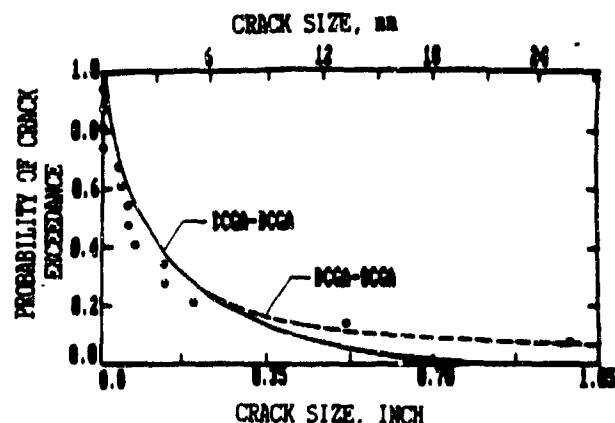


Fig. 4  Correlations Between Theoretical Predictions and Experimental Results (WAFXMR4 Data Set) for Crack Exceedance Probability $p(i, \mathcal{T})$ at $\mathcal{T} = 11606$ Flight Hours

Table 2  Summary of Crack Growth Parameters for Double Reversed Dog-Bone Specimen Data Sets with 76.2 mm Width and 15% Bolt Load Transfer

| DATA SET (1) | NO. SPEC. | $\sigma$ (MPa) | % BOLT LT | (2) $Q_1 \times 10^4$ (1/HR) | (3) $Q_2 \times 10^4$ (1/HR) | (4) $\sigma_z$ |
|---|---|---|---|---|---|---|
| WAFXMR4 | 14 | 234.4 | 15 | 2.851 | 2.908 | .449 |
| WAFXHR4 | 12 | 261.3 | 15 | 9.126 | 3.854 | .322 |

Notes:  (1)  Specimen details shown in Fig. 3
        (2)  AL-AU = .2564 mm - 1.27 mm
        (3)  AL-AU = 1.27 mm - 12.7 mm
        (4)  Natural log basis
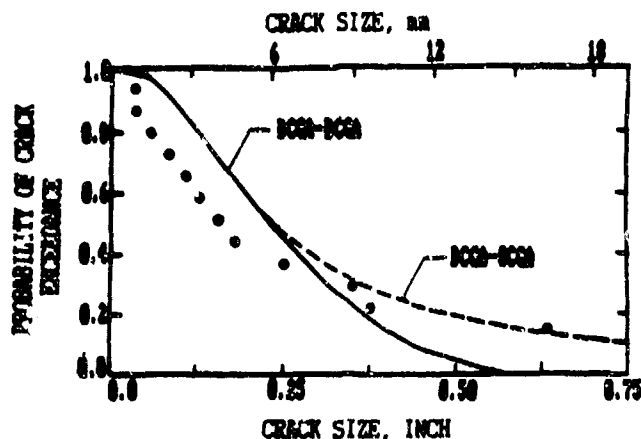
Fig. 5 Correlations Between Theoretical Predictions and Experimental Results (WAFXMR4 Data Set) for Crack Exceedance Probability $p(i,\mathcal{T})$ at $\mathcal{T}$ = 7000 Flight Hours

crack exceedance probabilities at $\mathcal{T}$ = 11408 flight hours are shown in Fig. 4; whereas those at $\mathcal{T}$ = 7000 flight hours are presented in Fig 5. Results for the DCGA-DCGA are shown as a solid curve; whereas results for the DCGA-SCGA are shown as a dashed curve. Both crack growth approaches give the same results for crack sizes $\leq a_0$ (1.27 mm). Experimental results are shown as solid circles.

Theoretical predictions for the distribution of service time to reach any given crack size $x_1$, $F_{T(x_1)}(\mathcal{T})$, for both crack growth approaches (Fig. 1) are correlated with experimental test results for the WAFXMR4 and the WAFXHR4 data sets in Figs. 6 and 7, respectively. The results shown in Fig. 6 are for a crack size of $x_1$ = 18.54 mm and those in Fig. 7 are for $x_1$ = 14.99 mm. Predictions for the DCGA-DCGA and the DCGA-SCGA are displayed as solid



Fig. 6 Correlations Between Theoretical Predictions and Experimental Results (WAFXMR4 Data Set) for Cumulative Distribution of Service Time to Reach Crack Size $x_1$ = 18.54 mm
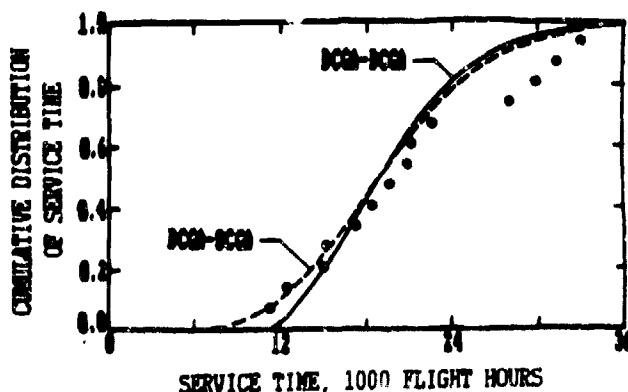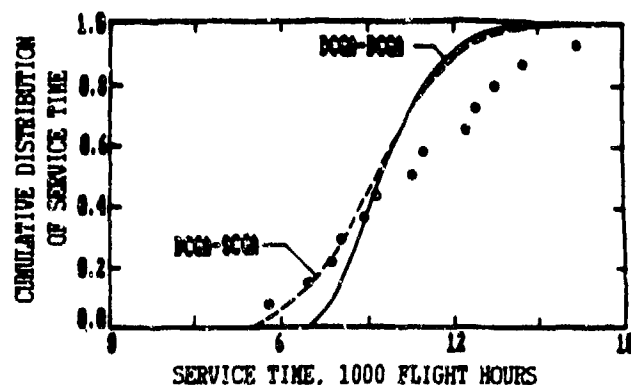


Fig. 7 Correlations Between Theoretical Predictions and Experimental Results (WAFXHR4 Data Set) for Cumulative Distribution of Service Time to Reach Crack Size $x_1$ = 14.99 mm

and dashed curves, respectively; whereas solid circles denote the experimental results.

From Figs. 4-7 it is observed that better overall correlations are obtained for the DCGA-SCGA than those for the DCGA-DCGA. Also, in the large crack size region (upper tail of Figs. 4 and 5) or the early service time (lower tail of Figs. 6 and 7), the DCGA-SCGA predictions are more accurate and conservative than those based on the DCGA-DCGA.

Lower Wing Skins

Fractographic results are available for the lower wing skins from a fighter durability test article [e.g., 25] that was fatigue tested under spectrum loading to 16000 flight hours. The wing skins are 7475-T7351 aluminum and include countersunk fasteners (i.e, MS 90353-08 blind pull-through rivets) of the same type used in the test specimens of Figs. 2 and 3. The durability analysis demonstration was conducted as follows:

1. The EIFSD parameters obtained previously for countersunk fastener holes were used for the fighter fastener holes, i.e., $x_u$ = .762 mm, $\alpha$ = 1.716 and $\phi$ = 6.308. These EIFSD parameters, representing the IFQ, were determined from three narrow width specimen data sets, i.e., AFXLR4, AFXMR4 and AFXHR4.

2. The lower wing skin was divided into ten stress regions as shown in Fig. 8. The maximum stress level, $\sigma_1$, and the number of fastener holes, $N_j$, in each stress region are shown in Table 3. Service crack growth rate parameters $Q_1$ and $Q_2$ for each stress region in the small and large crack size regions were estimated using five fractographic data sets available and a crack growth model proposed by Yang and Manning [5,12-14].

$$Q_i = \xi \sigma_i^\psi \qquad (24)$$

In Eq. 24, $Q_i$ = service crack growth parameter for the ith stress region, $\sigma_i$ = maximum stress level in the ith stress region; $\xi$ and $\psi$ are empirical constants determined from available base-line data or suitable analytical crack growth results. Fractographic results for three narrow width specimen data sets (i.e., AFXLR4, AFXMR4 and AFXHR4) and two 76.2 mm wide specimen data sets (i,e,, WAFXMR4 and WAFXHR4) were used in Eq. 24 to determine $\xi$ and $\psi$; with the following results: $\xi = 2.2274 \times 10^{-19}$ and $\psi = 6.3744$ for $x_1 < a_0$; $\xi = 6.2883 \times 10^{-8}$ and $\psi = 1.5463$ for $x_1 > a_0$. Parameter values for $\xi$ and $\psi$ reflect $\sigma_i$ in MPa units. Once $\xi$ and $\psi$ are determined from these base-line fractographic data, the crack growth rate parameter $Q_i$ in each of the ten stress regions with a maximum stress level of $\sigma_i$ is computed from Eq. 24. The resulting crack growth rate parameters $Q_1$ and $Q_2$ in the small and large crack size regions for each of the ten stress regions are presented in Table 3.

3. Typical predictions for crack exceedance probability, $p(i,\mathcal{T})$, in each of the ten stress regions at $\mathcal{T} = 16000$ flight hours for five different crack sizes (i.e., $x_1 = .762$ mm, 1.27 mm, 2.54 mm, 7.62 mm and 12.7 mm) are shown only for the DCGA-SCGA in Table 4, due to space limitations. Analysis details and results for both crack growth approaches, Fig. 1, are given elsewhere [13]. The analysis for the DCGA-SCGA was conducted using $\sigma_z = .3$ (natural log basis), which is reasonable for countersunk fastener holes in 7475-T7351 aluminum [13]. The average number of fastener holes, $\bar{N}(i,\mathcal{T})$, with a crack size > $x_1$ at $\mathcal{T} = 16000$ flight hours

are predicted and shown in Table 4 for each of the ten stress regions. Further, predictions for the average number of fastener holes in the lower wing skin with a crack size > $x_1$ at 16000 flight hours, $\bar{L}(\mathcal{T})$, and its standard deviation, $\sigma_L(\mathcal{T})$, are shown in Table 5 for the DCGA-SCGA. $\bar{L}(\mathcal{T})$ and $\sigma_L(\mathcal{T})$ values are computed based on the Binomial distribution [12,13], as given by Eqs. 25 and 26.

$$\bar{L}(\tau) = \sum_{i=1}^{10} \bar{N}(i,\tau) \qquad (25)$$

$$\sigma_L(\tau) = \left\{ \sum_{i=1}^{10} N_i \, p(i,\tau) \left[ 1 - p(i,\tau) \right] \right\}^{1/2} \qquad (26)$$

Using $\bar{L}(\mathcal{T})$ and $\sigma_L(\mathcal{T})$, the extent of damage for the lower wing skin can be estimated for selected probabilities. Such results can be used to determine the mean and upper/lower bound limits for the extent of damage.
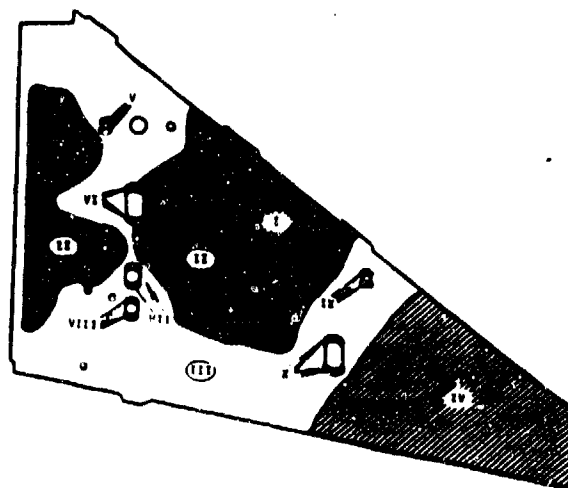


Fig. 8    Stress Regions for Fighter Lower Wing Skin

Table 3    Stress Levels, Number of Fastener Holes and Crack Growth Rate Parameters for Fighter Lower Wing Skin

| STRESS REGION | MAX. STRESS $\sigma_i$(MPa) | NO. HOLES $N_i$ | CRACK GROWTH PARAMETERS | |
|---|---|---|---|---|
| | | | $Q_1 \times 10^4$ (1/HR.) | $Q_2 \times 10^4$ (1/HR.) |
| 1 | 195.1 | 59 | .384 | 2.187 |
| 2 | 186.1 | 320 | .655 | 2.033 |
| 3 | 167.5 | 680 | .334 | 1.727 |
| 4 | 115.1 | 469 | .031 | .967 |
| 5 | 195.8 | 8 | .904 | 2.199 |
| 6 | 201.3 | 30 | 1.080 | 2.296 |
| 7 | 223.4 | 8 | 2.097 | 2.697 |
| 8 | 190.6 | 8 | .541 | 1.941 |
| 9 | 190.6 | 12 | .541 | 1.941 |
| 10 | 177.2 | 20 | .478 | 1.885 |

Theoretical predictions for the average number of fastener holes, $L(\mathcal{T})$, with a crack size $> x_1$ at $\mathcal{T} = 16000$ flight hours in the entire lower wing skin are plotted in Fig. 9 for both of the two-segment crack growth approaches. In this figure, the results for the DCGA-DCGA and the DCGA-SCGA are depicted by a solid curve and a dashed curve, respectively. Results for both approaches are identical for the crack size $x_1 \leq 1.27$ mm in the first crack growth segment. The tear-down inspection results are shown in Table 5 and Fig. 9 as solid circles for comparison. These results reflect the average extent of damage for a lower wing skin based on the total extent of damage for left and right lower wing skins combined.

It is observed that the durability analysis predictions based on specimen test results correlate well with the tear-down inspections results and that the predictions for the DCGA-SCGA are slightly more conservative than the results for the DCGA-DCGA.

## Conclusions

Two different durability analysis approaches for the large crack size region have been demonstrated and evaluated using fractographic results for both coupon specimens and lower wing skins from a fighter aircraft. Both approaches (i.e., DCGA-DCGA and DCGA-SCGA) were evaluated for fatigue cracking in countersunk fastener holes with clearance-fit fasteners. Similar demonstrations and evaluations for straight-bore fastener hole fractographic data are given elsewhere [11,13]. Both two-segment crack growth approaches are considered reasonable for evaluating functional impairment due to fuel leakage/ligament breakage in metallic aircraft structures. However, the DCGA-SCGA is recommended for durability analysis because predictions are more accurate and slightly more conservative than those based on the DCGA-DCGA.
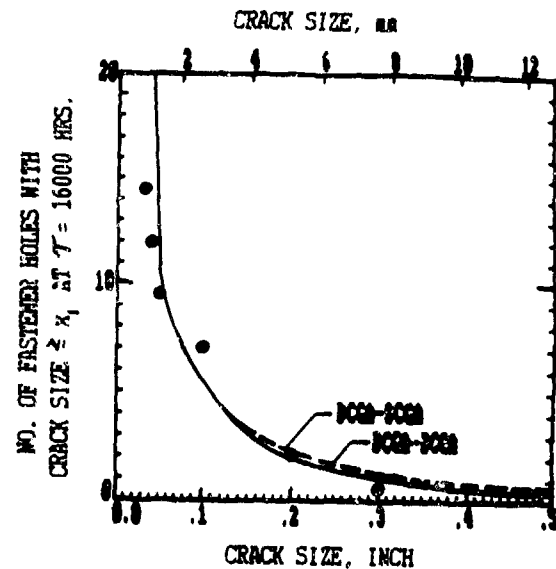
Fig. 9  Correlations Between Theoretical Predictions and Experimental Results for Fighter Lower Wing Skin for Extent of Damage at $\mathcal{T} = 16000$ Flight Hours

Table 5  Statistics for Number of Fastener Holes with Crack Size Exceeding $x_1$ in Fighter Lower Wing Skin [1]

| $x_1$ (mm) | $\bar{L}(\mathcal{T})$ | $\sigma_L(\mathcal{T})$ | EXPERIMENTAL RESULTS (Ave.) |
|---|---|---|---|
| .762 | 35.80 | 5.800 | 14.5 |
| 1.27 | 10.81 | 3.185 | 9.5 |
| 2.54 | 5.38 | 2.262 | 7.0 |
| 5.08 | 2.19 | 1.450 | 1.0 |
| 7.62 | 1.24 | 1.097 | .5 |

Table 4  Crack Exceedance Probability and Average Number of Fastener Holes with Crack Exceeding $x_1$ at $\mathcal{T} = 16000$ Flight Hours in Each Stress Region

| STRESS REGION | $x_1 = .762$ mm | | $x_1 = 1.27$ mm | | $x_1 = 2.54$ mm | | $x_1 = 5.08$ mm | | $x_1 = 7.62$ mm | |
|---|---|---|---|---|---|---|---|---|---|---|
| | $p(1,\mathcal{T})$ | $\bar{N}(1,\mathcal{T})$ | $p(1,\mathcal{T})$ | $\bar{N}(1,\mathcal{T})$ | $p(1,\mathcal{T})$ | $\bar{N}(1,\mathcal{T})$ | $p(1,\mathcal{T})$ | $\bar{N}(1,\mathcal{T})$ | $p(1,\mathcal{T})$ | $\bar{N}(1,\mathcal{T})$ |
| 1 | .0739 | 4.36 | .0350 | 2.07 | .0183 | 1.08 | .0071 | .42 | .00348 | .20 |
| 2 | .0449 | 14.37 | .0145 | 4.64 | .00566 | 1.81 | .00126 | .40 | .000419 | .13 |
| 3 | .0144 | 9.79 | .0000663 | .05 | .0000066 | .004 | .0000066 | .004 | .0000066 | .004 |
| 4 | .000239 | .11 | .00 | .00 | .0000066 | .003 | .0000066 | .003 | .0000066 | .003 |
| 5 | .0768 | .61 | .0371 | .29 | .0196 | .16 | .00783 | .06 | .00392 | .03 |
| 6 | .103 | 3.09 | .0577 | 1.73 | .0335 | 1.00 | .0158 | .47 | .00894 | .27 |
| 7 | .287 | 2.29 | .225 | 1.80 | .160 | 1.28 | .104 | .83 | .0756 | .60 |
| 8 | .0326 | .26 | .00014 | .06 | .00187 | .01 | .000196 | .002 | .0000451 | .00 |
| 9 | .0326 | .39 | .00714 | .09 | .00187 | .02 | .000196 | .002 | .0000451 | .00 |
| 10 | .0264 | .53 | .00403 | .08 | .000621 | .01 | .000031 | .001 | .0000096 | .00 |
| | | 35.80 | | 10.81 | | 5.377 | | 2.192 | | 1.237 |

## References

1. Military Specification, Aircraft Structures, Military Standard MIL-A-87221 (USAF), Air Force Aeronautical System Division, WPAFB, OH, February 28, 1985.

2. Aircraft Structural Integrity Program, Airplane Requirements, Military Standard MIL-STD-1530A, Air Force Aeronautical Systems Division, WPAFB, OH, December 1975.

3. Airplane Damage Tolerance Program Requirement, Military Standard MIL-A-83444, Air Force Aeronautical Systems Division, WPAFB, OH, July 1974.

4. Airplane Strength, Rigidity and Reliability Requirement; Repeated Loads and Fatigue, Military Standard MIL-A-8866B, Air Force Aeronautical Systems Division, WPAFB, OH, August 1975.

5. Manning, S. D. and Yang, J. N., USAF Durability Design Handbook; Guidelines for the Analysis and Design of Durable Aircraft Structures, AFWAL-TR-83-3027, Second Edition, Air Force Wright Aeronautical Laboratories, WPAFB, OH, August 1987.

6. Rudd, J. L., Yang, J. N., Manning, S. D., and Garver, W. R., "Durability Design Requirements and Analysis for Metallic Airframes," Design of Fatigue and Fracture Resistant Structures, ASTM STP 761, P. R. Abelkis and C. M. Hudson, Eds., American Society for Testing and Materials, 1982, pp. 133-151.

7. Rudd, J. L., Yang, J. N., Manning, S. D., and Yee, B. G. W., "Damage Assessment of Mechanical Fastened Joints in the Small Crack Size Range," Proc., Ninth U. S. National Congress of Applied Mechanics, Symposium on Structural Reliability and Damage Assessment, Cornell University, Ithaca, NY, June 21-25, 1982, pp. 329-338.

8. Rudd, J. L., Yang, J. N., Manning, S. D., and Yee, B. G. W., "Probabilistic Fracture Mechanics Analysis Methods for Structural Durability," Proc., Conference on the Behavior of Short Cracks in Airframe Components, AGARD-CP-328, Toronto, Canada, September 1982, pp. 10-1 through 10-23.

9. Yang, J. N., Manning, S. D., and Rudd, J. L., "Evaluation of a Stochastic Initial Fatigue Quality Model for Fastener Holes," Fatigue in Mechanically Fastened Composite and Metallic Joints, ASTM STP 927, John M. Potter, Ed., American Society for Testing and Materials, Philadelphia, 1986, pp. 118-149.

10. Yang, J. N., Manning, S. D., Rudd, J. L., and Artley, M. E., "Probabilistic Durability Analysis Methods for Metallic Airframes," Journal of Probabilistic Engineering Mechanics, Vol. 1, No. 4, December 1986.

11. Yang, J. N., Manning, S. D., Rudd, J. L., Artley, M. E., and Lincoln, J. W., "Stochastic Approach for Predicting Functional Impairment of Metallic Airframes," Proceedings of the 28th AIAA/ASME/ASCE/AHS Structures, Structural Dynamics and Materials Conference, Paper No. 8707520CP, Monterey, CA, April 6-8, 1987, pp. 215-223.

12. Manning, S. D., and Yang, J. N., "Advanced Durability Analysis, Volume I - Analytical Methods," AFWAL-TR-86-3017, Air Force Wright Aeronautical Laboratories, Wright-Patterson Air Force Base, OH, July 1987.

13. Manning, S. D., and Yang, J. N., "Advanced Durability Analysis, Volume II - Analytical Predictions, Test Results and Analytical Correlations," AFWAL-TR-86-3017, Air Force Wright Aeronautical Laboratories, Wright-Patterson Air Force Base, OH, August 1987.

14. Yang, J. N., Manning, S. D., and Garver, W. R., "Durability Methods Development, Volume V - Durability Analysis Methodology Development" AFFDL-TR-3118, Air Force Wright Aeronautical Laboratories, Wright-Patterson Air Force Base, OH, September 1979.

15. Yang, J. N., and Manning, S. D., "Distribution of Equivalent Initial Flaw Size," 1980 Proceedings of Annual Reliability and Maintainability Symposium, San Francisco, CA, 22-24 January 1980, pp. 112-120.

16. Yang, J. N., and Donath, R. C., "Statistical Fatigue Crack Propagation in Fastener Holes Under Spectrum Loading," Journal of Aircraft, AIAA, Vol. 20, No. 12, December 1983, pp. 1028-1032.

17. Yang, J. N., Manning, S. D., Rudd, J. L, and Hsi, W. H., "Stochastic Crack Propagation in Fastener Holes," Journal of Aircraft, AIAA, Vol. 22, No. 9, September 1985, 810-817.

18. Yang, J. N., Salivar, G. C., and Annis, C. G., "Statistical Modeling of Fatigue Crack Growth in a Nickel-Based Superalloy," Journal of Engineering Fracture Mechanics, Vol. 18, No. 2, June 1983, pp. 257-270.

19. Yang, J. N., and Chen, S., "Fatigue Reliability of Gas Turbine Engine Components Under Schedule Inspection Maintenance," Journal of Aircraft, AIAA, Vol. 22, No. 5, May 1985, pp. 415-422.

20. Yang, J. N., and Chen, S., "An Exploratory Study of Retirement-for-Cause for Gas Turbine Engine Components," _Journal of Propulsion and Power_, AIAA, Vol. 2, No. 1, January 1986, 38-49.

21. Yang, J. N., and Hsi, W. H., Manning, S. D., and Rudd, J. L., "Stochastic Crack Growth Models for Application to Aircraft Structures," _Probabilistic Fracture Mechanics and Reliability_, Edited by J. W. Provan, Chapter IV, Martinus Nijhoff Publishers, The Netherlands, 1987, pp. 171-211.

22. Manning, S. D., and Yang, J. N., "Advanced Durability Analysis, Volume IV - Executive Summary," AFWAL-TR-86-3017, Air Force Flight Dynamics Laboratory, Wright-Patterson Air Force Base, OH, September 1987.

23. Speaker, S. M., et al., "Durability Methods Development, Volume VIII - Test and Fractography Data," AFFDL-79-3118, Air Force Flight Dynamics Laboratory, Wright-Patterson Air Force Base, OH, November 1982.

24. Gordon, D. E., et al., "Advanced Durability Analysis, Volume III - Fractographic Data," AFWAL-TR-86-3017, Air Force Flight Dynamics Laboratory, Wright-Patterson Air Force Base, OH, August 1, 1986.

25. Manning, S. D., Yang, J. N., Shinozuka, M., Speaker, S. M., and Gordon, D. E., "Durability Methods Development, Volume VII - Phase II Documentation," AFFDL-TR-79-3118, Air Force Flight Dynamics Laboratory, Wright-Patterson Air Force Base, OH, January 1984.

Note: Appendix J is AIAA Paper No. 88-2421 presented at AIAA/ASME/ASCE/AHS 29th Structures, Structural Dynamics and Material Coonference, Williamsburg, VA, April 18-20, 1988.